DOCTORAL THESIS

Physics-of-Failure Based Performance Modeling of Critical Electronic Components

Adithya Thaduri

LULEÅ UNIVERSITY OF TECHNOLOGY

DOCTORAL THESIS

Physics-of-Failure Based Performance Modeling of Critical Electronic Components

Adithya Thaduri

Division of Operation and Maintenance Engineering

Luleå University of Technology, Luleå, Sweden

Printed by Universitetstryckeriet, Luleå 2013

ISSN: 1402-1544
ISBN 978-91-7439-696-6 (print)
ISBN 978-91-7439-697-3 (pdf)

Luleå 2013

www.ltu.se

PREFACE

The PhD work involves a thorough understanding of the some of the key electronic components that ensure the safety of certain process control systems. Earlier studies in this area to predict the life-time of semiconductor devices using reliability standards such as MIL-HDBK 217F, Telcordia, CNET etc. were inconsistent; and these methods do not apply to operating conditions that require accurate prediction. Therefore, this study applies the physics-of-failure approach to determine the time to failure of these devices. This work at Luleå University of Technology was through a sponsored research project at Indian Institute of Technology Bombay.

I am grateful to my supervisors Professor Ajit Kumar Verma (Stord/Haugesund University College, Norway) and Professor Uday Kumar for providing the opportunity to pursue doctoral study. Their extensive co-operation, support and guidance at every stage helped me to complete this dissertation in time and without them it would not have been possible. I am also grateful to Professor A. Srividya for her constant support, guidance and motivation.

I would like to thank the project collaborators Dr. Gopika Vinod, Rajesh Gopinath and Dr. Hari Prasad for their guidance, useful suggestions and practical advice for better understanding the project objective. I would also like to thank Professor V Ramgopal Rao, IIT Bombay and I have benefited from his extensive knowledge of the concept of physics-of-failure.

I thank all my colleagues in the Reliability Group at IIT Bombay especially Dr. Krishnamohan, Dr. Suraj Rane, Cdr. Dr. Anil Rana, Cdr. Dr. P G Ramesh, Dr. Srinivas, Dr. Manoj Singh and several others who helped me overcome the obstacles I encountered on this project with their willing support, generosity and time.

I would also like to thank Dr. Rupesh Kumar, Dr. Ram Sateesh Pasupuleti, Dr. Yuan Fuqing, Mr. Madhav Mishra, Mr. Ganesh Mainali and several people from Luleå University of Technology who had helped me in completing this work.

Finally, I am exceedingly grateful to my beloved family for their loving support and inspiration. I would also like to thank all my friends for their assistance.

ABSTRACT

Reliability prediction of the electronic components used in industrial safety systems requires high accuracy and compatibility with the working environment. The traditional reliability prediction methods that draw on standard handbooks such as MIL-HDBK 217F, Telcordia, CNET etc., are not appropriate to determine the reliability indices of these components. For one thing, technology is constantly advancing; for another, the empirical data do not always match the actual working environment.

The newest reliability prediction methodology, the physics-of-failure (PoF), emphasizes the root cause of failure, failure analysis, and failure mechanisms based on the analysis of parameter characteristics. It involves a focused examination of failure point locations, considering the fabrication technology, process, materials and circuit layout obtained from the manufacturer. This methodology is capable of providing recommendations for the increased reliability of components using intuitive analysis.

However, there is a limitation: it is sometimes difficult to obtain manufacturer's details for failure analysis and quality information. Several statistical and probability modeling methods can be performed on the experimental data of these components to measure the time to failure. These experiments can be conducted using the accelerated-testing of dominant stress parameters such as Voltage, Current, Temperature, Radiation etc.

In this thesis, the combination of qualitative data from PoF approach and quantitative data from the statistical analysis is used to create a modified physics-of-failure approach. This methodology overcomes the limitations of the standard PoF approach as it involves detailed analysis of stress factors, data modeling and prediction. A decision support system is created to select the best option from failure data models, failure mechanisms, failure criteria and other factors to ensure a growth in reliability.

In this study, the critical electronic components used in certain safety systems from different technologies are chosen for reliability prediction: Optocoupler, Constant Fraction Discriminator, BJT Transistor, Voltage Comparator, Voltage Follower and Instrumentation amplifier. The study finds that the modified physics-of-failure methodology provides more accurate reliability indices than the traditional approaches using field data. Stress based degradation models are developed for each of the components. The modified PoF models developed using Response Surface Regression and Support Vector Machine (SVM) show better performance.

Keywords: *Physics-of-failure; Reliability Prediction; Failure Modeling; time to failure; Design of Experiments; accelerated testing*

LIST OF APPENDED PAPERS

PAPER I: P1	Thaduri, A., Verma, A.K., Vinod, G., Rajesh, M.G., Kumar, U. (2012). Two-Stage Design of Experiments Approach for Prediction of Reliability of Optocouplers. *International Journal Of Reliability, Quality And Safety Engineering*, 19(2), pp. 1250007-1 - 1250007-24.
PAPER II: P2	Thaduri, A., Verma, A.K., Vinod, G., Rajesh, M.G., Kumar, U. (2013). Reliability prediction of semiconductor devices using modified physics-of-failure approach. *International Journal of Systems Assurance Engineering and Management*, 4(1), pp. 33-47.
PAPER III: P3	Thaduri, A., Verma, A.K., Vinod, G., Rajesh, M.G., Kumar, U. (2012). Degradation modeling of Voltage comparator using modified physics-of-failure approach. *Communications in Dependability and Quality Management (CDQM)*, 15(1), pp. 76-87.
PAPER IV: P4	Thaduri, A., Verma, A.K., Vinod, G., Rajesh, M.G., Kumar, U. (2013). Stress Factor and Failure Analysis of Constant Fraction Discriminator using Design of Experiments. *International Journal of Reliability, Quality and Safety Engineering*, 20(3), pp. 134003-1 – 134003-28.
PAPER V: P5	Thaduri, A., Verma, A.K., Vinod, G., Rajesh, M.G., Kumar, U. (2013). Failure Modeling of Constant Fraction Discriminator using Physics-of-failure Approach. *International Journal of Reliability, Quality and Safety Engineering*, 20(3), pp. 134002-1 – 134002-26.
PAPER VI: P6	Thaduri, A., Verma, A.K., Vinod, G., Rajesh, M.G., Kumar, U. (2012). Support Vector Regression degradation modeling for Constant Fraction Discriminator. *Communications in Dependability and Quality Management (CDQM)*, 15(1), pp. 101-122.

DIVISION OF WORK

This section presents the division of the research work for the appended papers, noting the roles of all co-authors and the thesis author. Each paper was jointly produced by the co-authors; all co-authors proof-read the manuscripts before submitting them for publication. The work on each paper can be divided up as follows:

Paper I: The procedure of a two-stage design of experiments was developed by the thesis authors. The literature review, design and experimentation, analysis and modelling reliability prediction of optocouplers was also done by the thesis author. The co-authors helped to improve the manuscript.

Paper II: The modified physics-of-failure approach for prediction of reliability for electronic components and this procedure was developed by the thesis author. The co-authors provided input on methodology and improving the manuscript.

Paper III: The literature review, design and experimentation, analysis and modelling reliability prediction of voltage comparators were done by the thesis author. The input for modelling came from Prof. A.K. Verma and Prof. Uday Kumar. The co-authors helped to improve the manuscript.

Paper IV: The literature review, design and experimentation, analysis and modelling reliability prediction of Constant Fraction Discriminator was done by the thesis author. The design of circuitry and implementation was discussed with Gopika Vinod and Rajesh Gopinath. Prof. A.K. Verma and Prof. Uday Kumar gave input on modelling.

Paper V: The study of literature, experiments, analysis and modelling was done by the thesis author. Prof. A.K. Verma, Prof. Uday Kumar, Gopika Vinod and Rajesh Gopinath gave input on modelling and helped to improve the manuscript.

Paper VI: The study of literature, experiments, analysis and modelling was done by the thesis author. Input on parametric analysis was provided by Prof. A.K. Verma, Prof. Uday Kumar, Gopika Vinod and Rajesh Gopinath; they also helped improve the manuscript.

LIST OF CONFERENCE PRESENTATIONS

CONF. I: C1	Thaduri, A., Rajesh, M.G., Vinod, G., Das, D., Bhatnagar, P.V., Pithawa, C.K., Verma, A.K. (2010). A study of failure mechanisms in CMOS & BJT ICs and their effect on device reliability. *2nd International Conference on Reliability, Safety and Hazard (ICRESH), (Published by IEEE*), December 14-16, Mumbai, India, pp. 425-430.
CONF. II: C2	Thaduri, A., Verma, A.K., Vinod, G., Rajesh, M.G. (2011). Reliability prediction of optocouplers for the safety of digital instrumentation. *IEEE International Conference on Quality and Reliability (ICQR),* September 14-17, Bangkok, Thailand, pp. 491-495.
CONF. III: C3	Thaduri, A., Verma, A.K., Vinod, G., Rajesh, M.G., Kumar, U. (2011). Study of Reliability aspects in Constant Fraction Discriminator. *5th International Conference on Quality, Reliability and Information Technology, (ICQRIT),* December 7-9, Kathmandu, Nepal, pp. 1-7 (20).
CONF. IV: C4	Thaduri, A., Verma, A.K., Vinod, G., Rajesh, M.G., Kumar, U. (2012). Modified physics-of-failure approach for reliability prediction of electronic components. *Proceedings of the 2nd International Workshop & Congress on eMaintenance,* December 12-14, Luleå, Sweden, pp. 181-190,
CONF. V: C5	Thaduri, A., Verma, A.K., Vinod, G., Kumar, U. (2013). Reliability Prediction of Constant Fraction Discriminator using modified PoF Approach. *IEEE Proceedings on the 59th Annual Reliability and Maintainability Symposium (RAMS 2013),* January 28-31, Orlando, Florida, USA, pp. 1-7.
CONF. VI: C6	Thaduri, A., Verma, A.K., Kumar, U. (2013). Comparison of Reliability Prediction Methods using Life Cycle Cost Analysis. *IEEE Proceedings on the 59th Annual Reliability and Maintainability Symposium (RAMS 2013),* January 28-31, Orlando, Florida, USA, pp. 1-7.

CONTENTS

CHAPTER 1

INTRODUCTION

1.1 Background

1.1.1 Electronics in Industry

The electronics industry is complex, consisting of several diverse components, technologies, process, materials and devices, ranging from higher order to nano order with multiple faces (Gordon, 1965). The use of electronics improves industrial performance, due to their size, price, speed and ability to store information. In virtually every segment of industry, the use of electronics and embedded software is increasing. In fact, we come into contact with them every day in such areas as transportation, communications, entertainment, instrumentation and control, aviation, IT, banking, medical appliances, home appliances, manufacturing etc. To remain competitive in a world of "electronics-driven products", the effective management of the whole electronics lifecycle in the context of the product is crucial.

In recent years, electronics have been used for various applications in numerous industries, including the following:

Aviation: Avionic systems include various communications, navigation, control, display and other factors which consist of thousands of electronic components that can fit into an aircraft. This industry demands higher safety, control, reliability prediction and maintenance to continue operations without experiencing failures.

Automobile: With the expansion of the automobile industry, there is a growing need for environmental protection, along with a demand from customers for greater fuel efficiency, security and safety. With the advances in technology, automobile manufacturers are able to offer a variety of electronic systems to their customers. For example, the safety systems depend on electronic circuits. The ECU (engine control unit) provides dashboard information on fuel and oil levels, speed, gearing and engine revolutions (via the tachometer). Other electronic systems include the automobile specific integrated circuit (ASIC), field programmable gate arrays (FPGAs) and application specific standard products (ASSPs) (Kulshreshtha and Chauhan, 2009).

Entertainment and Communications: Only a few decades ago, the main application of electronics in entertainment and communications was in telephony and telegraphy. With the advent of radio waves, however, any message could travel from one place to another without the use of wires, and the communications industry was revolutionised. Telephone systems now use digital ICs for switching and memory. Communication satellites became possible with the advent of microelectronics. A new generation of electronics, called digital signal processing (DSP), has evolved because ICs have made the merging of communications and computation possible (Kulshreshtha and Chauhan, 2009).

Defence Applications: Defence applications are totally controlled by electronic circuits. Radar (radio detection and ranging) was first used during the Second World War and has led to many significant developments in electronics. With radar, it is possible to identify and find the exact location of enemy aircraft. Today, radar and anti-aircraft guns can be linked to an automatic control system to make a complete unit. Radar, sonar and infrared systems have been used to determine the location of enemy jet fighters, war-ships and submarines and to control the aiming and firing of guns. Guided missiles are fully controlled electronically. Finally, electronic circuits can provide a means of secret communication between military headquarters and individual units.

Industrial Application: Electronics circuits are widely used in industrial applications, for example, to control the thickness, quality, weight and moisture content of a material. Electronic amplifier circuits used to amplify signals can control automatic door openers, power systems and safety devices. Electronically controlled systems are used for heating and cooling. Power stations producing thousands of megawatts of power are controlled by tiny electronic devices and circuits.

Medical Services: The use of electronics in medical science has grown quickly. Doctors and scientists are finding new uses for electronic systems in the diagnosis and treatment of diseases. Electrocardiographs (ECG), X-rays, short-wave diathermy units, ultrasound scanners, endoscopy machines, etc. are in common use. Even thermometers, blood-pressure and blood-sugar measuring instruments, etc. are so user-friendly because of electronic circuits that the patient can handle them (Kulshreshtha and Chauhan, 2009).

Instrumentation - Application of Electronics: Electronics instruments, such as cathode-ray oscilloscopes, frequency counters, signal generators, strain gauges, are of immense help in the precise measurement of various quantities. Without these electronic instruments, no research laboratory is complete. Automation of industrial processes is also made possible by electronic circuits. For example, silicon controlled rectifiers (SCRs) are used in the speed-control of motors, power rectifiers and inverters. With microelectronics, computers have become integral components of control systems. Accurate and user-friendly instruments, such as the digital voltmeter (DVM), cathode ray oscilloscope (CRO), frequency counter, signal generator, strain gauge, pH-meter, spectrum analyzers, etc., are now available.

Challenges: Major concerns about the use of electronics in industry include safety, security, reliability, maintainability, cost of failure, risk factors etc. When a component breaks down, the consequences could be severe. There is a need to predict reliability to determine a suitable replacement policy for electronic components.

1.1.2 Reliability Prediction

Reliability became a field of study with the advent of complex and advanced electronic equipment, due to its high failure rates. Accurate reliability modelling and prediction are needed if electronic systems are to function well. Reliability modelling and prediction can

estimate an item's ability to meet specified reliability requirements. A basic reliability prediction estimates the need for maintenance and logistic support caused by an item's unreliability (Mil-HDBK-781D, 1986).

Reliability models and predictions can be formulated using results from different methods such as Mil-HDBK-781D (1986), Telcordia, CNET, or Physics-of-failure (PoF).

Reliability modelling and prediction should be started early, in the system specification stage of the design. This provides a basis for item reliability allocation and for the establishment of corrective action priorities. The models must be updated when the item design is modified, when environmental requirements change, or when new stress data, failure rate data or service use profiles are available.

The uses of reliability models are described below (Mil-HDBK-338B1, 2007):

- To assess reliability requirements in planning reports, making initial design specifications and requests for proposals, and arranging proposed reliability requirements.
- To compare existing reliability requirements with the latest technology trends, and provide guidance in costing and scheduling decisions.
- To provide a basis for item selection among components and vendors.
- To identify and rank dominant problem areas and suggest possible solutions.
- To allocate reliability requirements among the subsystems and lower-level items to attain the reliability target.
- To evaluate the range of proposed parts, technology, materials, and processes.
- To evaluate the design before making a prototype.
- To provide a basis for trade-off studies and to evaluate design alternatives.

The accuracy of reliability modelling and prediction depends on the assumptions, data sources and other relevant influences. The primary value of reliability prediction as a design tool is to assess and compare various possible approaches. Although the absolute value of item reliability derived by the prediction may be used in calculations, operating reliability must include the data sources and assumptions. For example, when field experience data for similar items in an environment are used, the prediction reflects anticipated field performance after design maturity has been achieved. Conversely, when laboratory data are utilised, the prediction reflects expected performance under laboratory conditions.

Until the 1980s, the exponential or constant failure rate (CFR) model was the only one used to describe the useful life of electronic components. Its six reliability prediction procedures led to the creation of the military handbook for the reliability prediction of electronic equipments (Military-Handbook-217F2, 1995). The CFR model mathematically describes the failure distribution of systems wherein the failures are due to random or chance events.

When electronic equipment complexity began to increase then several inherent failure mechanisms were combined to result in a constant failure rate (White, 2008).

1.1.2.1 Constant Failure Rate

During the 1980s and early 1990s, with the introduction of integrated circuits (ICs), evidence increasingly suggested that the CFR model was no longer relevant. Phenomena such as device wear-out dominated failures could not be described using the CFR model. A number of studies, including McLeish (2010), Pecht (2009) and White (2008), recommended that the exponential distribution should not be applied to every electronic component and system without proper understanding (Murphy, 2002).

The methods to find failure rate are the following:

1. The constant-failure-rate reliability model is used for most empirical-electronic reliability prediction approaches. The failure rate of the system containing different components is the summation of its components; in this case, all system components are in series (Mil-HDBK-217F2, 1995).

2. Most traditional prediction methods have a base failure rate modified by several π factors. These factors are included in the overall failure rate prediction, as defined in MIL-HDBK-217F2 (1995); they are based on different configuration levels, environmental stress levels, and quality levels. They can be applied to the parts and packaging of microcircuits, gate/logic arrays, and microprocessors. Examples of π factors include πCF (Configuration Factor), πE (Environmental Factor), and πQ (Quality Factor). According to equation (1.1):

$$\lambda_S = \sum_{i=1}^{n} N_i (\lambda_g \pi_Q)_i \qquad \text{Eqn} \quad 1.1$$

3. Two basic methods for performing reliability prediction based on the data observation include the parts count and the parts stress analysis. The parts count reliability prediction method is used for the early design phases, when not enough data are available but the numbers of component parts are known. The information for parts count method includes generic part types, part quantity, part quality levels (when known or can be assumed), and environmental factors.

MIL-HDBK-217, as the basis for almost all traditional reliability approaches, has limitations. It has not been updated since 1995, and most ICs have not been updated since 1991. Therefore, more recent technologies are not included or defined. Despite a variety of empirical prediction models now available and in spite of its deficiencies, the majority of engineers still use MIL- HDBK-217. An advanced 217 plus was also proposed in RIAC (2006). In a Crane study, almost 80 percent of the respondents report using it, with CNET and Telcordia coming second and third respectively (White, 2008). Inconsistency among different traditional prediction methods is the main problem facing engineers.

1.1.2.2 Physics-of-failure Approach

The application of the traditional reliability handbooks to the military and other industries has led to failures in the field. The need for a physics-of-failure methodology became obvious with the development of diverse technologies and the realisation that the military handbook was unable to handle them.

Recommendations to improve the military handbook address the weaknesses of traditional approaches (White, 2008), including the following:

(1) Misleading use of constant physics-of-failure,

(2) Use of the Arrhenius temperature model,

(3) No modelling of wear-out mechanisms, and

(4) No modelling mechanisms such as brittle die fracture.

The physics-of-failure approach now dominates reliability modelling. Physics-of-failure tries to discover and model the root cause processes of device failures (Hillman, 2002). This branch of reliability combines information about the device with the statistical aspects of failure occurrences, considering failure mechanisms and models, failure modes and failure analysis (Perry, 1999 and ASM, 2004).

Since wear-out mechanisms are better understood, the goal of reliability engineers has been to develop failure mechanisms to determine the life of components (Ohring, 1998). A weakness of this approach is that the expected wear-out failures are unlikely to occur during the normal service life of microelectronic devices. Nonetheless, failures occur in the real world, and reliability prediction has had to adapt the new theoretical approach to eliminating failure mechanisms that limit the useful life of an electronic device. It depends on process, technology, manufacturer location, post processing techniques etc.

The physics-of-failure methodology can be summarized as the following (White, 2008 and Pecht, 2009):

- Identify potential failure mechanisms, e.g., chemical, electrical, physical, mechanical, structural, or thermal processes leading to failure, and the failure sites on each device.
- Expose the product to highly accelerated stresses to find the dominant root cause of failure.
- Identify the dominant failure mechanism as the weakest link.
- Model the dominant mechanism (the failure and why it takes place).
- Combine the information gathered from acceleration tests and statistical distributions.
- Develop an equation for the dominant failure mechanism at the site and its mean time-to-failure (MTTF).

Physics-of-failure is not widely used by engineers, however, a clear indication that it has not achieved its goals. A key problem is the difficulty of modelling the time to failure (TTF) of devices based on the underlying root causes (McPherson, 2010). Nor has the physics of device failures been clearly formulated. Scientists are still working on formulating the reasons behind each failure. Therefore, applying complex statistical tools to approximate scientific principles adds parameters to the equations, leading to a higher level of complexity. A scientific model should provide a clear explanation for the instances and then generalize the model. Until now, the physics-of-failure approach could not make accurate predictions and thus was unable to replace traditional approaches completely.

The upcoming electronic system (circuit/processor) reliability approach builds on the advantages of both traditional and physics-of-failure methodologies. It combines the physics-of-failure mechanisms with the constant failure rate model and applies them to the electronic system, providing both a physical explanation for the electronic system failures and a simplified statistical tool for reliability prediction.

The PoF approach can be performed in the following ways (White, 2008):

- Using traditional prediction tools in particular field studies to obtain an approximate numerosity.
- Updating the previous models based on statistical methods (like the Bayesian approach) and trying to calculate the uncertainty growth of the electronic systems.
- Unifying electronic-device failure mechanisms.
- Trying to implement the latest scientific models to electronic systems.

1.2 Research Motivation

In certain industries like the military, as well as nuclear, space and communications fields, safety, reliability and maintainability are major concerns. Since electronics are used in a number of critical systems, an efficient mechanism for reliability prediction is required to assess and monitor the behaviour of the relevant components to reduce risk factors. The physics-of-failure method applies root cause failure information on degradation to find failure mechanics and also uses reliability growth techniques to reduce the failure rate. As many different technologies are now available, the present work emphasises critical electronic components from several technologies to compare the behaviour and impact of these components on the performance of the whole system.

1.3 Problem Statement

"Inaccurate reliability prediction of electronic components at critical sites leads to safety issues, higher cost and resources and also improper applicability of standards to different electronic technologies dependent on available data."

Inappropriate shutdowns and delays in the functioning of safety subsystems can occur when there are problems in certain critical electronic components that ensure the safety of the signal conditioning circuitry in safety systems. Optocoupler, Constant Fraction Discriminator, BJT (Bipolar Junction Transistor) Transistor, Voltage Follower, Voltage Comparator and Instrumentation Amplifier are examples of these components. Undesired shutdowns result from poor predictions made by the reliability indices at the site that governs the repair/replacement and maintenance policy of the items. They also occur when there is minimal or no knowledge of component failures. The time to failure used to be calculated using traditional methodologies but discrepancies were discovered in the prediction methodology. These methodologies do not correctly handle the field failure data within the prescribed operating conditions.

Other reliability predictions, such as physics-of-failure, are called for if we are to find the root cause of failure of the mechanisms under consideration here. These components need an effective reliability prediction method which will reflect real-world failures in the field and provide greater availability of sub-systems.

1.4 Research Questions

The literature review, industrial experience and discussions with academics led to a number of interesting research questions in the area of reliability prediction:

1. How can we develop an efficient and flexible reliability prediction methodology with the available resources?
2. What are the reliability and stress characteristics of each of the failing components in real-world experience?
3. How can we develop failure models to find time-to-failure for these components?
4. How can we make decisions on the failure phenomenon in different technologies?

1.5 Research Purpose and Objectives

The purpose of this research is to develop an effective reliability prediction methodology to evaluate the reliability indices and find cost-effective failure mechanisms of the specified critical components within the limits of the available information. This information can help redefine maintenance issues and ensure a growth in reliability. Following the sponsor's suggestions, the present study seeks to do the following:

1. Design an efficient prediction methodology to find time to failure.
2. Study and identify the stress factors and dominant failure mechanisms of each of the components.

3. Conduct experiments on the components to develop the failure models.
4. Provide decision support for different technologies to select the right reliability growth recommendation.

1.6 Research Scope and Limitations

This project deals with reliability prediction using a modified physics-of-failure approach. Specific electronic ICs (listed in Table 1.1) are selected to monitor reliability and time to failure using existing failure mechanisms already studied in the literature or using statistical modelling techniques, depending on the behaviour of individual ICs under electrical and/or environmental stresses. The scope of this research is limited to reliability issues pertaining to stress analysis of the parameters at the integrated circuit level.

The work makes the following assumptions and limitations:

1. All components are assumed to be independent, and there is no interaction between them.
2. Most components do not include the manufacturer's details for failure point locations, and they have not undergone non-destructive testing.
3. The testing data reflect the operating environment in the field to the maximum extent.
4. During the load testing, the acceleration of stress parameters will not cause another failure mechanism.
5. The account of soldier joint failures and other failure mechanisms outside the IC is accommodated so that its influence can be ignored.
6. The selection of samples and testing time can depend on cost, time and accuracy.

Table 1.1 Selected ICs for Reliability Prediction

Name	**Item No.**	**Technology**	**Parts**
Optocoupler	4N 36	GaAs	LED and phototransistor
Comparator	LM 311	JFET	Op-Amp
Buffer	OP07	CMOS	Op-Amp
Instrumentation amplifier	AD 620	CMOS	Op-Amp
BJT Transistor	2N2222	BJT	Transistor
Constant Fraction Discriminator	CFD 2004	BJT	Comparators and flipflops

1.7 Organization of Thesis

This thesis consists of 7 chapters with 6 appended papers (P1 to P6) and 1 conference paper (C1) illustrating the modified prediction methodology and results and discussions of the selected components with research questions (R1 to R4) as shown in Figure 1.1.

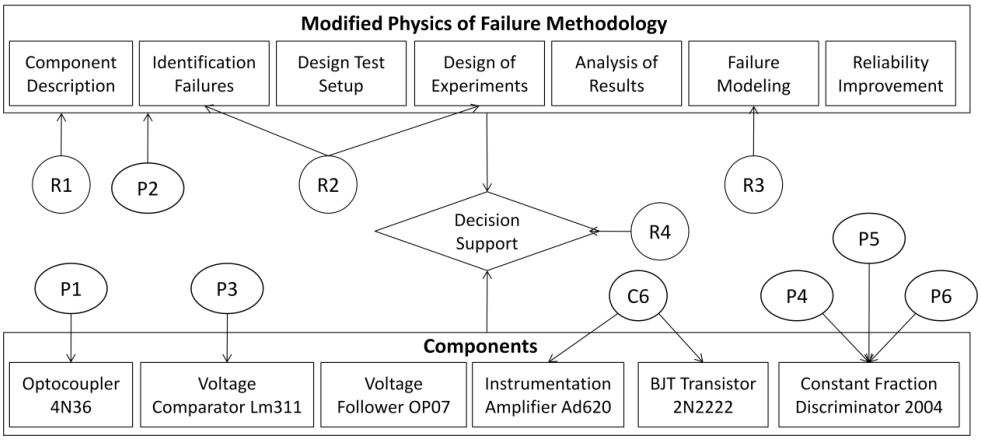

Figure 1.1 Organization of Thesis

Chapter 1 deals with the background of the inclusion of electronics in industries at different stages. It discusses the reliability prediction of electronic components.

Chapter 2 provides a literature review of the reliability prediction methodologies and compares their applicability.

Chapter 3 provides Research methodology applicable to the present work.

Chapter 4 is a more important section, as it gives the step by step procedure for finding out reliability or time to failure of a specific item; this approach is implemented in all aspects of the project.

Chapter 5 summarises the appended papers and the results obtained by implementing the methodology proposed in Chapter 4 on the specified components.

Chapter 6 presents the results and a discussion, building on Chapter 5.

Chapter 7 provides a conclusion, notes the research contributions and proposes future work.

References are listed in chronological order.

Appended papers of six journal papers and one conference paper are listed at the end of the thesis.

CHAPTER 2

LITERATURE REVIEW

Reliability assessment of electronics has traditionally been based on empirical failure-rate models using Mil-HDBK-217F, HRD4, Siemens, CNET, Bellcore, PRISM, Physics-of-failure etc. Pecht (1988) suggested that reliability can only be predicted when the layout of the components and exact mapping are known. O'Connor (1990) questioned the validity of the prediction models and their concept of assigning a failure rate to a component. Bowles (1992) compared these methods by calculating the failure rate of 64K DRAM and found large differences in values under similar operating and environmental conditions; as a result, Bowles raised questions about the difficulty of assigning the proper quality level of a specific component. Cushing (1993) broadly compared Mil-HDBK-217F and Physics-of-failure (POF) approaches and concluded that the former does not provide the designer or manufacturer with any insight into or control of the actual causes of failure. Nor does it provide strong indications of design parameters on reliability. Meanwhile, the POF approach proactively incorporates reliability into the design process by establishing a scientific basis for evaluating new materials, structures, and electronic technologies. Deckert (1994) compared traditional and physics-of-failure approaches for high reliability applications. Jeff (1999) compared traditional methods for different electronic components and found prediction values varied greatly from the observed field behaviour. Further analysis showed that each prediction model was sensitive to widely different physical parameters. EPSMA (2005) found differences in TTF values of a 1 watt DC-DC converter and suggested that the selection of prediction model is complex. Taken together, these studies show that traditional methods are not advisable for studying electronic components used in high reliability applications.

Goel (2006) provided an historical overview of traditional models and compared Mil-HDBK-217 to a PRISM model. Bisschop (2007) reviewed several reliability methods and standards and noted the importance of achieving world-wide standardisation in existing and new models. Jais (2013) emphasized the misuse of the Mil-HDBK 217 method, noting that the reliability assessment methodology includes utilising reliability data from comparable systems, historical test data, leveraging subject-matter-expert and applying fault-tree analysis (or similar analyses) to identify design weaknesses in the system. Finally, Pecht (1994) discussed the importance of reliability prediction and assessment in the design, development, and deployment of electronic equipment, along with the advantages and disadvantages of some of the current methods.

Pecht (1996) developed a comprehensive physics-of-failure methodology and studied a specific failure mechanism on conductive filament formation using insightful failure analysis. Ramakrishnan (2001) emphasized that a physics-of-failure approach is not only a tool to provide better and more effective designs; it also helps develop cost-effective ways to

improve the whole approach to building electronic products. Snook (2003) stated that physics-of-failure method has limitations, as it is essentially a bottom-up approach for assessing time to failure due to known failure mechanisms. Hillman (2004) studied failure analysis techniques on printed circuit boards with physics-of-failure prediction, SQUID microscopy, and ion chromatography and provided the identification of root-cause of failure with reliability growth recommendations. William (2006) reviewed various failure mechanisms on compound semiconductors and their impact on ageing. Bernstein (2006) reviewed some important failure mechanisms and used two state-of-the-art degradation-based reliability simulation methodologies with a new failure rate-based SPICE reliability simulation methodology to address reliability issues and the limitations inherent in other methods. Xiaolin (2006) studied the interactions of software and hardware enhancements on impact of reliability. Qin (2007) proposed physics-of-failure based VLSI circuit simulation tool for prediction methodologies of reliability for different failure mechanisms. Lori (2010) studied a physics-of-failure based industry consensus group VITA (VMEbus International Trade Association) using a multi-level approach. Jiang (2011) utilised several CAD simulation tools of stress analysis with a physics-of-failure approach on electronic modules to determine the design weaknesses. Chatterjee (2012) reviewed 50 years of the physics-of-failure, noting the important breakthroughs in the methodology. Yang (2013) reviewed the use of physics-of-failure methods on Wire bonding interconnects in power electronic modules and found that temperature and other sensitive processes had an impact on the bond degradation rate in the generated model. Wang (2012) proposed a FORM and physics-of-failure based approach using Monte-Carlo simulations. Challa (2013) incorporated physics-of-failure with history standards in qualification testing for prognostics health management.

Due to limitations in available resources like manufacturer data, sophisticated equipment and simulation tools, Ramakrishnan (2001) suggested incorporating physics-of-failure concepts with probabilistic techniques to find potential problems and trade-offs. Foucher (2002) compared bottom-up statistical methods, external databases and bottom-up physics-of-failure approaches using several criteria, including accuracy, time to calculate, customization etc., and found that the best reliability prediction can be achieved with the combined usage of the above methods. Cassanellia (2005) proposed a model combining empirical methods with graphical failure analysis by POF of failed parts; this would appeal to medium-size and small scale industries. Klaas, Jack and Van (2006) suggested using statistical and deterministic approaches simultaneously to obtain accurate life expectancy information and to create a reliable product. Dirk (2007) combined design of experiments with FEM based physics-of-failure models to define response surface methods for plastic IC packages and makes recommendations on increasing reliability. Baik (2008) discussed the challenges in the estimation of reliability based on warranty data and proposed a method for estimating component reliability using an accelerated life test model. Turner (2010), Varde and Naikan (2010) and Varde (2010) incorporated design of experiments and accelerated testing into physics-of-failure analysis and models to find the component's reliability. Guang (2012) proposed stochastic based physics-of-failure reliability based modelling to determine the momentum of a wheel with accelerated testing. Lundkvist (2013) had conducted a two-level full factorial experiment to find depth and variation of oscillation marks formed during

casting and found that depth of these marks can be reduced by decreasing the oscillation frequency from the Analysis of Variance (ANOVA) results obtained from design of experiments.

Due to cost, most medium and small scale industries do not have adequate information or enough available resources, including manufacturer data, intrinsic and extrinsic device parameters on wafer levels, high end sophisticated instruments and expensive CAD simulation tools to observe the critical areas of failure. Despite the cost and their limited resources such companies need accurate figures of time to failure to make good recommendations. An effective and flexible reliability prediction model is required to assess the failure of components within optimisation limits. This methodology would combine aspects of physics-of-failure, experimental data and statistical analysis to determine failure. Several process technologies are available in electronics, for example, BJT, JFET, CMOS and GaAs, and these industries need an overview of what they can do. They need to understand possible failure mechanisms, failure modes, failure models and failure analysis for the components they use.

To that end, this work suggests a flexible reliability prediction methodology for various electronic technologies and compares its efficiency with other methods.

CHAPTER 3

RESEARCH METHODOLOGY

Research can be defined in many different ways. In general, research is a process through which questions are asked and answered systematically. As a form of criticism, research can also need to include the question of whether or not we are asking the right questions (Dane, 1990). Research has its special significance in solving various operational and planning problems of business and industry (Kothari, 2004). Research is a systematic examination of observed information, performed to find answers to problems. Research methodology is the link between thinking and evidence (Sumser, 2000). To conduct research, it is essential to choose a clear and defined methodology. This provides a framework for integration of the different technical, commercial, and managerial aspects of study. The study of research methodologies provides the researcher with the knowledge and skills that are needed to solve the problems and meet the challenges of a fast paced decision making environment (Cooper and Schindler, 2006). The modeling involves a repeated switching between the functional and physical characteristics of a system, i.e., the determination of the expected change in the functioning of a physical system if a specific physical characteristic is changed to a certain extent (Lategan and Jordaan, 2006).

There are distinctive ways to carry out research (Kothari, 2004), but the purpose of research can be classified into three main categories i.e. the exploratory purpose (to explore a new topic), the descriptive purpose (to describe a phenomenon) and the explanatory purpose (to explain why something occurs). The details of these are described in Table 3.1.

Table 3.1: Different kinds of research purposes (Neuman, 2003)

Exploratory	Descriptive	Explanatory
- Become familiar with the basic facts, setting, and concerns - Create a general mental picture of conditions - Formulate and focus questions for future research - Generate new ideas, conjectures, or hypotheses - Determine the feasibility of conducting research - Develop techniques for measuring and locating failure data	- Provide a detailed, highly accurate picture - Locate new data that contradict past data - Create a set of categories or classify types - Clarify a sequence of steps or stages - Document a casual process of mechanism - Report on the background or context of a situation	- Test a theory's predictions or principle - Elaborate and enrich a theory's explanation - Extend a theory to new issues or topics - Support or refute an explanation or prediction - Link issues or topics with a general principle - Determine which of several explanations is best

The methodologies used in the present research are combination of descriptive, exploratory and explanatory. The research purpose of this study is to develop a prediction methodology that involves understanding of failure phenomenon of electronic components with mathematical modeling and physical modeling.

3.1 Research Approach

Research may be fundamental or applied in nature, depending upon the knowledge acquired about a certain area and the solution intended. Fundamental research aims to widen the knowledge of a particular subject so that future research initiatives may based on the extended knowledge. This research is design to solve problems of a theoretical nature, with little direct impact on strategic decisions. Applied research addresses existing problems and opportunities (Cooper and Schindler, 2006).

This thesis concerns applied research with a purpose to apply failure characteristics of devices to find time to failure of the critical electronics components in industrial context. The knowledge gathered from an extensive literature study, industrial discussions and the academic consultations scrutinized to achieve impact of physical failure phenomenon on the time to failure of the electronic components.

The research approach can categorize as induction or deduction (Sullivan, 2001).

- The induction approach uses observations, a knowledge base and empirical data to explain and develop theories. The approach involves inferring something about a whole group or class of objects from our knowledge of one or a few members of the group or class.

- The deduction approach can applied to generate hypotheses based on existing theories, the results of which derived by logical conclusions. The research approach can be quantitative or qualitative. In simple terms, quantitative research uses numbers, counts, and measures of things whereas qualitative research adopts questioning and verbal analysis (Sullivan, 2001).

In the present research, a both deductive and inductive approach had applied. An inductive approach has been applied to study failure mechanisms of the individual components in addition to a deductive approach has been applied to develop physics based failure models. Both qualitative and quantitative research methodologies have applied in this research.

3.2 Reliability and Validity

According to Neuman (2003), reliability means dependability or consistency. It suggests that the same things are repeated or reoccur under identical or very similar conditions. Reliability means that somebody else with the same result can apply the implementation methods of a study, such as data collection procedures. Validity is concerned with whether or not the study actually elicits the intended information. Validity suggests fruitfulness and refers to the match between a construct, or the way in which a researcher conceptualizes an idea in a conceptual definition, and a measure. It refers to how well an idea about reality fits in with actual reality (Neuman, 2003).

The data and information used in this research have collected from reputed peer reviewed journals, books from renowned authors, refereed conference proceedings and reports, or from company databases, which positively contributes to the research's reliability. In this research, different failure models have developed using physics-of-failure and statistical methodologies. The obtained results are believed to support the validity of the research, as they matched the theoretical and logical expectations. These models can be implemented in different industrial applications in future to support the validity further.

3.3 Data Collection

Data can be defined as the facts presented to the researchers from the studied environment. Data may be divided into primary and secondary types. Data collected by the researcher for the purpose of study through various experiments or onsite data recording are called primary data. Primary data are sought for their proximity to the truth and control over error. Data collected by other people/organizations and used by the researchers are called secondary data (Bhattacharyya, 2006). They have at least one level of interpretation inserted between the event and its recording (Cooper and Schindler, 2006).

Qualitative data were collected through relevant scientific papers and articles from online databases. Relevant books were searched for from IIT Bombay's library and then per used, and relevant reports and licentiate and PhD theses from various universities were also studied. The selection of the critical components is based on inputs from Bhabha Atomic Research Centre (BARC), Bombay. Different databases were searched to extract both qualitative and quantitative data. Relevant scientific papers and articles were extracted from online databases, such as Elsevier Science Direct, Emerald, IEEE Xplore, World Scientific etc. Some of the articles were searched from the references of other relevant articles. Different keywords were used for searching these articles as mentioned in the abstract. Different combinations of these keywords were also used to narrow down the number of hits. Some of the known articles were searched directly from the journal databases. Different types of statistical methods were examined and their parameters were characterized by using Reliasoft (2001), Minitab (2010) and other tools.

Researchers generate information by analyzing data after their collection. Data analysis is one step, and an important one, in the research process. Data analysis usually involves the reduction of accumulated data to a manageable size, developing summaries, looking for patterns, and applying statistical techniques. Further, the researcher must interpret these findings in the light of the client's research questions or determine if the results are consistent with the hypotheses and theories (Cooper and Schindler, 2006).

CHAPTER 4

POF RESEARCH METHODOLOGY FOR RELIABILITY PREDICTION

Physics-of-failure (PoF) is a procedure that tries to develop and model the root cause processes of device failures (White, 2008). The evaluation of possible component failure mechanisms considers basic phenomena involved in the degradation / failure of components. The resulting models recreate the life of the component, looking at operating stresses and load profiles. This method overcomes some of the limitations of traditional approaches in the following areas:

- Estimation of life and root causes of failure,
- Incorporation of operational load profiles of the component,
- Evaluation of associated failure mechanisms and detailed modelling for identified dominant failure mechanisms.

The physics-of-failure approach includes a systematic test method for finding the dominant failure mechanisms which might be indicated during the service of the component. The procedure followed for the modified physics of approach is detailed below and appears in Figure 4.1 as shown in Paper P2.

1. Description of component
2. Identification of possible failure mechanism and stress parameters
3. Design of test setup
4. Design of experiments
5. Analysis of test results
6. Failure modelling
7. Reliability Improvement.

This procedure is implemented on the components specified in this project. It acts as a basis for reliability prediction. Some of the steps cannot be used depending on the information available. Sufficient information on the unit's performance, literature related to previous studies, potential failure mechanisms, and comprehensive manufacturer's information are all required for an accurate understanding of the component.

4.1 Description of component

To start with a POF model of a component, information from multiple sources must be collected and analysed. This information includes the basic operation/function of the component, the materials and process used in its fabrication, details of packaging and assembly, CAD layout of IC's, the systems into which the part/component goes and their operation.

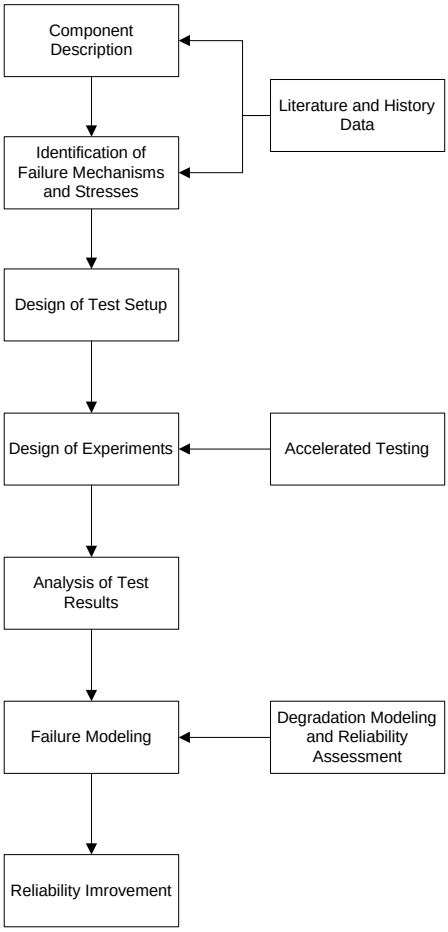

Figure 4.1 Proposed PoF methodology for reliability assessment

4.2 Identification of possible failure mechanism and stress parameters

Depending on the component's design, manufacturing and operational conditions, various failure mechanisms are possible (Bisschop (2007), Foucher (2002), Sematech (2000)). Accordingly, there is a need to determine the stresses such as thermal (Guijie (2000), Christou (2006), Theodre, Jeffrey and Guillerno (2009) and Zeghbroeck (2011)), electrical,

radiation (Witczak, 1993 and 1997, Kulkarni (2001)) and environmental that can cause the degradation mechanisms leading to its failure.

4.3 Design of test setup

After the identification of stress parameters, a setup needs to be designed for the accelerated test. The typical design of the setup for an accelerated test (hardware/software) includes a Printed Circuit Board (PCB), measurement equipments (CRO, waveform analyzers), heaters, power suppliers, function generator, voltage and current sources, environmental chamber etc.

4.4 Design of experiments

Design of experiments (DOE) is important. The DOE must take a systematic, extensive, and rigorous approach to the problems inherent to the collected data to ensure valid, supportable and effective results leading to interpretation (Lloyd, 2001). In this case, a statistical technique was used to study the effects and correlation of multiple variables simultaneously. The study's DOE applied response surface designs to the shape of the dependent variables (output) with each independent variable on a quantitative basis to determine the estimated position of maximum or minimum response and produce a region with the desirable effect.

The selection of sample size of the components was based on stress levels. The implementation of DOE is in two stages, screening and testing, as shown in Figure 4.2.

Screening stage gave us a better understanding of the influence of stress levels on the various performance indices and parameters. Testing stage gives appropriate stress levels were selected and tested based on the results of the screening stage in Paper P1.

It was then created a response table (including the two stages) that provides information on the impact of various stress levels on performance parameters.

Accelerated Testing

Traditional life data analysis involves analyzing times-to-failure data (of a product, system or component) obtained under normal operating conditions in order to quantify the lifetime characteristics of the product, system or component. In some situations, determining lifetime is extremely problematic. Reasons include the long lifetimes of today's products, the short time interval between design and release and the challenge of testing products that continuously operate under normal conditions (Nelson, 2008).

Because of the need to observe failures of products to better understand their failure modes and their life characteristics, reliability practitioners have attempted to devise methods to force these products to fail more quickly than under normal use conditions. In other words, they have attempted to accelerate their failures. Accelerated life testing is now used to describe all such practices, as shown in the figure below.

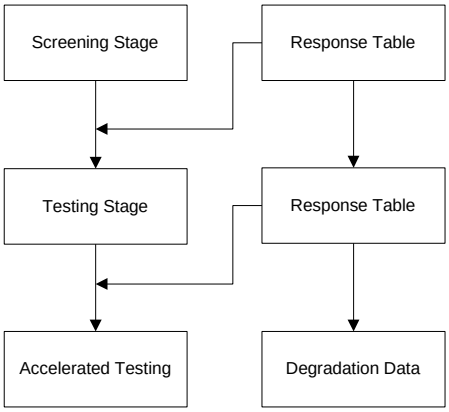

Figure 4.2: Two stage DOE with accelerated testing

4.5 Analysis of test results

The generated data can be used for detailed failure analysis (ASM, 2004 and Perry, 1999) and failure modelling. Certain statistical and graphical methods are required to determine the variation/degradation of the observed parameters.

4.6 Failure modelling

After the selection of stress parameters and failure mechanisms, an appropriate failure model must be created (Pham (2003), Pham (2006), Blischke and Murthy (2000), Sematech (2002) and JEDEC (2009)). Failure models can be designed from the degradation data using statistical methods for electronic components (Verma, 1987 and Verma, Srividya and Karanki, 2010). There are several failure models for each failure mechanism at various levels. In some instances, dominant failure mechanisms can be obtained from other studies or the literature. The generation of failure models can be formulated from the degradation data by statistical methods such as response surface methodology (Bradley (2007) and Raymond, Douglas and Christine (2009) and support vector regression (Vapnik (1995), Smola (1998), Cristianini and Shawe (2000) and Fuqing (2010)) with sequential minimal optimization algorithm (Platt (1998), Shevade (2000) and Flake (2001), Benett (2000)).

4.7 Reliability improvement

The examination of input parameters determines which contribute to the reliability growth of a component. The failure model and results provide feedback to the designer, manufacturer and supplier, enabling them to make changes to those parameters that increase the time to failure.

CHAPTER 5

SUMMARY OF APPENDED PAPERS

This chapter summarises six appended papers. Each paper contributes to the problem statement and research questions. More detailed information is available in the papers.

Paper I proposed a two-stage design of experiments (DOE) method and implemented it for Optocoupler. It studied the failure aspects of optocouplers and found that LED degradation was the prominent failure mechanism. The implementation of two-stage DOE on optocouplers led to the determination of the levels of dominant stress parameters and the stress level to conduct accelerated testing. Experimentation and analysis showed that higher current and higher temperature led to degradation of the optocoupler. The existing Lindquist model was compared with the model generated from Response Surface Regression (RSR). The characteristic of each parameter in the physics model was also studied; the effect was prominent after an accelerated time of 200 hours.

Paper II proposed using the modified physics-of-failure approach to predict the reliability of electronic components. This paper studied the most important failure mechanisms at the wafer level. It identified a research gap between traditional handbooks and the physics-of-failure approach. By inputting two methods, an advanced methodology was generated to achieve maximum confidence on the failure characteristics of the component. This methodology was flexible enough to meet the requirements while depending on the available resources.

Paper III studied the degradation mechanism of voltage comparators using dominant stress parameters. The paper examined the failure phenomenon of the voltage comparator and applied the methodology proposed in Paper II to determine its reliability characteristics. It found that both the higher radiation dose rate and higher temperature led to degradation of the voltage comparator, but radiation was the dominant stress parameter. A time to failure model was generated from the results by using Response Surface Regression (RSR).

Paper IV studied the stress factors and failure analysis of a constant fraction discriminator (CFD) using the physics-of-failure approach and vector regression. CFD was the important part of the project as this component defines the safety of a critical module. This device was fabricated using custom design specifications; hence, we had sufficient information on the wafer level of the device. The methodology proposed in Paper II was implemented on this device. The literature and experimentation results showed that radiation and temperature were the dominant stress parameters. Parametric analysis with different methods was applied to the data to determine the characteristics of the stress variables. Failure analysis was carried out on the device using a Scanning Electron Microscope (SEM); results indicated that radiation exposure and temperature had an adverse effect on the performance of the device.

Paper V developed a degradation model using Response Surface Regression. The experimentation results and parametric analysis in Paper IV were used to generate a time to failure model from the response surface regression.

Paper VI developed a degradation model using a Support Vector Machine (SVM). The experimentation results and parametric analysis in Paper IV were used to generate an SVM model. The support vector machine was discussed as a possibility for modelling the reliability prediction of this electronic component; a model was proposed to obtain the optimum kernel function with the respective tuning parameters. The sensitivity analysis of all functions showed that sequential minimal optimization (SMO) algorithm regression with the RBF kernel was best suited to determine the degradation of the output parameters with least amount of error.

Conf. V considered a critical component as Instrumentation Amplifier and a non-critical component as BJT transistor to compare Life Cycle Costing analysis with RIAC Mil-HDBK 217 PLUS and proposed a modified physics-of-failure (PoF) approach to reliability prediction methodologies. It concluded that when using the RIAC prediction method, the total cost of the BJT transistor is less than the Instrumentation Amplifier whereas when using the modified PoF method, the total cost of the Instrumentation Amplifier is less than the BJT transistor. This paper also compared several other features used in decision making in the reliability prediction method.

CHAPTER 6

RESULTS AND DISCUSSION

The application of a modified physics-of-failure approach to reliability prediction for the specified electronic components (see Table 1.1) led to the following observations:

1. The performance parameter (or output parameter) selection should be based on the field/ application environment.

2. The selection of stress parameters depends on the component type, literature, usage profile and working conditions. Most electronic components suffer from the thermal excitation caused by the application of direct temperature/heat or from intrinsic stresses.

3. Optocoupler devices experience a significant reduction in the current transfer ratio with gradual degradation of light output mainly due to the input light emitter (LED or LASER) inefficiency (Paper P1).

4. For CMOS technology, input voltage or input current may degrade the performance over time but this also depends on the usage environment (Paper C6).

5. The impact of radiation dose on BJT technology and JFET Technology is more than that of CMOS Technology. Radiation is one of the stress parameters for BJT components (2N2222 and CFD2004). The effect is reduced for CMOS devices due to radiation-hardened techniques that are now available (Paper P3, P4, P5, P6, C6).

6. Electromigration may occur on any of the metal contacts and is independent of technology. Especially significant is the electromigration found by the Constant Fraction Discriminator using SEM analysis. However, this effect is not verified for other components due to technology limitations (Paper P4).

7. The effect of Time Dependent Dielectric Breakdown (TDDB) is pronounced on devices with low oxide thickness. The time to failure is proportional to oxide thickness in the 1/E model since temperature is stress parameter. The CMOS and JFET components studied in this work are LM311, OP07 and AD62. These components have higher oxide thickness. As this does not demand a lower aspect ratio for scaling, the impact of TDDB is remarkably low (Paper P1, P3, P4, C6).

8. The radiation dose is a dominant stress parameter for JFET and BJT technology components, as shown by the Pareto Chart (Graeb, 2007) (Paper P3, P4).

9. Stress levels can be selected by using a two-stage experimental design. In the first stage, parameters are verified; in the next stage, the higher stress levels are subjected to get higher degradation. Parametric analysis can indicate the impact of each stress parameter. The selection of the stress level can be a useful input to accelerated testing (Paper P1, P2).

10. When this approach is used, the testing time (and cost implications) can be reduced, and the failures observed earlier (Paper C6).

11. The resistors and capacitors in the design circuitry degrade with temperature during accelerated testing. Hence, the main circuit should be segregated into a measuring circuit and a testing circuit (Paper P1, P5). The three technologies are shown in Table 6.1:

Table 6.1 Comparison of reliability w.r.t different technologies

Technology	CMOS	BJT	JFET
Stress Parameters	Temperature/Voltage	Temperature/Radiation	Temperature/Voltage
Possible FM	Electromigration/TDDB	Electromigration	Electromigration/TDDB
Failure Model	Blacks Eqn/ 1/E Model	Blacks Eqn	Blacks Eqn/ 1/E Model

12. The failure modelling for the components can be performed using the response surface regression method. The time to failure can be related to design considerations (Paper P1, P5, C6).

13. The equation for the time to failure for CMOS technology takes the form as in Eqn 6.1 (Paper C6)

$$Vout = K + \alpha 1R + \alpha 2T + \alpha 3t + \alpha 11R^2 + \alpha 22T^2 + \alpha 33t^2 + \alpha 12RT \qquad \text{Eqn 6.1}$$

where α represents the coefficients and K is constant. The time to failure is calculated by considering the *Vout* as a degradation percentage of the input design voltage *Vin*. By substituting the design values of Temperature T, the accelerated time t can be calculated.

14. The equation for the time to failure for components of BJT/JFET technology takes the form as in Eqn 6.2 (Paper P1, P3)

$$Vout = K + \alpha 1Vin + \alpha 2T + \alpha 3t + \alpha 11Vin^2 + \alpha 22T^2 + \alpha 33t^2 + \alpha 12VinT + \alpha 13Vint$$

Eqn 6.2

where α represents the coefficients and K is constant. The time to failure is calculated by considering the *Vout* as a degradation percentage of the input design voltage *Vin*. By substituting the design values of Temperature T and Radiation dose R, the accelerated time t can be calculated.

15. Several enhancement techniques, including temperature compensation circuitry, high quality devices, better isolation assembly, cooling schemes in the circuit board, changes in fabrication design etc., can be used to reduce the impact of temperature on the devices.

16. The use of radiation hardened techniques in fabrication can reduce the impact of external radiation exposure (Paper P4).

17. The design parameters are reduced for the components when current/voltage acts as one of the stress parameters (Paper P1).

18. This methodology can be applied to items with insufficient information on failure, optimising experimental setups to determine the time to failure.

19. The time to failure can be calculated with greater confidence using this method, as the prediction depends on field data, previous studies in the literature and experimental data.

20. The cost value resulting from this approach's accuracy of prediction is higher; it involves more insight into the failure phenomenon and experimentation.

21. From the LCC analysis of the Instrumentation Amplifier, we can conclude that for critical components, although the initial cost of physics-of-failure prediction is prohibitively high, the total cost incurred, including the penalty costs, are lower than those incurred by a traditional reliability prediction method. For non-critical components like BJT transistor, the total cost of physics-of-failure approach is also higher than the traditional approach; hence, in this instance, the traditional approach is more effective (Paper C6).

Summary of Results

The modified physics-of-failure methodology developed in Chapter 4 was applied on the components listed in Table 1.1. In Table 6.2, the failure phenomenon of each component is compared using a literature survey, experimentation and analysis. The dominant failure modes are showed as bold.

Table 6.2 Physics-of-failure information for the components

Name	**Parts**	**Stresses**	**Failure Mechanism**	**Failure Mode**	**Failure Analysis**
Opto-Coupler (4N36)-GaAs	LED and phototransistor	Current Temperature	LED ageing	output flux and **diffusion current degradation**	Functional Characteristics, external observation
Comparator (LM 311)-JFET	Op-Amp	Radiation Temperature	Radiation dependent Electromigration, Junction Degradation, surface contamination	Resistance fluctuation, Short, open, **increase in leakage current, Voltage degradation,** V_T, h_{FE} shift	Functional Characteristics, external observation
Voltage Follower (OP07)-CMOS	Op-Amp	Voltage Temperature	Junction Degradation, Gate Oxide Interface level Electromigration	Short, increase in **leakage current, Voltage degradation, V_T, h_{FE} shift** and Resistance fluctuation	Functional Characteristics, external observation
Instrumentation amplifier (AD 620)-CMOS	Op-Amp	Voltage Temperature	Junction Degradation, Gate Oxide Interface level Electromigration,	Short, increase in **leakage current, Voltage degradation, V_T, h_{FE} shift** and Resistance fluctuation	Functional Characteristics, external observation
BJT Transistor (2N2222)-BJT	Transistor	Radiation Temperature	Radiation dependent Electromigration, Junction Degradation, surface contamination	Resistance fluctuation, **Short, open, increase in leakage current, Voltage degradation,** V_T, h_{FE} shift	Functional Characteristics, external observation
Constant Fraction Discriminator (2004)-BJT	Comparators and flipflops	Radiation Temperature	Radiation dependent Electromigration, Junction Degradation, surface contamination	Resistance fluctuation, **Short, opem, increase in leakage current, Voltage degradation,** V_T, h_{FE} shift	Functional Characteristics, external observation, SEM

Table 6.3 summarises the results for the selected components. The table provides performance and stress parameters, models developed, time to failure figures and reliability growth information of all the components listed in Table 1.1.

Table 6.3 Comparison of selected electronic components w.r.t Reliability

Component	**Performance Parameter**	**Stress Parameters and levels**	**Model Used**	**Operating Conditions and Failure criteria**	**Time to failure from design specs**	**Reliability Growth**
Opto-Coupler (4N36)-GaAs	Current Transfer Ratio	Input Current = 90mA Temperature = 90^0C	Lindquist Model RSM	Input Current = 8mA Temperature = 30^0C Fc = 10%	24750 Hours and 27864 Hours	Reduce input current value and temp. compensation
Comparator (LM 311)-JFET	Output Voltage	Radiation = 10 KGy Temperature = 90^0C	RSM	Radiation = 0 KGy Temperature = 30^0C Fc = 5%	$58.54x10^6$ Hours	Rad-Hard manufacturing techniques and temp. compensation
Voltage Follower (OP07)-CMOS	Output Voltage	Input Voltage= +16 and -16V Temperature = 80^0C	RSM and SVM	Gain = 1 Temperature = 40^0C Fc = 5%	$11.2x10^8$ Hours SMO Reg with RBF Kernel (C=50, gamma = 1, Epsilon = 0.01)	Reduce input voltage and temp. compensation
Instrumentation amplifier (AD 620)-CMOS	Gain	Input Voltage= +16 and -16V Temperature = 80^0C	RSM and SVM	Gain = 1 Temperature = 30^0C Fc = 5%	$78.56x10^7$ Hours SMO Reg with RBF Kernel (C=50, gamma = 1, Epsilon = 0.01)	Reduce input voltage and temp. compensation
BJT Transistor (2N2222)-BJT	Output Voltage	Radiation = 10 KGy Temperature = 90^0C	RSM	Radiation = 0 KGy Temperature = 30^0C Fc = 5%	$1.5x10^{10}$ Hours	Rad-Hard manufacturing techniques and temp. compensation
Constant Fraction Discriminator (2004)-BJT	Output Voltage Pulse	Radiation = 10 KGy Temperature = 90^0C	RSM and SVM	Radiation = 0 KGy Temperature = 30^0C Fc = 5%	$5.7x10^7$ Hours SMO Reg with RBF Kernel (C=100, gamma = 15, Epsilon = 0.0001)	Rad-Hard manufacturing techniques and temp. compensation

Decision Support System

The decision support system consists of results obtained from the experimentation. The conclusions are divided into Design, Technology, Methodology and Management, as shown in Figure 6.1. Figure 6.2 shows the decision analysis for design and technology oriented methods and Figure 6.3 shows the decision analysis for methodology and management oriented methods

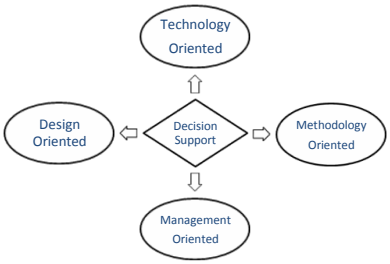

Figure 6.1 Decision Support System

Design Oriented

GaAs	BJT	JFET	CMOS
Reduce input current levels	Radiation isolation packaging	Radiation isolation packaging	Reduce input voltage and current levels
	Selection of components that are insensitive to radiation		
Temperature is stress parameter & independent of technology better isolation assembly, cooling schemes in circuit board			
Electromigration can occur on metal contacts and is independent of technology used Optimized metal thickness in design			

Technology Oriented

GaAs	BJT	JFET	CMOS
Degradation of i/p LED due to current and temperature	Higher impact of Radiation Dose than CMOS Electromigration is verified using SEM	Higher impact of Radiation Dose than CMOS No TDDB due to higher oxide thickness	Input electrical parameters dependence No TDDB due to higher oxide thickness
	Radiation Hardened Techniques		
Temperature is stress parameter & independent of technology High Quality Materials, Process Stability			
Electromigration can occur on metal contacts and is independent of technology used Optimize metal thickness and uniformity			

Figure 6.2 Design oriented and technology oriented recommendations

Methodology Oriented

GaAs	BJT	JFET	CMOS
Comparison of PoF model and RSM model	SEM analysis of CFD 2004	Failure models from RSM, SVM	Failure models from RSM, SVM
A Modified Physics of Failure Approach for finding time to failure			
Testing component was separated from measurement circuit to reduce sparse effects from other components			
The stress levels are selected by using two-stage DOE. In the first stage, verification of parameters is analyzed and in the second stage higher the stress levels are subjected to make higher degradation			
Accelerated time was optimized from DOE			
Finding weights of dominant stress parameters with interactions using Pareto Chart			

Management Oriented

Non-Critical – 2N2222	Critical – AD620
Initial cost of Traditional is lower than PoF	
Total cost of Traditional is lower than PoF	Total cost of PoF is lower than traditional
The effective usage of stress samples and testing time wrt cost implications can be reduced	
Physics of Failure method for resources like equipments, manufacturing data and analysis	
The selection of prediction model was presented depends on accuracy, criticality, cost and resources	

Figure 6.3 Methodology oriented and management oriented recommendations

CHAPTER 7

CONCLUSION & FUTURE WORK

7.1 Conclusion

The electronic components prescribed in this project require greater safety and longer time to failures. Accordingly, this paper seeks to improve failure models and failure prediction.

Constant failure rate prediction models have been found to lack accuracy and consistency, as they use different methodologies when handling the field data. Nor do they provide sufficient reliability improvement methods. Thus, an alternative prediction methodology is called for. The physics-of-failure approach is an advanced methodology that can assess the reliability of an item by investigating the root cause of failure using failure mechanisms and modes. This methodology depends on the fabrication technology, materials, process, layout etc., which vary according to the stress and environmental parameters of the field. It is often difficult to get information required for the analysis from the manufacturer. Hence, a model must be created from the experimental data using statistical methods.

The modified physics-of-failure model was applied to specified components for reliability analysis. From the knowledge acquired from the root cause analysis, stress parameters were determined. The behaviour of the performance parameter was then observed in accelerated testing. The experimental data were used for degradation modelling to calculate the time to failure. These data can also be used in parametric analysis to determine the dominant parameter that affects the performance of the device. Stress levels were calculated using a two-stage experimental design to plot the higher degradation on a response surface diagram.

The failure models generated from experimental data from the devices use Response Surface Regression and Support Vector Machine. These models consist of input stress parameters, output stress parameters and time variables. The time to failure is calculated from the design values. This approach can be useful to analyse how variability affects reliability. The data from this analysis are also useful for indicating design enhancements that will extend the time to failure.

The methodology offers a balance of resources, time spent and accuracy. The coordination of the physics-of-failure methodology and statistical methods provides better reliability prediction as it depends on available information. This methodology is better able to parametrically analyse a device and to suggest options for reliability improvement.

7.2 Research Contribution

The research presented in this doctoral thesis has focussed on the applicability of modified physics-of-failure approach on the selected critical components presented in Table 1.1. The literature study shows that there is significant research gap in prediction methodologies considering amount of information available with engineer. Furthermore, these methodologies have a limited use in some of the applications.

The research contributions can be listed as follows:

1. A modified Physics-of-failure methodology was developed for reliability prediction involving decision making factors (Paper P2).

2. The dominant stress parameters of each of the components were verified and validated (Paper P1, P3, P4, P5 and P6).

3. A two-stage design of experiments was developed to generate the stress levels required to carry out effective accelerated testing (Paper P1).

4. The failure models developed from the experimental data were used to obtain reliability indices (Paper P1, P3, P4, P5 and P6).

5. The design for reliability and reliability growth considerations was used to reduce the failure rate (Paper P1, P4).

7.3 Future Work

As extensions of this work and research conducted, the following areas can be considered for further investigation:

- With the implementation of a three-parameter stress model, we can obtain the time to failure figure, perform parametric analysis and discuss reliability growth techniques.
- Analysis must be carried out at the wafer level of each component to emphasise the failure mechanism
- Parametric analysis and failure modelling must lead to a higher level of confidence using inputs from statistical methods.
- Maintenance issues for each component must be considered.
- The methodology needs to apply new technologies in a simulation study.

REFERENCES

ASM International (2004), *Microelectronics Failure Analysis Desk Reference*, 5th Edition, Materials Park, Ohio, ISBN: 9780871708045

Baik, J. & Murthy, D.N.P. (2008). Reliability assessment based on two-dimensional warranty data and an accelerated failure time model. *International Journal of Reliability and Safety*, 2(3), 190-208.

Bennett, K.P. & Campbell, C. (2000). Support Vector Machines: Hype or Hallelujah. *SIGKKD Explorations*, December, New York, 2(2), 1-13.

Bernstein, J.B., Moshe, G., Xiaojun, L., Jorg, W., Yoram, S. & Michael, T. (2006). Electronic circuit reliability modeling, *Microelectronic Reliability*, 46, 1957–1979.

Bhattacharyya, D.K. (2006). *Research Methodology*, 2nd Edition, Excel Books, ISBN: 81-7446-497-2

Bisschop, J. (2007). Reliability methods and standards, *Microelectronics Reliability*, 47, 1330–1335.

Blischke, W.R. & Murthy, D.N.P (2000). *Reliability Modelling, Prediction and Optimization*, Wiley, New York, ISBN: ISBN-13: 978-0471184508.

Bowles, J.B. (1992). A Survey of Reliability-Prediction Procedures for Microelectronic Devices. *IEEE Transactions on Reliability*, 41(1), 2-12.

Bradley, N. (2007). *Response Surface Methodology*, Thesis, Indiana University, [Online], Available at: https://www.iusb.edu/math-compsci/_prior-thesis/NBradley_thesis.pdf.

Cassanellia, G., Murab, G., Cesarettic, F., Vanzib, M. & Fantini, F. (2005). Reliability predictions in electronic industrial applications, *Microelectronics Reliability*, 45, 1321–1326.

Challa, V., Peter, R. & Pecht, M. (2013). Challenges in the Qualification of Electronic Components and Systems, *IEEE Transactions on Device and Materials Reliability*, March 13(1), 26-35.

Chatterjee, K., Mohammad, M. & Bernstein, J.B. (2012). Fifty Years of Physics-of-failure, *The Journal of the Reliability Information Analysis Center*, January.

Christou, A. (2006). *Reliability of High Temperature Electronics*, Center for risk and reliability, University of Maryland, ISBN: 0-9652669-4-X.

Cooper, D.R. & Schindler, P.S. (2006). *Business Research Methods*, 9th Edition, McGraw-Hill Companies, Singapore, ISBN 0-07-124430-1.

Cristianini, N. & Shawe, T.J. (2000). *An Introduction to Support Vector Machines and Other Kernel-based Learning Methods*, Cambridge University Press, UK, ISBN-13: 978-0521780193.

Dane, F.C. (1990), *Research method*, Brooks/Cole Publishing Company, California.

Dirk, W.V.D. (2007). *Virtual Thermo-Mechanical Prototyping of Microelectronics Devices*, Printed by PrintPartners Ipskamp, The Netherlands, ISBN: 9789090221793.

Flake, G.W. & Lawrence, S. (2001). Efficient SVM Regression Training with SMO. *Machine Learning*, 46(1-3), 271-290.

Foucher, B., Boulli, J., Meslet, B. & Das, D. (2002). A review of reliability prediction methods for electronic devices, *Microelectronics Reliability*, 42, 1155–1162.

Goel, A. & Robert, G.J. (2006). Electronic System Reliability: Collating Prediction Models, *IEEE Transactions on Device and Materials Reliability*, June, 6(2), 258-265.

Graeb, H., Mueller, D. & Schlichtmann, U. (2007). Pareto optimization of analog circuits considering variability. 18th European Conference on Circuit Theory and Design, ECCTD, August 27-30, Seville, 28- 31.

Guang, J., Liu, Q., Zhou, J. & Zhou, Z. (2012). RePofe: Reliability physics-of-failure estimation based on stochastic performance degradation for the momentum wheel, *Engineering Failure Analysis*, 22, 50–63.

Guijie, W. & Meijer, G.C.M. (2000). The temperature characteristics of bipolar transistors fabricated in CMOS technology, *Sensors and Actuator (Elsevier)*, 87, 81–89.

Hillman, C. (2002). *Improved Methodologies for Identifying Root-Cause of Printed Board Failures*, CALCE Electronic Products & Systems Center, Mechanical Engineering Department, College Park, MD, University of Maryland.

Jais, C., Benjamin, W. & Das, D. (2013). Reliability Predictions – Continued Reliance on a Misleading Approach, *Proceedings of Annual Reliability and Maintainability Symposium*, January 28-31, Orlando, 1-6.

JEDEC Publication (2009). *Failure mechanisms and models for semiconductor devices*, JEP122E, (Revision of JEP122D, October 2008), Originally published as JEP122D.01 [Online], Available at: http://www.sematech.org/docubase/document/3955axfr.pdf [31 May 2000].

Jiang, S., Chenhui, Z. & Yonghong, L. (2011). Application of Physics-of-failure Method in Reliability Design of Electronic Products, *Applied Mechanics and Materials*, vols.44-47, 819-823.

Jones, J. & Hayes, J. (1999). A Comparison of Electronic-Reliability Prediction Models. IEEE Transactions on Reliability, June, 48(2), 127-134.

Klaas, B.K., Jack, C.L. & Van, P. (2006). *System Reliability: Concepts and Applications*, VSSD, ISBN-13: 978-9071301681.

Kulshreshtha, D.C. & Chauhan, D.S. (2009). *Electronics Engineering*, New Age Publications (Academic), ISBN: 978-81-224-2564-2.

Lori, E.B. (2010). Industry Consensus Approach to Physics-of-failure in Reliability Prediction, *Proceedings of Annual Reliability and Maintainability Symposium*, January 25-28, San Jose, 1-4.

McLeish, J.G. (2010). Enhancing MIL-HDBK-217 reliability predictions with physics-of-failure methods, *Proceedings of Annual Reliability and Maintainability Symposium*, January 25-28, San Jose, 1-6.

Michael, J.C., Mortin, D.E., Stadterman, T.J. & Malhotra, A. (1993). Comparison of electronics-reliability assessment approaches. *IEEE Transactions on Reliability*, December, 42(4), 542–546.

Mil-HDBK-217F2 (1995). *Reliability prediction of Electronic Equipment*, [Online], Available at: http://www.weibull.com/mil_std/mil_hdbk_217f_2.pdf [28 February 1995].

Mil-HDBK-338B1 (2007). *Electronic Reliability Design Handbook*, [Online], Available at http://www.weibull.com/mil_std/mil_hdbk_338b_1.pdf: [29 June 2007].

Mil-HDBK-781D (1986). *Reliability Methods and Standards*, [Online], Available at: http://www.weibull.com/mil_std/mil_std_781d.pdf [17 October 1986].

Fuqing, Y., Kumar, U. & Galar, D. (2010). Reliability prediction using support vector regression. International Journal of Systems Assurance Engineering and Management, 1(3), 263–268.

Gordon, E.M. (1965). Cramming more components onto integrated circuits. *Electronics Magazine*, p.1-4.

Kothari, C.R. (2004). *Research Methodology: Methods & Techniques*, 2nd Edition, New Age International, ISBN: 81-224-1522-9

Kulkarni, R. & Agarwal, V. (2001). Reliability Prediction of Electronic Power Electronic Devices Subjected to Gamma Radiation, *Proceedings of the International Conference on Quality, Reliability and Control*, December 27-28, Mumbai, India, R27-1-7.

Lategan, L.O.L & Jordaan, G.D. (2006). *Modelling as Research Methodology*, Sun Press, ISBN: 978-1-920383-05-3

Lundkvist, P., & Bergquist, B. (2013). Experimental study of oscillation mark depth in continuous casting of steel. *Ironmaking & Steelmaking*, [online], Available at: http://www.ingentaconnect.com/content/maney/ias/pre-prints/1743281213Y.0000000132 [July 1, 2013].

McPherson, J.W. (2010). *Reliability Physics and Engineering: Time-To-Failure Modeling*, Springer, New York, ISBN-13: 978-1441963475.

Minitab (2010). *Meet Minitab 16*, User Guide [Online], Available at http://www.minitab.com/uploadedFiles/Shared_Resources/Documents/MeetMinitab/EN16_MeetMinitab.pdf [6 April 2009]:.

Murphy, K.E., Carter, C.M. & Brown, S.O. (2002). The exponential distribution: the good, the bad and the ugly, A practical guide to its implementation, *Proceedings of Annual Reliability and Maintainability Symposium*, January 28-31, Seattle, WA, USA, 550-555.

Neuman, W.L. (2003). *Social Research Method*, 5th edition, USA

O'Connor (1990). Reliability prediction—Help or hoax?. *Solid State Technology*, August, 33, 59–61.

Ohring, M. (1998). *Reliability and Failure of Electronic Materials and Devices*, Academic Press, San Diego, USA, ISBN-13: 978-0125249850.

Pecht, M. & Dasgupta, A. (1995). Physics-Of-Failure: An Approach to Reliable Product Development. *International Integrated Reliability Workshop*, October 22-25, Lake Tahoe, CA, USA, 1-4.

Pecht, M. & Kang, W. (1988). A Critique of Mil-Hdbk-217E Reliability Prediction Methods. *IEEE Transactions on Reliability*, December, 37(5), 453-457.

Pecht, M. & Nash, F.R. (1994). Predicting the Reliability of Electronic Equipment. *Proceedings of the IEEE*, July, 82(7), 992-1004.

Pecht, M. (2001). Electronic Reliability Engineering in the 21st Century. *International Symposium on Advances in Electronic Materials and Packaging*, November 19-22, Jeju Island, South Korea, 1-7.

Pecht, M. & Gu, J. (2009). Physics-of-failure-based prognostics for electronic products. *Transactions of the Institute of Measurement and Control*, 31(3/4), 309–322.

Pecht, M. (2009). *Prognostics and Health Management of Electronics*, John Wiley & Sons Ltd, ISBN: 978-0-470-27802-4.

Perry, L.M. (1999). *Electronic Failure Analysis Handbook Techniques and Applications for Electronic and Electrical Packages, Components, and Assemblies*, McGraw-Hill, New York, ISBN: 9780071626347.

Pham, H. (2003). *Handbook of Reliability Engineering*, Springer, New Jersey, USA, ISBN: 978-1-85233-841-1.

Pham, H. (2006). *Reliability Modeling, Analysis and Optimization*, World Scientific, ISBN: 978-981-256-388-0.

Platt, J.C. (1998). Sequential Minimal Optimization: A Fast Algorithm for Training Support Vector Machines. *Microsoft Research*, Technical Report MSR-TR-98-14, April 21.

Qin, J. (2007). *A New Physics-of-Failure based VLSI Circuit Reliability Simulation and Prediction Methodology*, Dissertation, University of Maryland [Online], Available at: http://drum.lib.umd.edu/bitstream/1903/7410/1/umi-umd-4832.pdf [27 August 2007].

Ramakrishnan, A., Syrus, T. & Pecht, M. (2001). *Electronics Hardware Reliability*, In Cary, R.S., *The Avionics Handbook*, CRC Press London, ISBN 0-8493-8348-X [Online], Available at: http://www.davi.ws/avionics/TheAvionicsHandbook_Cap_22.pdf.

Raymond, H.M., Douglas, C.M. & Christine, M.A. (2009). *Response Surface Methodology: Process and Product Optimization using Designed Experiments*, Wiley Series in Probability and Statistics, New Jersey, USA, ISBN-13: 978-0470174463.

RIAC, Reliability Information Analysis Center (2006). *Handbook of 217 Plus Reliability Prediction Models*, Utica, New York, ISBN-13: 978-1-933904-03-0 [Online], Available at: http://sthelp.ru/sites/default/files/userfiles/2619/2012-06-05/spravochnik.pdf [26 May 2006].

ReliaSoft (2001). *Accelerated Life Testing Reference*, Reliasoft Publishing [Online], Available at: http://reliawiki.com/index.php/Accelerated_Life_Testing_Data_Analysis_Reference

Sematech (2000). *Semiconductor Device Reliability Failure Models*, Technology Transfer # 00053955A-XFR [Online], Available at: http://www.sematech.org/docubase/document/3955axfr.pdf [31 May 2000].

Shevade, S.K., Keerthi, S.S., Bhattacharyya, C. & Murthy, K.R.K. (2000). Improvements to the SMO Algorithm for SVM Regression. *IEEE Transactions on Neural Networks*, September, 11(5), 1188-1193.

Smola, A. & Schölkopfm, B. (1998). A tutorial on support vector regression. *NeuroCOLT2*, Technical Report NC2- TR-1998-030 [Online], Available at: http://alex.smola.org/papers/2003/SmoSch03b.pdf [30 September 2003].

Sullivan, T.J. (2001). *Methods of Social Research*, Harcourt Inc., USA, ISBN: 0-15-507463-6

Sumser, J.R. (2000). *A Guide to Empirical Research in Communication*, Sage Publications Inc, ISBN: 0761922229.

Theodore, F.B., Jeffrey, B. & Guillerno, R. (2009). *Electronic Devices and Circuits*, Pearson Prentice Hall, USA, ISBN13: 9780131111424.

Vapnik, V.N. (1995). *The Nature of Statistical Learning Theory*, Springer, New York, ISBN-13: 978-0387987804.

Verma, A.K. & Murthy, A.S.R. (1987). Reliability Modeling of Electronic Components. *Microelectronics and Reliability*, Pergamon Press, 27(1), 29-32.

Verma, A.K., Srividya, A. & Karanki, D.R. (2010). *Reliability and Safety Engineering*, Springer Series in Reliability Engineering, London, ISBN: 978-1-84996-231-5.

Wang, X., Shao, J. & Liu, X. (2012). A new Reliability Prediction Method based on Physics-of-failure Method for Product Design and Manufacture. *Advanced Materials Research*, 548, 521-526.

White, M. & Bernstein, J.B. (2008). Microelectronics Reliability: Physics-of-Failure based modeling and lifetime evaluation. *JPL Publication*, NASA Technical Report WBS: 939904.01.11.10, 08-5 2/08 [Online], Available at: http://trs-new.jpl.nasa.gov/dspace/bitstream/2014/40791/1/08-05.pdf [February 2008].

William, J.R. (2006). Historical review of compound semiconductor reliability. *Microelectronics Reliability*, 46(8), 1218–1227.

Witczak, S.C., Schrimpf, R.D., Fleetwood, D.M., Galloway, K.F., Lacoe, R.C., Mayer, D.C., Puhl, J.M., Pease, R.L. & Suehle, J.S. (1993). Charge separation for bipolar transistors. *IEEE transaction on Nuclear Science*, 40(6), 1276-1285.

Witczak, S.C., Schrimpf, R.D., Fleetwood, D.M., Galloway, K.F., Lacoe, R.C., Mayer, D.C., Puhl, J.M., Pease, R.L. & Suehle, J.S. (1997). Hardness assurance testing of bipolar junction transistors at elevated irradiation temperatures. *IEEE transaction on Nuclear Science*, 44(6), 1989-2000.

Xiaolin, T., Pham, H. & Jeske, D.R. (2006). Reliability Modeling of Hardware and Software Interactions, and Its Applications. *IEEE Transactions on Reliability*, 55(4), 571-577.

Yang, L., Pearl, A.A. & Johnson, C.M. (2013). Physics-of-Failure Lifetime Prediction Models for Wire Bond Interconnects in Power Electronic Modules. *IEEE Transactions on Device and Materials Reliability*, 13(1), 9-17.

Zeghbroeck, V.B. (2011). *Principles of Electronic Devices*, University of Colorado [Online], Available at: http://ecee.colorado.edu/~bart/book/book/title.htm [2011]

APPENDED PAPERS

Paper I

P1

Two-Stage Design of Experiments Approach for Prediction of Reliability of Optocouplers

Thaduri, A., Verma, A.K., Vinod, G., Rajesh, M.G., Kumar, U. (2012). Two-Stage Design of Experiments Approach for Prediction of Reliability of Optocouplers. *International Journal Of Reliability, Quality And Safety Engineering*, 19(2), pp. 1250007-1 - 1250007-24.

International Journal of Reliability, Quality and Safety Engineering
Vol. 19, No. 2 (2012) 1250007 (24 pages)

DOI: 10.1142/S0218539312500076

World Scientific
www.worldscientific.com

TWO-STAGE DESIGN OF EXPERIMENTS APPROACH FOR PREDICTION OF RELIABILITY OF OPTOCOUPLERS

ADITHYA THADURI* and A. K. VERMA†

Department of Electrical Engineering
Indian Institute of Technology, Bombay, India
**adithya.thaduri@gmail.com*
†*akvmanas@gmail.com*

GOPIKA VINOD‡ and M. G. RAJESH§

Bhabha Atomic Research Centre
Trombay, Mumbai, India
‡*vgopika@barc.gov.in*
§*rajeshgopalan@gmail.com*

UDAY KUMAR

Lulea University of Technology
Lulea, Sweden
Uday.Kumar@ltu.se

Received 10 October 2011
Revised 2 January 2012

Conventionally, reliability prediction of electronic components is carried out using standard handbooks such as MIL STD 217 plus, Telcordia, etc. But these methods fail to provide a realistic estimate of reliability for upcoming technologies. Currently, electronic reliability prediction is moving towards applying the Physics of Failure approach which considers information on process, technology, fabrication techniques, materials used, etc. Industries employ different technologies like CMOS, BJT and BICMOS for various applications. The possibility of chance of failure at interdependencies of materials, processes, and characteristics under operating conditions is the major concern which affects the performance of the devices. They are characterized by several failure mechanisms at various stages such as wafer level, interconnection, etc. For this, the dominant failure mechanisms and stress parameters needs to be identified.

Optocouplers are used in input protection of several instrumentation systems providing safety under over-stress conditions. Hence, there is a need to study the reliability and safety aspects of optocouplers. Design of experiments is an efficient and prominent methodology for finding the reliability of the item, as the experiment provides a proof for the hypothesis under consideration. One of the important techniques involved is Taguchi method which is employed for finding the prominent failure mechanisms in semiconductor devices. By physics of failure approach, the factors that are affecting the performance on both environmental and electrical parameters with stress levels for optocouplers are identified. By constructing a 2-stage Taguchi array with these parameters where output parameters decides the effect of top two dominant failure mechanisms and their extent

of chance of failure can be predicted. This analysis helps us in making the appropriate modifications considering both the failure mechanisms for the reliability growth of these devices. This paper highlights the application of design of experiments for finding the dominant failure mechanisms towards using physics of failure approach in electronic reliability prediction of optocouplers for application of instrumentation.

Keywords: Design of experiments; accelerated testing; optocouplers; degradation; failure mechanism; electronics; physics of failure.

1. Introduction

Industries employ different technologies like CMOS, BJT and BICMOS for various applications. The possibility of chance of failure at interdependencies of materials, processes, and characteristics under operating conditions is the major concern which affects the performance of the devices. They are characterized by several failure mechanisms and hence failure models of these devices should consider them at various stages such as wafer level, interconnection, etc. For this, the dominant failure mechanisms and stress parameters needs to be identified.

Design of experiments is an efficient and prominent methodology for finding the reliability of the item, as the experiment provides a proof for the hypothesis under consideration. One of the important techniques involved is Taguchi method[1] which is employed for finding the prominent failure mechanisms in semiconductor devices. By physics of failure approach, the factors that are affecting the performance on both environmental and electrical parameters with stress levels are identified. By constructing Taguchi array with these parameters where output parameters decides the effect of top two dominant failure mechanisms and their extent of chance of failure can be predicted. This analysis helps us in making the appropriate modifications considering both the failure mechanisms for the reliability growth of these devices. This paper highlights the application of design of experiments for finding the dominant failure mechanisms towards using physics of failure approach in optocoupler reliability prediction.

2. Optocouplers

An optocoupler (in Fig. 1) is a little cool device that allows you to completely separate sections of an electric circuit. An optocoupler or sometimes referred to as opto-isolator allows two circuits to exchange signals yet remain electrically isolated. It consists of LED at the input and Photo-transistor at the output and the isolation is implemented by light medium.[2]

In most of the circuits, electrical isolation has major effect on the performance which includes noise exerted by the wire medium. So, for better isolation, optocouplers are used since here light acts as a medium.

Due to the degradation of optocouplers, reliability plays important role. Current transfer ratio (CTR) is the main characteristic for operation of optocouplers. For

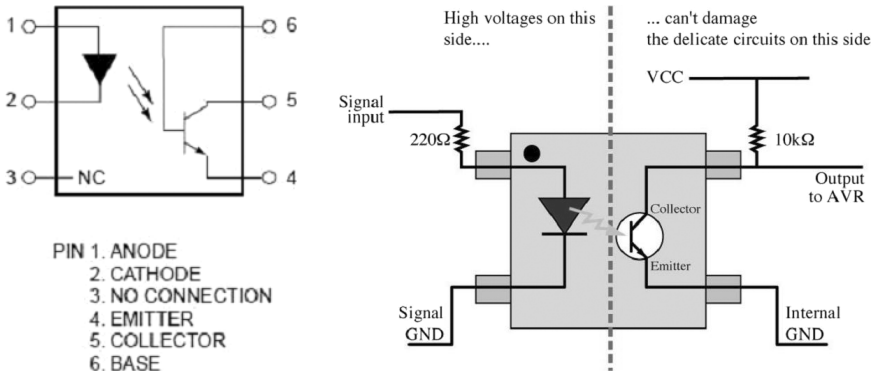

Fig. 1. Block Diagram of 4N36.

fixed V_{ce}, CTR as in Eq. (1)

$$\text{CTR} = \frac{I_{\text{Collector}}}{I_{\text{Diode}}}. \tag{1}$$

CTR is measured as from the circuit diagram shown in Fig. 2. One of the optocoupler ICs, 4N36 consists of six pins described in Fig. 1. Input voltage is given to pin1 with reference to the ground at JP3. The output voltage is calculated from pin5 with reference to ground at JP4. Input and output currents are calculated by dividing currents to the resistances of input as R1 and output as R3 respectively.

The CTR is the amount of output current derived from the amount of input current. CTR is normally expressed as a percent. CTR is affected by a variety of influences, including LED output power, hFE of the transistor, temperature, diode current and device geometry. If all these factors remain constant, the principle cause

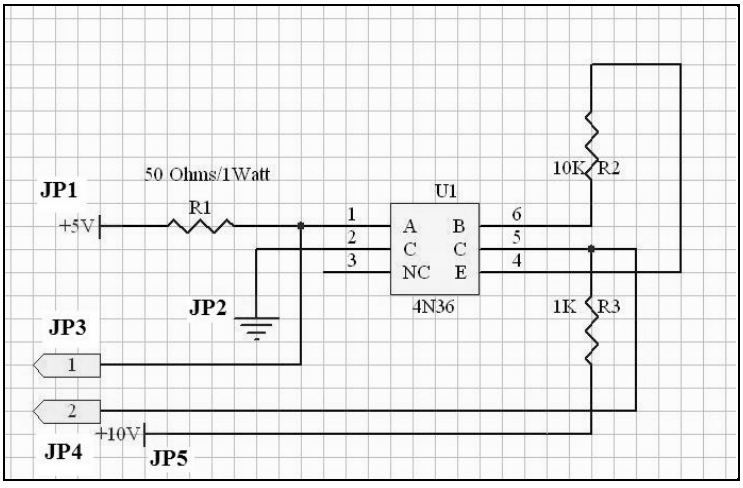

Fig. 2. Circuit diagram of 4N36.

of CTR degradation is the degradation of the input LED. Other characteristics include Id versus Vd, transmission speed and operating temperature range.

2.1. *Optocoupler input* (*LED*)[3]

The area of greatest concern in optocoupler reliability has been the infrared LED. The decrease in LED light output power over current flow affects the performance. Companies are focused on the infrared LED to improve CTR degradation and consequently achieved a significant improvement in coupler reliability. The improvements have included die geometry to improve coupling efficiency, metallization techniques to increase die shear strength and to increase yields while reducing user cost, and junction coating techniques to protect against mechanical stresses, thus stabilizing long-term output.

2.2. *Optocoupler output* (*photo-transistor*)

There are varieties of outputs available like bipolar transistors, MOS, SCR with different ratings to suit particular applications. The slow change in the electrical parameters over time when voltage is applied is termed as electric field. This is extreme at 100 C with high voltage 1 kV. This is due to the release of charge carriers which results in change of gain, reverse current and reverse voltage where direction of field is important. To improve characteristics, pn junctions are protected by transparent ion screen.

3. Experimental Setup

Ageing Tests: There were several accelerated wear-out tests for ageing tests of optocouplers. Many parameters including LED ageing and ambient temperature on photo-detector is suspected.

Circuit Diagram for 4N36: Two types of tests are carried out; temperature and input current in Fig. 3. In order to highlight the ageing tests of optocouplers, first measure their functional characteristics after that ageing tests should be implemented.

Optocoupler Parameter Drift: Ageing tests are carried out in two batches: LED side and photo-transistor side. Two batches of 20 4N36 ICs with ambient temperature as 30°C and junction temperature as 105°C using Fig. 3. By studying the variation of CTR on the input measurement current on both the batches, degradation of components stressed in photo-transistor is insignificant event after 1000 h. Significant degradation exists in LED ageing where for smaller currents it is more rapid up to 100 h and after that rate decreases with time.

4. Modeling

Variation of CTR with current and time: From the above results, drift in CTR depends on I and t. Failure is considered as if CTR reaches 50% lesser than original

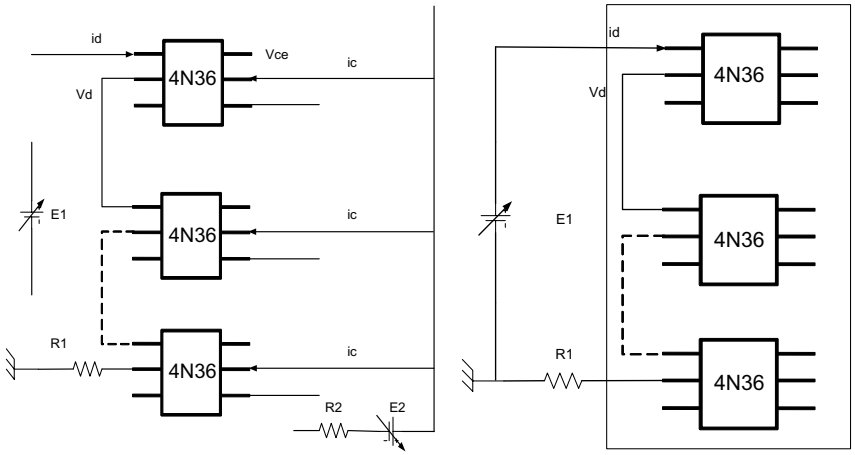

Fig. 3. (a) Photo detector ageing and (b) LED ageing.

value.

$$D(t) = \frac{\mathrm{CTR}(0) - \mathrm{CTR}(t)}{\mathrm{CTR}(0)}. \tag{2}$$

Modeling of Optocouplers ageing[2]: Bajenesco proposed a model for optocouplers ageing in terms of life time as Eq. (11), junction temperature and current across LED.

$$t_1 = \frac{A}{I_\mathrm{d} e^{-\frac{E_\mathrm{a}}{KT_\mathrm{j}}}}, \tag{3}$$

where t_1 is lifetime, I_d is ageing (LED) Current, E_a is Activation Energy, $E_\mathrm{a} = 0.15\,\mathrm{eV}$, K is Boltzman Constant, T_j is Junction Temperature and A is Time factor A.s.

The main cause for CTR degradation is the reduction in efficiency of the LED in the optocoupler. Its quantum efficiency (total photons per electron of input current) decreases with time at a constant current. The LED current in Eq. (12) consists of two components diffusion current and a space–charge recombination current.

$$I_\mathrm{f}(V_\mathrm{f}) = Ae^{qV_\mathrm{f}/KT} + Be^{qV_\mathrm{f}/KT}. \tag{4}$$

For constant current, if recombination current increases due to B, then diffusion current, the radiative component will decrease. This reduction is due to both current density and junction temperature. In general, emitter current density is a function of current, junction geometry, resistivity of both the regions of diode. Junction temperature is a function of coupler packaging, power dissipation and temperature. As with current density, high T_j will increase rapidly in proportion with recombination

current. From the block diagram of abstract optocoupler,[4] CTR expression is given as in Eq. (13),

$$\mathrm{CTR} = I0/I_{\mathrm{f}}(100\%) = KR\eta(I_{\mathrm{f}}, t)\beta(Ip, t), \tag{5}$$

where K is Transmission factor, R is Resistivity of photodetector, η is Quantum efficiency with function of input current and time and β is Gain of output amplifier with function of photo current and time.

Temperature variation affects the efficiency and gain. The normalized CTR is given as in Eq. (6)

$$\frac{\Delta\mathrm{CTR}}{\mathrm{CTR}} = \frac{\Delta\eta}{\eta} + \frac{\Delta\eta}{\eta}\left(\frac{\delta \ln \beta}{\delta \ln Ip}\right) + \frac{\Delta\beta}{\beta}. \tag{6}$$

1st term: Major contribution to normalized CTR. In general, it is negative over time.
2nd term: Second-order effect of shift in Q point of amplifier as efficiency changes.
3rd term: Negligible effect with change in gain over time.

Lindquist Model[5]: Lindquist also suggested a model describing the relative (CTR) degradation in terms of ageing current and measurement current as Eq. (15).

$$D(\%) = \frac{j(0) - j(t)}{j(0)} = 1 - e^{q\Delta V/KT}. \tag{7}$$

Since the transistor life is more compared to LED, the optocoupler ageing mainly depends on degradation of LED light output which is flux.

$$\frac{\Delta\mathrm{CTR}}{\mathrm{CTR}} = \frac{\Delta j}{j}, \tag{8}$$

where output flux as in Eq. (17) is a function of efficiency of optcoupler and diffusion current.

$$j = \eta \cdot I_{\mathrm{diff}} = \eta \cdot \alpha \cdot e^{qV/KT}. \tag{9}$$

By the above model, the increase in ΔV with decreasing current means degradation increases as measurement current increases. For direct bandgap emitters, the degradation is due to nonradiative component at which flux is measured. Current density $J(V)$ in Eq. (18) is combination of radiation and nonradiation current densities

$$J(V) = \frac{I(V)}{A} = \alpha e^{q\Delta V/KT} + \gamma e^{q\Delta V/2KT}, \tag{10}$$

where α denotes the coefficient of diffusion (Radiation) and γ denotes the coefficient of recombination current (Nonradiation). Taking the boundary values into consideration in current density equation, by solving, change in gamma coefficient

with respect to initial value can be found in Eq. (11)

$$\frac{\Delta\gamma}{\gamma(0)} = -2\xi_0 \sinh\left(\frac{q\Delta V}{2KT}\right) + e^{-q\Delta V/2KT} - 1, \tag{11}$$

where ξ, the ratio of diffusion current and recombination current is given as in Eq. (12)

$$\xi = \frac{\alpha}{\gamma} e^{qV/2KT}. \tag{12}$$

Substituting this value in the degradation mechanism, the final equation is in Eq. (13)

$$\frac{D(\%)}{100} = 1 - \frac{\left(1 + \frac{\Delta\gamma}{\gamma(0)}\right)^2}{4\xi_0^2} \left\{ \sqrt{1 + \frac{4\xi 0(\xi 0 + 1)}{\left(1 + \frac{\Delta\gamma}{\gamma(0)}\right)^2}} - 1 \right\}^2, \tag{13}$$

where: $\Delta\gamma = \gamma(t) - \gamma(0)$ and ξ, for the values of $\gamma(0)$ and $V(0)$. Suppose, change in γ is proportional to current, $d\gamma/dt = b.I_\mathrm{s}$, then the drift model of CTR is in Eq. (14)

$$\frac{\Delta\mathrm{CTR}(t, I_\mathrm{s}, I_\mathrm{m})}{\mathrm{CTR}} = 1 - \frac{\left(1 + \frac{b.I_\mathrm{s}.t}{\gamma(0)}\right)^2}{4.C^2.I_\mathrm{m}} \left\{ \sqrt{1} + \frac{4.C.\sqrt{I_\mathrm{m}}(C.\sqrt{I_\mathrm{m}} + 1)}{\left(1 + \frac{b.I_\mathrm{s}.t}{\gamma(0)}\right)^2} - 1 \right\}^2, \tag{14}$$

where t = time in hours, I_s = ageing current in A, I_m = measurement current in A, $\gamma(0) = 10$–$12(A)$, $C = 80(A - 1/2)$ and b = constant related to optocoupler.

Causes of CTR Degradation: Total electron flux emitted by LED degrades slightly over operating time of the device. At higher stress currents, change of light output increased over time. Main causes include reduction in emitter efficiency, decrease in transmission ratio, and reduction in responsiveness of photo detector or change in gain of amplifier which all are dependent on time. The critical cause is the result of electrical and thermal stressing of PN junction. Assuming degradation mechanism establishes a resistive shunt parallel to active PN Junction. At low values of input current, resistance path exhibits appreciable impact on the performance which offers low resistance. As current increases further, junction experiences low resistance which draws more current.

Reliability of optocouplers: Important area of investigation is the light output test of LED, assembly area in die attach and wire bond. Temperature cycle is a more effective screen than stabilization bake. Temperature coefficient of expansion and low glass transition temperature of unfilled, clear plastics is much greater than that of the other components. To maintain reasonable device integrity requires temperature range of operation and stronger mechanical construction; some clear plastics build up mechanical stress on the encapsulated parts during curing. This stress has been likened to rapid, inconsistent degradation of IRED light output.

Although a filled plastic would stop these phenomena, the filler also spoils the light transmission properties of the plastic. The decrease in quantum efficiency of LEDs is the main reason for CTR degradation of optocouplers. Other less important causes of CTR degradation are a decrease in the transmission of the transparent epoxy, a change in sensitivity of the photodetector and a change in gain of the output amplifier. It is now known that the rate of CTR degradation is influenced by the materials and processing parameters used to manufacture the LED, and the junction temperature of the LED in addition to the current density through the LED.

5. Design of Experiments

From the above study, input current to LED is dominant for the degradation of CTR for optocouplers whose interim is dominant stress parameter. Temperature is second dominant parameter for optocoupler which also degrades CTR. Other stress parameters radiation effects[6] and humidity are negligible. Statistically, the effect of both the stress parameters is not quantified. To define this, the prominent Design of experiments by Taguchi method[1] is implemented here which also involves screening of stress parameters. It gives the statistical measure of amount of S/N generated by specific parameter at specific level. This also helps in choosing the design parameter for extended MTTF of the item. From the traditional approach, runs are selected based on the stress parameters and its levels as in the example given in Table 1. But in this paper, a modified approach of Taguchi method is implemented in which the runs entirely depends on the behavior of stress parameters and levels variation on the performance parameter. This extended Taguchi method is shown below:

Extended Taguchi Method: The Design of experiments is carried out in two stages.

Stage 1: It provides information on effective variation of stress parameters that leads to CTR deviation. From the response table, it was concluded that as current and temperature increased CTR decreased.

Stage 2: Select the parameter levels from the feedback of stage 1. From the experiment results, estimate the parameter levels for the accelerated testing for CTR degradation.

Experimental parameters are selected as:

Item: 4N36 (I_f: 10 mA, 25°C, CTR = 100), I_f (0, 100 mA) and T (−55°C, 150°C).

Table 1. L4 Array.

Run no:	A (I_f)	B (T)	AXB
1	1	1	1
2	1	2	2
3	2	1	2
4	2	2	1

Failure Mechanisms: LED ageing Stress Parameters: Input LED current and Temperature.
Levels: I_f (H: 70 mA; L: 10 mA) and T (H: 100°C, L: 30°C)
Samples: For each run, $n = 5$ samples are selected.
Measurement Parameter: CTR is calculated by measuring currents on both input and output. Bigger is better (B-Type Statistics).

Using the above two level parameters, L4 Array is constructed as in Table 1 and modified with above levels.
The average of CTR is

$$\bar{Y} = \frac{Y1 + Y2 + Y3 + Y4 + Y5}{n}. \tag{15}$$

Signal to Noise Ratio is defined as S/N $= -10$log MSD where

$$\text{MSD} = \frac{1/Y1^2 + 1/Y2^2 + 1/Y3^2 + 1/Y4^2 + 1/Y5^2}{n}, \tag{16}$$

where Y_Y = Average of Y_{AVG} value for that level.

By calculating results table and response table, the effect of both the parameters are quantified and will maximize the CTR for the respective selection of parameters.

Accelerated Testing: After finding the levels of stress parameters, accelerated testing is carried out at different times and effective CTR is calculated at each point. From the model in Eq. (14), value of 'b' is calculated for $t = 200$ h. Then, time to failure is calculated at different values of CTR. Even from the above model, we can define the relation between the design current and degradation ratios of CTR to time to failure.

Validation of parameters of Eq. (14) is also studied based on the experimental data at different times. This provides the dissimilarity of values of parameters and deviation according to times.

Response Surface Method: Response surface methodology (RSM) explores the relationships between several explanatory variables and one or more response variables.[7] The main idea of RSM is to use a sequence of designed experiments to obtain an optimal response. An easy way to estimate a first-degree polynomial model is to use a factorial experiment or a fractional factorial designs. This is sufficient to determine which explanatory variables have an impact on the response variable(s) of interest.

Methodologies that help the experimenter reach the goal of optimum response are referred to as *Response Surface Methods.* These methods are exclusively used to examine the "surface" or the relationship between the response and the factors affecting the response.

Regression models are used for the analysis of the response. The RSM is used to determine the settings for the important factors that result in the optimum value of the response. Select the operation conditions and its limits that affect the performance parameter.

A second-order model (Eq. (17)) is generally used to approximate the response once it is realized that the experiment is close to the optimum response region. It is possible that a number of responses may have to be optimized at the same time.

$$y = \beta_0 + \beta_1 x_1 + \beta_2 x_2 + \cdots + \beta_k x_k + \beta_{11} x_1^2 + \beta_{22} x_2^2 + \cdots + \beta_{kk} x_k^2 + \beta_{12} x_1 x_2 + \cdots + \beta_{k-1,k} x_{k-1} x_k + \varepsilon \quad (17)$$

In this context, time, temperature and current are the operating conditions or input parameters and CTR is the performance parameter. In order to find the relation between these parameters, regression coefficients of each 1^{st}- and 2^{nd}-order constants are calculated and analysis of variance with linear, square and interaction are calculated. The constants in the above equation were found out by the above calculations.

6. Experimental Results

Design of Experiments: As discussed in Sec. 5, the experimental results of two-stage DOE are tabulated as in Table 2. In order to achieve the effect of individual parameter stress levels on CTR, a response table is constructed using results from Table 2. This Response table provides information on the variation of input parameters that depicts the performance of output parameter CTR as in Table 3.[1]

From Table 3, as both current and temperature increases, the performance of CTR degrades considerably as depicted in Fig. 4 which indeed plotted on the values of response table.

From this analysis, we can be able to represent the effect of variation of input parameters on the output parameter. The main motto of these experiments is to find out the input parameter stress levels which degrades the output parameter and given as an input to Accelerated testing. In this case, current of 90 mA and temperature of 90°C are selected.

Accelerated Testing: The input from DOE is fed to Accelerated testing with 20 samples and tested for 0 h, 150 h, 200 h, 300 h, 400 h and 500 h and results of CTR degradation is plotted as in Fig. 5. As time increases with input stress parameters, the CTR is affected with considerable degradation.

From the Fig. 5, it was concluded that the effective stress parameters for the degradation of CTR of optocouplers are temperature, current and accelerated over time.

Analysis of data and degradation model:

Calculation of 'b' in model:
To find b: at $t = 150$ h, $D(150) = 0.05$,
$I_{\mathrm{m}} = I_{\mathrm{o}} = 0.5129$ A,
$I_{\mathrm{s}} = I_{\mathrm{i}} = 90\,\mathrm{mA} = 0.09$ A,
$C = 80$: $\gamma(0) = 10^{-12}$.

Table 2. Design of experiments.

Run	I (mA)	T(°C)	S1	S2	S3	S4	S5	Sum	Avg (%)	MSD	S/N	COV
DOE - Stage 1												
1	1	30	37.1	34.6	35.94	34.1	33.8	175.54	35.108	0.00081	30.8923	2.32E-05
2	1	50	33.2	28	29.1	27.3	27.6	145.2	29.04	0.0012	26.1951	4.38E-05
3	5	30	12.1	11.5	11.85	11.1	11.2	57.75	11.55	0.00752	21.2377	0.00065
4	5	50	11.5	10.1	10.5	10	9.8	51.9	10.38	0.00937	20.2829	0.0009
5	10	30	9.1	8.58	8.59	8.6	8.6	43.47	8.694	0.01325	18.7776	0.00167
DOE - Stage 2												
6	50	30	6.5	6.2	6.3	6.13	6.08	31.21	6.242	0.02571	15.8992	0.00412
7	50	50	6.5	6.15	6.19	5.9	5.82	30.56	6.112	0.02689	15.7039	0.0044
8	50	90	6.28	6.2	6.18	6.02	5.94	30.62	6.124	0.0267	15.7352	0.00436
9	90	30	6.45	6.1	6.07	5.78	5.9	30.3	6.06	0.02734	15.6316	0.00451
10	90	90	6.2	5.96	5.92	5.97	5.95	30	6	0.027801	15.55942	0.004824

Table 3. Response table of CTR.

Factor	Levels	Σ of Y	n	Σ of Yb	MSD	S/nb
A:I	1	64.148	2	32.074	0.0008831	30.539901
	5	21.93	2	10.965	0.00480209	23.185698
	10	8.44	1	8.44	0.00344398	24.629391
	50	18.478	3	6.1593	0.01790355	17.470608
	90	11.982	2	5.991	0.02787239	15.548258
B:T	30	67.4	5	13.48	0.01288332	18.899721
	50	45.532	3	15.177	0.00155819	28.073785
	90	12.046	2	6.023	0.0275893	15.592593

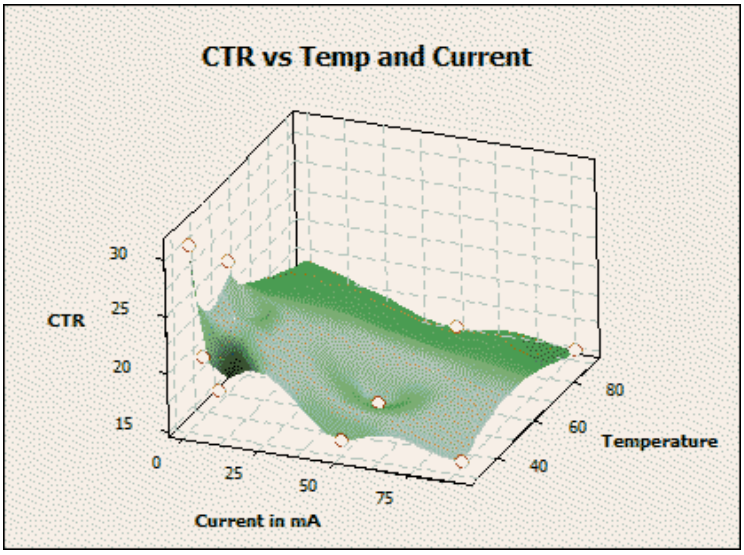

Fig. 4. Plotted in Response Table.

Substituting the above values in the below equation.

$$\frac{\Delta \mathrm{CTR}(t, I_\mathrm{s}, I_\mathrm{m})}{\mathrm{CTR}} = 1 - \frac{\left(1 + \frac{b.I_\mathrm{s}.t}{\gamma(0)}\right)^2}{4.C^2.I_\mathrm{m}} \left\{ \sqrt{1 + \frac{4.C.\sqrt{I_\mathrm{m}}(C.\sqrt{I_\mathrm{m}} + 1)}{\left(1 + \frac{b.I_\mathrm{s}.t}{\gamma(0)}\right)^2}} - 1 \right\}^2 \quad (18)$$

The value of b is found out to be 28×10^{-14}.

Failure Time: The time tf at which $D(\mathrm{tf}) = 0.5$,
$b = 28 \times 10^{-14}$,
$I_s = I_i = 10\,\mathrm{mA} = 0.01$ A,
$I_m = I_o$ at 30°C $= 0.08695$ A,
$C = 80$: $\gamma(0) = 10^{-12}$.

Substituting the above values in the degradation equation, the failure time is 6110 h.

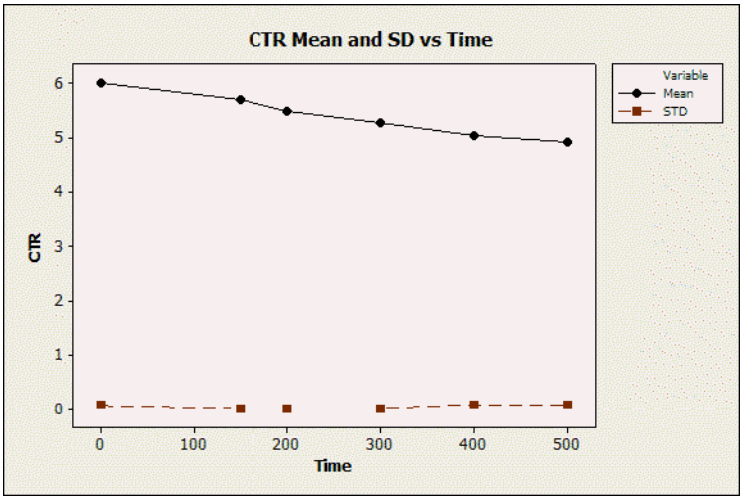

Fig. 5. Variation of CTR with time.

From this analysis, the failure time can be calculated for any of the input currents. As from the above equation, the temperature parameter is influenced as an indirect phenomenon from the modeling discussed in Sec. 5. The below analysis shows the effect of various device parameters like T_f, b, $\gamma(0)$ and C from the experimental data.

(a) T_f *versus* $D(t)$:
Failure criteria of the optocoupler depend on the selection of degradation ratio. So the variation of time to failure with respect to $D(t)$ is analyzed. Reframing the above model equation, T_f in terms of D is

$$T_{\mathrm{f}} = \frac{\gamma(0)}{b.I_{\mathrm{s}}}\left[\frac{CD(t)\sqrt{I_{\mathrm{m}}}+1}{\sqrt{(1-D(t))}}-1\right], \tag{19}$$

where $\gamma(0) = 10^{-12}$:

$b = 28 \times 10^{-14}$ at 150 h,
$C = 80$,
$I_s = 0.01$ A,
$I_m = 0.08695$ A at 30°C,
$D(t)$ = Degradation Ratio
$= [\mathrm{CTR})0 - \mathrm{CTR})t]/\mathrm{CTR})0.$

Similarly the above data is reproduced with input current to 8 mA.

$I_{\mathrm{s}} = 0.008$ A,
$I_{\mathrm{m}} = 0.06956$ A at 30°C.

Table 4. Accelerated testing results.

S	CTR (I_m/I_s) in %					
t.H	0	150	200	300	400	500
1	6.1023	5.7289	5.4963	5.2566	5.0111	5.016
2	5.9887	5.6122	5.5073	5.2699	5.0285	4.856
3	6.05	5.5167	5.5129	5.256	5.0367	4.9125
4	6.105	5.7833	5.4813	5.2713	5.0399	4.903
5	5.995	5.7622	5.5101	5.2746	5.0456	4.907
6	6.01	5.7833	5.5012	5.2733	5.0313	5
7	5.98	5.7656	5.4986	5.2666	5.0455	4.9133
8	6.05	5.6989	5.4999	5.262	5.0396	4.9033
9	5.9633	5.7311	5.5012	5.25	5.0456	4.9178
10	5.95	5.7333	5.4851	5.2587	5.0455	4.85
11	6.02	5.7011	5.4857	5.2643	5.0389	4.879
12	6.0511	5.7511	5.4811	5.2577	5.0278	4.9133
13	5.9777	5.6733	5.4965	5.2778	5.0395	4.91
14	5.9877	5.6578	5.5123	5.2633	5.05	4.88
15	6.025	5.7611	5.4986	5.2514	5.04	5.1
16	6.00	5.6944	5.4767	5.26	5.00	5.0125
17	5.9633	5.7044	5.4787	5.2514	5.045	4.6999
18	5.981	5.7478	5.4899	5.2547	5.0489	4.81
19	6.11	5.7411	5.49	5.27	5.0512	4.9102
20	5.95	5.6689	5.5015	5.2515	5.0365	4.8799
Avg	6.0131	5.6989	5.4953	5.2621	5.0373	4.9087
ST	0.0504	0.0698	0.011	0.0086	0.0128	0.0826

From the data selected from the above parameters, time to failure for different degradation ration per each current is calculated from the above equation and tabulated as in Table 5.

From the Fig. 6, time to failure depends on the selection of input current parameter and degradation ratio. This data is further sent to designer for feedback for particular selection of parameters which results in time to failure of the optocoupler.

(b) *b versus t and T_f versus t — D@0.5*

In the calculation of '*b*', the time sample is taken as 150 h. Here, this analysis is performed by calculating '*b*' at different samples and accordingly time to failure is calculated at $D(t) = 0.5$.

Using accelerated t values, calculate b value taking I_{m} and D values at t.

$$b = \frac{\gamma(0)}{t.I_{\mathrm{s}}}\left[\frac{CD(t)\sqrt{I_{\mathrm{m}}}+1}{\sqrt{(1-D(t))}}-1\right] \tag{20}$$

After obtaining value of b from the above equation, calculate Time to failure at $D(t) = 0.5$ from the equation provided in section (a), at use conditions are calculated using Table 6 and plotted as in Fig. 7.

From this analysis, device parameter is not constant as provided in the model and interim it depends on the accelerated time. Figure 7 depicts that this device parameter b degrades over time in consistent with the performance of CTR.

Table 5. Time to failure versus $D(t)$ for input currents.

$D(t)$ (mA)	0.1	0.15	0.2	0.25	0.3	0.35	0.4	0.45	0.5	0.55	0.6	0.65	0.7	0.75	0.8	0.85	0.9	0.95
12	826.7	1276	1755	2266	2815	3410	4058	4770	5610	6451	7469	8655	10074	11833	14125	17349	22531	33706
10	900	1401	1926	2488	3092	3746	4271	4791	6107	7083	8200	9503	11602	12994	15512	19055	24750	37033
8	1017	1570	2159	2788	3464	4196	4994	5871	6845	7941	9195	10657	12406	14575	17401	21378	27773	41568

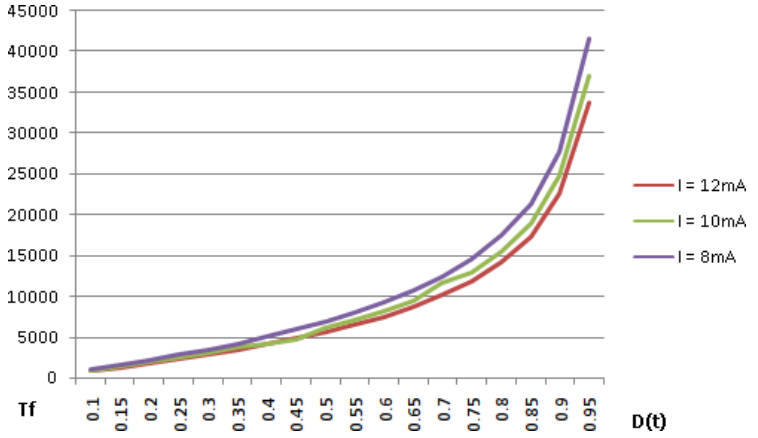

Fig. 6. Input Current D versus Time to Failure.

Table 6. b versus t and T_f versus t.

Time, t	b (in 10^{-14})	T_f (h)
150	28	6110
200	27.7	6174
300	27	6335
400	26.7	6405
500	24	7126

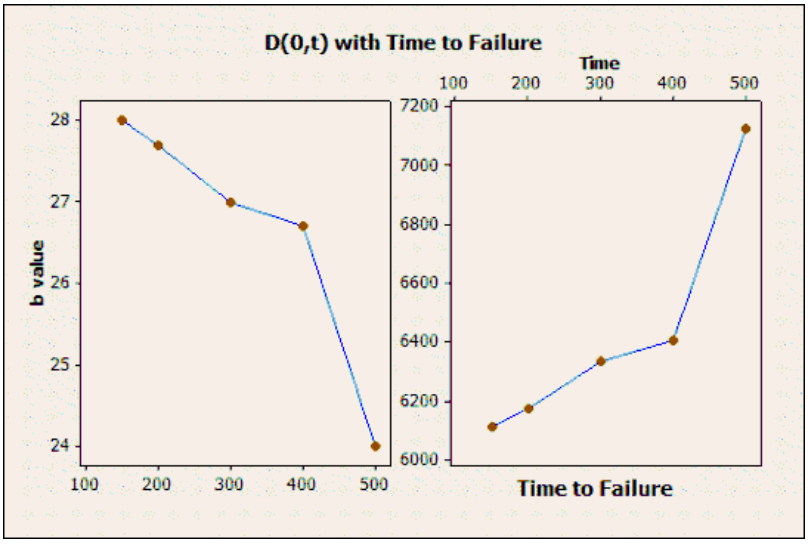

Fig. 7. b versus t and T_f versus t.

(c) *$\gamma(0)$ versus t and T_f versus t — D@0.5*

Similarly, as above, $\gamma(0)$ is calculated to know the variation at sample intervals. Using accelerated t values, calculate $\gamma(0)$ value taking I_{m} and D values at t.

$$\gamma(0) = t.I_{\mathrm{s}}.b.\left[\frac{CD(t)\sqrt{I_{\mathrm{m}}}+1}{\sqrt{(1-D(t))}}-1\right]^{-1}. \tag{21}$$

After calculating $\gamma(0)$ value from the above equation, calculate time to failure at $D(t) = 0.5$ from the equation in section (a) under use conditions and is tabulated as in Table 7 and plotted results in Fig. 8.

From this analysis, value of device parameter $\gamma(0)$ also degrades over time but it has disturbance at the value of 150 h. The reason for this implication was explained in Ref. 2 which is due to the fact that b is not really constant and has nonlinear behavior during the first 200 h. Thus, the model does not take into account the early ageing time.

(d) *C versus t and T_f versus t — D@0.5*

Table 7. $\gamma(0)$ versus t and T_f versus t — D@0.5.

Time, t	$\gamma(0)$ in 10^{-12}	T_f
150	1.27	7753.755
200	1.0099	6165.924
300	1.0358	6324.371
400	1.05844	6462.082
500	1.16686	7123.985

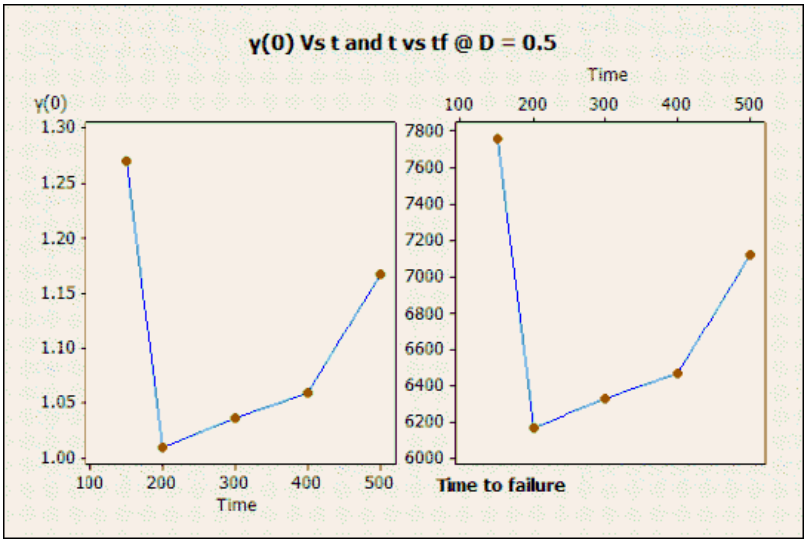

Fig. 8. $\gamma(0)$ versus t and T_f versus t — D@0.5.

Similarly, as above, C is calculated to know the variation at sample intervals. Using accelerated t values, calculate C value taking I_{m} and D values at t.

$$C = \frac{1}{D(t)\sqrt{I_{\mathrm{m}}}} \left(\sqrt{(1 - D(t))}. \left(1 + \frac{t.I_{\mathrm{s}}.b}{\gamma(0)} \right) - 1 \right). \tag{22}$$

After calculating $\gamma(0)$ value from the above equation, calculate time to failure at $D(t) = 0.5$ from the equation in section (a) under use conditions and is tabulated as in Table 7 and plotted results in Fig. 8.

From this analysis, value of device parameter $\gamma(0)$ degrades over time but it has disturbance also at the value of 150 h. Similarly in the above case for the operation of below 200 h, the value of C is not really constant and experiences nonlinear behavior. So this model is not applicable for below 200 h of operation.

Response Surface Method – Minitab: There are various softwares available for performing response surface method and one of them is Minitab. A particular data set is given as input to it as provided in Table 9, it calculates regression and ANOVA parameters in order to find the coefficients.

Table 8. C versus t and T_f versus t — D@0.5.

Time , t	C	T_f
150	101.7918	7728.03
200	80.80207	6164.99
300	82.89798	6321.07
400	84.72084	6456.81
500	93.48056	7109.12

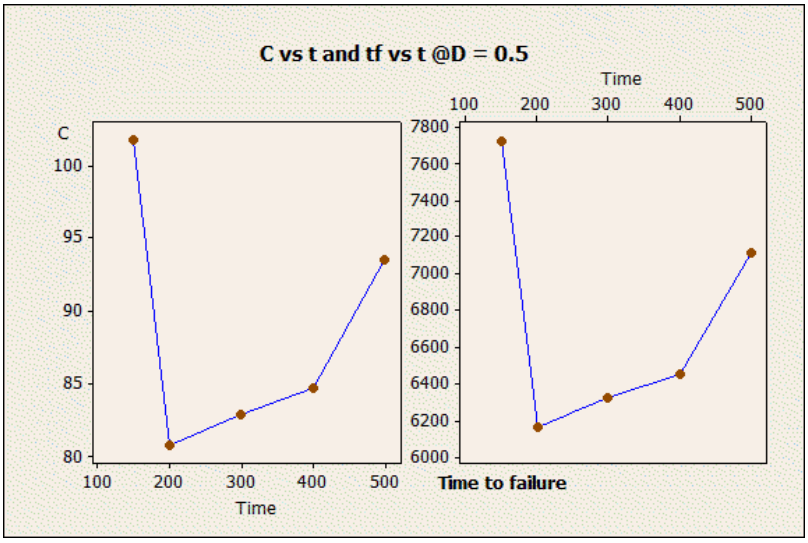

Fig. 9. C versus t and T_f versus t — D@0.5.

Table 9. Test data for RSM.

Step	Time	Current	Temp	CTR
1	0	1	30	35.108
2	0	5	50	10.38
3	0	10	30	8.44
4	0	50	50	6.112
5	0	90	30	6.06
6	0	1	50	28.4
7	0	5	30	11.55
8	0	50	30	6.242
9	0	50	90	6.124
10	0	90	90	5.922
11	150	90	90	5.698889
12	200	90	90	5.495252
13	300	90	90	5.262064
14	400	90	90	5.037347
15	500	90	90	4.908688

Response Surface Regression: (*Results from Minitab*)

C13 versus C10, C11, C12
C10 = Time,
C11 = Current,
C12 = Temperature,
C13 = CTR.

The following terms cannot be estimated, and were removed because the data has null values.

C10*C11,
C10*C12.

The analysis was done using coded units.

Estimated Regression Coefficients for C13

Term	Coef	SE Coef	T	P
Constant	3.1589	11.156	0.283	0.785
C10	−0.8459	4.933	−0.171	0.869
C11	−8.2490	5.945	−1.388	0.208
C12	0.9052	4.814	0.188	0.856
C10*C10	0.4427	7.835	0.057	0.957
C11*C11	9.7269	6.553	1.484	0.181
C12*C12	0.8680	8.029	0.108	0.917
C11*C12	−1.0621	6.837	−0.155	0.881

Each of the estimates (coefficients, indicated with Coef) has a standard error — this is a measure of how variable the estimate is likely to be. To gain the 95% confidence intervals of the coefficient, we multiply the standard error by 1.96, and add and subtract this from the coefficient. The standard error of a coefficient (SE Coef) is the square root of the corresponding diagonal element of the covariance

matrix of the coefficient estimates. The variances are the diagonal elements of the X'X inverse matrix times the mean square error (MSE). T-value (T) computed from the data for testing the hypothesis that the corresponding population coefficient is 0. The p-values for the test that the population value is 0 are given in the P column. Large t-values go with small p-values and suggest a term contributes to the model. T is not very useful on its own, but it does give us P that is the probability of the occurrence of result, if the real value in the population is zero. Each term is contributing the overall effect as P value is higher for C10*C10 and C12*C12.

$S = 8.00050$ PRESS $= 2208.87$,
R-Sq $= 61.45\%$, R-Sq(pred) $= 0.00\%$, R-Sq(adj) $= 22.89\%$.

The above results show stability and how well is the prediction of parameters. S is the square-root of MSE and PRESS statistic in the original units of the response when a power transformation of the response is applied in a linear regression. R-Sq evaluates how closely the data fall next to the fitted line. Here prediction R-Sq is 0% because of the missing null values exists in time parameter. So R-Sq is adjusted to 23% which is still quite low but the calculated value is 61%. Due to the assumption of null values of time, we are proceeding with analysis.

Analysis of Variance for C13

Source	DF	*SeqSS*	*AdjSS*	*AdjMS*	F	P
Regression	7	714.07	714.066	102.009	1.59	0.277
Linear	3	554.38	332.244	110.748	1.73	0.247
Square	3	158.14	142.967	47.656	0.74	0.559
Interaction	1	1.54	1.545	1.545	0.02	0.881
Residual Error	7	448.06	448.056	64.008		
Total	14	1162.12				

DF refers to the degrees of freedom for each source. The SS column gives, top to bottom, the sums of squares SSR, SSE and SST. The SSE is used (with the formula and a calculator) for the F-test for testing some subset of the independent variables. Here P-value is also significant predictor as how well the term contributes to the overall output parameter. Interaction has significant value which concludes the interaction of temperature and current has essential effect on CTR.

Unusual Observations for C13

Obs	Std	Order	C13 Fit	SE Fit	Residual	St Resid
1	1	35.108	21.324	4.808	13.784	2.16 R

R denotes an observation with a large standardized residual.

The final part of the output is some diagnostics, to help you to interpret the equation. Minitab has selected some cases it believes you might want to look at. It bases this on the residuals and the influence.

Estimated Regression Coefficients for C13 using data in uncoded units

Term	Coef
Constant	22.5408
C10	−0.00692511
C11	−0.584629

C12	−0.0493666
C10*C10	7.08293E-06 (Neglected)
C11*C11	0.00491198
C12*C12	0.000964470
C11*C12	−7.95547E-04 (Neglected)

So, from the above analysis, CTR calculated in terms of time, temperature and current is

$$\text{CTR} = 22.541 - 0.007t - 0.5846i - 0.0494T + 0.0049i^2 + 0.0009T^2 \tag{23}$$

Comparison of two models: The time to failure is calculated using the physics of failure approach by the CTR degradation model and using Response Surface Model which uses the regression.

The difference between LED degradation model and RSM model is calculated from Eqs. (19) and (23) respectively illustrated in Fig. 10 with respect to time to failure. As the above RSM model selects the linear method when compared to actual degradation model, Lindquist model provides characteristic curve which considers the nonlinear behavior of device parameters. It is interesting to note that both models have increasing failure rate with degradation rate. This analysis explains the fact that the regression mechanism from the experimental results deviates from the physics of failure model, Lindquist model and latter model is more comprehensive approach for calculating the reliability indexes.

7. Conclusion

In this paper, a detailed study, operation and modeling of an optocoupler 4N36 is selected and reliability analysis is carried out. LED ageing is responsible for the

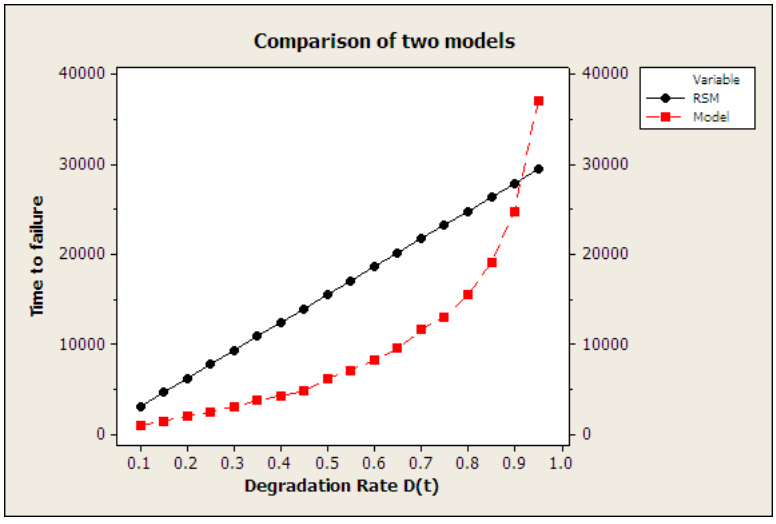

Fig. 10. Comparison of two models Lindquist and RSM.

Table 10. Comparison of two models: Lindquist and RSM.

$D(t)$	0.1	0.15	0.2	0.25	0.3	0.35	0.4	0.45	0.5	0.55	0.6	0.65	0.7	0.75	0.8	0.85	0.9	0.95
RSM	3096	4644	6192	7740	9288	10836	12384	13932	15480	17028	18576	20124	21672	23220	24768	26316	27864	29412
Model	900	1401	1926	2488	3092	3746	4271	4791	6107	7083	8200	9503	11602	12994	15512	19055	24750	37033

degradation of CTR of optocoupler and mainly due to increase in the input current and temperature. Statistical analysis using design of experiments is implemented here for the screening of the stress parameter and also the selection of the design parameter level for increase in the CTR thus by improving the reliability. The dominant failure mechanism which affects the performance is found to be degradation of LED by input current and temperature. Analysis of model parameters are carried out and their variation to the input stress parameters are studied. RSM model is also designed from the input data and verified with the Lindquist model.

References

1. L. W. Condra, *Reliability Improvement with Design of Experiments*, 2nd edn. (Marcel Dekker, 2001).
2. J. B. H. Slama, H. Helali, A. Lahyani, K. Louati, P. Venet and G. Rojat, Study and modelling of optocouplers ageing, *J. Autom. Syst. Eng.* **2**(3) (2008) 3.
3. Vishay Semiconductors, Manufacturing and reliability of optocouplers (2006).
4. I. Bajenesco, Ageing problem of optocouplers (IEEE, 1944).
5. P. F. Lindquist, A New model for light output degradation of direct band gap emitters, HP (1980).
6. R. Mangeret, L. Bonara *et al.*, Radiation characterization and test methodology study of optocouplers devices for space applications, *6th European Conf. Radiation and Its Effects on Components and Systems* (2002), pp. 166–171.
7. N. Bradley, Response surface methodology, thesis, Indiana University (2007).

About the Authors

Adithya Thaduri did his M.Tech in Reliability Engineering from IIT Bombay. He has obtained his B.E. from Electronics and Instrumentation Engineering from Bapatla Engineering College. He has widely studied electronic reliability at the device and component levels. His area of research is on the reliability prediction mechanism using physics of failure approach. His work is for finding out failure mechanisms and modes occurring at device level and performs failure analysis using sophisticated instruments for root cause and providing reliability growth techniques. He is currently pursuing research at IIT Bombay and also working on Ph.D. topic at Lulea University of Technology, Sweden.

A. K. Verma received B.Tech (Hons) and Ph.D. (Engg.) degrees from IIT Kharagpur. He has been with IIT Bombay as a faculty since 1988. He is a Professor in the Department of Electrical Engineering at IIT Bombay. He has over 225 research papers to his credit and has supervised 31 Ph.D. thesis and 92 Masters Thesis. He is the Editor in Chief of the International Journal of Systems Assurance and Engineering Management. He has been a guest editor of a dozen special issues of various international journals. He is a senior member of IEEE and life fellow of IETE. His research interests in reliability engineering include interdisciplinary applications in software engineering, computing, maintenance, and power systems.

Gopika Vinod, a graduate of 37th batch of BARC Training School, joined Reactor Safety Division, BARC in 1994. She has made significant contributions in the area of Probabilistic Safety Assessment (PSA). She has actively participated in the PSA Studies of AHWR and research reactors, Fire PSA, Risk Informed In-Service Inspection methods for piping systems in DAE facilities and in the development of Risk Monitor. She has conducted extensive research on applicability of Risk Informed In-Service Inspection methods which have resulted in formulating a complete framework. She has successfully translated the research methods into the application framework. The most important contributions are the introduction of a new importance measure, incorporating the effects of In-service inspection through markov model and using genetic algorithm for optimizing inspection. She could later extend her research for chalking out the RI-ISI program me for nuclear power plants as well as in heavy water plants. She has co-authored a standard for applying the risk-based inspection and maintenance procedures, for European industry.

M. G. Rajesh is working at Electronics division at Bhabha Atomic Research Centre, Bombay, India for eight years. His research includes the selection and design of electronic parts which are used in the signal conditioning unit of nuclear reactor. He analyzes the reason for failure of components and accordingly design the circuits for effective performance.

Uday Kumar obtained his B.Tech from India in the year 1979. After working for six years in Indian mining industries, he joined the postgraduate program of Lulea University of Technology, Lulea, Sweden and obtained a Ph.D. degree in field of Reliability and Maintenance in 1990. Afterwards, he worked as a Senior Lecturer and Associate Professor at Lulea University during 1990–1996. In 1997, he was appointed as a Professor of Mechanical Engineering (Maintenance) at University of Stavanger, Stavanger, Norway. Presently, he is Professor of Operation and Maintenance Engineering at Lulea University of Technology, Lulea, Sweden. His research interests are equipment maintenance, equipment selection, reliability and maintainability analysis, System analysis, etc. He has published more than 170 papers in International Journals and Conference Proceedings.

Paper II

P2

Reliability prediction of semiconductor devices using modified physics-of-failure approach

Thaduri, A., Verma, A.K., Vinod, G., Rajesh, M.G., Kumar, U. (2013), "Reliability prediction of semiconductor devices using modified physics-of-failure approach", *International Journal of Systems Assurance Engineering and Management*, 4(1), pp. 33-47.

Int J Syst Assur Eng Manag (Jan-Mar 2013) 4(1):33–47
DOI 10.1007/s13198-013-0146-9

ORIGINAL ARTICLE

Reliability prediction of semiconductor devices using modified physics of failure approach

Adithya Thaduri · Ajit Kumar Verma · V. Gopika · Rajesh Gopinath · Uday Kumar

Received: 17 July 2012 / Revised: 12 November 2012 / Published online: 14 February 2013

Abstract Traditional approaches like MIL-HDBK, Telcordia, and PRISM etc. have limitation in accurately predicting the reliability due to advancement in technology, process, materials etc. As predicting the reliability is the major concern in the field of electronics, physics of failure approach gained considerable importance as it involves investigating the root-cause which further helps in reliability growth by redesigning the structure, changing the parameters at manufacturer level and modifying the items at circuit level. On the other hand, probability and statistics methods provide quantitative data with reliability indices from testing by experimentation and by simulations. In this paper, qualitative data from PoF approach and quantitative data from the statistical analysis is combined to form a modified physics of failure approach. This methodology overcomes some of the challenges faced by PoF approach as it involves detailed analysis of stress factors, data modeling and prediction. A decision support system is added to this approach to choose the best option from different failure data models, failure mechanisms, failure criteria and other factors.

Keywords Physics of failure · Reliability prediction · Time to failure · Failure mechanism · Failure mode · Failure modeling

A. Thaduri (✉)
Department of Electrical Engineering, IIT Bombay, Powai, Mumbai, India
e-mail: adithya.thaduri@gmail.com

A. Thaduri · U. Kumar
Division of Operation and Maintenance,
Lulea University of Technology, Lulea, Sweden
e-mail: Uday.Kumar@ltu.se

A. K. Verma
Stord/Haugesund University College, Haugesund, Norway
e-mail: akvmanas@gmail.com

V. Gopika · R. Gopinath
RSD, BARC, Trombay, Bombay, India
e-mail: vgopika@barc.gov.in

R. Gopinath
e-mail: rajeshgopin@gmail.com

1 Introduction

The basic idea of the project is to predict the reliability of some specific components, which are used in the nuclear industry by methods called Reliability Prediction and Modeling Techniques. Reliability modeling and prediction is a relatively new discipline. Only since World War II reliability has become subject of study due to the relatively complex electronic equipment used during the war and the high failure rates observed. Reliability modeling and prediction is a methodology for estimating an item's ability to meet specified reliability requirements. A Mission Reliability prediction estimates the probability that an item will perform its required functions during the mission. A basic Reliability prediction estimates the demand for maintenance and logistic support caused by an item's unreliability. Reliability models and predictions are not used as a basis for determining the attainment of reliability requirements. Attainment of these requirements is based on representative test results such as those obtained by using tests plans from MIL-HDBK-781, Telcordia, PRISM, Physics of Failure etc. Reliability modeling and prediction should be initiated early in the configuration definition stage to aid in the evaluation of the design and to provide a basis for item reliability allocation and establishing corrective action

priorities. Reliability models and predictions are updated when there is a significant change in the item design, availability of design details, environmental requirements, stress data, failure rate data, or service use profile.

1.1 Reliability prediction

There have been two eras of Reliability Prediction. Until the 1980s, the exponential, or constant failure rate (CFR), had been the only model used for describing the useful life of electronic components. It was common to the six reliability prediction procedures that and was the foundation of the military handbook for reliability prediction of electronic equipments (MIL-HDBK-338B). Although the CFR model was used without physical justification, it is not difficult to reconstruct the rationale for the use of the CFR model, which mathematically describes the failure distribution of systems wherein the failures are due to completely random or chance events. Throughout that period, electronic equipment complexity began to increase significantly. Similarly, the earlier devices were fragile and had several intrinsic failure mechanisms that combined to result in a constant failure rate.

1.1.1 MIL-HDBK-217

During the 1980s and early 1990s, with the introduction of integrated circuits (ICs), more and more evidence was gathered suggesting that the CFR model was no longer applicable. Phenomena such as infant mortality and device wear out dominated failures; these failures could not be described using the CFR model. They further recommended that the exponential distribution should not be applied to every type of component and system without due awareness. The methods to find failure rate are (MIL-HDBK-338B; MIL-HDBK-217F):

1. The constant-failure-rate: The constant-failure-rate reliability model is used by most of the empirical-electronic reliability prediction approaches.
2. π factors: Almost all of the traditional prediction methods have a base failure rate modified by several π factors.
3. Two basic methods for performing reliability prediction based on the data observation include the parts count and the parts stress analysis. The parts count reliability prediction method is used for the early design phases, when not enough data is available but the numbers of component parts are known.

$$\lambda_S = \sum_{i=1}^{n} N_i(\lambda_g \pi_Q)_i \tag{1}$$

The inconsistency among different traditional prediction methods is the main problem facing designers.

1.1.2 Physics of failure approach

Attempts, which began during the 1970s, to include physics-of-failure into military handbooks were not very successful. Although the need for a physics-of-failure methodology was realized in the 1970s, a physics-of-failure-like model for small-scale CMOS technology was not introduced until 1989. Even so, this approach, as an independent methodology, only started to attract attention during the 1990s in the form of recommendations to update the military handbook (Pecht and Kang 1988). The recommendations addressed the weaknesses of traditional approaches (White 2008):

- the misleading use of constant physics-of-failure,
- the use of the Arrhenius temperature model,
- the modeling of wear out mechanisms, and
- modeling mechanisms such as brittle die fracture.

Since then, the physics-of-failure approach has dominated reliability modeling. In this approach, the root cause of an individual failure mechanism is studied and corrected to achieve some determined lifetime. Since wear out mechanisms are better understood, the goal of reliability engineers has been to design dominant mechanisms out of the useful life of the components by applying strict rules for every design feature. The theoretical result of this approach is, of course, that the expected wears out failures are unlikely to occur during the normal service life of microelectronic devices. Nonetheless, failures do occur in the field and reliability prediction has had to accommodate this new theoretical approach to the virtual elimination of any one failure mechanism limiting the useful life of an electronic device. It depends on process, technology, manufacturer location, post processing techniques etc.

Physics-of-failure is an approach that tries to reveal and model the root cause processes of device failures. This branch of reliability combines knowledge about the device with the statistical aspects of failure occurrences. The fact that physics-of-failure is not widely used by engineers shows that it was not successful in achieving its goals. It seems that the key element of this lack of success is the complexity of modeling the MTTF of devices based on the underlying root causes. Moreover, the physics of device failures has not yet been clearly formulated. Scientists are still working on formulating the reasons behind each failure.

Moreover reliability aspects and prediction is critical to these components and this paper provides advanced physics of failure methodology for finding failure characteristics and reliability indices. The following Table 1 demonstrates various traditional prediction methods the differences between the values of time to failures of DC–DC converter constraints the ambiguity and risk in selecting appropriate figure.

There were significant advantages to this methodology like reliability design, condition monitoring, improvement in LCC and component selection to the application involved. This method requires sophisticated tools for failure analysis and advanced tools for analyzing the simulated data. Still, this methodology also has challenges like insufficient data from the manufacturer, needs expert judgment and also time taking process (MIL-HDBK-217F; White 2008; Panasonic Corporation 2000; Renesas Technology Corp 2008).

On the other hand, statistical methods were widely available in order to find out the reliability indices from the test data. This method was also considered as black box testing which concentrate on available data and proper model was selected depends on the application. There were possibilities to analyze the data and generated model to extract enormous amount of information to characterize the performance parameters. Some of them include design of experiments, accelerated testing, regression analysis, etc. Even, there were several tools available for model selection, mathematical formulation and model analysis. This methodology has some advantages like time consuming, no need for manufacturer data and parameter analysis.

Therefore, applying complex statistical tools to vague scientific principles adds several parameters to the equations, leading to a higher level of complexity. In contrast, a scientific model should give a simple explanation for the instances and then generalize the model. Until now, the physics-of-failure approach was not able to make accurate predictions or replace traditional approaches.

The electronic system reliability approach is a method built upon the advantages of both traditional and physics-of-failure methodologies; this approach combines the device physics-of-failure mechanisms with the constant failure rate model and applies them to the electronic system, which provides both a physical explanation for the electronic system failures, and a simplified statistical tool for reliability prediction. However, these approaches can still (White 2008):

- Use traditional prediction tools in specific field studies to obtain an approximate numerosity.
- Update the previous models based on statistical methods (like the Bayesian approach) and try to calculate the uncertainty growth of the electronic systems.
- Unify electronic-device failure mechanisms.
- Try to apply the new scientific models to electronic systems.

The inclusion of multidisciplinary science and engineering approaches was very effective in solving of real life problems and our modified approach was combination of both physics of failure (deterministic) and statistical (probabilistic) approaches in Fig. 1. This advancement methodology first starts with the proper understanding of basic failure physics of the component and process the physics of failure methodology. This knowledge was fed to the statistical approach to further refining of data for accurate models. Finally, we get three faces of models; history and literature, white box and black box models and these were sent to decision support system. The other inputs to this system were life cycle costs and regulatory requirements.

2 Failure mechanisms at wafer level

Advanced integrated circuits (ICs) are very complex, both in terms of their design and in their usage of many dissimilar materials (semiconductors, insulators, metals, plastic molding compounds, etc.). For cost reductions per device and improved performance, scaling of device geometries has

Table 1 Comparisons of different reliability prediction models (MTBF Report 2005)

Reliability prediction model	Company	1 Watt DC–DC converter				100 W AC-DC PSU	
		25 °C		85 °C		40 °C	
		Hours	Years	Hours	Years	Hours	Years
MIL-HDBK-217F EXAR	A	31,596,574	3,606.9			686,771	78.4
MIL-HDBK-217F Notice2	B	832,000	95	86,000	9.8		
MIL-HDBK-217F Notice2	C	156,000	17.8	124,000	14.2		
Telcordia SR332 Parts count	D	89,380,000	10,203.2	29,260,000	3,340.2		
Telcordia SR332 Parts stress	D	104,200,000	11,895	57,160,000	6,525.1		
Siemens SN29500	A	80,978,217	9,244.1			1,554,055	177.4
HRD5 Parts Stress	B	2,465,000	281.1	849,000	96.9		
HRD4 Parts count	B	1,132,000	129.2	1,132,000	129.2		
MIL-HDBK-217F EXAR	A	31,596,574	3,606.9			686,771	78.4
Telcordia SR332 Parts count	E					1,418,000	16.2

played a critically important role in the success of semiconductors. This scaling—where device geometries are generally reduced by 0.7 × for each new technology node and tend to conform to Moore's Law—has caused the electric fields in the materials to rise (bringing the materials ever closer to their breakdown strength) and current densities in the metallization to rise causing electromigration (EM) concerns. The higher electric fields can accelerate reliability issues such as: time-dependent dielectric breakdown (TDDB), hot-carrier injection (HCI), and negative-bias temperature instability (NBTI). This failure mechanisms behave differently depends on the technology such as CMOS, BJT and other semiconductors, process, manufacturer etc. In addition, the use of dissimilar materials in a chip and in the assembly process produces a number of thermal expansion mismatches which can drive large thermomechanical stresses. These thermomechanical stresses can result in failure mechanisms such as stress migration (SM), creep, fatigue, cracking, delaminating interfaces, etc. Several of them are described below (White 2008; Ohring 1998; Panasonic Corporation 2000; Renesas Technology Corp 2008; JEDEC Publication 2008; MOSIS Technical notes; Semiconductor Device Reliability Failure Models 2000; Semiconductor Reliability Handbook 2011; SONY—Sony semiconductor quality and reliability handbook 2000; Joseph Bernstein et al. 2006; Foucher et al. 2002; Shahrzad Salemi et al. 2008; MTBF Report 2005).

The following failure mechanisms have possibility to appear at wafer level in device including all technologies. Certainty of occurrence of these failure mechanisms on particular device depends on stress factors, process, technology and application.

Failure Mechanisms:

1. Electro Migration (EM)
2. Temperature Dependence Die-electric Breakdown (TDDB)
3. Hot Carrier Injection (HCI)
4. Negative Bias Temperature Instability (Slow Trap)
5. Stress Migration
6. Soft Error (Radiation)

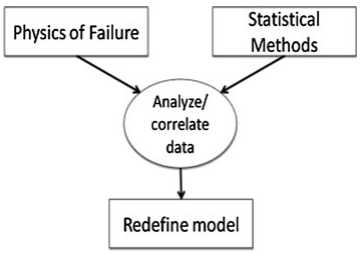

Fig. 1 Short idea of Modified approach

7. Corrosions
8. Surface Inversion
9. Reliability Problem of non-volatile memory
10. Thermal Fatigue (Cycling)

Scaling of devices is big advantage over the past technologies and apparently they found so many reliability issues which are so random at 45 nm technology. Out of the above list, there is a possibility that these failure mechanisms occurred at wafer level.

2.1 Electro migration (EM)

Failure occurs mainly due to the blocking (or voids) of interconnects through transport momentum at conductor-metal interface forming open-circuit failure mode. Also, atoms of one conductor pile up to another conductor cause short-circuit (hillock Failure or whisker failure). This mechanism happens predominantly at higher current density levels ($>10^5$ A/cm^2) and at higher temperatures. Activation energy, Ea has variable effect on Electro migration and it ranges between 0.5 and 0.8 eV. The following forms of EM are

i. Grain boundary diffusion on Al wires and surface diffusion in Cu wires.
ii. Thermal Effects: high power collide scattering joule heating.

Aluminum and Copper are the mostly used metals for contacts. Aluminum (Ea = 0.6 ± 0.1 eV) has good conductivity, good ohmic contacts and adherence to substrate where pure Copper is more robust (Jcu = 5JAl) to currents. Activation energy and mobility increases by adding 1 % palladium to metals. Electromigration causes due to increase in current density and mainly occurs in smaller grain boundaries. For a Bamboo structure; if, width is proportional to average grain size then the effect of electromigration decreases. For large magnitude currents, slotted wires are used to meet power requirements. Blech Length, the lower limit of length of interconnects at which electromigration is allowed, is used as design parameter. Solder joints made up of occurs at lower current densities. Electromigration is characterized using the time to failure model (Joseph Bernstein et al. 2006; Foucher et al. 2002), given below: Black's Equation,

$$MTTF = A(J^{-n})e^{\left(\frac{E_g}{KT}\right)} \quad (2)$$

Where Ea = 0.5–0.8 eV, J is Current Density, K is Boltzman Constant, T is Temperature, $n = 2$, and A is Acceleration Factor.

The following are preventive methods for electromigration:

i. Adding 2–4 % of Cu increases resistance to EM by 50 times or adding W & Ti 0.95 eV

ii. Controlling the quality of wiring
iii. Smoothing of the process
iv. Prescribed current densities and enforcing rules on accelerated life testing

2.2 Temperature dependence die-electric breakdown (TDDB)

This mechanism occurs by continuously applying stress to Gate oxide film causing di-electric falling shorting anode and cathode (Panasonic Corporation 2000). This mechanism was also prominent while increasing/decreasing in electric field across the device. Time to failure increases with increasing electric field and temperature. But as electric field decreases, activation energy also increases which results in increase in internal stresses. For higher fields (>10 MV/cm), a mechanism called field enhanced thermal bond breakage is activated. The decrease in the activation energy also leads to electron reaction rate (Shahrzad Salemi et al. 2008).

2.2.1 E-Model

An electric field on oxide film causes injection of holes on anode side induces traps (Renesas Technology Corp 2008). Increase of traps leads to the formation of stress induced leakage current because of tunneling effect and further increase of these traps between gate and silicon substrate corresponds to increase in leakage current leads to gate oxide break down.

$$MTTF = Ax10^{-\beta \mathbf{E}} xe^{\left(\frac{Ea}{KT}\right)} \quad (3)$$

A, arbitrary scale factor, dependent upon materials and process; Eox, electric field across the dielectric in MV/cm; ß, Electric field intensity coefficient (cm/MV); K, Boltzman Constant; T, Temperature in K; Ea, $(\Delta H)_0$-a Eox; Ea, effective activation energy (eV); (ΔH)0, the enthalpy of activation for bond breakage in the absence of external E (∼2.0 eV); a, effective molecular dipole-moment for the breaking bonds which value is ∼7.2 eÅ.

2.2.2 1/E Model

This model is applicable for lower electric fields and current mechanism follows Fowler–Nordheim conduction. Electrons experience impact ionization at lower electric fields that damages the di-electric, which degrades further by accelerated field (MOSIS Technical notes). These accelerated electrons reaching anode produces hot holes which tunnel back to dielectric and this phenomena is known as hot hole injection mechanism (Semiconductor Device Reliability Failure Models 2000). 1/E Model:

$$TF = \tau_0(T)e^{\left(\frac{G(T)}{Eox}\right)} \quad (4)$$

Where τo(T), a temperature dependent prefactor, $\sim 1 \times 10^{-11}$ s; G, field acceleration parameter, ∼350 MV/cm with a weak temperature dependence; Eox, electric field across the dielectric in MV/cm.

For ultra-thin oxides, Temp is non-Arrhenius,

$$MTTF = T_{BD0}(V)e\left(\frac{a(V)}{T} + \frac{b(V)}{T^2}\right) \quad (5)$$

2.3 Hot carrier injection

2.3.1 Hot carrier injection in CMOS

Charge carriers in high electric field are accelerated by gaining energy. Some charges have acquired hot energy and capable to overcome potential between Gate and Substrate. These carriers injected to Gate (some are trapped), form a space charge region, which results in change in threshold and transconductance. Injected carriers which are not trapped are drawn as gate current and other carriers are drawn as substrate current. Hot carrier Injection generated by these four mechanisms (Semiconductor Reliability Handbook 2011):

i. Drain Avalanche Hot Carrier DAHC injection Electrons from Source lead to impact ionization because of high electric field at Drain, which generates electron–hole pairs and has sufficient higher energy injected into Gate. Vgs = ½ Vds. This is the greatest factor at normal temperatures.
ii. Channel Hot Electron CHE injection (Vgs = Vds, lucky electrons which are not energy dissipation).
iii. Secondary generated hot electron SGHE injection.
iv. Substrate hot electron SHE injection.

Hot carrier injection is prominent at lower temperatures. Thermal vibrations of the charges increase and hence collisions decreases, thus have higher probability for mean free path of electrons to absorb more energy. Higher electric field injects carriers in the substrate thus increasing the probability of occurrence. The impact provides higher secondary electrons. As voltage of the source decreases, the impact of ionization modes depends on temperature.

The degradation by HCI is given by following equation

$$\Delta P = At^n \quad (6)$$

Where P, parameter gm; Vth, isat. The following models for n-channel and p-channel describes HCI failure mechanism.

$$\text{n-channel, Eyring Model } MTTF = B(I_{sub})^{-N}e^{(Ea/KT)} \quad (7)$$

p-channel $MTTF = B(I_{gate})^{-M} e^{(Eg/KT)}$ (8)

Where Igate is gate current, Isub is substrate current, Ea is activation energy, K is boltzman constant, T is absolute temperature and M,N and B are constants.

Substrate current and voltage in p-channel substrate doubles for each 0.5 V increase in voltage between source and drain (Semiconductor Device Reliability Failure Models 2000). The acceleration factor is thus given as

$$AF = e^{(B(1/Vdd - 1/Vdd,\max))} \quad (9)$$

The effect of HCI can be reduced by moderating electric field using lightly doped drain (LDD) structure with higher resistance at Drain and further reducing source voltage.

2.3.2 *Hot carrier injection in BJT*

HCI behaves differently to BJT technology. Berkeley (Hu 1989) simulated the circuit waveforms at arbitrary time in the future considering the hot-carrier degradation of the transistors in the circuit. The key physical model is the realization of transistor parameters are the functions of Age where

$$Age = \int \frac{I_{ds}}{WH}\left(\frac{I_{sub}}{I_{ds}}\right)^{m} dt \quad (10)$$

Where W is the transistor width, W and M are the functions of the oxide field, i.e., functions of Vgd, and are determined from dc transistor stress tests.

Under emitter–base reverse bias, a small reverse current, IR, flows through the junction due to band-to-band tunneling and impact ionization. These carriers apparently generate interface traps near the junction and introduce a component of non-ideal base forward current, ΔIB, which causes the current gain to decrease. It can be shown that

$$\Delta I_B = DJ_c^a \left(\int I_R^b dt\right)^c \quad (11)$$

This mechanism is not important in ECL circuits, where the base-emitter junctions do not experience revere bias stress. It is a potential factor in BICMOS circuits.

2.4 Negative bias temperature instability (NBTI)

The failure mode in NBTI is shift in threshold voltage; Vt. Holes are trapped between Si/SiO2 interfaces degrade the performance of device and happen mostly in PMOS. Holes are thermally activated and gains sufficient energy to disassociate Si/SiO2 defects near LDD. Concentration of holes increases with temperature rise. Due to NBTI, there is predominant degradation in Idsat and transconductance gm and off current. The increase in these currents leads to increase in Vth. Critical value of electric field is 6MV/cm and temperature from 25 to 100 °C.

Silicon dangling bond on interface inactivated by Hydrogen (Renesas Technology Corp 2008), Si–H, stress (high temperature), increase in bias, holes gives to electro-thermal reaction, freeing Hydrogen atom. Silicon dangling bond becomes interface state and H diffuses in oxide film. Some diffusing Hydrogen joins with defects to form traps. Increase in interface state and charge resulting from traps in oxide for degrading Vth. Recovery can be done by removing stress bias and applying reverse bias. NBTI is predominant in circuits where DC stress is applied. Time to failure is found out using the following equation in Equation 12 (Renesas Technology Corp 2008).

$$MTTF = A10^{-\beta \mathbf{E}} e^{\left(\frac{Ea}{kT}\right)} \quad (12)$$

Where MTTF: Time to Failure, A: Constant, E: Electric field intensity (MV/cm), k: Boltzmann constant, Ea: Activation energy (eV) 1 eV, β: Electric field intensity coefficient (cm/MV) 1 to 1.5

2.5 Stress migration

Metal atoms in wiring migrate due to stress (SONY—Sony semiconductor quality and reliability handbook 2000). Increase in temperature and difference in thermal expansion between materials causes increase in further. If it is beyond critical level, metal ions with thermal capabilities diffuse through grain boundaries and defects scattered in each grain boundary migrate creating voids. There are two types of causes of stress: intrinsic stress and molding method cause distortion in crystal lattice. Thermal stress produces with difference in coefficient of thermal expansion of different materials. Stress also depends on structure. At lower temperatures, disconnection of wire happens after long-term and at higher temperature (200 °C) for short-term wherever voids exhibit heat treatment. At lower temperatures, metal atom diffusion speed increases by increase in temperature, stress by insulating film and metal wiring are smaller. At higher temperatures, decrease in heat-treatment process and adjusting heating and cooling reduces migration.

Movement of metal atoms under stress-flux divergence results in voids. In metals, there is decrease in grain boundary diffusion only when grain size is less than line width. Stress Migration baking temperature (150–200 °C) at maximum creep rate leads to higher stress, lower mobility and lower temperature. Using of refractory metal barriers or layered metallization nullify voids.

Mechanical Stress Model:

$$MTTF = A_0 \sigma^{-n} e^{(Ea/KT)} \quad (13)$$

Thermo-mechanical Stress Model: σ α (ΔT)

$$MTTF = B_0(T_0 - T)^{-n}e^{(Ea/KT)} \quad (14)$$

Where σ,constant stress load; $n = 2$–3 for ductile metals; n is usually ~5 if creep, thus T < Tm/2; T0, stress free temperature for metal and Ea = 0.5–0.6 eV for grain boundary diffusion; ~1 eV for single grain (bamboo-like) diffusion.

2.6 Soft errors (Radiation)

Semiconductor memory defects recovered by rewriting data are called soft errors (SONY—Sony semiconductor quality and reliability handbook 2000). Source voltage, ground and α rays from Uranium and Thorium in packaging leads to degradation on materials. When α rays incident on silicon, electron and hole pairs are generated. Electric field causes holes to p-well and e- cluster in n diffusion area. Cluster electron node potential to drop. As Vs decreases, charge level accumulated at node, soft errors occur more easily.

The following precautions to be taken to reduce the effect of radiation:

i. Reducing level of α rays to penetrate; coating chip surface to attenuate,
ii. Difficult to e- makes cluster at nodes; less diffusion layer area or increase in substrate density,
iii. Increasing memory node Capacitance; decrease in insulating film thickness or adding Capacitance.

2.7 Corrosions

Corrosion failures can occur when ICs are exposed to moisture and contaminants (Semiconductor Device Reliability Failure Models 2000). IC corrosion failures are usually classified as one of two broad groups: bonding pad corrosion or internal-chip corrosion. The bonding pad is a rather large piece of on-chip metallization on the order of 50 μm × 50 μm. These bonding pads, historically, have provided the metallization contact surface for eventual Au or Cu-wire ball bonding. Internal corrosion (internal to the chip, away from the bonding pads) can also occur if some weakness or damage exists in the die passivation layer which could permit moisture and contaminants (e.g., chlorides) to reach the exposed metallization. The internal corrosion can cause electrical discontinuities at localized regions of die (McPherson 2010). Corrosion can be generally described in terms of a corrosion cell.

The corrosion cell must have four key components in order for corrosion to occur: an anode (a region for the oxidation reaction to occur), a cathode (a region for the reduction reaction to occur), an electrolyte (through which the ions can diffuse), and a conductor to provide a pathway for the electron flow from the oxidation region to reduction region.

Aluminium with Copper and Silicon increases corrosion failures. Bonding pad: die passivation does not cover metallization. Internal: damage in die passivation leads to moisture to reach metal. Standards for testing are 85/85 (Temperature & Humidity), Autoclave (2 atm absolute pressure) and HAST (85 %RH, steam pressure > ambient pressure).

There are several models demonstrated here which depends on applicability.

2.7.1 Experimental reciprocal method

The time-to-failure equation for IC failure due to corrosion is

$$TF = A_0 e^{\left(\frac{b}{RH}\right)} e^{\left(\frac{Q}{K_B T}\right)} \quad (15)$$

Where A0 is a process/material dependent parameter and serves to produce a distribution of times-to-failure (Weibull or lognormal distributions), b is the reciprocal humidity dependence parameter (approximately equal ~300 %), RH is the relative humidity expressed as a 3 % and

Q is the activation energy (approximately equal to 0.3 eV for phosphoric acid induced corrosion of aluminum and generally consistent with wet corrosion.

This model was developed when phosphosilicate glass (PSG) was used for interconnect dielectric and/or passivation.

2.7.2 Power law humidity model

The time-to-failure equation for IC failure due to corrosion is

$$TF = A_0 (RH)^{-n} e^{\left(\frac{Q}{K_B T}\right)} \quad (16)$$

where n is the power-law exponent and equal to 2.7, RH = % relative humidity, and Q is the activation energy and equal to 0.7–0.8 eV for chloride-induced corrosion of aluminum.

This model was developed for chloride-induced corrosion in plastic-packaged chips. Cl-based dry etches are generally used for the aluminum-alloy metallization. If excessive amounts of chlorides are left on the die after post-etch cleanups, corrosion can occur with the addition of moisture.

2.7.3 Exponential humidity model

The time-to-failure equation for IC failure due to corrosion is

$$TF = A_0 e^{(-a.RH)} e^{\left(\frac{Q}{K_B T}\right)} \quad (17)$$

where a is humidity acceleration parameter and is equal to 0.10–0.15 (%RH) -1, RH is the % relative humidity, and Q is the activation energy and is equal to 0.7–0.8 eV for chloride-induced corrosion of aluminum in plastic packages. This corrosion model was developed when it was shown that, over a wide range of humidity (20–80 %), the surface conductivity is exponentially dependent on the humidity.

2.7.4 *Exponential humidity-voltage model*

The time-to-failure equation for IC failure due to corrosion is

$$TF = A_0 RH^{-N} f(V) e^{\left(\frac{Q}{K_B T}\right)} \tag{18}$$

Where A0, arbitrary scale factor; N, ~2.7; Ea, 0.7–0.8 eV (appropriate for aluminum corrosion with chlorides are present) and f(V) = an unknown function of applied voltage.

Originally used for Al corrosion, but applied to other failure mechanisms with different N & Ea values. From all these models, the power-law model is a widely used corrosion model in the IC industry for plastic-package chips.

2.8 Surface inversion

Mobile ions contaminate over time and accumulation causes drifts the ions at the interface (Semiconductor Device Reliability Failure Models 2000). Impure ions like sodium and potassium increase mobility of ions. Eventually at the Gate, there is a drift of charge carriers from poly anode to silicon substrate cathode. Positive ions at interface invert the surface and severely degrade oxide isolation. Ionic drift in SiO2 gate dielectric cause premature TDDB. Devices isolation leakage failures recover at unbiased temperature bake causes redistribution. It happens at E = 0.5 MV/cm and temperature at 100 °C.

2.9 Reliability problem of non-volatile memory

Electrons isolated from floating gate gain sufficient thermal energy to overcome energy barrier of surrounding oxide film (Renesas Technology Corp 2008). Designing of higher energy barrier leads to better quality.

Thermal excitation:

$$\frac{Vcc(t)}{Vcc(0)} = \frac{N(t)}{N(0)} = e^{[-vte^{(-Ea/KT)}]} \tag{19}$$

Data retention in memories happens generally at 10 years at room temperature. Degradation happens due to (Renesas Technology Corp 2008)

(a) Charge loss/gain due to initial effect in oxide; leakage path or particles
(b) Ionic contamination;
(c) Excessive electrical stress
(d) Stress from too many writes/erasures.

If there is a defect in interlayer film and no failure in erased state, then there is a failure in written state due to loss of electrons in floating gate (JEDEC Publication 2008). Failure occurs in both modes with less time and higher temperature. To prevent these failures, baking temperature at manufacture is to be raised. Intrinsic degradation leads to repeated cycles of Read/Write. Electrons trapped in oxide results in reduce in threshold voltage of 0/1 states.

2.10 Thermal fatigue

Fatigue failures can occur in ULSI devices due to temperature cycling and thermal shock (JEDEC Publication 2008; Semiconductor Device Reliability Failure Models 2000; McPherson 2010). Permanent damage accumulates during thermal cycling or temperature shock. Damage from thermal cycling can also accumulate each time the device undergoes a normal power-up and power-down cycle. Such cycles can induce a cyclical stress that tends to weaken materials, and may cause a number of different types of failures (MIL-HDBK-217F), including

- Dielectric/thin-film cracking.
- Lifted bonds.
- Fractured/broken bond wires.
- Solder fatigue (joint/bump/ball).
- Cracked die.
- Lifted die.

2.10.1 *Coffin-Manson model*

For ductile materials, low-cycle fatigue data are described well by the Coffin-Manson equation:

$$N_f = C_0(\Delta T - \Delta T_0)^{-q} N_f = A_0[1/\Delta\varepsilon_\rho]^B \tag{20}$$

Low cycle fatigue is defined as a stress condition in which some hundreds or thousands of cycles cause failure, while high cycle fatigue would require millions of cycles. The Coffin-Manson model was originally developed for ductile materials (iron and aluminum alloys for aircraft), but has been successfully applied to brittle materials also under all stress conditions.

2.10.2 *Modified Coffin-Mansion model*

$$\Delta\varepsilon_\rho \propto (\Delta T - \Delta T_0)^\beta \tag{21}$$

The Coffin-Manson equation works well, even for brittle material failures, where failure is dominated by crack initiation and growth, rather than simple plastic deformation.

During a temperature cycle, not all of the stress (temperature range, ΔT) may be inducing plastic deformation. If a portion of te cycle, ΔT0, is actually elastic, then the elastic portion should be subtracted from the total strain range.

3 Modified physics of failure approach

Initially, the component was described thoroughly to get enough failure information. First need to check whether that component was existed in the field, and if it's available similar item analysis and if failures were present an extensive methodology was carried out and correspondingly failure analysis, failure mechanism and failure modeling was implemented to get an idea of the component. We need also to check whether the component was analyzed in the literature that information was also stored. After an extensive research and inputs from the similar and failure analysis, a detailed methodology needs to be planned in the sequential order of failure modeling, experimentation, simulations and statistical and data modeling. According to the plan, everything was executed simultaneously to reduce the amount of time in testing. After getting the data, several analyses of factors was conducted and modeling was developed from various methods. The essential information from all the blocks were given as inputs to the decision support system where it provides the best alternative was selected and considered as technique for reliability growth. This information was stored in the component database where it was useful for further analysis. The modified physics of failure will be implemented as in Fig. 2.

3.1 Component description

As informed above, this analysis requires as much as information for the pre- and post processing examination. Hence, the component was collected from the various data and sources are essential in building up data (MIL-HDBK-338B). The resources required for data part are:

i. Materials used for fabrication and its properties.
ii. Diagrams for layout of internal chip structure.
iii. Various stresses effecting at the field and its performance.
iv. Architecture used for design.
v. Processes carried out during the fabrication.
vi. Design of the circuitry.
vii. and technology implemented for fabrication.

The resources required for data part are:

i. Manufacturer of the product/item.
ii. Consumer data supplied.
iii. Similar items that was earlier carried out in house.
iv. Manuals for that component.
v. Field information.
vi. And design team for information.

3.2 Literature and History Data

As for the failure study, learning the literature was necessary for understanding the behavior of the component under the failure considerations (MIL-HDBK-338B). The aspects need to be considered in literature are:

i. Stress parameters in and off the field.
ii. Reliability growth techniques available.
iii. Testing information and setup.
iv. Possible failure point locations (weak areas).
v. Failure modeling methods and techniques and failure criteria.
vi. Failure analysis using sophisticated equipments.
vii. Failure mechanisms that effect the behavior of performance parameters.
viii. Operational life cycle of the component.

The aspects to be considered were provided as:

i. Field information.
ii. Prediction of life using MilHdbk and other standard handbooks.
iii. Reliability indices to be considered.
iv. Datasheets from the manufacturer.
v. Failure data provided in the research.

3.3 Similar item analysis

Several techniques have been developed and used in performing very early predictions of item reliability before any characteristics of the system design have been established (MIL-HDBK-338B).

i. Defining the new item.
ii. Identifying an existing item with nearly comparison.
iii. Obtaining and analyzing historical data.
iv. Drawing conclusions on the level of reliability.

Major factors for a direct comparison of similar items should include: Item physical and performance comparison, design similarity, manufacturing similarity, similarity of the service use profile, program and project similarity and proof of reliability achievement.

3.4 Reliability indices

There are several indices are present to define reliability of the component. They are time to failure, failure rate, percentage of degradation and probability. An appropriate parameter was selected by limiting with the failure criteria of the component. It comes under one of the parameters in the design considerations.

3.5 Failure analysis

Failure analysis consists of confirming reported failures and clarifying failure modes or mechanisms using electrical measurements and various scientific analysis technologies. This section introduces specific failure analysis methods. However, before performing the actual analysis work it is necessary to thoroughly investigate failure circumstances and accurately understand the failure contents. This makes it possible to determine the optimum analysis methods and carry out swift processing.

As semiconductor devices become more highly integrated and incorporate more advanced functions, manufacturing processes are becoming more miniaturized and complex, and include diverse reliability factors. In addition, semiconductor devices have come to be used over an extremely wide range of fields, so failure causes and mechanisms are also complex. Under these circumstances, an extremely high reliability level is required of semiconductor devices. Reliability must be built in from the device development stage to the manufacturing stage in order to ensure a high level of reliability.

There are several destructive and non-destructive sophisticated methods are available at several handbooks and simulations in order to characterize the device at various levels, to implement failure analysis and also to find failure point location (MIL-HDBK-217F; White 2008; Panasonic Corporation 2000; Perry Martin 1999). This is the comprehensive list of several non destructive failure analysis techniques applicable for each failure mechanism.

- Hot carrier injection: hot spot: photo emission analysis, thermal analysis, SEM, Liquid Crystal method.
- TDDB: oscilloscope for detection of breakdown voltage.
- Electromigration: Electron Probe Micro analysis.
- To quantify the internal Image: Image Analyzing System.
- Temperature and heat related failures: Thermal Analysis System.
- Impurities like S, P, F, Cl, Br and I: X-Ray Fluorescence Spectrometer and also FTIR.
- Corrosion: Time of flight secondary ion mass spectrometer.
- ESD: Optical beam induced current analysis (OBIC), TEM, Optical Microscope, SEM.
- Latchup: Optical beam induced current analysis (OBIC).
- For Electric Measurements: IC Tester, Oscilloscope and Curve Tracer.
- Surface Analysis: Transmission Electron Microscope (TEM).

3.6 Failure mechanisms

Advanced integrated circuits (ICs) are very complex, both in terms of their design and in their usage of many dissimilar materials (semiconductors, insulators, metals, plastic molding compounds, etc.). For cost reductions per device and improved performance, scaling of device geometries has played a critically important role in the success of semiconductors. This scaling—where device geometries are generally reduced by 0.7 × for each new technology node and tend to conform to Moore's Law—has caused the electric fields in the materials to rise (bringing the materials ever closer to their breakdown strength) and current densities in the metallization to rise causing electromigration (EM) concerns. The higher electric fields can accelerate reliability issues such as: time-dependent dielectric breakdown (TDDB), hot-carrier injection (HCI), and negative-bias temperature instability (NBTI). This failure mechanisms behave differently depends on the technology such as CMOS, BJT and other semiconductors, process, manufacturer etc. (MIL-HDBK-217F; White 2008; Panasonic Corporation 2000). In addition, the use of dissimilar materials in a chip and in the assembly process produces a number of thermal expansion mismatches which can drive large thermo-mechanical stresses. These thermo-mechanical stresses can result in failure mechanisms such as stress migration (SM), creep, fatigue, cracking, delaminating interfaces, etc. (Renesas Technology Corp 2008; JEDEC Publication 2008; MOSIS Technical notes).

3.7 Failure modeling

In order to predict the life time of the component, an appropriate model was designed or developed or selected which depends on the data generated from the experimental and simulation results. Apart from the standard physics of failure models, several models that were generated from the statistical results were also compared to define behavior of the stress and performance parameters (JEDEC Publication 2008; MOSIS Technical notes; McPherson 2010). As mentioned in Fig. 3, the model depends on the field and testing data, failure mechanisms and modes, stress parameters involved and by reference as failure criteria; it can be compared with the existing models.

3.8 Design of experiments

This technique was well established technique to find the variability of the input stress parameters and its effect on the performance parameter. Design of Experiments (DOE) techniques enables the designers and fabrication engineers to determine simultaneously the individual and interactive effects of many stress factors with respective levels that could affect the output results in any design (Condra 2001). DOE also provides a full insight of interaction between parameters and thus efficient in converting standard design into a robust one. DOE helps to make concentrate on the sensitive stress-levels and sensitive areas in designs that

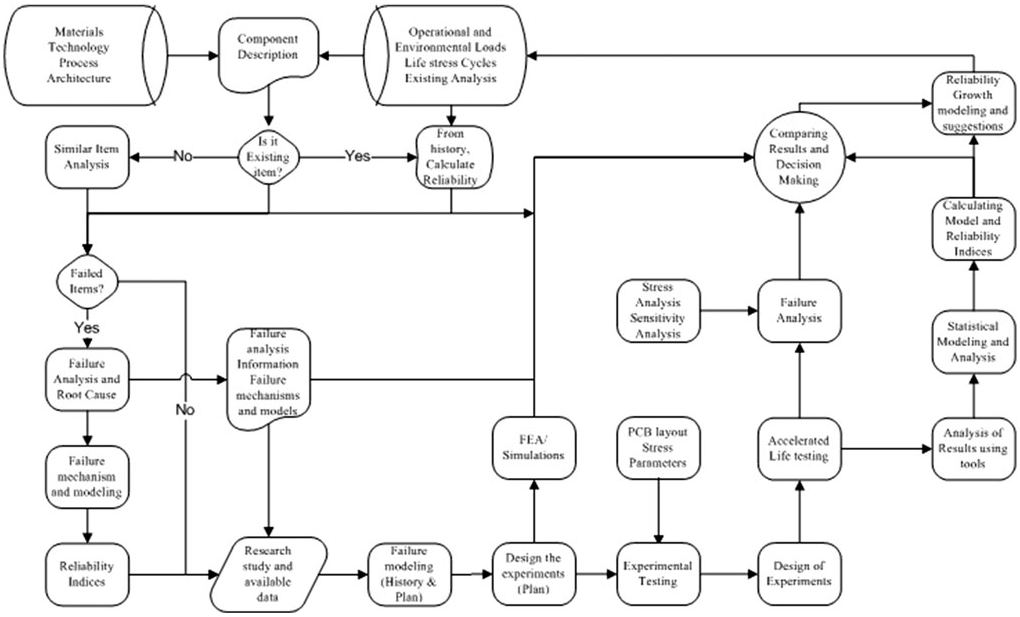

Fig. 2 Advanced block diagram of proposed physics of failure approach

cause problems in degradation, best performance and yield. Designers are then capable to reconfigure these parameters to reduce problems and correspondingly produce robust and higher designs before production. Design of experiments (DOE) is the design of any information-gathering exercises where variation is present, whether under the full control of the experimenter or not. Stress factors, levels and their interactions are tabulated for response curve and provides and runs that will best and worst solutions. In standard procedure, Taguchi method was implemented by considering the stress factors with levels with some number of runs. In general, there was a risk in selecting in levels of parameters.

In our work, we modified the conventional DOE into two steps: screening step and testing step. Initially appropriate samples were selected for each stage for repeatability and accuracy. The first step demonstrates the observance of input stress parameters on the output parameter. The response curve generated from this step provides the increase/decrease of respective stress parameter results in the degradation of performance output parameter. Then in accordingly the worst levels of the stress was selected for second testing step in constraints with the datasheet of the component. In the testing step, the experiments were conducted from the inputs of step 1. By this methodology, the ambiguity and risk in the selecting the stress levels was eliminated.

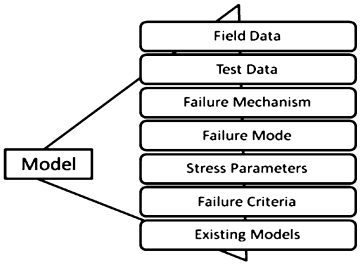

Fig. 3 Model dependence parameters

3.9 PCB design and layout

In order the experiment the electronic component, an appropriate circuit was designed and fabricated using Printed Circuit Board. There were several tools available to design the circuitry to compatible with PCB. The board layout was properly designed to reduce the interspatial effects, size and interoperability. As the experiment was needed to be exposed under stressed accelerated testing, the

circuitry need to be designed in such a way that the component under stress was segregated with the other control and power circuitry. This technique helps to reduce the effect the trace changes of other components such as resistor, capacitor and other miscellaneous components on the measured parameters as this components may vary their parameters in according with stress.

3.10 Experimental testing

After developing the circuit, the items were subjected to the stresses and monitor the output variables using various instruments. The experimental setup consists of various instruments such as voltage suppliers, oscilloscopes, voltage and current meters etc. ("EIAJ ED-4701 semiconductor device environment and durability testing methods" 1994). Accordingly, it was properly maintained in controlled environments to reduce the external noises. As it was needed to be subjected to the accelerated testing, the experiment stage needs to be properly monitored periodically for the effective control. The following stress parameters are temperature, voltage, current, radiation exposure etc. The planned Design of Experiments was subsequently applied on this circuitry to find the results.

3.11 Simulations

The simulation tools present a virtual environment and also gather information of the respective dimensions by graphical illustration (MIL-HDBK-217F). Simulations are carried out using advanced softwares tools such as Cadence, SPICE, etc. by providing inputs of stress parameters, device parameters and limits. This step will run simultaneously with the experimental testing for purpose of comparison with results from experimentation. Finite Element Analysis tools such as Ansys, Comsol, nanoHUB etc. are also carried to study the behavior of device and material characteristics.

3.12 Accelerated testing

In normal operating conditions, the component takes more amount of time to degrade and subsequently results in failure. In order to speed up the testing time, the applied parameters need to be stressed and correspondingly the testing time was reduced (Wayne Nelson 2004). Then using extrapolation and considering the acceleration factor, the failure time at operating conditions was calculated. Hence, accelerated life testing involves acceleration of failures with the single purpose of quantification of the life characteristics of the product at normal use conditions. In the most of the electronic components, the failure time was quite high and hence more rigorous stress levels need to be considered. Accelerating factors and stressed applied, either singly or in combination, include

i. More frequent power cycling.
ii. Higher vibration levels.
iii. High humidity.
iv. More severe temperature cycling.
v. Higher temperatures.

Most common model for temperature is Arrhenius model

$$AF = e^{\frac{Ea}{k}\left(\frac{1}{T_1} - \frac{1}{T_2}\right)} \quad t_f = Ae^{\frac{E_a}{kT}} \tag{22}$$

where AF, acceleration factor; Ea, activation energy; k, Boltzmann constant; T1, T2, operating and stress temperatures; tf, TTF.

From the normal and operating temperatures, acceleration factor was calculated by substituting this value, time to failure was calculated.

3.13 Analysis of results

The data generated from both experimentation and simulation was fed to this step. This step involves the behavior study of input stress parameters, design parameters, model parameters with respect to the performance and failure criteria. Individual graphs were also drawn to make some conclusions on the performance. It's like pre-processing stage to characterize the interdependence of the variables and observe the phenomenon of the imminent illustrations. The results were properly analyzed using some of the advanced statistical methods and tools to acquire essential information for further processing.

3.14 Stress and sensitivity analysis

This is pre-processing step for failure analysis which provides the affect of stress inputs on the variability of material characteristics using simulations and sensitivity data. This analysis is sub-section of failure analysis in which after acquiring information from the non-destructive testing techniques and simulation data, each and every stress parameter was demonstrated using contour graphs and 3D modeling information. This analysis provides parameters affecting the performance of the component. The sensitivity part provides the interaction between variability of each stress with the output variable.

3.15 Statistical modeling and data analysis

The preprocessing data was applied in this stage to qualify and quantify the data to assess the information. Using some of the statistical methods such as regression, response

surface regression, parametric analysis, DOE, quality methods, reliability/survival analysis, accelerated life testing, and support vector machine and other techniques to model the input–output interactions by illustrating the several graphical analysis were generated. This extensive examination of the parameters provides enormous amount of information at which we can judge the performance of the component. The models generated in the stage were considered as basis for the next steps as it decides the reliability growth techniques. The consideration and analyis the physics of failure models was also taken into account and further modify these models in accordance to the customized design.

3.16 Reliability indices

From the selected reliability indices at the planning stage, these figures were calculated using developed models such as Physics of Failure, MilHdbk standard handbooks, Response Surface Regression, other regression techniques and support vector machine. All these figures need to be calculated in consideration with the failure criteria. These figures were further compared in a common platform to assess the variability and degradation of the performance parameters with the operating conditions. The outputs of this stage are reliability indices, design range and metrics, safety limits and best parameters for maximum performance.

3.17 Reliability growth

The final objective of this overall methodology is to find the best design and manufacture alternatives to increase the life time of the component. The techniques required for enhancement in TTF and reduction in degradation of parameters is called reliability growth (Chary et al. 2012). This step provides only the prediction so such that uncertainty and confidence levels were also included. The possible reliability growth techniques cover in

i. Changes in design parameters.
ii. Incorporation of additional circuitry.
iii. Selection of different manufacturer.
iv. Failure site improvement.
v. Fabrication suggestions to manufacture for in-house components.

3.18 Non-technical factors

In deciding the optimal characteristics of the component, several other factors need to be considered at the managerial level. These include risk analysis, government policies, management choices, availability, life cycle cost, human interaction etc. to be considered.

3.19 Decision support system

This is the final stage of the entire proposed modified block diagram which involves much more productive decision can be made by the information gathered from different parts of the Fig 4. The following figure demonstrates the various factors required as an inputs to the decision support system to finalize the judgment on the component for reliability growth and further to take necessary measures. The inputs to the system are:

(a) Failure AnalysisFrom acquiring the information of failure point locations at different parts of the block diagram, such as similar item analysis, tested failure analysis, in the literature and from historical data, a final conclusion needs to be stated as input to the support system. This was considered as quality input.
(b) Statistical ModelsModels were generated at different parts of the diagram such as in the literature, historical data, failed items and the tested data. An appropriate prediction model was selected for quantitative analysis and thus decisive finding was fed to system.
(c) SimulationsSimultaneously we carried out simulations on the component to identify the stress behavior on the performance parameters and any other essential information was provided to the central system.
(d) RiskThe possible risk associated with each alternative was considered as input.
(e) Life Cycle CostAs cost was one of the main criteria for a business, total cost accumulated for each alternative was considered.
(f) Non-technical factorsOther non-technical factors were also discussed.

An expert group consists of reliability engineers, electronic design and fabrication engineers, material engineers, statisticians, field engineers and management need to be discussed on the several alternatives and appropriate solution was to be selected by optimal suggestions from all the people in the group. Each alternative was excessively discussed and generates report considering all the factors and this information will feed back to the database of the component in which this information is useful in further analysis.

4 Predicted outcomes

By implementing this advanced methodology, the following productive outcomes provides efficient information as

- Root cause analysis provides the exact failure site location which provides pin pointed improvement area.
- Suggesting different alternatives for the enhancement in reliability.

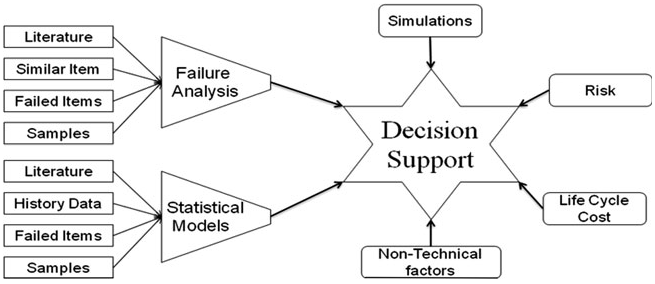

Fig. 4 Decision Support System

- Reduction in the repair/recall/replacement cost.
- Feasible for flexible reliability design using the data w.r.t the application.
- Also available for similar item analysis.

4.1 Advantages

The advantages by using this methodology are

- Proper learning of failures so that future product development, design, strategy and implementation will be more successful.
- Reputation in market due to reliable product outcomes.
- Cost, time and human work for recalling, repairing and replacement decreases.
- Qualitative and quantitative data is available for the selected component and consider as a basis for advance in design with less time.
- Modeling the component as per requirement and provides in-house research.
- Increase in time to market depends on supply of products.

4.2 Challenges

This methodology has following challenges and limitations

- Materials, process and technologies are always not available to the customer datasheet by companies due to confidentiality.
- Requires more sophisticated instruments (also cost) for analysis which are always not possible.
- Modeling of the failure criteria/degradation phenomena of new materials needs insightful research.
- It takes time to carry out and require cost for all analysis.
- Need expert reviews on the cause of failure.

5 Conclusion

Physics of failure methodology alone does not provide enough information on the component and hence incorporation of statistical methods will improve the effectiveness of the prediction of the reliability indices. The proposed modified approach accommodates enormous amount of information which also provides several other alternatives which improves the mechanism. But this method is only applicable to the critical parts and components which is very important and provide safety to the costly equipment. This type of rigorous analysis does not require for less important components.

Acknowledgments The authors acknowledge the several people at BARC, Mumbai for their extensive support on writing this paper. In addition, authors thank Prof. V Ramgopal Rao, IIT Bombay for his knowledge and support on technology perspective on electronic devices and failure mechanisms.

References

"EIAJ ED-4701 Semiconductor device environment and durability testing methods" (1994) Electronic industries association of Japan

"European power supply manufacturers association", MTBF Report, June 2005

Analysis of thermal failure of electronic components, MPE 635, Electronic cooling, Cairo University, Egypt, 2007

Chary Geetha V, Habtour Ed, Drake Gary S (2012) Improving the reliability in the next generation of US Army platforms through physics of failure analysis. J Fail Anal Prev 2(1):74–85

Lloyd W Condra (2001) Reliability improvement with design of experiments, 2nd edn, Marcel Dekker, New York

Foucher B, Boulli J, Meslet B, Das D (2002) A review of reliability prediction methods for electronic devices. Microelectron Reliab 42:1155–1162

Hu C (1989) Reliability issues of MOS and bipolar ICs. IEEE International conference on Computer Design pp. 438–442

JEDEC Publication, Failure mechanisms and models for semiconductor devices, JEP122E, (Revision of JEP122D, October 2008), Originaly published as JEP122D.01 March 2009, China

Joseph Bernstein B, Gurfinkel Moshe, Li Xiaojun, Walters Jorg, Shapira Yoram, Talmor Michael (2006) Electronic circuit reliability modeling. Microelectron Reliab 46:1957–1979

Kim Vu (2003) Silver Migration—and Effects on thick-film conductors, Material Science Engineering 234–Spring

McPherson JW (2010) Reliability physics and engineering: time-to-failure modeling. Springer, New York

Ohring Milton (1998) Reliability and failure of electronic materials and devices. Academic Press, New York

Panasonic—reliability of semiconductor devices (2000), T04007BE-2, Panasonic Corporation, USA

Pecht Michael, Kang Wen-Chang (1988) A Critique of Mil-Hdbk-217E reliability prediction methods. IEEE Trans Reliab 37(5): 453–457

D.S.Peck and C.H.Zierdt (1973) Temperature-humidity acceleration of metal-electrolysis in semiconductor devices, The 11th Annual Proceedings of International Reliability Physics Symp., p 146

Perry Martin L (1999) Electronic failure analysis handbook: techniques and applications for electronic and electrical packages, components, and assemblies. McGraw Hill, New York

Ramakrishnan Arun, Syrus Toby, Pecht Michael (2001) Electronic hardware reliability. CRC Press, Florida, Avoinics Handbook

Renesas—Semiconductor reliability handbook (2008), REJ27L0001-0101, Rev.1.01, Renesas Technology Corp., Nov 28

Semiconductor device reliability failure models, International SEMATECH, May 31, 2000

Semiconductor reliability handbook (2011) Toshiba, No. BDE0128H

Shahrzad Salemi, Shahrzad Salemi, Liyu Yang, Jun Dai, Jin Qin, Joseph B. Bernstein (2008) Physics-of-failure based handbook of microelectronic systems, Reliability Information Analysis Center

SONY—Sony semiconductor quality and reliability handbook (2000) Sony Corporation

Wayne Nelson B (2004) Accelerated testing: statistical models, test plans, and data analysis (Wiley series in probability and statistics). Wiley, New York

White Mark (2008) Microelectronics reliability: physics-of-failure based modeling and lifetime evaluation. JPL Publication 08-05, NASA, California

Military handbook, Electronic eeliability design handbook, MIL-HDBK-338B

Military handbook, Reliability prediction of electronic component, MIL-HDBK-217F

Reliability in CMOS IC design: physical failure mechanisms and their modeling, MOSIS Technical notes

Paper III

P3

Degradation modeling of Voltage comparator using modified physics-of-failure approach

Thaduri, A., Verma, A.K., Vinod, G., Rajesh, M.G., Kumar, U. (2012), "Degradation modeling of Voltage comparator using modified physics-of-failure approach", *Communications in Dependability and Quality Management (CDQM)*, 15(1), pp. 76-87.

Degradation modelling of Voltage comparator using modified physics of failure approach

Adithya Thaduri[#$]1, A K Verma[&]2, V Gopika[*]3, Rajesh Gopinath[*]4, Uday Kumar[$]5

Department of Electrical Engineering, IIT Bombay, Powai, Mumbai, India

1adithya.thaduri@gmail.com

& Stord/Haugesund University College, Haugesund, Norway

2akvmanas@gmail.com

*RSD, BARC, Trombay, Bombay, India

3vgopika@barc.gov.in

4rajeshgopin@gmail.com

$Division of Operation and Maintenance, Lulea University of Technology, Lulea, Sweden

5Uday.Kumar@ltu.se

Abstract

There are several electronic systems running continuously to control and monitor the various activities in the nuclear industry and reliability and safety of these systems is taken care of utmost importance. The Neutron Flux Monitoring System has individual electronic components is one of the modules present in the signal processing unit. This unit consists of numerous components such as Optocoupler, Constant fraction discriminator, Voltage Comparator, Instrumentation Amplifier etc., and this paper studies the degradation aspects of the Voltage comparator. The prediction of reliability was conducted at earlier phases of electronics but in the present advances in the technology that methods were no longer obsolete. Hence, the other alternative, physics of failure approach laid emphasis on the root cause analysis and degradation of the performance parameters. Apart from that, we combined physics of failure approach with the statistical methods such as Design of Experiments, Accelerated testing and failure distribution models to quantify time to failure of this electronic component by radiation and temperature as stress parameters. The degradation of the performance parameter is modelled and compared using regression analysis, parametric analysis, several response plots and response surface method.

Keywords

Accelerated Testing, Design of Experiments, Physics of Failure, Radiation testing, Reliability Prediction, Voltage Comparator

1. Introduction

The nuclear industry consists of numerous critical components at various stages of the operation. The incorrect prediction of these critical components poses safety and quality issues which leads to the improper shutdown. Hence there is a need to concentrate on the prediction methodologies that was implemented in selection, installation and working conditions of the respective components.

Electronics division of BARC is engaged in design & fabrication of CMOS and BJT ASICs for nuclear pulse processing unit. These new microelectronic devices often exhibit infant mortality and wear-out phenomena in operation of the unit. The reliability of electronic systems, used in nuclear power plants, is traditionally estimated with empirical databases such as MIL-HDBK-217, PRISM etc. These methods assigns constant failure rate to the electronic devices, during their entire course of useful life. The constant failure rate assumption treats failures as random events. In the advancements in science and technology,

electronic reliability prediction is moving towards applying the Physics of Failure (PoF) approach which illustrates information on materials, process, technology, fabrication techniques etc. It depicts competing degradation mechanisms such as electro migration, hot carrier injection, dielectric breakdown etc.-that makes a device's useful life contrast to the predicted life by empirical methods [1]. The robust understanding of the dominant mechanisms that leads to device failure –Physics of Failure– is a more realistic approach to reliability prediction.

In practical considerations, it was not possible to get the sufficient device information and also has serious limitations from the manufacturers. There are even other limitations such as failure analysis using sophisticated instruments, amount of time and cost to conduct the physics of failure approach. In contrast, there were highly developed methodologies available in the statistical domain of the reliability prediction using data from design of experiments and accelerated testing which characterises various parameters leading to the failure. In order to get advantage from both the methodologies, a modified physics of failure approach was developed with inputs from failure characteristics of PoF approach and data and analysis of statistical approach.

Neutron Flux Monitoring System-NFMS- comprises of different modules (Pulse Translator, Logarithmic Count Rate, Mean-Square Value Processor etc) that process pulse and current signals from detector. Besides, there are modules that generate trip signals [2]. Trip signals are of 24V level and optically isolated.

It is worthwhile to study the failure mechanisms of the components involved in the signal processing chain of NFMS, as its reliability is being evaluated with conventional MIL-HDBK-217 method [3]. The physics of failure study of these components will generate reliability data that can be eventually compared with the MTBF figures provided by MIL-HDBK-217. A few components have been identified in this regard-They form a part of trip signal generation which has direct implication on safety. 4N-36: Optocoupler, AD-620: Instrumentation Amplifier, OP-07: A general purpose operational amplifier etc., are widely used in the trip modules of NFMS.

Another candidate chosen for study, Voltage comparator was used in the pulse processing circuits of NFMS. This component generates a pulse when the input voltage exceeds the threshold voltage. From the field studies and literature available [4, 5], the degradation of the output voltage was due to the effect of temperature and radiation excitation over the extended life time. Hence, both these parameters were selected as stress parameters. There was a constraint in the experimentation that both the stress parameters cannot be applied simultaneously and instead excited with one after another. The effect of individual parameter was quantified on voltage output and degradation of device was studied. In order to select the stress levels, design of experiments (DOE) to provide maximum degradation considering different runs. These stress levels was then fed to accelerating testing for extended period of time. Since there is no sufficient physical model present for this device, modelling was to be carried out by probabilistic methods such as linear regression, response surface regression and support vector machine. From these models, relation between design parameters and time to failure was observed and provided to designer for the reliability growth.

2. Block diagram for reliability prediction

2.1 Component Description

The first step in this methodology was to describe the component with all the necessary and essential information for analysing the failure and calculating the reliability indices. The sources required for the information on the component were: materials, processes, layout

diagrams, technology, architecture, design, criticality, cost, datasheet, manuals, field data and any similar item analysis that was analysed earlier.

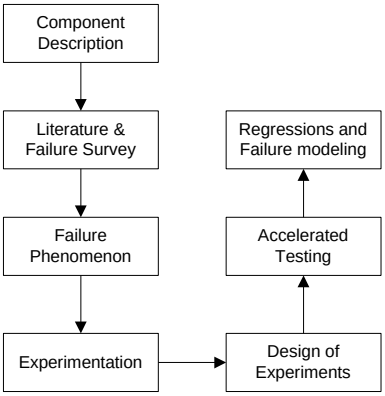

Fig 1: Block Diagram of Modified Physics of Failure approach

2.2 Literature Survey and Failure Survey

To study the failure behaviour of the component, the literature survey was required to understand the behaviour of several factors that affecting the performance. The information essential for this study were: expert reviews, stress factors, failure criteria, failure mechanisms, failure modes, failure analysis, degradation analysis and other factors.

The advanced methodology, physics of failure lay emphasis on the root cause of failure inherently depends on the operational stress factors, environment and physical characteristics of the device [6]. From the information on component description and literature survey, appropriate failure phenomenon and failure criteria were selected.

2.3 Failure Phenomenon

There was several failure mechanisms reported in the literature characterized on operational environment, stress parameters, level of approach, technology etc [1,6]. There were several failure time to failure models associated with each mechanism and appropriate model was picked for the application. According to the selected component, the appropriate failure mechanism or degradation mechanisms were studied. From the literature, an appropriate failure analysis was selected to examine and illustrate the failure of the component and root cause of failure by electrical characterization or by using non-destructive testing by making use of sophisticated instruments like scanning electron microscope, infrared spectroscopy, thermal analysis etc [7]. For some of the components where there was no information on the failure mechanism, this step was need to be implemented beforehand to acquire information on failure characteristics.

2.4 Experimentation

From the acquired data, the next process of experimentation was planned for testing and reliability prediction. The desired circuitry was designed and fabricated using printed circuit board. This step also includes the number of samples, stress parameters and experimental setup for further testing of the component.

2.5 Design of Experiments

Design of Experiments was very advanced and efficient methodology to find the prominent factors, component selection and variability analysis of the component [8]. The prominent approach, Taguchi method was implemented here. In order to get best out of design of experiments, a modified methodology was designed as two-step DOE. In general, there was uncertainty in selecting the stress factors for design of experiments and accelerated testing. Hence, at first screening step, the test was designed to know variability of stress on

the effect of performance parameters. In the second testing step, the levels of the stress were aggressive which defines the degradation of the performance parameters.

2.6 Accelerated Testing

The input pattern obtained for degradation from modified design of experiments was applied in the accelerated testing step [9]. As from the analysis, this particular pattern leads to further degradation over the accelerated time.

2.7 Regressions and Failure Modelling

The data collected from both design of experiments and accelerated testing was used for statistical data and modelling analysis using various methods such as response surface regressions, regression methods and other tools to quantify the stress parameters and its behaviour on the performance of the device. This data was also useful for failure models obtained from failure mechanisms.

3. Voltage Comparator: Component Description

The voltage comparator consists of an operational amplifier (op-amp) which amplifies the small difference between the two input signals. The output voltage depends on the voltages between inverting input (-ve) and non-inverting input (+ve). In the general operation, one of the inputs was set to the threshold value which can be tuned by a potentiometer [10]. The Voltage comparators were not perfect devices as the operation and suffer from the intrinsic effects of Input Offset Voltage due to the fabrication constraints. This problem normally occurs when the Input voltage changes very slowly and in the order of few milli volts. The net result of the Input Offset Voltage and input base current resulted that the output transistor does not fully turn on or off when the input voltage is close to the reference voltage.

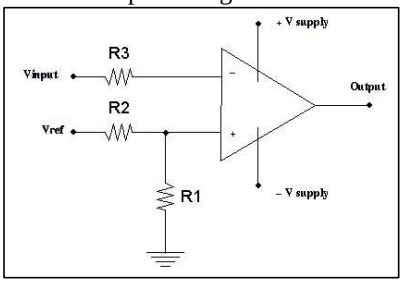

Fig 1: Voltage Comparator

4. Literature Survey and Failure phenomenon of Voltage Comparator

Failure possibly happened due to the degradation of internal transistor parameters with the applied stress parameters. By the physics of failure approach, the stress parameters affect the transistors to change their behavior of electrical h-parameters. Commonly, when an electrical or temperature stress applied on the transistor, it develop reverse current from emitter to base to increase in such a way to degrade the performance of output electrical characteristics such as collector current and output voltage. If the values of this device parameter vary, the effective voltages and currents tend to vary at the larger levels of the operational amplifier and output pulse width changes. If the value of the output voltage was not sufficient to generate signal to the next component, it was considered as failure. The failure criterion was selected when output voltage reduces to 5% of its initial value with inputs from the field.

A. Effect of Temperature

The temperature dependence of bipolar transistors depends on a multitude of parameters affecting the bipolar transistor characteristics in different ways. Important effect is the temperature dependence of the current gain. Since the current gain depends on both the emitter efficiency and base transport factor [4].

The emitter efficiency depends on the ratio of the carrier density, diffusion constant and width of the emitter and base. As a result, it is not expected to be very temperature dependent. The carrier densities are linked to the doping densities. Barring incomplete ionization, which can be very temperature dependent, the carrier densities are independent of temperature as long as the intrinsic carrier density does not exceed the doping density in either region. The width is very unlikely to be temperature dependent and therefore also the ratio of the emitter and base width. The ratio of the mobility is expected to be somewhat temperature dependent due to the different temperature dependence of the mobility in n-type and p-type material.

The base transport is more likely to be temperature dependent since it depends on the product of the diffusion constant and carrier lifetime. The diffusion constant in turn equals the product of the thermal voltage and the minority carrier mobility in the base. The recombination lifetime depends on the thermal velocity. The result is therefore moderately dependent on temperature. Typically the base transport reduces with temperature, primarily because the mobility and recombination lifetime are reduced with increasing temperature. Occasionally the transport factor initially increases with temperature, but then reduces again.

Temperature affects the AC and DC characteristics of transistors. The two aspects to this problem are environmental temperature variation and self-heating. Some applications, like military and automotive, require operation over an extended temperature range. Circuits in a benign environment are subject to self-heating, in particular high power circuits.

Leakage current ICO and β increase with temperature. The DC β hFE increases exponentially. The AC β hfe increases, but not as rapidly. It doubles over the range of -55o to 85o C. As temperature increases, the increase in hfe will yield a larger common-emitter output, which could be clipped in extreme cases. The increase in hFE shifts the bias point, possibly clipping one peak. The shift in bias point is amplified in multi-stage direct-coupled amplifiers. The solution is some form of negative feedback to stabilize the bias point. This also stabilizes AC gain [4].

As from the studies from BJT technology, temperature and radiation is selected as stress parameters. The emitter and collector current of npn BJT is given as Equation (1) and (2).

$$I_E = I_{ES}\left(e^{\frac{V_{BE}}{V_T}} - 1\right) \tag{1}$$

$$I_C = \alpha_T I_{ES}\left(e^{\frac{V_{BE}}{V_T}} - 1\right) \tag{2}$$

The output voltage VCE is given as in (3)

$$V_{CE} = V_{CC} - I_C R_{eff} \tag{3}$$

where R_{eff} is effective output resistance at the output, I_{ES} = reverse saturation current at base-emitter diode, α_T = common base forward short circuit gain, V_T = Thermal Voltage kT/q, V_{BE} = base-emitter Voltage, V_{CE} = base-collector Voltage, V_{CC} = Source Voltage typically 5V/10V.

In Eber-Moll Model, IC grows at about 9%/^{0}C if you hold VBE constant and VBE decreases by 2.1mV / ^{0}C if you hold IC constant with the temperature. Since both the currents depend on temperature parameter V_T, the raise in the temperature leads to vary these parameters which finally lead to degrade the performance of component.

B. Effect of Radiation

Another stress parameter which degrades the BJT devices is β-radiation. Degradation of many types of bipolar transistors and circuits is known to depend strongly on dose rate. For a given total dose, degradation is more severe in low dose rate exposure than high dose rate exposure. This effect has been attributed to space charge effects from trapped holes and hydrogen related species through oxygen vacancies in base oxide. There are several hardness assurance tests and most popular has been high dose rate irradiation at elevated temperatures [5].

Although radiation exposure generally leads to grain degradation in npn and pnp devices, the mechanisms by which radiation effects their gains are quite different. Ionizing radiation degrades the current gain of npn bipolar transistors by introducing net trapped positive charge and interface traps into the oxide base. This positive oxide trapped charge spreads the emitter-base depletion region into the extrinsic base results in increase of base recombination current under forward-bias operation at the junction. Radiation-induced interface traps, especially those near mid-gap, serve as generation-recombination centers through which recombination current in the base is further increased due to enhanced surface recombination velocity. In pnp transistors [6], near-midgap interface traps in the base oxide also increase the base current by surface recombination. Compared with npn transistors, radiation-induced net positive oxide trapped charge can mitigate gain degradation by creating an imbalance in carrier concentrations at the surface of the base.

From the statistical results explained in et al. Witczak [5], Current gain degradation grows worse with decreasing dose rate regardless of dose. Excess base current, an increase in base current due to radiation exposure, increases gradually with decreasing dose rate. This effect is due to weak dependence of excess base current on radiation-induced defect densities at large total dose. Changes in collector current as compared to base current is small because it provides meaningful assessment of amount of gain degradation while relating closely to the physical mechanisms, excess base current is a convenient parameter to evaluate radiation-induced damage in these devices [5].

Although much progress has been made in understanding the effects of dose rate and temperature on radiation-induced bipolar gain degradation, still there is ambiguity in selecting the optimum values for assurance testing. From the analysis carried out by Ronald [13], the combined influence of both radiation and temperature has considerable dependence on gain degradation and excess base current enhancement. The combined effect of temperature and radiation results in degradation of pulse amplitude of Voltage Comparator.

5. Experimentation, Design of Experiments and Accelerated Testing

A printed circuit board was developed for five samples of LM311 of each with the testing circuit of voltage comparator as shown in fig 2. In the earlier section it was studied that temperature and radiation was considered as stress parameters and also noted that both the parameters cannot be applied simultaneously. Initially each lot was subjected to 4 steps of radiation 0, 3Kgray, 6Kgray and 9Kgray respectively. Then each lot was ramped from 30^0C to 90^0C in steps of 5^0C from the source of temperature controller. Then design of experiments was conducted to achieve and select a run which poses higher degradation of the output voltage. This particular run further fed to the accelerated testing up to several hours to impact further degradation. The table 1 was the results for both the exposure of radiation and temperature at different stress levels. This result was graphically depicted in the figure 3. This information showed that increase of both radiation and temperature leads to the degradation of the output voltage.

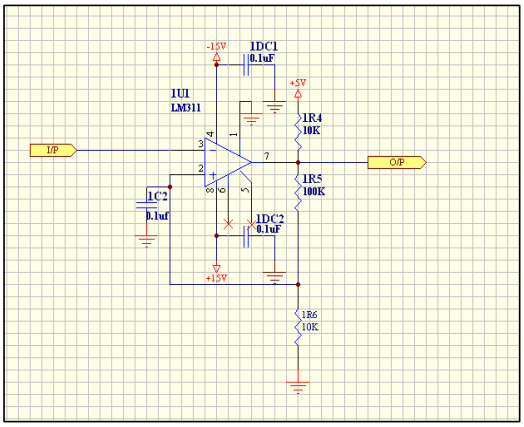

Fig 2: Experimental Testing circuit for Voltage Comparator

Table 1: Impact of Temperature and Radiation at different runs

R/T	30	35	40	45	50	55	60	65	70	75	80	85	90
0	4.9864	4.984	4.9814	4.9772	4.9748	4.972	4.9694	4.9654	4.961	4.9566	4.9518	4.9466	4.9414
3	4.964	4.9614	4.9588	4.9566	4.9542	4.9514	4.9488	4.9452	4.941	4.9368	4.9318	4.9264	4.9212
6	4.9316	4.9294	4.9274	4.9252	4.9224	4.9198	4.9168	4.9138	4.9098	4.9054	4.9026	4.8978	4.892
9	4.9016	4.8994	4.8974	4.895	4.8924	4.8902	4.8878	4.8842	4.8792	4.8742	4.8688	4.863	4.8572

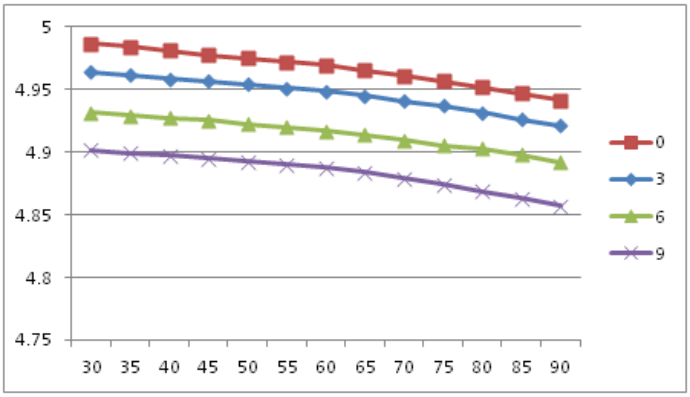

Fig 3: Impact of Temperature and Radiation at different runs

The stress level of 9Kgray of radiation and 90^0C of temperature has higher degradation and this stress levels was controlled at extended period of time by conducting accelerated testing. The Table 2 and Figure shows the degradation of the output voltage with time.

Table 2: Impact of accelerated time at each radiation step (T = 90^0C)

R/t	0	50	100	150
0	4.9654	4.9544	4.9434	4.9318
3	4.9452	4.9346	4.921	4.9086
6	4.9138	4.9016	4.8904	4.8784
9	4.8842	4.8728	4.8604	4.848

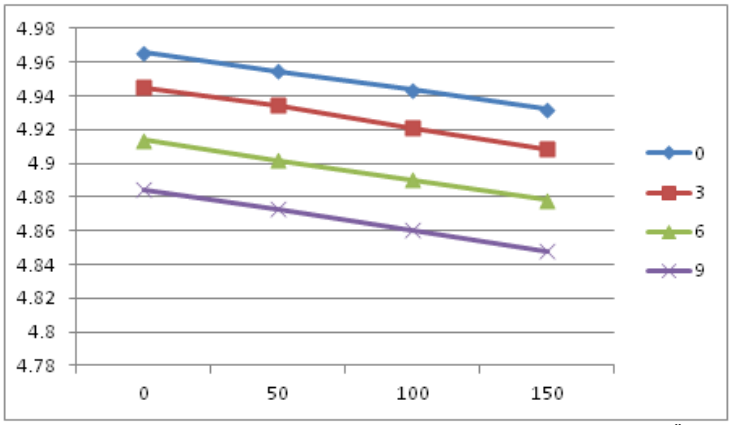

Fig 4: Impact of accelerated time at each radiation step (T = 90^0C)

From the Table 2 and figure 4, the output parameter further degrades over the accelerated time. This procedure was extended until the voltage comparator lead to failure (i.e., 5% of initial value). The 3D plots in fig 5, interactions plot in fig 6 and main effects plot in fig 7 characterizes the effect of stress parameters on the output voltage. These parametric analysis illustrates that the increase in all the stress parameters leads to higher degradation and also shows the non-linear and independent behaviour of each stress parameter.

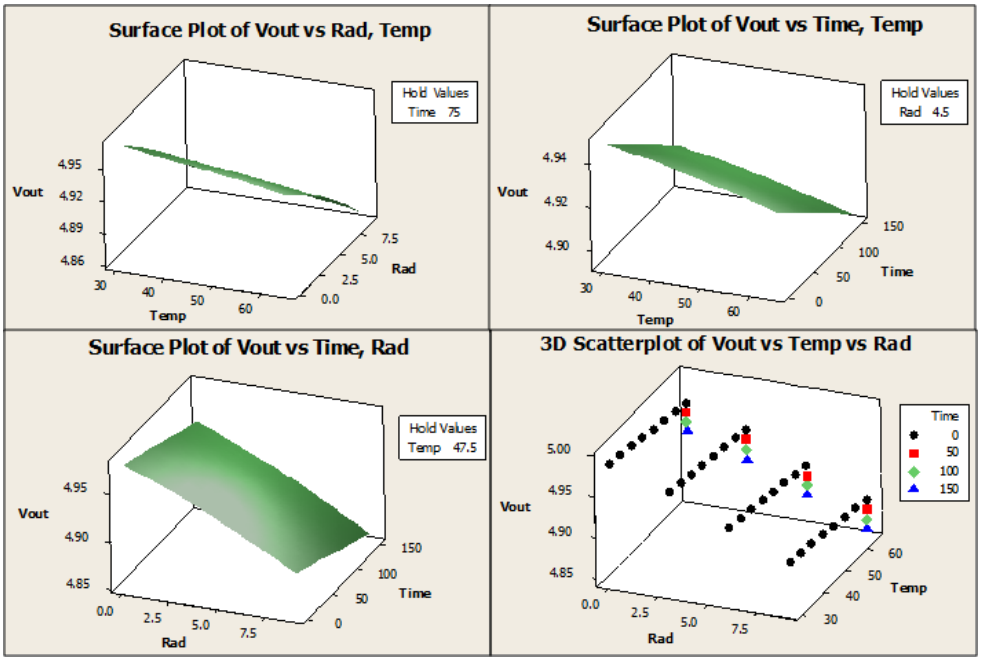

Fig 5: 3D surface plots of stress parameters with output voltage

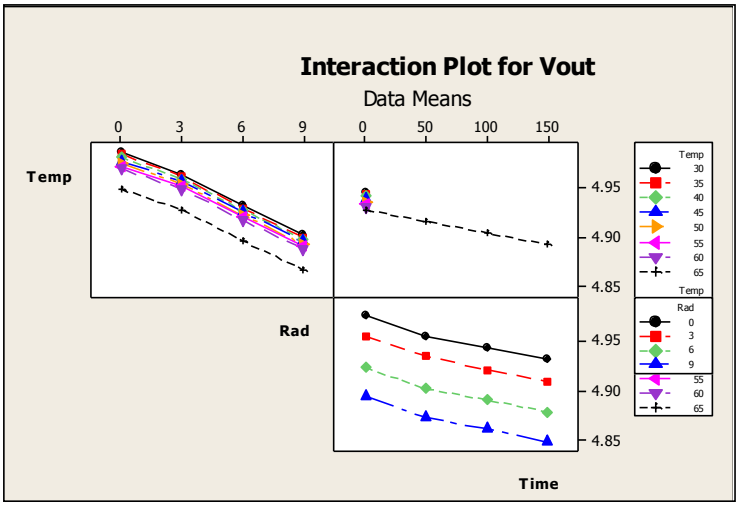

Fig 6: Interaction plot of stress parameters

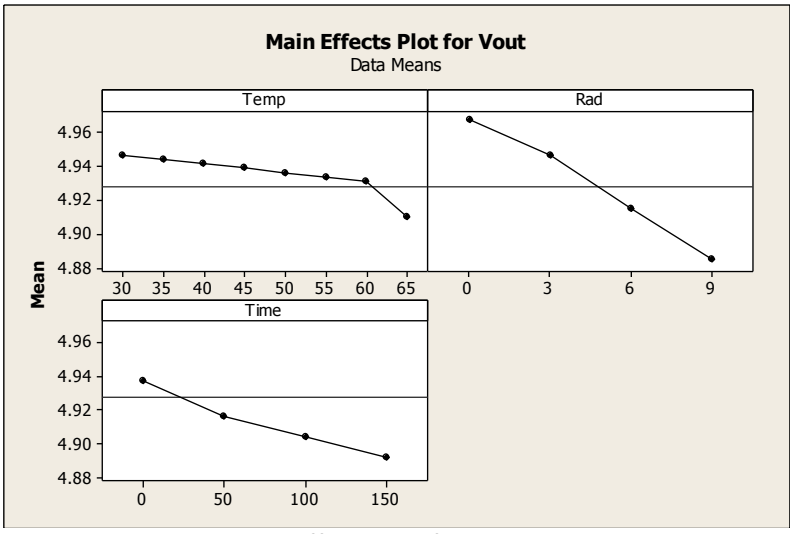

Fig 7: Main effects plot of stress parameters

Identify the Best Factor Settings with Analyze Variability

A traditional analysis of a designed experiment helps you to determine the factor settings that produce the best average response [11]. But to identify the factor settings those not only perform well on average, but also perform the most consistently can be found out by using this variability analysis available in Minitab. The pareto chart was generated by considering the standard deviations calculated at each of different run subsequently finding out the the parameters or interaction of the parameters that defines higher variability. From the data obtained from the experimentation, it was found out that the radiation was the dominant stress parameter for variability and quality factor as shown in fig 8.

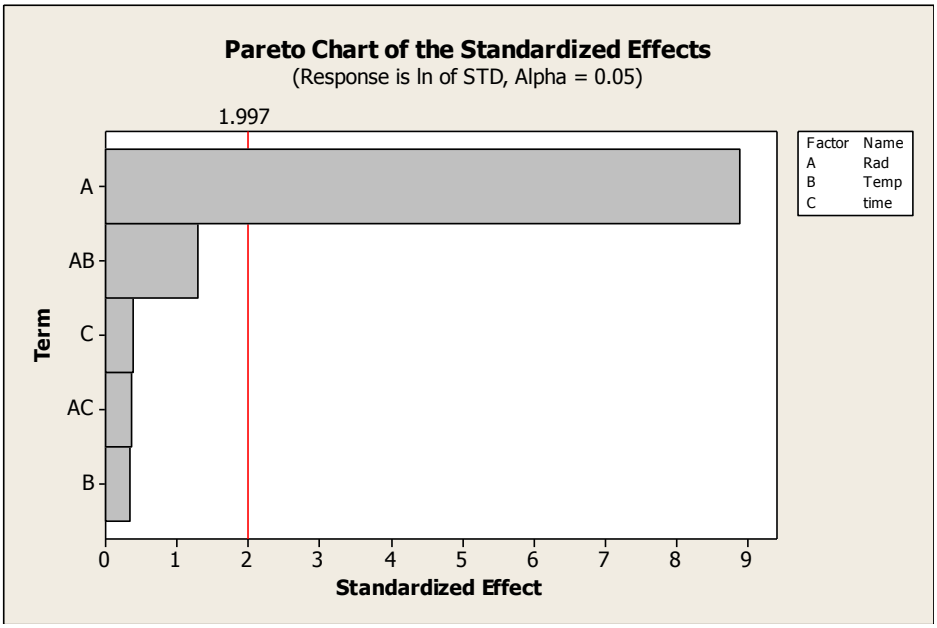

Fig 8: Pareto Chart using variability analysis

6. Regression and Data Modelling

The response surface regression procedure fits a quadratic response-surface model with the input and out parameters, which is useful in searching for factor values that optimizes the response according to the application. The following features make it preferable to other regression procedures for analysing response surfaces: automatic generation of quadratic effects, a lack-of-fit test, and solutions for critical values of the surface, eigen values of the associated quadratic form, a ridge analysis to search for the direction of optimum response [12]. The response equation (4) that was generated from the above data with the interactions and its coefficients as

$$V = 4.98791-0.00650306R+8.96032E^{-05}T-2.07619E^{-04}t-3.32099E^{-04}R^2-6.68796E^{-06}T^2-8.01589E^{-08}t^2+2.69630E^{-06}RT-1.27303E^{-06}Rt \quad (4)$$

The time to failure was calculated with the required value of failure criteria and operating parameters in the above equation.

7. Conclusion

In this paper, the need of reliability study of voltage comparator was studied. Furthermore, reliability and degradation mechanisms that affects the performance of output pulse with temperature and dose rates acts as input characteristics was properly explained and verified with the experiments. A modified physics of failure approach considering the inputs from the PoF analysis and statistical analysis was implemented on the testing of Voltage Comparator. Design of experiments and Accelerated testing was carried out and the data obtained from these methods was characterized by several parametric analyses. The failure model was obtained from the more accurate response surface regression considering the above data.

8. References

[1]. B. Foucher, J. Boullie, B. Meslet, D. Das, "A review of reliability prediction methods for electronic devices", *Microelectronics Reliability* 42 (2002) 1155–1162

[2]. Susumu Harasawa, Atsushi Nakamoto, Yoshinori Hayakawa, Jun Egawa, Otohiko Aizawa, Tetsuya Nozaki, Takashi Minobe, Hiroshi Hatanaka, "Improved Monitoring System of Neutron Flux during Boron-Neutron Capture Therapy", *Radiation Research*, 88, 187-193 (1981)

[3]. "Military Handbook, Reliability prediction of electronic component, MIL-HDBK-217F"

[4]. Guijie Wang, Gerard C.M. Meijer,"The temperature characteristics of bipolar transistors fabricated in CMOS technology", *Elsevier, Sensors and Actuators* 87 2000 81–89.

[5]. S.C. Witczak, R.D. Schrimpf, D.M. Fleetwood, K. F. Galloway, R.C.Lacoe, D.C. Mayer, J.M. Puhl, R.L.Pease, J.S. Suehle, "Hardness assurance testing of bipolar junction transistors at elevated irradiation temperatures", *IEEE transaction on Nuclear Science*, Vol 44, No. 6, Dec 1997.

[6]. "Failure Mechanisms and Models for Semiconductor Devices", *JEDEC Publication*, JEP122E, Originally published as JEP122D.01 March 2009

[7]. Perry L Martin, "Electronic Failure Analysis Handbook, Techniques and Applications for Electronic and Electrical Packages, Components, and Assemblies", *McGraw Hill*, 1999

[8]. Lloyd W. Condra, "Reliability improvement with design of experiments", 2nd edn, *Marcel Dekker*, 2001.

[9]. Wayne Nelson, "Accelerated Testing: Statistical Models, Test Plans, and Data Analysis", *John Wiley & Sons*, 2004

[10]. Theodore F Bogart, Jeffrey Beasley, Guillerno Rico, "Electronic Devices and Circuits", *Pearson Prentice Hall*, 2009

[11]. Graeb H., Mueller, D., Schlichtmann, U., "Pareto optimization of analog circuits considering variability", *18th European Conference on Circuit Theory and Design, 2007. ECCTD 2007*, 28 - 31, 27-30 Aug, 2007

[12]. Raymond H Myers, Douglas C Montgomery, Christine M Anderson-Cook, "Response Surface Methodology: Process and Product Optimization using Designed Experiments", *Wiley Series in Probability and Statistics*, 2009

[13]. Ronald L. Pease, M. C. Maher, M. R. Shaneyfelt, M. W. Savage, P. Baker, J. Krieg, T. L. Turflinger, "Total-Dose Hardening of a Bipolar-Voltage Comparator", *IEEE Transactions on Nuclear Science*, vol. 49, no. 6, December 2002

Paper IV

P4

Stress Factor and Failure Analysis of Constant Fraction Discriminator using Design of Experiments

Thaduri, A., Verma, A.K., Vinod, G., Rajesh, M.G., Kumar, U. (2013). Stress Factor and Failure Analysis of Constant Fraction Discriminator using Design of Experiments. *International Journal of Reliability, Quality and Safety Engineering*, 20(3), pp. 134003-1 – 134003-28.

International Journal of Reliability, Quality and Safety Engineering
Vol. 20, No. 3 (2013) 1340003 (28 pages)

DOI: 10.1142/S0218539313400032

STRESS FACTOR AND FAILURE ANALYSIS OF CONSTANT FRACTION DISCRIMINATOR USING DESIGN OF EXPERIMENTS

ADITHYA THADURI

Division of Operation and Maintenance
Luleå University of Technology, Luleå, Sweden
adithya.thaduri@gmail.com

A. K. VERMA

Stord/Haugesund University College, Haugesund, Norway
akvmanas@gmail.com

V. GOPIKA* and RAJESH GOPINATH†

RSD, BARC, Trombay, Bombay, India
**vgopika@barc.gov.in*
†*rajeshgopin@gmail.com*

UDAY KUMAR

Division of Operation and Maintenance
Luleå University of Technology, Luleå, Sweden
Uday.Kumar@ltu.se

Received 30 August 2012
Revised 31 October 2012
Accepted 6 May 2013
Published 21 June 2013

Reliability prediction using traditional approaches were implemented at earlier stages of electronics. But due to advancements in science and technology, the above models are outdated. The alternative approach, physics of failure provides exhaustive information on basic failure phenomenon with failure mechanisms, failure modes and failure analysis becomes prominent because this method depends on factors like materials, processes, technology, etc., of the component. Constant fraction discriminators which is important component in NFMS needs to study failure characteristics and this paper provides this information on failure characteristics using physics of failure approach. Apart from that, the combined physics of failure approach with the statistical methods such as design of experiments, accelerated testing and failure distribution models to quantify time to failure of this electronic component by radiation and temperature as stress parameters. The SEM analysis of the component is carried out by decapsulating the samples and studied the impact of stress parameters on the device layout.

Keywords: Constant fraction discriminator; physics of failure; failure analysis; design of experiments; accelerated testing.

1. Introduction

There are several methods available for prediction of reliability for electronic systems such as MIL-HDBK 217F,[15] PRISM, Telcordia, etc., using constant failure method considering random failures. This assumption is inaccurate for some components as the recent trends in technology are changing rapidly in electronics and semiconductor fabrication. The other advanced methodology, physics of failure approach, investigates the real reason for failure using root cause analysis.[16,17] In some of the cases, the physics of failure approach along with statistical methods are needed to be implemented to assess the parametric analysis of stress parameters.

Electronics division of Bhabha Atomic Research Center, BARC is engaged in design and fabrication of CMOS and BJT ASICs for nuclear pulse processing. Earlier, reliability was calculated by using constant failure methods without any information on stress parameters lead to inaccurate prediction. There exist several failure mechanisms in the field like electromigration, hot carrier injection, corrosion, etc., which cannot be evaluated using the empirical methods and which may results in inefficient prediction. The physics of failure approach investigates the failures using stress analysis and failure analysis by advanced methods with higher accuracy and provide valuable inputs for reliability growth.

Neutron flux monitoring system (NFMS) comprises of different modules (Pulse Translator, Logarithmic Count Rate, Mean-Square Value Processor, etc.) that process pulse and current signals from detector. Besides, there are modules that generate trip signals. Trip signals are of 24 V level and optically isolated.

It is worthwhile to study the failure mechanisms of the components involved in the signal processing chain of NFMS, as its reliability is being evaluated with conventional MIL-HDBK-217 method. The physics of failure study of these components will generate reliability data that can be eventually compared with the MTTF figures provided by MIL-HDBK-217. A few components have been identified in this regard. They form a part of trip signal generation which has direct implication on safety.

Constant fraction discriminator (CFD) is one of the critical components in NFMS which provides an input pulse if the input amplitude reaches a particular threshold voltage. This detector is an important part since it provides safety to the system and detailed stress analysis and failure analysis are of higher priority and need to be studied.

2. Methodology

The following methodology was applied for failure analysis of CFD as shown in Fig. 1.

2.1. *Description of component*

To start with POF model of a component data from diverse sources need to be collected and analyzed. It includes basic operation/function of the components,

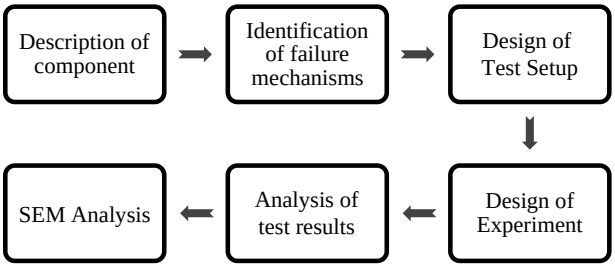

Fig. 1. Methodology for reliability prediction of CFD.

materials and process used in its fabrication, details of packaging and assembly, CAD layout of IC's. The operations of individual subsystems consist of parts/component should be analyzed.

2.2. *Identification of possible failure mechanism and stress parameters*

The conditions under which a component operates (thermal, electrical and environmental) are needed to be identified and analyzed. Data also from literature are needed to be collated. The stresses that a component is subjected to during its operation may induce different failure mechanisms in the long run. The stresses that a component experiences spell out dominant failure/degradation mechanisms which lead to failure.

2.3. *Experimental setup*

After the stress parameters are identified, the particular input/output profile that a component should see during an accelerated test becomes known. An appropriate test fixture can be designed (hardware/software). It includes PCB, bread board, measurement equipments (CRO, waveform analyzers), heaters, power suppliers, function generator, voltage and current sources, environmental chamber, etc., which might be required during accelerated test.

2.4. *Design of experiments*

After selection of all stress and performance parameters, the next step is to run design of experiments (DOE).[1] Appropriate stress levels and sample size are selected. DOE is carried out in two stages: screening stage and testing stage.

2.4.1. *Screening stage*

To know the influence of stress parameter levels on the performance parameter, this stage is implemented. Effects of stress levels are studied and further action is

taken on next stage for further expanding the range of stress levels by considering the effect on performance parameters.

2.4.2. *Testing stage*

From the feedback of the screening stage, appropriate stress levels are selected and it is tested. Response table is generated including the two stages which provide information on effect of variation of stress parameter levels on performance parameters.

2.4.3. *Accelerated testing*

In many situations, and for many reasons, such life data is very difficult, if not impossible, to obtain. The reasons for this difficulty can include the long life times of today's products, the small time period between design and release and the challenge of testing products that are used under normal conditions. They have attempted to accelerate their failures.[2] From the selected stress levels in response table, accelerated testing is carried out. A failure criterion is also mentioned here for further analysis.

2.5. *Analysis of test results*

From the enormous data generated from experimental setup, a detailed analysis is carried out including failure modeling. Failure analysis is performed on failed items to know if the failure happened or not. Some statistical and graphical methods are also utilized to find out the variation/degradation of the observed parameters.

2.6. *SEM analysis*

The selected samples of the component, CFD, are decapsulated using chemical process to access the internal layout of the circuitry. These samples are then analyzed by using scanning electron microscope (SEM) to visualize the defects caused by the accelerated stress parameters and studied accordingly.

3. Constant Fraction Discriminator

3.1. *Description of component*

CFD is another device which is failing regularly in the field. This device is made up of BJT technology. It is a level discriminator at which it provides a pulse when the analog input reaches particular voltage level. Temperature and cobalt radiation are considered as stress parameters. These parameters effects the operation of BJT transistors inside to behave as it reduces the output voltage which further reduces the performance parameter, which is in this case, is voltage of output pulse. There is a limitation that both the stress parameters cannot be applied simultaneously.

Effect of individual parameter is quantified on voltage output and degradation of whole device is studied. Selection of stress levels can be carried out by using DOE and accelerating testing is implemented.

In general, discriminators generate logic pulses in response to input signals exceeding a particular threshold. The leading edge discriminator suffers from a problem such that if the amplitude is changed, the rise time of the input pulse remains the same, a sort of "time walk" occurs.[3] An input pulse with smaller amplitude but with the same rise time as a larger pulse will cross the threshold at a later time. Thus, the timing of the output pulse is shifted by this change in amplitude.

The CFD alleviates this problem by using a constant fraction, f, of the input pulse to precisely determine the timing of the output pulse relative to the input signal. It does this by splitting the input signal, attenuating one half so that it is a certain fraction, f, of the original amplitude, and delaying and inverting the other half.

The attenuated pulse and the delayed and inverted pulse are then added together, and the zero crossing is computed. The zero crossing gives the time at which the CFD should create an output pulse, and is always independent of amplitude. For a simple linear ramp, like the one shown above, the equations for its input pulse, attenuated pulse, and delayed and inverted pulse are as follows: $td =$ delay, $f =$ fraction, $A =$ initial amplitude, $Vi = At =$ input pulse and $Vd = A(t - td) =$ delayed and inverted pulse.

To find the zero crossing, set $V_c + V_d = 0$ and solve for t:

$$0 = -fAt + A(t - td) \Rightarrow t_{\text{cross}} = \frac{\varepsilon d}{1 - f}. \tag{1}$$

Ideally, the delay is chosen such that the maximum of the attenuated pulse crosses at the desired fraction of the delayed pulse. In that case, $t_{d\_\text{ideal}} = t_{\text{rise}}(1-f)$. However, if the delay is chosen smaller than t_{d_ideal}, CFD will operate at a fraction less than that of f. From Eq. (1), it was seen that t_{cross} is independent of the amplitude of the input pulse. The CFD has a monitor output feature, which outputs the bipolar signal created by summing the attenuated and the delayed and inverted pulses, so that it can be viewed on how it is calculating the zero crossing.[4] In order to achieve a constant timing edge, it is customary to use an attenuator and a delay. The input signal is split. One part is delayed, and the other is attenuated. After these two signals are re-mixed, a comparator detects the zero cross points. The timing of the zero cross point is not influenced by the amplitude of the input signal.

3.2. *Identification of possible failure mechanism and stress parameters*

The principle of operation of CFD is demonstrated as in the block diagram shown in Fig. 2. The Constant Fraction Discriminator CFD 2004 is made by Bharat Electronics Limited (BEL) Bangalore, India. The comparators and flip flops as shown

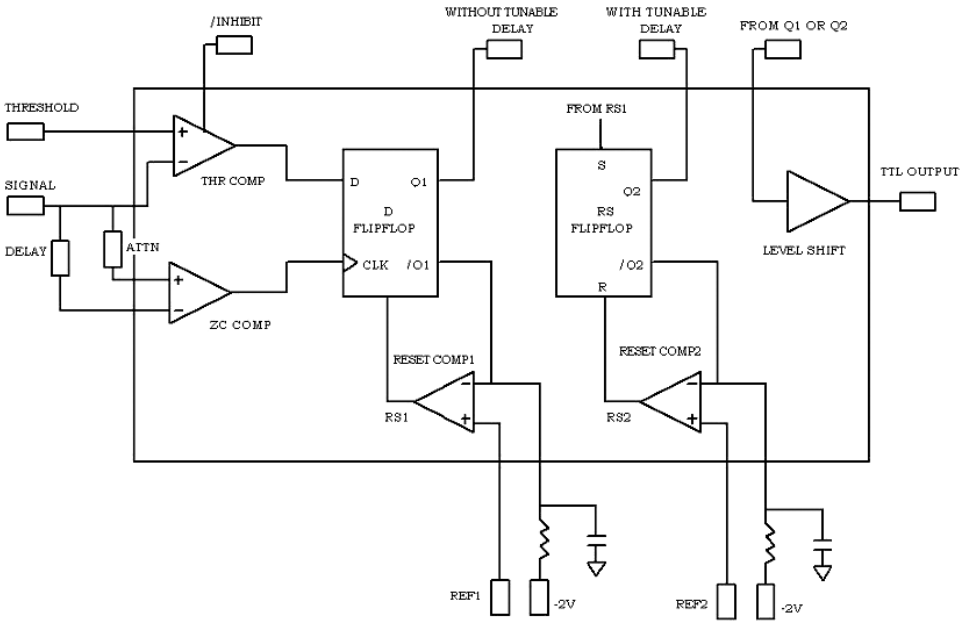

Fig. 2. Block diagram of CFD.

in Fig. 2 consist of transistors made up of BJT Technology. The failure physics of these transistors at wafer level adversely affects the performance and failure of the component. As from the description, if the wave from the counter expects to cross at a threshold level, CFD must provide TTL pulse. The failure may possibly happen if the threshold level at the input and the pulse width at the output vary in accordance with the prescribed level with the existing internal parameters. By the physics of failure approach, the stress parameters affect the BJT transistors to change their behavior of electrical h-parameters. Commonly, when an electrical or temperature stress applied on the transistor, they develops reverse current from emitter to base to increase in such a way to degrade the performance of output electrical characteristics such as collector current and V_{CE} voltage at the output. If these values changes inside the device, as all other devices are interconnected, this effective voltages and currents tend to vary at the larger levels of the whole device and output pulse width and time periods change. If this change is large such that it cannot detect the input pulse providing the output TTL, then it is considered as failure.

3.2.1. *Effect of temperature*

The temperature dependence of bipolar transistors depends on a multitude of parameters affecting the bipolar transistor characteristics in different ways. Important effect is the temperature dependence of the current gain since the current gain depends on both the emitter efficiency and base transport factor.[5]

The emitter efficiency depends on the ratio of the carrier density, diffusion constant and width of the emitter and base. As a result, it is not expected to be very temperature-dependent. The carrier densities are linked to the doping densities. Barring incomplete ionization, which can be very temperature-dependent, the carrier densities are independent of temperature as long as the intrinsic carrier density does not exceed the doping density in either region. The width is very unlikely to be temperature-dependent and therefore also the ratio of the emitter and base width. The ratio of the mobility is expected to be somewhat temperature-dependent due to the different temperature dependence of the mobility in n-type and p-type material.

The base transport is more likely to be temperature-dependent since it depends on the product of the diffusion constant and carrier lifetime. The diffusion constant in turn equals the product of the thermal voltage and the minority carrier mobility in the base. The recombination lifetime depends on the thermal velocity. The result is therefore moderately dependent on temperature. Typically the base transport reduces with temperature, primarily because the mobility and recombination lifetime are reduced with increasing temperature. Occasionally the transport factor initially increases with temperature, but then reduces again.

Temperature affects the AC and DC characteristics of transistors. The two aspects to this problem are environmental temperature variation and self-heating. Some applications, like military and automotive, require operation over an extended temperature range. Circuits in a benign environment are subject to self-heating, in particular high power circuits.

The increase in hFE shifts the bias point, possibly clipping one peak. The shift in bias point is amplified in multi-stage direct-coupled amplifiers. The solution is some form of negative feedback to stabilize the bias point. This also stabilizes AC gain.[6] The change in the device parameters with the temperature is shown in Fig. 3.

In Eber–Moll Model, I_C grows at about 9%/°C if you hold V_{BE} constant and V_{BE} decreases by 2.1 mV/°C if you hold I_C constant with the temperature. Since both

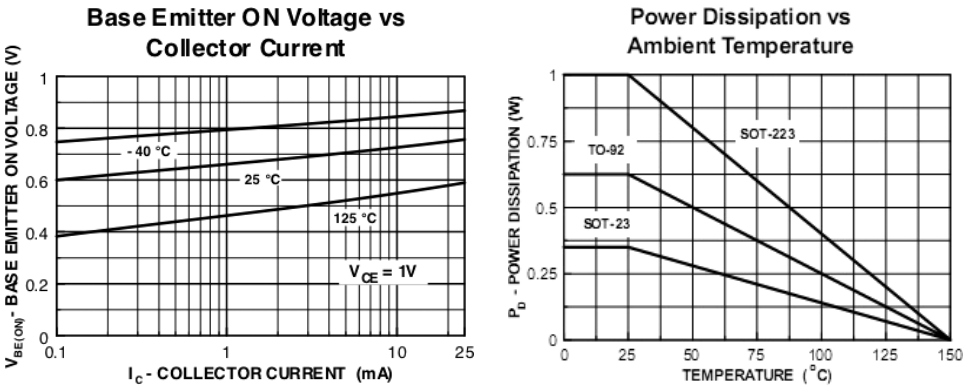

Fig. 3. I_c versus V_{BE} and power dissipation versus temperature.[7]

the currents depend on temperature parameter V_T, the raise in the temperature leads to vary these parameters which finally lead to degrade the performance of CFD.

3.2.2. *Effect of radiation*

Degradation of many types of bipolar transistors and circuits is known to depend strongly on dose rate. For a given total dose, degradation is more severe in low dose rate exposure than high dose rate exposure. This effect has been attributed to space charge effects from trapped holes and hydrogen related species through oxygen vacancies in base oxide. There are several hardness assurance tests and most popular has been high dose rate irradiation at elevated temperatures[8] as shown in Fig. 4.

Although radiation exposure generally leads to grain degradation in npn and pnp devices, the mechanisms by which radiation affects their gains are quite different. Ionizing radiation degrades the current gain of npn bipolar transistors by introducing net trapped positive charge and interface traps into the oxide base. This positive oxide trapped charge spreads the emitter-base depletion region into the extrinsic base results in increase of base recombination current under forward-bias operation at the junction. Radiation-induced interface traps, especially those near midgap, serve as generation-recombination centers through which recombination current in the base is further increased due to enhanced surface recombination velocity. In pnp transistors,[9] near-midgap interface traps in the base oxide also

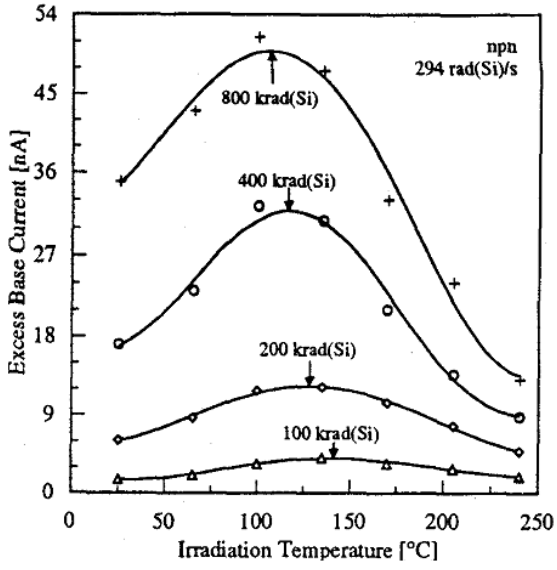

Fig. 4. Effect of excess base current with irradiation temperature.[8]

increase the base current by surface recombination. Compared with npn transistors, radiation-induced net positive oxide trapped charge can mitigate gain degradation by creating an imbalance in carrier concentrations at the surface of the base.

From the statistical results explained in Witczak *et al.*,[8] current gain degradation grows worse with decreasing dose rate regardless of dose. Excess base current, an increase in base current due to radiation exposure, increases gradually with decreasing dose rate. This effect is due to weak dependence of excess base current on radiation-induced defect densities at large total dose. Changes in collector current as compared to base current is small because it provides meaningful assessment of amount of gain degradation while relating closely to the physical mechanisms, excess base current is a convenient parameter to evaluate radiation-induced damage in these devices.[10]

From the analysis carried out by Witczak *et al.*,[8] the combined influence of both radiation and temperature has considerable dependence on gain degradation and excess base current enhancement. The combined effect of temperature and radiation results in degradation of performance parameters such as threshold voltage, pulse amplitude and time period of CFD.

3.3. *Experimental setup*

CFD 2004 of BJT technology from manufacturers of BEL is considered for this study. It is 24-pin DIP plastic package with operating conditions −5.2 V to 5 V and temperature 100°C. In order to monitor and test this IC for temperature and radiation considering time, a circuit is required to assess and measure it. Figure 5 shows the conditional measuring circuit for this failure testing.

3.4. *Design of experiment*

From the research, temperature and radiation dose rate are considered as stress parameters for the degradation of performance of CFD. The performance parameters include threshold voltage which is at the input and TTL pulse amplitude at the output. From the Taguchi method of DOE,[1] selection of this temperature levels is considered such that IC provides optimum performance. Testing can be done in two steps: Basic and Extensive testing for analysis of CFD.

3.4.1. *Stage* 1: *Basic testing*

3.4.1.1. Screen testing

The radiation and temperature are the dominant stress parameters. Initially the device is exposed to radiation under biased conditions. Thereafter it is exposed to temperature. The selection parameters can be done using 2-stage DOE. Accelerated testing is carried out from the data acquired from DOE to define time to failure of device using Response Surface graph.[11]

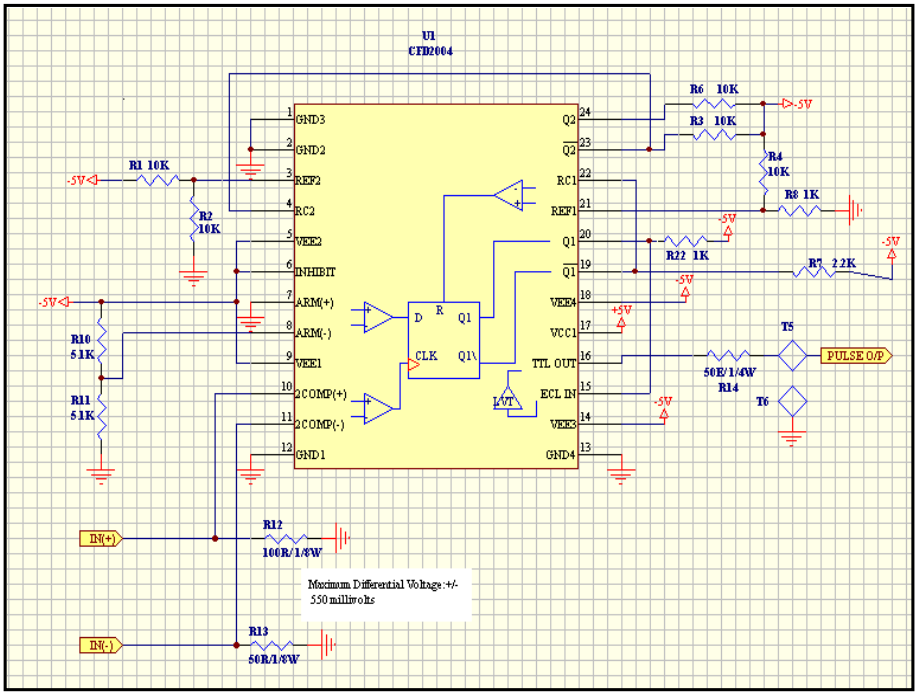

Fig. 5. Circuit diagram of CFD.

Radiation testing

In this study, variation of pulse amplitude in accordance with the Cobalt dose rate is calculated. The sample size is 3, radiation levels: 20 min and 40 min, temperature: 30°C, time is 0 h. Figure 6 shows the variation of output pulse amplitude with respect to the dose rate. There is some little degradation in the output at higher dose rate.

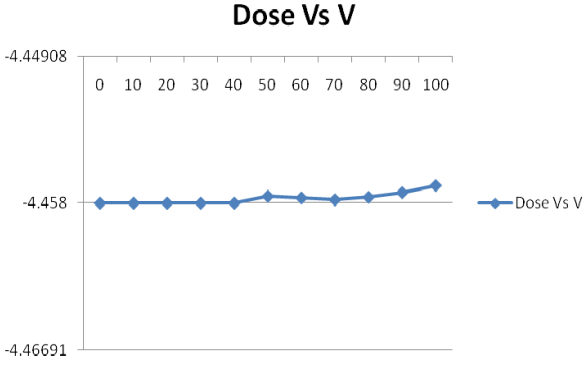

Fig. 6. Variation of pulse voltage with dose rate.

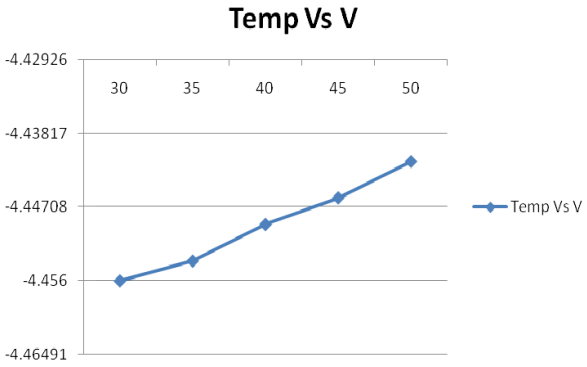

Fig. 7. Voltage with temperature acceleration.

Temperature testing

In this study, variation of pulse amplitude in accordance with the temperature is calculated. Range of temperature is considered from 30°C to 50°C. Figure 7 shows considerable decrease in the amplitude as the temperature increased nonlinearly to 50°C because of explanation given in above section. From the screening results, it was known that both radiation and temperature degrades the performance parameters as both the parameters increase. This experiment provides a proof of the discussion on degradation mechanisms that was explained in above section.

3.4.1.2. Design of experiments

In this stage, stress levels of both radiation and temperature are subjected to CFD circuit. The response surface graph results are shown in Fig. 8. The sample size is 3, the radiation levels: 20 min and 40 min, temperature: 30°C and 50°C and time is 0. From DOE and the response surface graphs, the levels of input parameters is selected such that maximum degradation of performance parameter is expected and acts as input to the accelerated testing of CFD for life testing analysis.

3.4.1.3. Accelerated testing

From the inputs of DOE, the levels are selected such that pulse amplitude has maximum degradation. The values are provided below and experiments are carried out at regular intervals after exposure of radiation and maintaining the temperature level. The sample size is 10, radiation: 40 min, temperature: 50°C and time: 0, 100, 200, 300 and 400 h. As in Fig. 9, the degradation of pulse amplitude happened over the time nonlinearly. To quantify and model this time to failure considering dose rate and temperature need to be studied as there are no physics of failure models available in the literature.

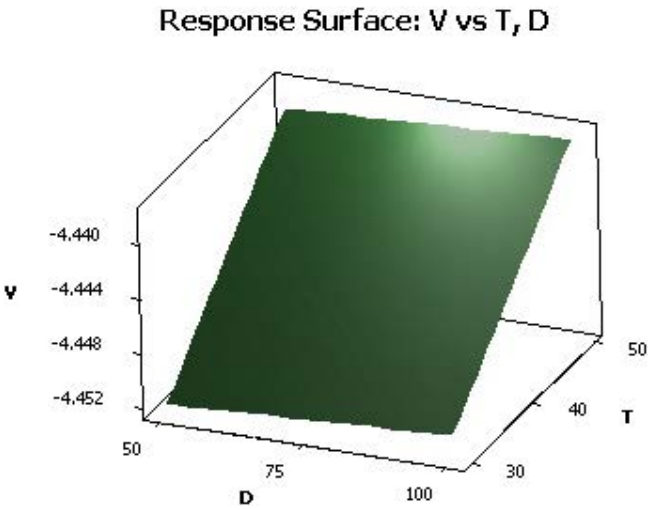

Fig. 8. RSG of V versus T, D.

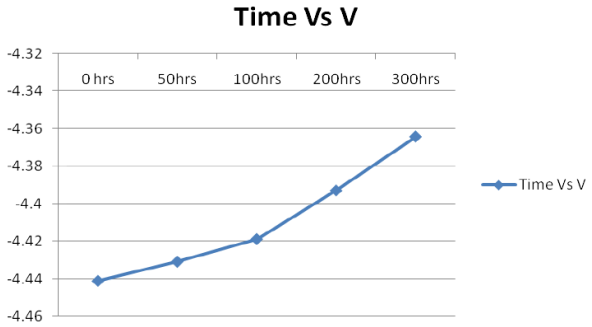

Fig. 9. Accelerated testing of CFD.

3.4.2. *Stage* 2: *Extensive testing*

From the input from Stage 1, as both the temperature and radiation parameters increase, the output performance factor further degrades. In this stage, the radiation parameters are selected at the higher dosages as 0, 3.14, 6.64 and 10 kGy. Similarly, the testing of IC is excited to higher temperatures of 30°C, 50°C, 70°C and 90°C. From the Witczak,[2] the degradation of the device by radiation increases further with the temperature. Hence the items are subjected at first to the radiation step and second to the temperature step. To get more extensive data, accelerated testing is carried out after the temperature step. This radiation-temperature-time sequence is carried out at all the stress levels of the radiation. The cumulative effect of both temperature and time factors with respect to radiation stress level is shown below.

From Table 1, temperature further degrades the effect of radiation step and shown graphically in Fig. 10 where $t = 0$.

Table 1. Radiation step with temperature.

Temp (°C)	V 0 kGy	V 3 kGy	V 6 kGy	V 10 kGy
30	−4.426	−4.368	−4.264	−4.146
50	−4.404	−4.352	−4.238	−4.124
70	−4.382	−4.334	−4.216	−4.1
90	−4.35	−4.304	−4.184	−4.068

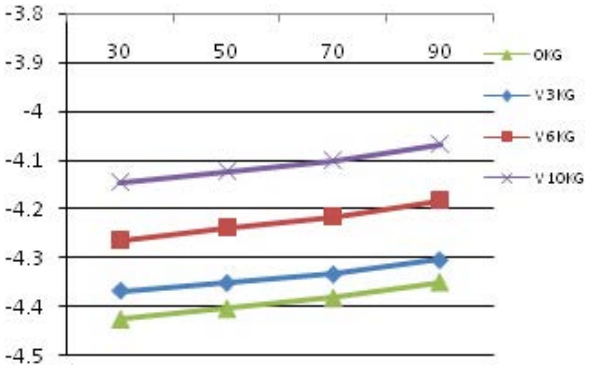

Fig. 10. Degradation with radiation and temperature.

Table 2. Radiation step with accelerated time.

Time (h)	V 0 kGy	V 3 kGy	V 6 kGy	V 10 kGy
0	−4.441	−4.304	−4.184	−4.068
50	−4.4308	−4.254	−4.134	−4.016
100	−4.4188	−4.194	−4.074	−3.952
150	−4.4059	−4.122	−3.992	−3.89

Similarly, the degradation characteristics are observed with accelerated testing carried out 90°C at each radiation step and results are provided in Table 2. From Table 2, the output parameter further degrades by the effect of accelerated time and shown graphically in Fig. 11. From the above figures, it was concluded that both radiation and temperature degrades the performance parameter, the voltage of the output pulse with further accelerated time.

3.5. *Analysis of test results*

From the results obtained from both the stages, analysis of results is carried out to find the behavior of individual parameters on the output performance parameter. In order to analyze and model the parameters, some tools such as Minitab[12] are used to characterize and model the output voltage parameter. The data selected for this Minitab analysis are taken as in Table 3.

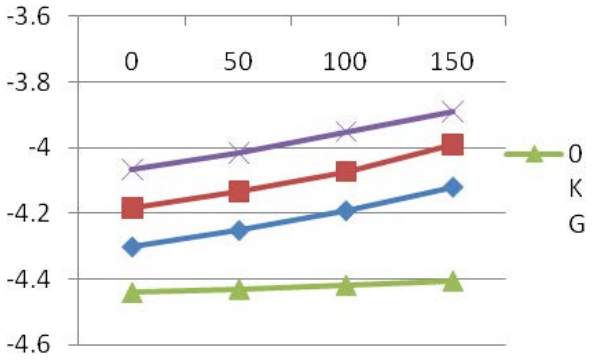

Fig. 11. Degradation with radiation and accelerated time.

The 3D scatterplot with radiation, temperature and accelerated time as axis parameters and output voltage as the points in Fig. 12. As discussed in the above section, the voltage degrades with increase in radiation, temperature and accelerated time.

Table 3. Data selected for Minitab analysis.

Temperature (°C)	Time (h)	R (in kGy)	O/P Voltage (V)
30	0	0	−4.426
30	0	3	−4.368
30	0	6.5	−4.264
30	0	10	−4.146
50	0	0	−4.404
50	0	3	−4.352
50	0	6.5	−4.238
50	0	10	−4.124
70	0	0	−4.382
70	0	3	−4.334
70	0	6.5	−4.216
70	0	10	−4.1
90	0	0	−4.35
90	0	3	−4.304
90	0	6.5	−4.184
90	0	10	−4.068
90	50	0	−4.4308
90	50	3	−4.254
90	50	6.5	−4.134
90	50	10	−4.016
90	100	0	−4.4188
90	100	3	−4.194
90	100	6.5	−4.074
90	100	10	−3.952
90	150	0	−4.4059
90	150	3	−4.122
90	150	6.5	−3.992
90	150	10	−3.89

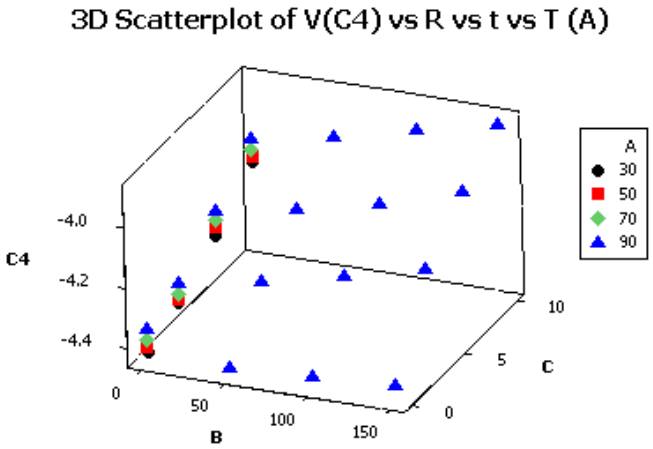

Fig. 12. 3D Scatterplot of stress parameters with output voltage.

3.5.1. *Characterization of stress parameters*

The characterization of each input stress parameter with the degraded output voltage carried out using response surface plots, contour plots and matrix plots is shown in Figs. 13–15. By observing the plots, the degraded parameter is characterized by each stress parameter and directly proportional to the degradation of output voltage pulse due to the fact that all these parameters induce defects into the device that reduces the response of the item.

Each stress parameter is solely fitted as linear plots with the output parameter along with ANOVA and regression life data.

3.5.1.1. Fitted line plots

The fitted line plot provides the linearity behavior of the one stress parameter at a time on the output parameter. The fitted line plot provides not only the estimated regression function, but also a scatterplot of the data adorned with the estimated regression function. The linearized plot of temperature, radiation and time stress parameters are shown in the order of Figs. 16–18.

3.5.1.2. One-way ANOVA

One-way ANOVA is a technique used to compare means of two or more samples. It tests the null hypothesis that samples in two or more groups are drawn from the same population. If the group means are drawn from the same population, the variance between the group means should be lower than the variance of the samples, following the Central Limit Theorem. A higher ratio therefore defines that samples are drawn from different samples. One-way ANOVA of temperature, radiation and time stress parameters with the output voltage is shown below.

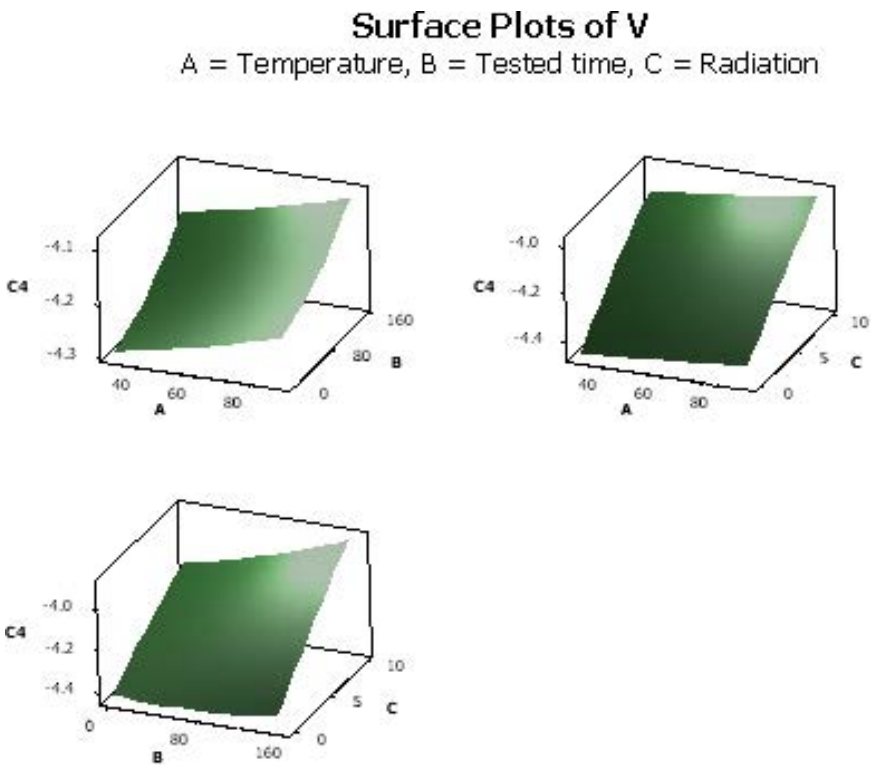

Fig. 13. Response surface plots of stress parameters.

3.5.1.3. Individual value plots

Minitab[12] new individual value plot allows you to view important data features, to find miscoded values, and to identify unusual cases. An individual value plot can help you to set the appropriate course for your analysis and to avoid wasted time and frustration. Individual value plots to identify possible outliers and other values of interest. It can also clearly illustrate characteristics of the data distribution. Here, the mean value at each stress level of the factor is plotted across the output voltage to assess its performance degradation over in increase of the stress value. In Fig. 19, there is sudden increase in the degradation of the voltage parameter from 70°C to 90°C. Hence, higher the temperature of the CFD leads to degradation of voltage parameter. In Fig. 20, the slope of the radiation line is steep and has higher effect on the voltage degradation. In comparison, in Fig. 21, the slope of the line is low and has less impact on the degradation.

3.5.1.4. Regression with life data

Using Regression with Life Data,[12] whether one or more predictors affect the failure time of a product can be found. The goal is to come up with a model which

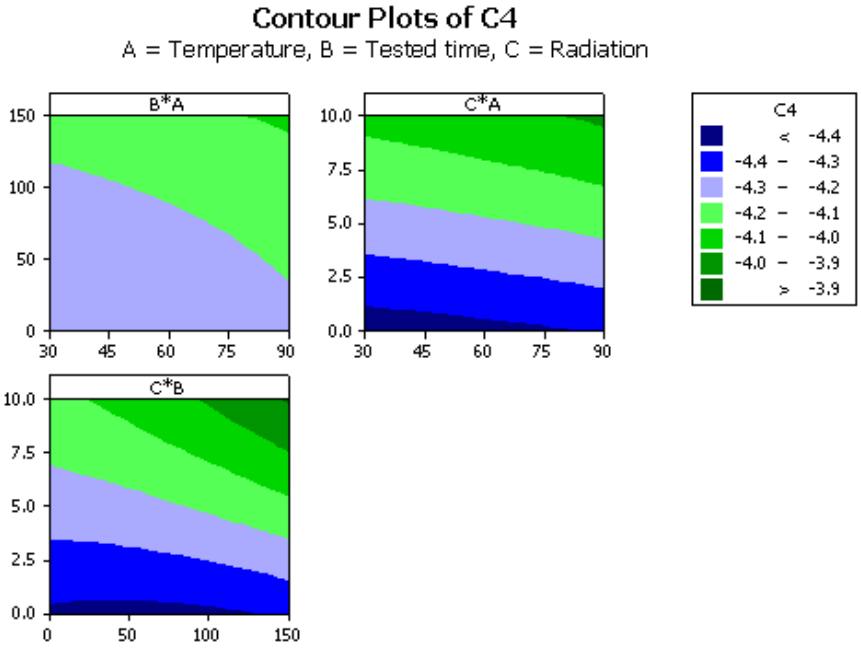

Fig. 14. Contour plots of stress parameters.

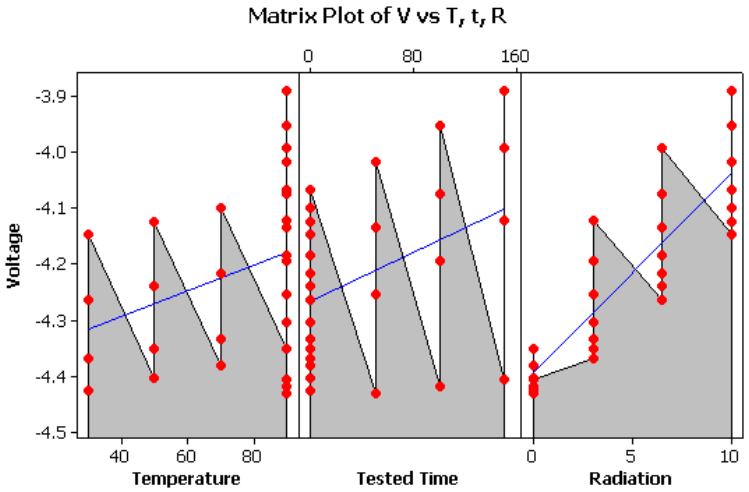

Fig. 15. Matrix plots of stress parameters.

predicts failure time. This model uses explanatory variables to explain changes in the response variable, for example why some products fail quickly and some survive for a long time. From the Regression Table, you get the coefficients for the regression model. For a Weibull distribution, this model describes the relationship between temperature and failure time for the insulation:

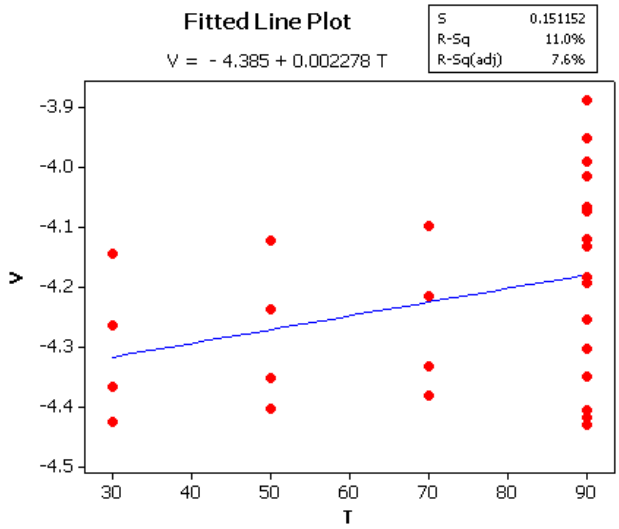

Fig. 16. Fitted line plot with temperature.

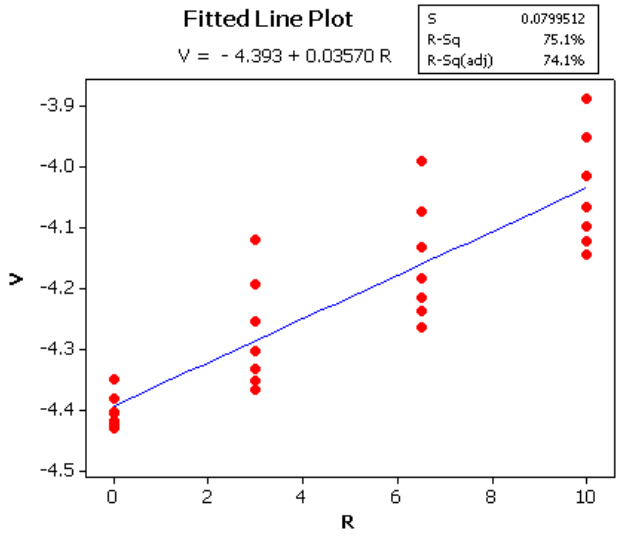

Fig. 17. Fitted line plot with radiation.

Log (failure time) = Intercept + V (Parameter) + Shape * εp (pth-percentile of the standard extreme value distribution).

The best factor analysis using variability of each parameter and its interactions are calculated using Pareto Chart in Fig. 22. From this figure, it was observed that the radiation has larger impact or dominant stress parameter of the CFD and second to that is temperature and radiation interaction.

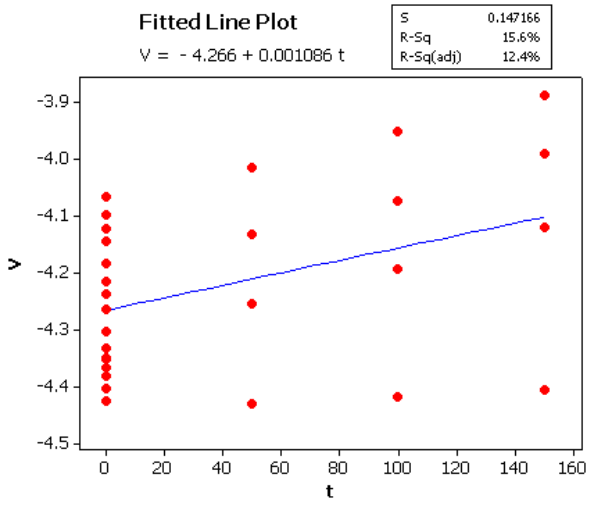

Fig. 18. Fitted line plot with time.

One-way ANOVA of temperature, radiation and time stress parameters with the output voltage is shown in Tables 4, 5 and 6.

Table 4. One-way ANOVA of temperature parameter.

Source	DF	SS	MS	F	P
A	3	0.0795	0.0265	1.08	0.376
Error	24	0.5880	0.0245		
Total	27	0.6676			

Note: $S = 0.1565$, $R - \text{Sq} = 11.91\%$, $R - \text{Sq(adj)} = 0.90\%$, Pooled StDev = 0.1565.

Table 5. One-way ANOVA of radiation parameter.

Source	DF	SS	MS	F	P
A	3	0.50312	0.16771	24.48	0.0000
Error	24	0.16444	0. 00685		
Total	27	0.66756			

Note: $S = 0.08277$, $R - \text{Sq} = 75.37\%$, $R - \text{Sq(adj)} = 72.29\%$, Pooled StDev = 0.0828.

Table 6. One-way ANOVA of temperature parameter.

Source	DF	SS	MS	F	P
A	3	0. 1045	0. 0348	1.49	0.244
Error	24	0.5630	0. 0235		
Total	27	0.6676			

Note: $S = 0.1532$, $R - \text{Sq} = 15.66\%$, $R - \text{Sq(adj)} = 5.11\%$, Pooled StDev = 0.1532.

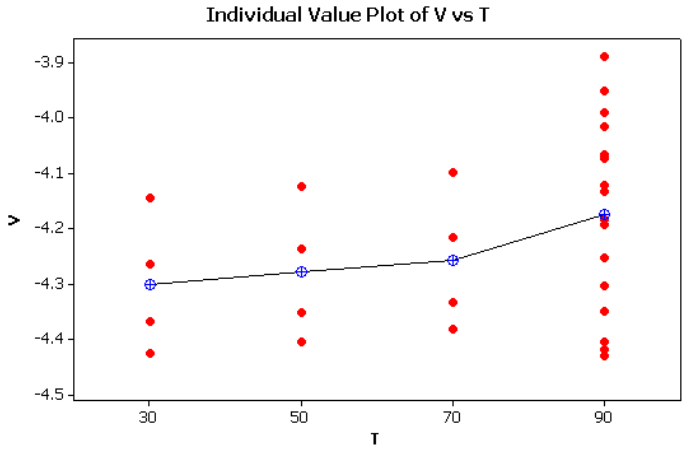

Fig. 19. Individual value plot of V versus T.

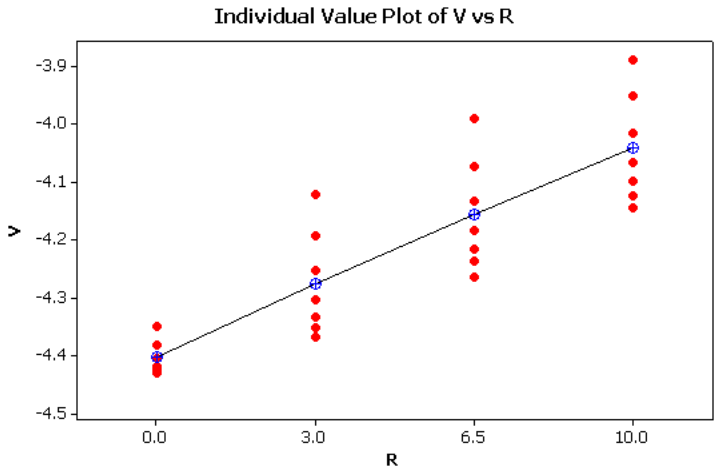

Fig. 20. Individual value plot of V versus R.

3.6. *SEM analysis*

The samples subjected to different stresses are inspected using Scanning Electron Microscope[13] after the decapsulation[14] of CFD ICs. The procedure is as follows:

(1) Grind the top layer of the plastic mould by grinder to etch the material faster.
(2) The following are the necessities for chemical etching; 95% Nitric Acid, Acetone, Beaker and plate, Tweezer and blower, Heater.
(3) Heat the nitric acid in the beaker for around 80°C to 100°C up to boiling.
(4) Remove the beaker from heater for controlled etching. Clip the IC with tweezers and carefully shake the IC and precaution to be taken care of not falling in the solution.

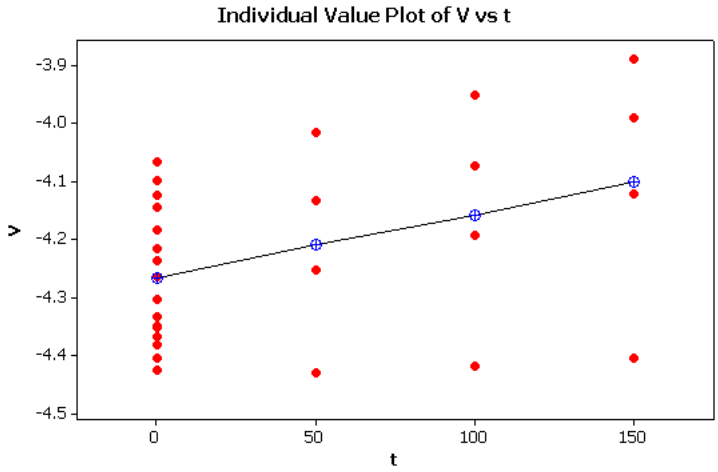

Fig. 21. Individual value plot of V versus t.

Table 7. Temperature versus voltage.

	Standard		90%		Normal CI	
Predictor	Coeff.	Error	Z	P	Lower	Upper
Intercept	29.851	18.071	1.65	0.099	−5.5678	65.2705
V	−6.7236	4.2868	−1.57	0.117	−15.126	1.67838
Shape	0.25104	0.0374			0.1875	0.33606

Note: Log − Likelihood = −62.457, Log (failure time) = 29.8513 − 6.72359T + 1/0.251041εp.

Table 8. Radiation versus voltage.

	Standard		90%		Normal CI	
Predictor	Coeff.	Error	Z	P	Lower	Upper
Intercept	37.395	10.172	3.68	0.0	17.4581	57.3322
V	−8.6109	2.4157	−3.56	0.0	−13.3455	−3.87614
Shape	0.71335	0.12031			0.512555	0.992812

Note: Log − Likelihood = −60.019, Log (failure time) = 5.74849−0.323077t + 1/4.17447εp.

Table 9. Accelerated time versus voltage.

	Standard		90%		Normal CI	
Predictor	Coeff.	Error	Z	P	Lower	Upper
Intercept	5.74849	1.1894	4.83	0	3.4173	8.07967
V	−0.3231	0.2821	−1.15	0.252	−0.876	0.229819
Shape	4.17447	0.7048			2.9984	5.81184

Note: Log − Likelihood = −125.202, Log (failure time) = 37.3952 − 8.61085T + 1/0.713352εp.

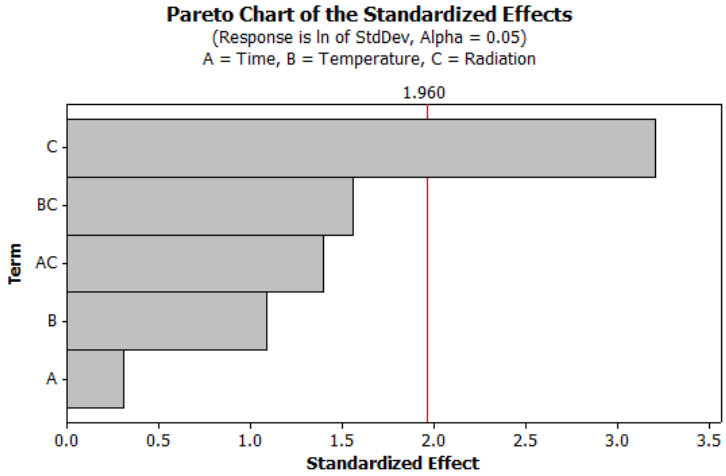

Fig. 22. Individual value plot of V versus t.

Table 10. Sample preparation for SEM analysis.

Screening	Radiation: 3 kGy	Radiation: 6 kGy	Radiation: 10 kGy
20	20	20	20
Temperature testing	5 samples at each step: 30, 50, 70 and 90		
Temperature testing	5 samples at each step: 30, 50, 70 and 90		
Decapsulation	2 Samples at each Radiation, temperature and accelerated test time.		
SEM	Taken 9 samples		

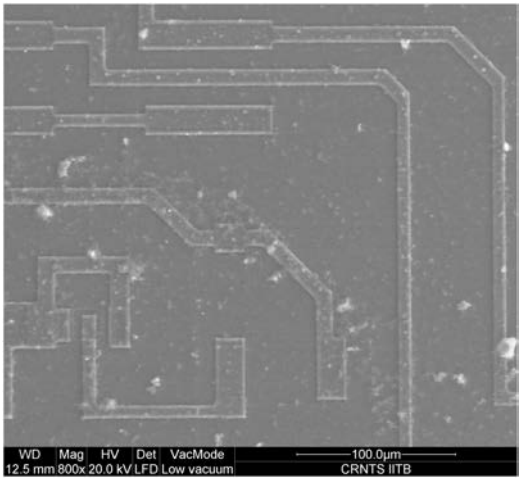

Fig. 23. SEM at $R = 0$, $T = 90°C$, Time $= 150$ h.

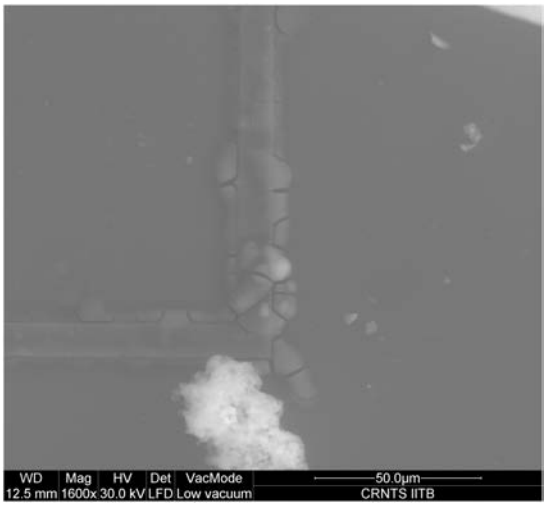

Fig. 24. SEM at $R = 3\,\text{kGy}$, $T = 90°\text{C}$, Time $= 0$.

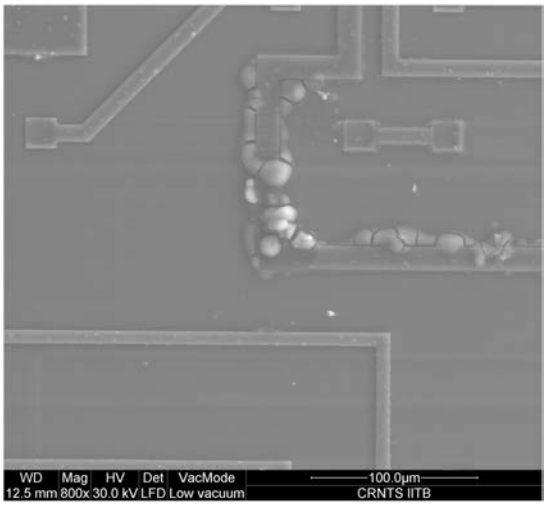

Fig. 25. SEM at $R = 3\,\text{kGy}$, $T = 90°\text{C}$, Time $= 150\,\text{h}$.

(5) Initially, the leads and plastic mould etches away and after careful controlled shaking and monitoring continuously to ensure that also the bond pads will not etch.
(6) To remove small traces of black spots of plastic mould, etch for few seconds in another clean nitric acid solution with moderate heat.
(7) Clean the etched IC with acetone in plate and blow the component to make it dry. Also, post-heat the IC for few seconds above heater plate.
(8) Inspect the layout of the component using microscope with 100X zoom.

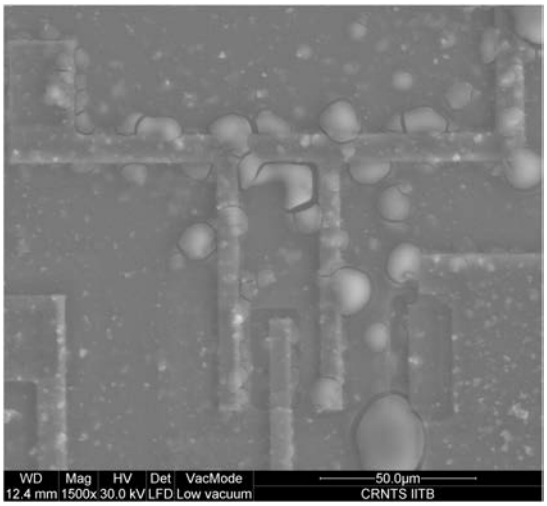

Fig. 26. SEM at $R = 6\,\text{kGy}$, $T = 30°\text{C}$, Time $= 0$.

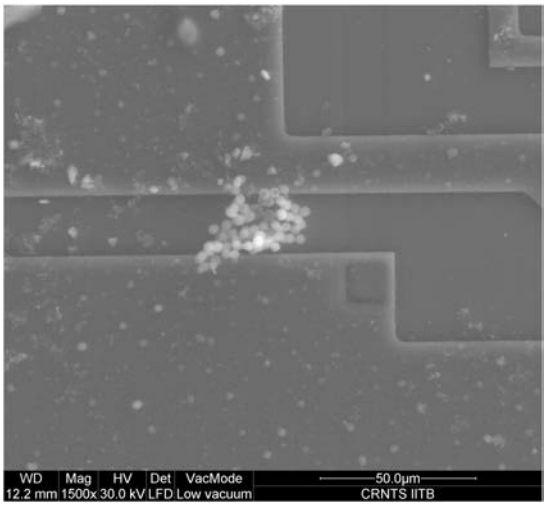

Fig. 27. SEM at $R = 6\,\text{kGy}$, $T = 90°\text{C}$, $t = 0\,\text{h}$.

The sample preparation for the failure analysis is collected as shown in Table 10. The SEM images at each of the stress steps are produced from Figs. 23–30.

The following observations are found out from the above SEM figures:

(1) The average defect size is from $10\,\mu$m to $50\,\mu$m.
(2) The defects in the layout increase with the increase in impact of radiation exposure.
(3) The effect temperature further degrades the material.

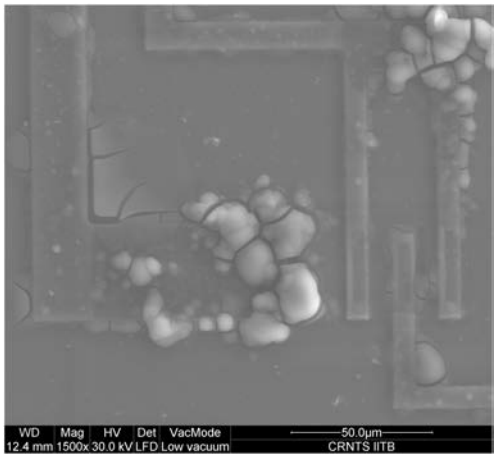

Fig. 28. SEM at $R = 6\,\text{kGy}$, $T = 90°\text{C}$, $t = 150\,\text{h}$.

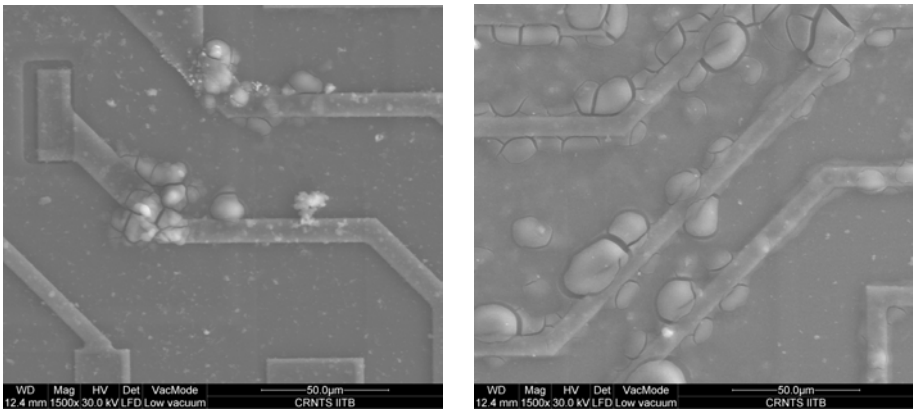

Fig. 29. SEM at $R = 10\,\text{kGy}$, $T = 90°\text{C}$, Time $= 0\,\text{h}$.

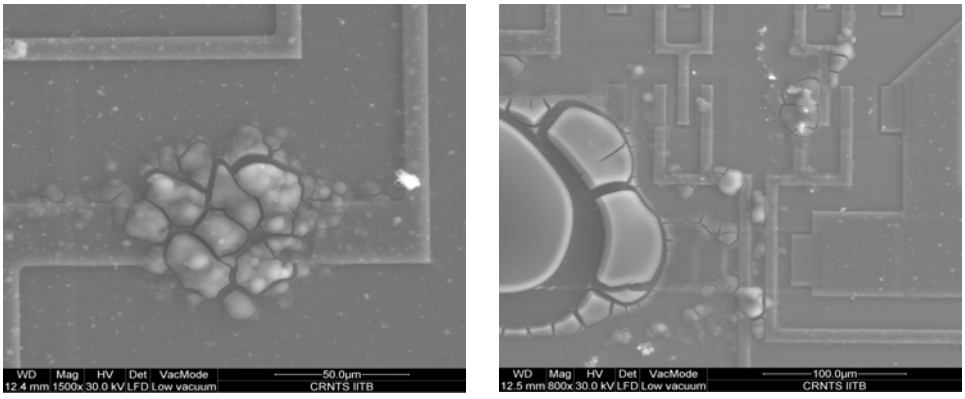

Fig. 30. SEM at $R = 6\,\text{kGy}$, $T = 30°\text{C}$, Time $= 0\,\text{h}$.

(4) Due to long extent of accelerated time on the sample, the defect density is enlarged by large amount.
(5) Most of the defects are found at the corners in the layout.
(6) To find the failure point locations from the layout information of CFD sample.

4. Conclusion

In this paper, functioning and importance of CFD in nuclear field is studied. Furthermore, reliability and degradation mechanisms that affects the performance of output pulse with temperature and dose rates acts as input characteristics was properly explained and verified with the experiments. Accelerated testing is carried out to define the life testing of the component with respect to degradation in output TTL pulse amplitude. The parametric analysis of stress variables are assessed with different methods to obtain detailed picture. The failure inspection was carried out on decapsulated samples of CFD by using SEM and it was found that the defect density generates more by increase in radiation dose and temperature which expose over the time.

References

1. L. W. Condra, *Reliability Improvement with Design of Experiments* (Marcel Dekker Inc., 2001).
2. W. Nelson, *Accelerated Testing: Statistical Models, Test Plans and Data Analysis* (John Wiley and Sons, 2004).
3. K. Luery, Failure of the constant fraction discriminator, Warsaw University of Technology (Jul 9, 2003).
4. K. Carnes, Constant fraction discriminators, *Tutorial*, James Macdonald Laboratory, Kansas State University (Jan 2003).
5. B. Van Zeghbroeck, Principles of electronic devices, University of Colorado (2011).
6. G. Wang and G. C. M. Meijer, The temperature characteristics of bipolar transistors fabricated in CMOS technology, *Sensors Actuators* **87** (2000) 81–89.
7. A. Christou, Reliability of high temperature electronics, Center for risk and reliability, University of Maryland (2006).
8. S. C. Witczak, R. D. Schrimpf, D. M. Fleetwood, K. F. Galloway, R. C. Lacoe, D. C. Mayer, J. M. Puhl, R. L. Pease and J. S. Suehle, Hardness assurance testing of bipolar junction transistors at elevated irradiation temperatures, *IEEE Trans. Nuclear Sci.* **44**(6) (1997) 1989–2000.
9. S. C. Witczak, R. D. Schrimpf, D. M. Fleetwood, K. F. Galloway, R. C. Lacoe, D. C. Mayer, J. M. Puhl, R. L. Pease and J. S. Suehle, Charge separation for bipolar transistors, *IEEE Trans. Nuclear Sci.* **40** (1993) 1276–1285.
10. R. D. Schrimpf, D. M. Schmidt, D. M. Fleetwood, R. L. Pease and W. E. Combs, Modeling ionizing radiation induced gain degradation of the lateral pnp bipolar junction transistor, *IEEE Trans. Nuclear Sci.* **43** (1996) 3032–3039.
11. R. H. Myers, D. C. Montgomery and C. M. Anderson-Cook, *Response Surface Methodology: Process and Product Optimization using Designed Experiments* (Wiley Series in Probability and Statistics, 2009).
12. *Meet Minitab 16*, Manual (2011).

13. P. L. Martin, *Electronic Failure Analysis Handbook Techniques and Applications for 42 Electronic and Electrical Packages, Components, and Assemblies* (McGraw-Hill, 1999).
14. ASM International, *Microelectronics Failure Analysis Desk Reference*, 5th edn. (ASM International, 2004).
15. Military Handbook, Mil-HDBK 217F: Reliability Prediction of Electronic Equipment (Dec 1991).
16. Joseph, Moshe, Electronic circuit reliability modeling, (2006).
17. Semiconductor device reliability failure models, SemaTech, AMD (2000).

About the Authors

Adithya Thaduri studied electronics and instrumentation engineering in Bachelors and reliability engineering in Masters. Presently, he is doing Ph.D. at Luleå University of Technology, Sweden and research fellowship at IIT Bombay, India in association with Bhabha Atomic Research Center, India. His core area of research is on predicting the life of critical electronic components using physics of failure approach.

A. K. Verma is currently a Professor in Engineering (Technical Safety), Stord/Haugesund University College, Haugesund, Norway and has been a Professor (since February 2001) with the Department of Electrical Engineering at IIT Bombay (away on lien from IIT Bombay). He was the Director of the International Institute of Information Technology Pune, on lien from IIT Bombay, from August 2009–September 2010. He is also a Guest Professor at Luleå University of Technology, Sweden. He has supervised/co-supervised 35 Ph.D.s and 95 Masters theses in the area of software reliability, reliable computing, power systems reliability (PSR), reliability centered maintenance (RCM) and probabilistic safety/risk assessment (PSA) and use of computational intelligence in system assurance engineering and management. He is the Chairman of the recently constituted Special Interest Group on System Assurance Engineering and Management of Berkeley Initiative in Soft Computing, Department of Electrical Engineering and Computer Science, University of California, Berkeley. He is an author of books titled *Fuzzy Reliability Engineering — Concepts and Applications* (Narosa), *Reliability and Safety Engineering* (Springer) and *Dependability of Networked Computer-Based Systems* (Springer) and *Optimal Maintenance of Large Engineering System* (published by Narosa). He has over 225 publications in various journals (over 100 papers) and conferences. He has been the Editor-in-Chief of OPSEARCH published by Springer (January 2008–January 2011) as well as the Founder Editor-in-Chief of International Journal of Systems Assurance Engineering and Management (IJSAEM) published by Springer and the Editor-in-Chief of *SRESA Newsletter* and *Journal of Life Cycle Reliability and Safety Engineering*. He is also the Series Editor along with Prof. Roy Billinton and Prof. Rajesh Karki of Springer Book Series "Reliable and Sustainable Electric Power and Energy Systems Management" and has jointly edited the book *Reliability and Risk Evaluation of Wind Integrated Power Systems* also published

by Springer. He has been a Guest Editor of a dozen issues of international journals including *IEEE Transactions on Reliability* and has been the Editor of several conference proceedings.

V. Gopika, a graduate of 37th batch of BARC Training School, joined Reactor Safety Division, BARC in 1994. She has made significant contributions in the area of probabilistic safety assessment (PSA). She has actively participated in the PSA studies of AHWR and research reactors, Fire PSA, risk informed in-service inspection methods for piping systems in DAE facilities and in the development of risk monitor. She has conducted extensive research on applicability of risk informed in-service inspection methods which have resulted in formulating a complete framework. She has successfully translated the research methods into the application framework. The most important contributions are the introduction of a new importance measure, incorporating the effects of in-service inspection through Markov model and using genetic algorithm for optimizing inspection. She would later extend her research for chalking out the RI-ISI program for nuclear power plants as well as in heavy water plants. She has co-authored a standard for applying the risk-based inspection and maintenance procedures, for European industry.

Rajesh Gopinath is working at Electronics Division at Bhabha Atomic Research Center, Bombay, India for eight years. His research includes the selection and design of electronic parts which are used in the signal conditioning unit of nuclear reactor. He analyzes the reason for failure of components and accordingly designs the circuits for effective performance.

Uday Kumar obtained his B.Tech from India during the year 1979. After working for six years in Indian mining industries, he joined the postgraduate program of Luleå University of Technology, Luleå, Sweden and obtained a Ph.D. degree in Field of Reliability and Maintenance during 1990. He worked as a Senior Lecturer and Associate Professor at Luleå University from 1990–1996. In 1997, he was appointed as a Professor of Mechanical Engineering (Maintenance) at University of Stavanger, Stavanger, Norway. Since July 2001, he has taken up the position as a Professor of Operation and Maintenance Engineering at Luleå University of Technology, Luleå, Sweden. Currently he is the Director of Luleå Railway Research Center. His research interests are equipment maintenance, reliability and maintainability analysis, etc. He is also Member of the editorial boards and reviewer for many international journals. He has published more than 150 papers in international journals and conference proceedings.

Paper V

P5

Failure Modeling of Constant Fraction Discriminator using Physics-of-failure Approach

Thaduri, A., Verma, A.K., Vinod, G., Rajesh, M.G., Kumar, U. (2013). Failure Modeling of Constant Fraction Discriminator using Physics-of-failure Approach. *International Journal of Reliability, Quality and Safety Engineering*, 20(3), pp. 134002-1 – 134002-26.

International Journal of Reliability, Quality and Safety Engineering
Vol. 20, No. 3 (2013) 1340002 (26 pages)

DOI: 10.1142/S0218539313400020

World Scientific
www.worldscientific.com

FAILURE MODELING OF CONSTANT FRACTION DISCRIMINATOR USING PHYSICS OF FAILURE APPROACH

ADITHYA THADURI
Division of Operation and Maintenance
Luleå University of Technology
Luleå, Sweden
adithya.thaduri@gmail.com

A. K. VERMA
Stord/Haugesund University College
Haugesund, Norway
akvmanas@gmail.com

V. GOPIKA* and RAJESH GOPINATH†
RSD, BARC, Trombay, Bombay, India
**vgopika@barc.gov.in*
†*rajeshgopin@gmail.com*

UDAY KUMAR
Division of Operation and Maintenance
Luleå University of Technology
Luleå, Sweden
Uday.Kumar@ltu.se

Received 30 August 2012
Revised 10 November 2012
Accepted 6 May 2013
Published 13 June 2013

Due to several advancements in the technology trends in electronics, the reliability prediction by the constant failure methods and standards no longer provide accurate time to failure. The physics of failure methodology provides a detailed insight on the operation, failure point location and causes of failure for old, existing and newly developed components with consideration of failure mechanisms. Since safety is a major criteria for the nuclear industries, the failure modeling of advanced custom made critical components that exists on signal conditioning module are need to be studied with higher confidence. One of the components, constant fraction discriminator, is the critical part at which the failure phenomenon and modeling by regression is studied in this paper using physics of failure methodology.

Keywords: Constant fraction discriminator; physics of failure; failure modeling; design of experiments; accelerated testing.

1. Introduction

The reliability of electronic systems, used in nuclear power plants, is traditionally estimated with empirical databases such as MIL-HDBK-217,[1] PRISM, etc. These methods assign a constant failure rate to electronic devices, during their useful life. The constant failure rate assumption stems from treating failures as random events. Currently, electronic reliability prediction is moving towards applying the Physics of Failure approach[2] which considers information on process, technology, fabrication techniques, materials used, etc.

The new microelectronic devices often exhibit infant mortality and wear-out phenomena while in operation in the nuclear field. It points to competing degradation mechanisms-electro-migration, hot carrier injection, dielectric breakdown, etc., that makes a device's useful life different from that predicted by empirical methods. The understanding that the dominant mechanisms lead to device failure — Physics of Failure — is a more realistic approach to reliability prediction. This paper describes degradation mechanisms and modeling encountered in constant fraction discriminator (CFD) with consideration of stress parameters like temperature and radiation over the accelerated time. Failure modeling has been carried out on the components considering the data acquired from experimentation with inputs from physics of failure.

Neutron flux monitoring system (NFMS) comprises of different modules (Pulse Translator, Logarithmic Count Rate, Mean-Square Value Processor, etc.) that process pulse and current signals from detector which is present in the signal conditioning circuitry. Besides, there are modules that generate trip signals. Trip signals are of 24V level and optically isolated.

There are different electronic components in NFMS namely, Optocoupler, Instrumentation Amplifier, voltage comparators, etc., and CFD is the most critical part of the module. This component provides safety to the system and early failure of the component results in breakdown of the whole module. Hence, the more efficient prediction of time to failure is needed to define the replacement policy for the component.

2. Methodology

The following methodology was applied for the reliability prediction of CFD as shown in Fig. 1.

2.1. *Description of component*

The basic initial step for this procedure is the detailed description of the component. The vast information is needed from all the sources either from the field data or from the available literature. The comprehensive information of the component at root level such as block diagram inside chip, wafer process, construction, and materials used, computer-aided design (CAD), etc., are required for conducting

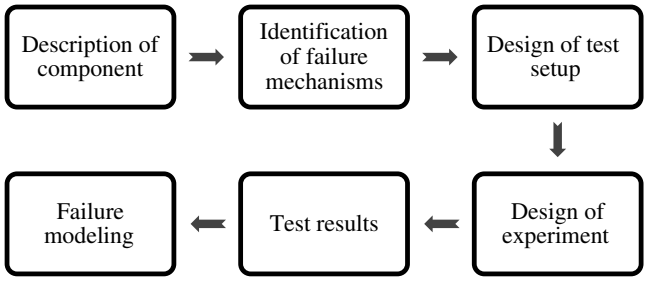

Fig. 1. Methodology for reliability prediction of CFD.

physics of failure. The functioning of the device also must and should consider to make appropriate idea of possible ways of failure mechanisms, failure modes and degradation mechanisms. Further this component is used at failure site, and environmental and electrical stress factors have major influence on the performance of the component pertaining to the operating conditions. The accuracy of the reliability prediction depends on the availability of the data.

2.2. *Identification of possible failure mechanism and stress parameters*

There are several failure mechanisms related to several environmental and electrical stress parameters.[3] This step involves finding out potential stress factors and consequently dominant failure mechanisms (or degradation) which relates to the functioning of component. Initially, performance factors are selected as output parameters and from the knowledge and functioning of component, possible ways of stress parameters and levels are to be identified. This is the critical part which makes sense to the overall procedure because incorrect selection of these parameters makes the component resistant to these stress parameters which lacks the basic idea of this approach. From the reliable sources of information, these stress parameters are chosen and correspondingly failure behavior also to be recognized. The degradation mechanism can be identified from experimental data, from the literature review and from the field data.

2.3. *Design of test setup*

As everything planned from stress levels and parameters, performance parameters and sample size, actual experiment is carried out using experimental setup. For each component it is different and depends on the stress and performance parameters. A printed circuit board (PCB) is designed using tools by making necessary circuit and all electrical and environmental source and measurable equipments are attached to make a robust experimental setup.

2.4. *Design of experiments*

After selection of all stress and performance parameters, the next step is to run design of experiments.[4] Appropriate stress levels and sample size are selected. The design of experiments (DOE) is carried out in two stages: screening stage and testing stage.

2.4.1. *Screening stage*

To know the influence of stress parameter levels on the performance parameter, this stage is implemented. Effects of stress levels are studied and further action is taken on next stage for further expanding the range of stress levels by considering the effect on performance parameters.

2.4.2. *Testing stage*

From the feedback of the screening stage, appropriate stress levels are selected and it is tested. Response table is generated including the two stages which provide information on effect of variation of stress parameter levels on performance parameters.

2.4.3. *Accelerated testing*

Traditional life data analysis involves analyzing times-to-failure data (of a product, system or component) obtained under normal operating conditions in order to quantify the life characteristics of the product, system or component. In many situations, and for many reasons, such life data (or times-to-failure data) is very difficult, if not impossible, to obtain. The reasons for this difficulty can include the long life times of today's products, the small time period between design and release and the challenge of testing products that are used continuously under normal conditions. Given this difficulty, and the need to observe failures of products to better understand their failure modes and their life characteristics, reliability practitioners have attempted to devise methods to force these products to fail more quickly than they would under normal use conditions. In other words, they have attempted to accelerate their failures.[5] Over the years, the term accelerated life testing has been used to describe all such practices. From the selected stress levels in response table, accelerated testing is carried out. A failure criterion is also mentioned here for further analysis.

2.5. *Test results*

From the enormous amount of data produced from experimental setup, the information required for the failure modeling can be selected.

2.6. *Failure modeling*

From the selection of stress parameters and failure mechanisms, appropriate failure modeling needs to be implemented. There is several failure models for each failure mechanism at various levels are described in literature. Depending upon the component specifications, time to failure model for particular failure mechanism is picked up. For the some of the cases, dominant failure mechanisms is not restricted to the above list but the literature or design of modeling needs to be considered. Reliability metrics are calculated on basis of failure modeling from experimental data.

3. Constant Fraction Discriminator

3.1. *Description of component*

CFD is another device which is failing regularly in the nuclear field at Bhabha Atomic Research Center (BARC). This device is made up of bipolar junction technology (BJT). It is a level discriminator at which it provides a pulse when the analog input reaches particular voltage level. The possible failure mechanisms for this device is electro-migration and hot carrier injection. Temperature and incident radiation are considered as stress parameters. These parameters effect the operation of BJT transistors inside to reduce the output voltage which further reduces the performance parameter which in this case is voltage of output pulse. There is a constraint in the experimentation that both the stress parameters cannot be applied simultaneously instead of one after another. The effect of individual parameter is quantified on voltage output and degradation of whole device is studied. The selection of stress levels can be carried out by using DOE and accelerating testing is implemented. Since there is no sufficient physics model available for this device, modeling is to be carried out by data acquired from experimental analysis. This model with failure information and experimentation has better confidence than conventional constant failure rate prediction models. From the model, relation between design parameters and time to failure is observed and provided to designer.

Discriminators generate logic pulses in response to input signals exceeding a particular threshold. In general, there are two main types of discriminators, the leading edge discriminator and the CFD. The leading edge discriminator is the simpler one. Given an input pulse, the leading edge discriminator produces an output pulse at the time when the input pulse crosses a given threshold voltage. This, however, causes a problem in situations where the timing is important. If the amplitude is changed, but the rise time of the input pulse remains the same, a sort of "time walk" occurs (Fig. 2)[6] with the output voltage over the operational time. That is, an input pulse with smaller amplitude but with the same rise time as a larger pulse will cross the threshold at a later time. Thus, the timing of the output pulse is shifted by this change in amplitude.

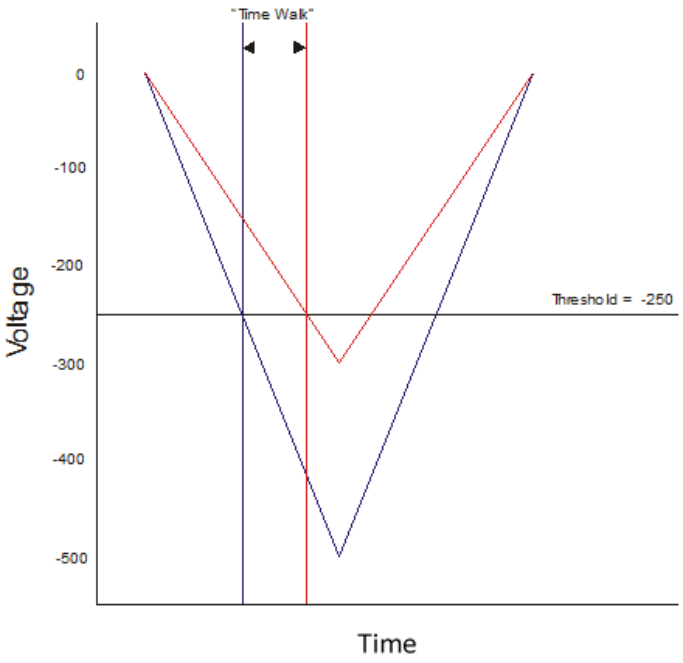

Fig. 2. Leading edge discriminator and "time walk".[6]

The CFD alleviates this problem by using a constant fraction, f, of the input pulse to precisely determine the timing of the output pulse relative to the input signal. It does this by splitting the input signal (Fig. 3): attenuating one half so that it is a certain fraction, f, of the original amplitude (Fig. 4), and delaying and inverting the other half (Fig. 5).

The attenuated pulse and the delayed and inverted pulse are then added together, and the zero crossing is computed (Fig. 6).

The zero crossing gives the time at which the CFD should create an output pulse, and is always independent of amplitude. For a simple linear ramp, like the one shown above, the equations for its input pulse, attenuated pulse, and delayed and inverted pulse are as follows: td = delay, f = fraction, A = initial amplitude, $Vi = At$ = input pulse and $Vd = A(t - td)$ = delayed and inverted pulse.

To find the zero crossing, set $Va + Vd = 0$ and solve for t:

$$0 = -fAt + A(t - td) \Rightarrow t_{\text{cross}} = \frac{td}{1 - f}. \tag{1}$$

Ideally, the delay is chosen such that the maximum of the attenuated pulse crosses at the desired fraction of the delayed pulse. In that case, $td_{\text{ideal}} = t_{\text{rise}}(1-f)$. However, if the delay is chosen smaller than t_{d_ideal}, CFD will operate at a fraction less than that of f. From Eq. (1), it was seen that t_{cross} is independent of the amplitude of the input pulse. The CFD has a monitor output feature, which outputs the bipolar

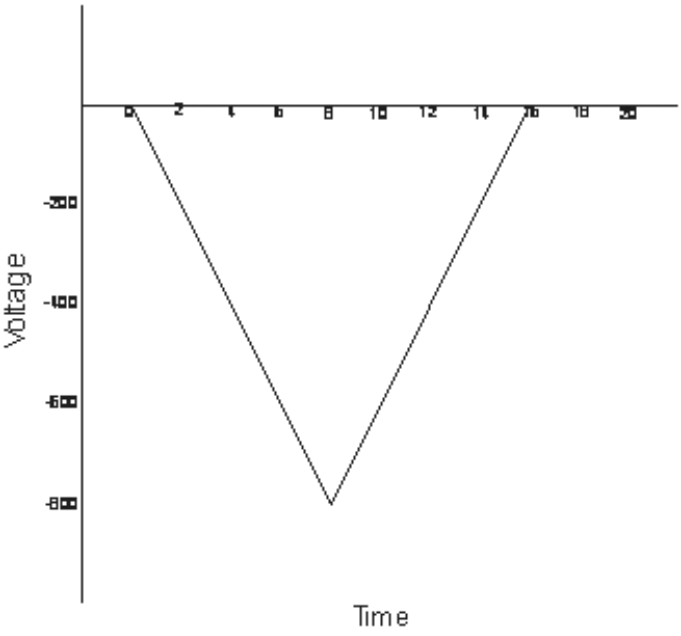

Fig. 3. Input pulse to CFD.[6]

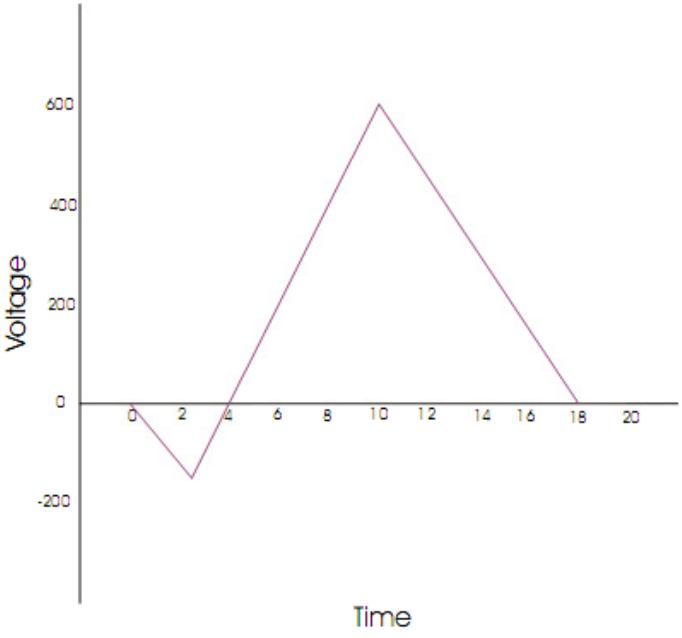

Fig. 4. Attenuated pulse.[6]

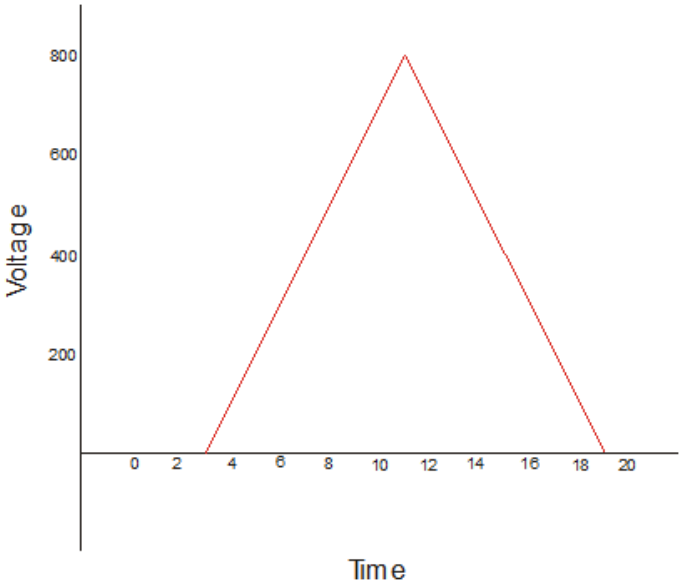

Fig. 5. Delayed and inverted pulse.[6]

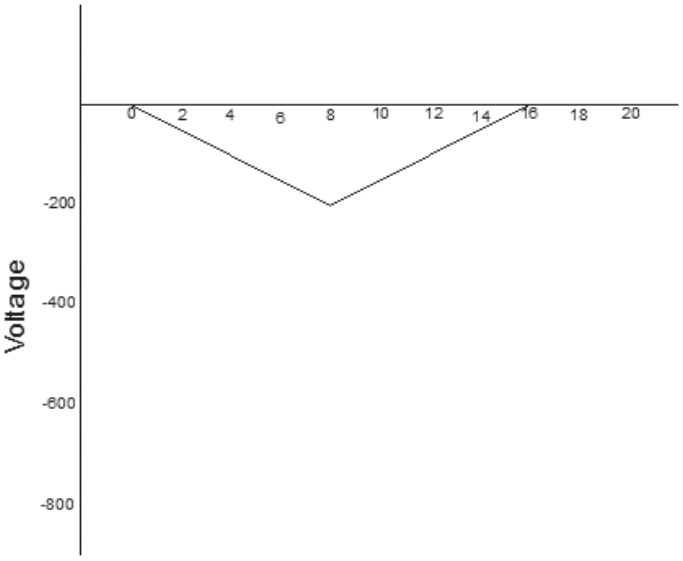

Fig. 6. Sum of attenuated and delayed inverted pulses.[6]

signal created by summing the attenuated and the delayed and inverted pulses, so that it can be viewed to how CFD is calculating the zero crossing.[7]

As in the block diagram, Fig. 7, in order to achieve a constant timing edge, it is customary to use an attenuator and a delay. The input signal is split. One

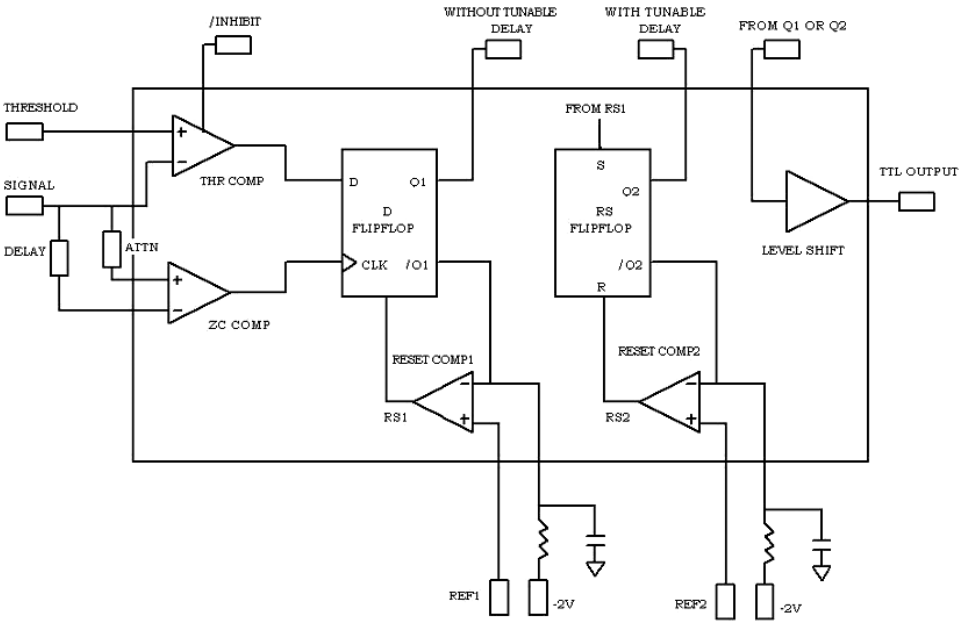

Fig. 7. Block diagram of CFD.

part is delayed, and the other is attenuated. After these two signals are re-mixed, a comparator detects the zero cross points. The timing of the zero cross point is not influenced by the amplitude of the input signal.

The output pulse from CFD is fed to the tripper and this tripper will trigger the system when it reaches a particular level of threshold voltage. If the level of the output pulse does not meet the specified level, the activation signal does not generate and will lead to the breakdown of the module which concerns the safety of the system. Hence the failure criteria are considered as 5% of the initial designed value.

3.1.1. *Block diagram of CFD* 2004

The principle of operation of CFD is demonstrated as in the block diagram shown in Fig. 7.

3.2. *Identification of possible failure mechanism and stress parameters*

The constant fraction discriminator (CFD) 2004 is made by Bharat Electronics Limited (BEL), Bangalore, India. Comparators and flip flops as shown in Fig. 7 consist of transistors made up of BJT Technology. So, the failure physics of these transistors at wafer level adversely affects the performance and failure of CFDs. As from the description, if the wave from the counter expects to cross at a threshold level,

CFD must provide TTL pulse. Failure possibly happens if the threshold level at the input and the pulse width at the output varies in accordance with the prescribed level with the existing internal parameters. By the physics of failure approach, the stress parameters affect the BJT transistors to change their behavior of electrical *h*-parameters. Commonly, when an electrical or temperature stress applied on the transistor, they develop reverse current from emitter to base to increase in such a way to degrade the performance of output electrical characteristics such as collector current and V_{CE} voltage at the output. If these values change inside the device, as all other devices are interconnected, these effective voltages and currents tend to vary at the larger levels of the whole device and output pulse width and time periods change. If this change is large such that it cannot detect the input pulse providing the output TTL, then it is considered as failure.

3.2.1. *Effect of temperature*

The temperature dependence of bipolar transistors depends on a multitude of parameters affecting the bipolar transistor characteristics in different ways. Important effect is the temperature dependence of the current gain since the current gain depends on both the emitter efficiency and base transport factor.[8]

The emitter efficiency depends on the ratio of the carrier density, diffusion constant and width of the emitter and base. As a result, it is not expected to be very temperature-dependent. The carrier densities are linked to the doping densities. Barring incomplete ionization, which can be very temperature-dependent, the carrier densities are independent of temperature as long as the intrinsic carrier density does not exceed the doping density in either region. The width is very unlikely to be temperature-dependent and therefore also the ratio of the emitter and base width. The ratio of the mobility is expected to be somewhat temperature-dependent due to the different temperature dependence of the mobility in *n*-type and *p*-type material.

The base transport is more likely to be temperature-dependent since it depends on the product of the diffusion constant and carrier lifetime. The diffusion constant in turn equals the product of the thermal voltage and the minority carrier mobility in the base. The recombination lifetime depends on the thermal velocity. The result is therefore moderately dependent on temperature. Typically the base transport reduces with temperature, primarily because the mobility and recombination lifetime are reduced with increasing temperature. Occasionally the transport factor initially increases with temperature, but then reduces again.

Temperature affects the AC and DC characteristics of transistors. The two aspects to this problem are environmental temperature variation and self-heating. Some applications, like military and automotive, require operation over an extended temperature range. Circuits in a benign environment are subject to self-heating, in particular high power circuits.

Leakage current ICO and β increase with temperature. The DC β hFE increases exponentially. The AC β hFe increases, but not as rapidly. It doubles over the

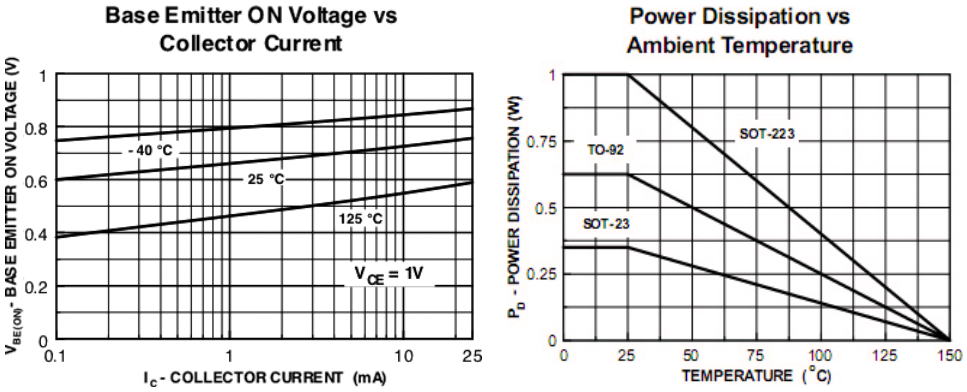

Fig. 8. I_c versus V_{BE} and power dissipation versus temperature.[10]

range of −55°C to 85°C. As temperature increases, the increase in hFe will yield a larger common-emitter output, which could be clipped in extreme cases. The increase in hFE shifts the bias point, possibly clipping one peak. The shift in bias point is amplified in multi-stage direct-coupled amplifiers. The solution is some form of negative feedback to stabilize the bias point. This also stabilizes AC gain.[9] The change in the device parameters with the temperature is shown in Fig. 8.

The impact of temperature changes the device parameters at different levels and it can be reflected in overall performance. The emitter and collector current of npn BJT is given as Eqs. (2) and (3).[9]

$$I_{\mathrm{E}} = I_{\mathrm{ES}} \left(e^{\frac{Vbe}{Vt}} - 1 \right), \tag{2}$$

$$I_{\mathrm{C}} = \alpha\, TIES \left(e^{\frac{Vbe}{Vt}} - 1 \right). \tag{3}$$

The output voltage V_{CE} is given as in Eq. (4)

$$V_{\mathrm{ce}} = V_{\mathrm{cc}} - IcR_{\mathrm{eff}}, \tag{4}$$

where R_{eff} is effective output resistance at the output, I_{ES} = reverse saturation current at base-emitter diode, α_{T} = common base forward short circuit gain, V_{T} = thermal voltage kT/q, V_{BE} = base-emitter voltage, V_{CE} = base-collector voltage, V_{CC} = source voltage typically 5 V/10V.

In Eber–Moll model, I_{C} grows at about 9%/°C if you hold V_{BE} constant and V_{BE} decreases by 2.1 mV/°C if you hold I_{C} constant with the temperature.

Since both the currents depend on temperature parameter V_{T}, the raise in the temperature leads to vary these parameters which finally lead to degrade the performance of CFD.

3.2.2. *Effect of radiation*

Another stress parameter which degrades the BJT devices is cobalt β-radiation. Degradation of many types of bipolar transistors and circuits is known to depend strongly on dose rate. For a given total dose, degradation is more severe in low dose rate exposure than high dose rate exposure. This effect has been attributed to space charge effects from trapped holes and hydrogen related species through oxygen vacancies in base oxide. There are several hardness assurance tests and most popular has been high dose rate irradiation at elevated temperatures[11] as shown in Fig. 9.

Although radiation exposure generally leads to grain degradation in npn and pnp devices, the mechanisms by which radiation affects their gains are quite different. Ionizing radiation degrades the current gain of npn bipolar transistors by introducing net trapped positive charge and interface traps into the oxide base. This positive oxide trapped charge spreads the emitter-base depletion region into the extrinsic base results in increase of base recombination current under forward-bias operation at the junction. Radiation-induced interface traps, especially those near mid-gap, serve as generation-recombination centers through which recombination current in the base is further increased due to enhanced surface recombination velocity. In pnp transistors,[12] near-midgap interface traps in the base oxide also increase the base current by surface recombination. Compared with npn transistors, radiation-induced net positive oxide trapped charge can mitigate gain degradation by creating an imbalance in carrier concentrations at the surface of the base.

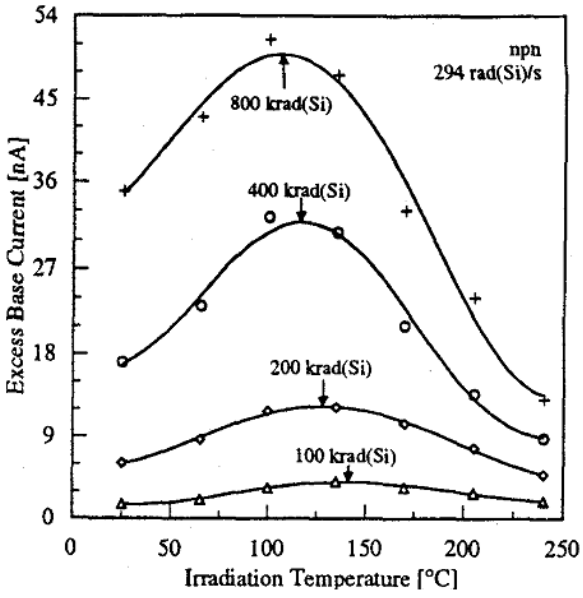

Fig. 9. Effect of excess base current with irradiation temperature.[11]

From the statistical results explained in Witczak *et al.*,[11] current gain degradation grows worse with decreasing dose rate regardless of dose. Excess base current, an increase in base current due to radiation exposure, increases gradually with decreasing dose rate. This effect is due to weak dependence of excess base current on radiation-induced defect densities at large total dose. Changes in collector current as compared to base current is small because it provides meaningful assessment of amount of gain degradation while relating closely to the physical mechanisms, excess base current is a convenient parameter to evaluate radiation-induced damage in these devices.[13]

Although much progress has been made in understanding the effects of dose rate and temperature on radiation-induced bipolar gain degradation, still there is ambiguity in selecting the optimum values for assurance testing. From the analysis carried out by Witczak *et al.*,[11] the combined influence of both radiation and temperature has considerable dependence on gain degradation and excess base current enhancement. The combined effect of temperature and radiation results in degradation of performance parameters such as threshold voltage, pulse amplitude and time period of CFD.

3.3. *Design of test setup*

CFD 2004 of BJT technology from manufacturers of BEL is considered for this study. It is 24-pin DIP plastic package with operating conditions as shown in Fig. 10: −5.2 to 5 V and temperature 100°C. In order to monitor and test this IC for temperature and radiation considering time, a circuit is required to assess and measure it. Figure 11 shows the conditional measuring circuit for this failure testing. This circuitry is designed such that the output voltage delivers irrespective of the external components and purely to provide output voltage dependence. As can be seen, along with IC, several other components are also required to measure the performance parameters such as Inverter (to invert the positive pulse to negative pulse input which is not shown in figure), resistors, capacitors, etc. These components are also sensitive to temperature which affects the measurement.

Hence, the circuit is divided to two parts: CFD part and measurement part as in Fig. 12. In this way, effect of temperature lies only on CFD. The board of CFD part is also holed out at the bottom of IC to expose it with sufficient temperature. A thermistor is placed across IC to continuously monitor the temperature of it.

3.4. *Design of experiment*

From the research, temperature and radiation dose rate are considered as stress parameters for the degradation of performance of CFD. The performance parameters include threshold voltage which is at the input and transistor-transistor logic (TTL) pulse amplitude at the output. From the Taguchi method of design of experiments,[4] selection of this temperature levels is considered such that integrated

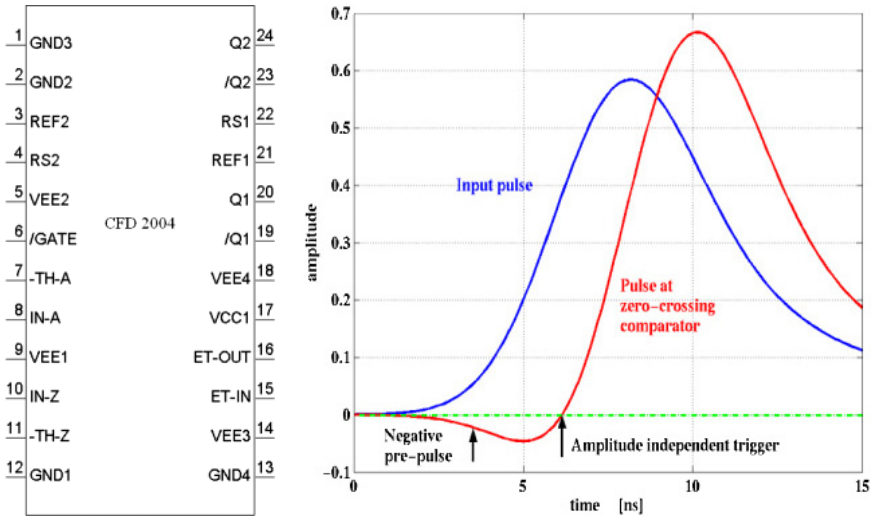

Fig. 10. CFD P in configuration and general demonstration of working of CFD with input pulse.

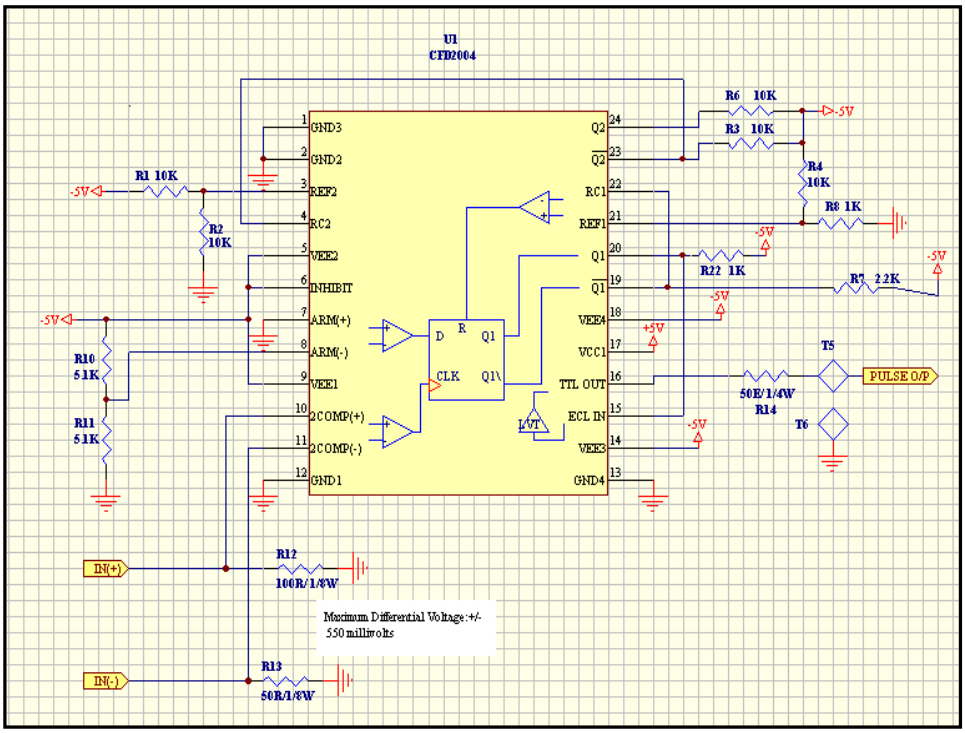

Fig. 11. Circuit diagram of CFD.

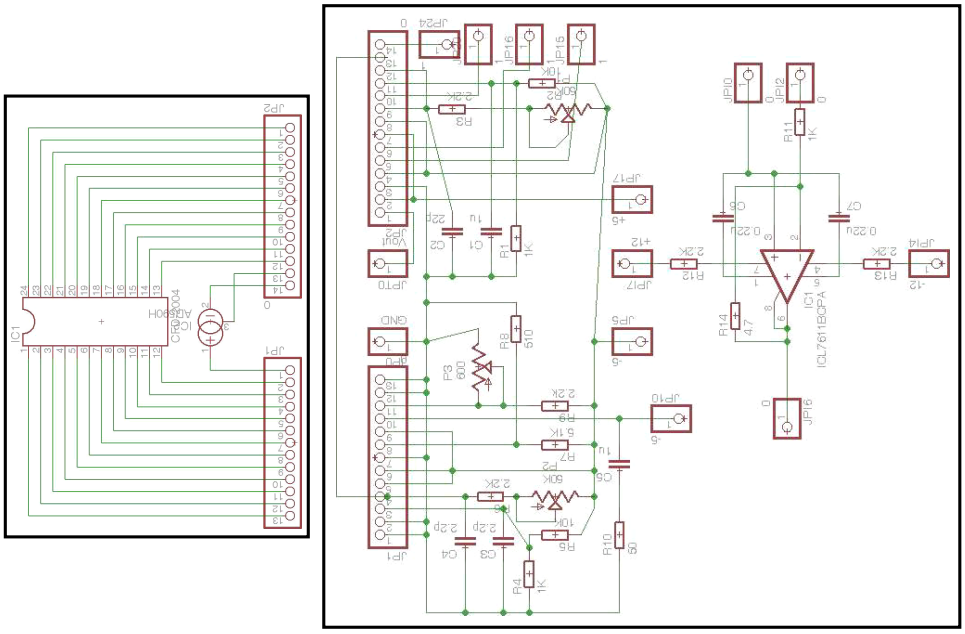

Fig. 12. Board diagram of CFD and measurement circuit.

circuit (IC) provides optimum performance. Testing can be done in two steps: Basic and Extensive testing for analysis of CFD.

3.4.1. *Stage* 1: *Basic testing*

3.4.1.1. Screen testing

The radiation and temperature are the dominant stress parameters. Initially the device is exposed to radiation under biased conditions. Thereafter it is exposed to temperature. The selection parameters can be done using 2-stage DOE. Accelerated testing is carried out from the data acquired from DOE to define time to failure of device using Response Surface method.[14]

The importance of DOE used here is to find out potential stress levels of each stress parameters to provide maximum degradation for accelerated testing. This step-by-step parametric analysis of stress levels has advantage of reducing the testing time and number of sample size.

Radiation testing

In this study, variation of pulse amplitude and time period in accordance with the radiation dose rate is calculated.

Figure 13 shows the variation of output pulse amplitude with respect to the dose rate. There is some little change in the output at higher dose rate.

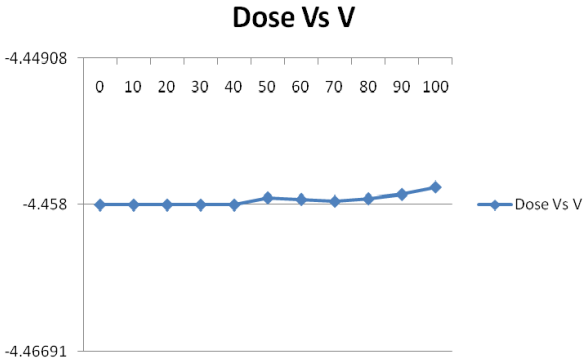

Fig. 13. Variation of pulse voltage versus dose rate.

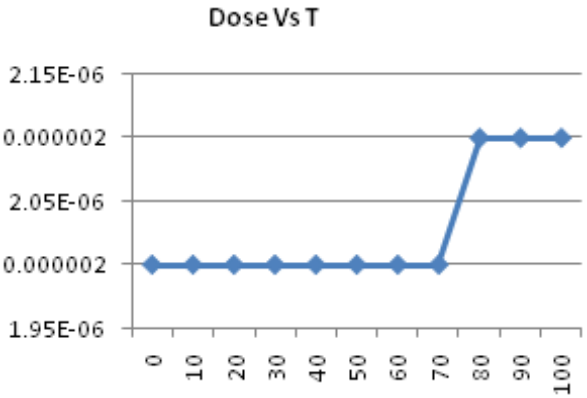

Fig. 14. Variation of time period versus dose rate.

Similarly, Fig. 14 shows the variation of time period with dose rate. As from these results, dose rate at 80 rads makes considerable change in the time period. This result depicts some change in performance parameters with radiation.

Temperature testing

In this study, variation of pulse amplitude and time period in accordance with the temperature is calculated. Range of temperature is considered from 30°C to 50°C. Figure 15 shows considerable decrease in the amplitude as the temperature increased nonlinearly to 50°C because of explanation given in above section. Similarly, Fig. 16 shows the variation of time period with temperature. As from these results, temperature variation on CFD decreases time period linearly. This result depicts some change in performance parameters with temperature. From the screening results, it was known that both radiation and temperature degrades the performance parameters as both the parameters increases. This experiment provides a proof of the discussion on degradation mechanisms that was explained in above section.

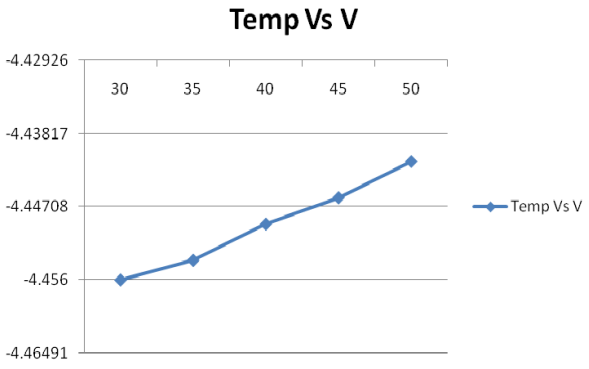

Fig. 15. Voltage versus temperature acceleration.

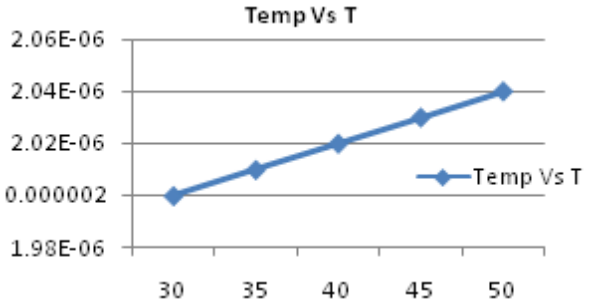

Fig. 16. Time period versus temperature acceleration.

3.4.1.2. Design of experiments

In this stage, stress levels of both radiation and temperature subjected to CFD circuit one after another are subjected. The response surface graph results are shown in Fig. 17 for voltage and Fig. 18 for time period.

The sample size is 3, the radiation levels: 20 min and 40 min, temperature: 30°C and 50°C and time is zero. From DOE and the response surface graphs, the levels of input parameters are selected such that maximum degradation of performance parameter is expected and acts as input to the accelerated testing of CFD for life testing analysis.

3.4.1.3. Accelerated testing

From the inputs of design of experiments, the levels are selected such that pulse amplitude has maximum degradation. The values are provided below and experiments are carried out at regular intervals after exposure of radiation and maintaining the temperature level. The sample size is 10, radiation: 40 min, temperature: 50°C and time: 0 h, 100 h, 200 h, 300 h and 400 h. As in Fig. 19, the degradation of pulse amplitude happened over the time nonlinearly. To quantify and model this

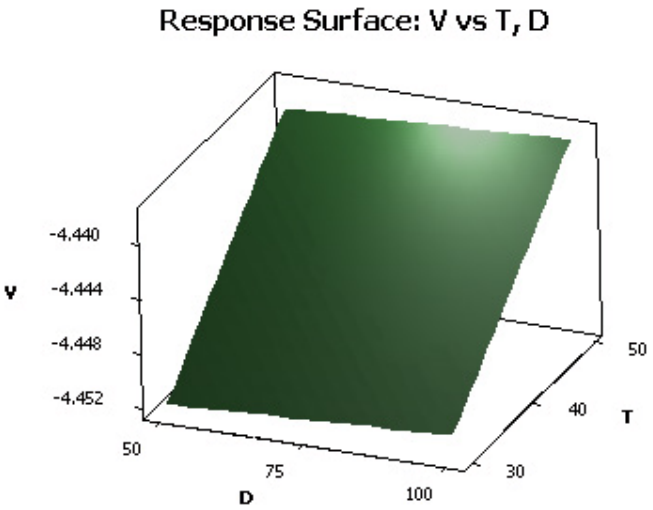

Fig. 17. RSG of V versus T, D.

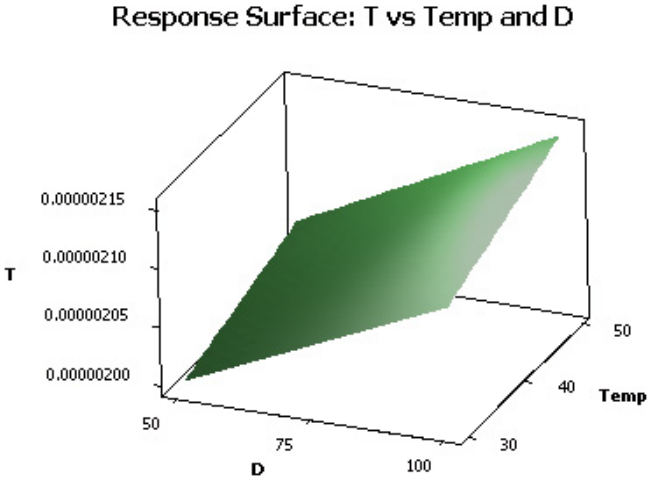

Fig. 18. RSG of T versus T, D.

time to failure considering dose rate and temperature need to be studied as there are no physics of failure models available in the literature.

3.4.2. *Stage* 2: *Extensive testing*

From the input from Stage 1, as both temperature and radiation parameters increases, the output performance factor further degrade. In this stage, the radiation parameters are selected at the higher dosages as 0, 3.14, 6.64 and 10 kGy. Similarly, the testing of IC is excited to higher temperatures of 30°C, 50°C, 70°C and 90°C.

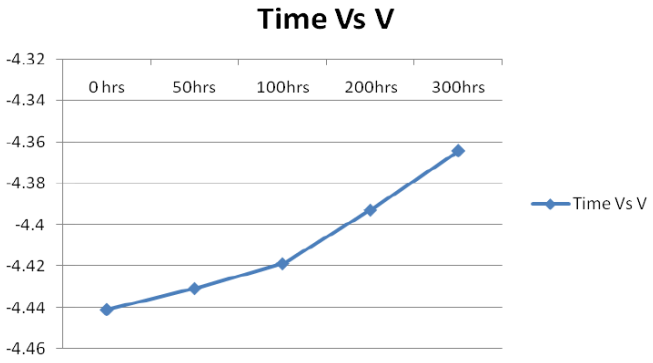

Fig. 19. Accelerated testing of CFD.

From the Witczak,[5] the degradation of the device by radiation increases further with the temperature. Hence, the items are subjected at first to the radiation step and second to the temperature step. To get more extensive data, accelerated testing is carried out after the temperature step. This radiation-temperature-time sequence is carried out at all the stress levels of the radiation. The cumulative effect of both temperature and time factors w.r.t radiation stress level is shown below.

From Table 1, temperature further degrades the effect of radiation step and shown graphically in Fig. 20 where $t = 0$.

Table 1. Radiation step with temperature.

Temp (°C)	V 0 kGy	V 3 kGy	V 6 kGy	V 10 kGy
30	−4.426	−4.368	−4.264	−4.146
50	−4.404	−4.352	−4.238	−4.124
70	−4.382	−4.334	−4.216	−4.1
90	−4.35	−4.304	−4.184	−4.068

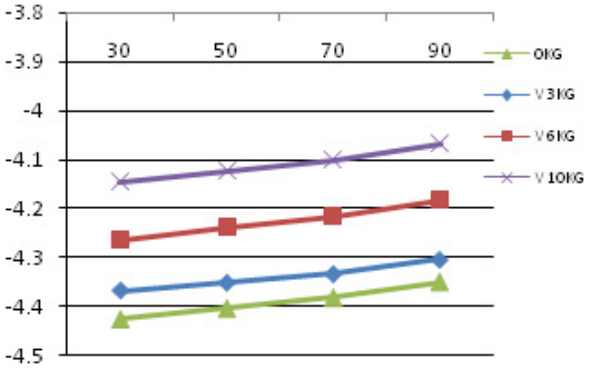

Fig. 20. Degradation with radiation and temperature (x-axis) on output voltage (y-axis).

Table 2. Radiation step with accelerated time.

Time (h)	V 0 kGy	V 3 kGy	V 6 kGy	V 10 kGy
0	−4.441	−4.304	−4.184	−4.068
50	−4.4308	−4.254	−4.134	−4.016
100	−4.4188	−4.194	−4.074	−3.952
150	−4.4059	−4.122	−3.992	−3.89

Table 3. Data selected for Minitab analysis.

Temperature (°C)	Time (h)	R (kGy)	O/P Voltage (V)
30	0	0	−4.426
30	0	3	−4.368
30	0	6.5	−4.264
30	0	10	−4.146
50	0	0	−4.404
50	0	3	−4.352
50	0	6.5	−4.238
50	0	10	−4.124
70	0	0	−4.382
70	0	3	−4.334
70	0	6.5	−4.216
70	0	10	−4.1
90	0	0	−4.35
90	0	3	−4.304
90	0	6.5	−4.184
90	0	10	−4.068
90	50	0	−4.4308
90	50	3	−4.254
90	50	6.5	−4.134
90	50	10	−4.016
90	100	0	−4.4188
90	100	3	−4.194
90	100	6.5	−4.074
90	100	10	−3.952
90	150	0	−4.4059
90	150	3	−4.122
90	150	6.5	−3.992
90	150	10	−3.89

Similarly, the degradation characteristics are observed with accelerated testing carried out at 90°C at each radiation step and results are provided in Table 2. From Table 3, the output parameter further degrades by the effect of accelerated time and shown graphically in Fig. 21. From the above figures, it was concluded that both radiation and temperature degrades the voltage of the output pulse with further accelerated time.

3.5. *Test results*

From the results obtained from both the stages, Table 3 is constructed.

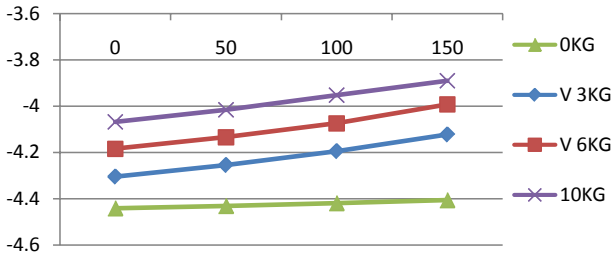

Fig. 21. Degradation with radiation and accelerated time (x-axis) with output voltage (y-axis).

3.6. *Failure modeling*

As there are no specified and existing models for this component in literature, the failure model can be generated by using the linear regression, response surface regression and the support vector learning machine with temperature and radiation as stress parameters.

Linear Regression Analysis (A = Temperature, B = Tested time, C = Radiation):

The regression equation is

$$V = -4.51 + 0.00106A + 0.000840B + 0.0357C. \tag{5}$$

Response Surface Regression (A = Temperature, B = Tested time, C = Radiation, $C4 = O/P$ Voltage):

A^*B term cannot be estimated, and was removed.

The analysis was done using coded units.

Each of the estimates (coefficients, indicated with Coeff.) has a standard error — this is a measure of how variable the estimate is likely to be as shown in Table 4. To gain 95% confidence intervals of the coefficient, it was multiplied by the standard

Table 4. Regression coefficients.

Predictor	Coeff.	SE Coeff.	T	P	Seq SS
Constant	−4.50659	0.03389	−132.3	0.000	
A	0.0010584	0.0004766	2.22	0.036	0.07354
B	0.0008402	0.0001906	4.41	0.000	0.04144
C	0.035703	0.002329	15.33	0.000	0.50137

Note: $S = 0.0461945$, $R - \text{Sq} = 92.3\%$, $R - \text{Sq(adj)} = 91.4\%$.

Table 5. Analysis of variance.

Source	DF	SS	MS	F	P
Regression	3	0.61635	0.20545	96.28	0.000
Residual error	24	0.05121	0.00213		
Total	27	0.66756			

Table 6. Estimated regression coefficients for V.

Term	Coeff.	SE	T	P
Constant	−4.21357	0.02718	−155.003	0
A	0.03642	0.01104	3.298	0.004
B	0.06464	0.01104	5.853	0
C	0.19755	0.01342	14.718	0
A^*A	0.00499	0.01861	−0.268	0.791
B^*B	0.02193	0.01861	1.178	0.253
C^*C	−0.01665	0.01436	−1.16	0.261
A^*C	0.00696	0.01375	0.506	0.618
B^*C	0.05105	0.01375	3.714	0.001

error of 1.96, and added and subtracted from the coefficient. The standard error of a coefficient (SE Coeff.) is the square root of the corresponding diagonal element of the covariance matrix of the coefficient estimates. The variances are the diagonal elements of the X′X inverse matrix times the mean square error (MSE). T-value (T) is computed from the data for testing the hypothesis that the population coefficient is 0. The p-values computed for testing that the population value is 0 are given in the P column. Large t-values go with small p-values and suggest a term that contributes to the model. T is not very useful on its own, but it does give us P — that is the probability of the result occurring, if the value in the population is zero.[16]

$$S = 0.0332874, \quad \text{PRESS} = 0.0607202,$$
$$R - \text{Sq} = 96.85\%, \quad R - \text{Sq(pred)} = 90.90\%, \quad R - \text{Sq(adj)} = 95.52\%.$$

The above results show stability and how well the prediction of parameters is. S is the square-root of mean square error and PRESS statistic in the original units of the response when a power transformation of the response is applied in a linear regression. $R - \text{Sq}$ evaluates how closely the data fall next to the fitted line. Here prediction $R - \text{Sq}$ is 90.9% because of the missing null values exist in time parameter. So $R - \text{Sq}$ is adjusted to 95.52% which is a quite reasonable prediction for the degradation of output variable.

DF refers to the degrees of freedom for each source. The analysis of variance (ANOVA) was calculated as in Table 5. The SS column gives, top to bottom, the sums of squares SSR, SSE and SST. The SSE is used (with the formula and a calculator) for the F-test for testing some subset of the independent variables. Here p-value is also significant predictor as to how well the term contributes to the overall output parameter. Interaction has significant value which concludes the interaction of temperature and radiation has essential effect on degradation of V using data in uncoded units is modeled from Tables 7 and 8.

The final part of the output is some diagnostics, to help you to interpret the equation. Minitab[15] has selected some cases it believes you might want to look and bases this on the residuals and the influence. Estimated Regression Coefficients for

Table 7. Analysis of variance for V.

Source	DF	Seq SS	Adj SS	Adj MS	F	P
Regression	8	0.64651	0.64651	0.080814	72.93	0
Linear	3	0.616349	0.327607	0.109202	98.55	0
Square	3	0.00303	0.00303	0.00101	0.91	0.454
Interaction	2	0.027131	0.027131	0.013566	12.24	0
Residual error	19	0.021053	0.021053	0.001108		
Total	27	0.667563				

Table 8. Unusual observations for V.

Obs	StdOrder	C4	Fit	SE Fit	Residual	St Resid
25	25	−4.406	−4.358	0.025	−0.048	$-2.19R$
26	26	−4.122	−4.19	0.019	0.068	$2.48R$
28	28	−3.89	−3.847	0.026	−0.043	$-2.04R$

Note: R denotes an observation with a large standardized residual.

V using data in uncoded units is modeled from Table 6.

$$V = -4.45838 + 0.00032T \pm 4.035t + 0.0332R + 5.546x10^{-6}T^2 + 3.898x10^{-6}t^2 - 6.6597x10^{-4}R^2 + 4.639x10^{-5}RT + 0.00014tR. \quad (6)$$

The failure criteria were measured as 5% degradation of the initial value. By substituting the initial operating conditions and solving for t results in time to failure as 5.7×10^7 h.

4. Conclusion

In this paper, the failure phenomenon of CFD is studied by following the physics of failure methodology. It was come to know that temperature and radiation are stress parameters and were responsible for degradation of the output voltage, and design of experiments was carried out to obtain the stress levels for accelerated testing. A response surface regression failure model with time to failure was generated from the collected data with inclusion of stress parameters with the inputs from the physics of failure concepts.

References

1. *Military Handbook, Reliability Prediction of Electronic Equipment*, Mil-HDBK 217F, February 1995.
2. J. Bernstein, M. Gurfinkel, X. Li, J. Walters, Y. Shapira and M. Talmor, Electronic circuit reliability modeling, *Microelect. Reliab.* **46**(12) (2006) 1957–1979.
3. Semiconductor Device Reliability Failure Models, SemaTech, AMD (2000).
4. L. W. Condra, *Reliability Improvement with Design of Experiments*, 2nd edn. (Marcel Dekker, 2001).

5. W. Nelson, *Accelerated Testing: Statistical Models, Test Plans and Data Analysis* (John Wiley, 2004).
6. K. Luery, Failure of the constant fraction discriminator, Galileo, University of Virginia, Memos, June 2003.
7. K. Carnes, *Constant Fraction Discriminators*, Electronics Manual, University of Indiana, January 2003.
8. B. Van Zeghbroeck, Principles of electronic devices, University of Colorado (2011).
9. G. Wang and G. C. M. Meijer, The temperature characteristics of bipolar transistors fabricated in CMOS technology, *Sensors Actuators* **87** (2000) 81–89.
10. A. Christou, Reliability of high temperature electronics, Center for Risk and Reliability, University of Maryland (2006).
11. S. C. Witczak, R. D. Schrimpf, D. M. Fleetwood, K. F. Galloway, R. C. Lacoe, D. C. Mayer, J. M. Puhl, R. L. Pease and J. S. Suehle, Hardness assurance testing of bipolar junction transistors at elevated irradiation temperatures, *IEEE Trans. Nuclear Sci.* **44**(6) (1997) 1989–2000.
12. S. C. Witczak, R. D. Schrimpf, D. M. Fleetwood, K. F. Galloway, R. C. Lacoe, D. C. Mayer, J. M. Puhl, R. L. Pease and J. S. Suehle, Charge separation for bipolar transistors, *IEEE Trans. Nuclear Sci.* **40** (1993) 1276–1285.
13. R. D. Schrimpf, D. M. Schmidt, D. M. Fleetwood, R. L. Pease and W. E. Combs, Modeling ionizing radiation induced gain degradation of the lateral pnp bipolar junction transistor, *IEEE Trans. Nuclear Sci.* **43** (1996) 3032–3039.
14. R. H. Myers, D. C. Montgomery and C. M. Anderson-Cook, *Response Surface Methodology: Process and Product Optimization using Designed Experiments* (Wiley Series in Probability and Statistics, 2009).
15. *Meet Minitab 16*, Manual (2010).
16. N. Bradley, Response Surface Methodology, Thesis, Indiana University (2007).

About the Authors

Adithya Thaduri studied electronics and instrumentation engineering in Bachelors and reliability engineering in Masters. Presently, he is doing Ph.D. at Luleå University of Technology, Sweden and research fellowship at IIT Bombay, India in association with Bhabha Atomic Research Center, India. His core area of research is on predicting the life of critical electronic components using physics of failure approach.

Ajit K. Verma is currently a Professor in Engineering (Technical Safety), Stord/Haugesund University College, Haugesund, Norway and has been a Professor (since February 2001) with the Department of Electrical Engineering at IIT Bombay (away on lien from IIT Bombay). He was the Director of the International Institute of Information Technology Pune, on lien from IIT Bombay, from August 2009–September 2010. He is also a Guest Professor at Luleå University of Technology, Sweden. He has supervised/co-supervised 35 Ph.D.s and 95 Masters theses in the area of software reliability, reliable computing, power systems reliability (PSR), reliability-centered maintenance (RCM) and probabilistic safety/risk assessment (PSA) and use of computational intelligence in system assurance engineering and management. He is the Chairman of the recently constituted Special Interest Group

on System Assurance Engineering and Management of Berkeley Initiative in Soft Computing, Department of Electrical Engineering and Computer Science, University of California, Berkeley. He is an author of books titled *Fuzzy Reliability Engineering-Concepts and Applications* (Narosa), *Reliability and Safety Engineering* (Springer), *Dependability of Networked Computer-Based Systems* (Springer) and *Optimal Maintenance of Large Engineering System* (published by Narosa). He has over 225 publications in various journals (over 100 papers) and conferences. He has been the Editor-in-Chief of OPSEARCH published by Springer (January 2008–January 2011) as well as the Founder Editor-in-Chief of *International Journal of Systems Assurance Engineering and Management* (IJSAEM) published by Springer and the Editor-in-Chief of *SRESA Newsletter* and *Journal of Life Cycle Reliability and Safety Engineering*. He is also the Series Editor along with Prof. Roy Billinton and Prof. Rajesh Karki of Springer Book Series "Reliable and Sustainable Electric Power and Energy Systems Management" and has jointly edited the book *Reliability and Risk Evaluation of Wind Integrated Power Systems* also published by Springer. He has been a Guest Editor of a dozen issues of international journals including *IEEE Transactions on Reliability* and has been the Editor of several conference proceedings.

Gopika V., a graduate of 37th batch of BARC Training School, joined Reactor Safety Division, BARC in 1994. She has made significant contributions in the area of probabilistic safety assessment (PSA). She has actively participated in the PSA Studies of AHWR and research reactors, Fire PSA, Risk Informed In-Service Inspection methods for piping systems in DAE facilities and in the development of Risk Monitor. She has conducted extensive research on applicability of Risk Informed In-Service Inspection methods which have resulted in formulating a complete framework. She has successfully translated the research methods into the application framework. The most important contributions are the introduction of a new importance measure, incorporating the effects of In-service inspection through Markov model and using genetic algorithm for optimizing inspection. She would later extend her research for chalking out the RI-ISI program for nuclear power plants as well as in heavy water plants. She has co-authored a standard for applying the risk-based inspection and maintenance procedures, for European industry.

M. G. Rajesh is working at electronics division at Bhabha Atomic Research Center, Bombay, India for eight years. His research includes the selection and design of electronic parts which are used in the signal conditioning unit of nuclear reactor. He analyzes the reason for failure of components and accordingly designs the circuits for effective performance.

Uday Kumar obtained his B.Tech from India during the year 1979. After working for six years in Indian mining industries, he joined the postgraduate program of

Luleå University of Technology, Luleå, Sweden and obtained a Ph.D. degree in field of reliability and maintenance during 1990. He worked as a Senior Lecturer and Associate Professor at Luleå University from 1990–1996. In 1997, he was appointed as a Professor of Mechanical Engineering (Maintenance) at University of Stavanger, Stavanger, Norway. Since July 2001, he has taken up the position as a Professor of Operation and Maintenance Engineering at Luleå University of Technology, Luleå, Sweden. Currently he is the Director of Luleå Railway Research Center. His research interests are equipment maintenance, reliability and maintainability analysis, etc. He is also member of the editorial boards and reviewer for many international journals. He has published more than 150 papers in international journals and conference proceedings.

Paper VI

P6

Support Vector Regression degradation modeling for Constant Fraction Discriminator

Thaduri, A., Verma, A.K., Vinod, G., Rajesh, M.G., Kumar, U. (2012). Support Vector Regression degradation modeling for Constant Fraction Discriminator. *Communications in Dependability and Quality Management (CDQM)*, 15(1), pp. 101-122.

Support Vector Regression degradation modeling for Constant Fraction Discriminator

Adithya Thaduri, Lulea University of Technology, Sweden
A K Verma, Stord/Haugesund University College, Norway
Uday Kumar, Lulea University of Technology, Sweden
V Gopika, Bhabha Atomic Research Centre, India
Rajesh Gopinath, Bhabha Atomic Research Centre, India
D Datta, Bhabha Atomic Research Centre, India

Abstract:

In the nuclear industries, the electronic signal processing unit plays a key role in the data processing, data analysis, control mechanism and more importantly safety of the nuclear reactor. The processing unit comprises of different modules that process pulse and current signals from detector and constant fraction discriminator which has higher criticality is one of them. Earlier the reliability was calculated using MilHdbk 217 standard and found discrepancies to the field failure. This paper studies the failure phenomenon using physics of failure approach by studying degradation and failure analysis and conducting the experiments using modified physics of failure methodology. Support vector machine (SVM) is a machine learning phenomenon using statistical learning theory. In this paper, failure data is fed to SVM for regression models intended for life prediction. From the parametric analysis, it was found that Sequential minimal optimization with RBF kernel represent the best model for degradation of the CFD. This method provides higher accuracy compared to response surface methodology.

Keywords: Constant Fraction Discriminator, Kernel, Physics of Failure, Regression, Response Surface Methodology, Support Vector Machine

1. Introduction

The reliability of electronic systems, used in nuclear power plants, is traditionally estimated with empirical databases such as MIL-HDBK-217 [1], PRISM etc. These methods assign a constant failure rate to electronic devices, during their useful life. The constant failure rate assumption stems from treating failures as random events. Currently, electronic reliability prediction is moving towards applying the Physics of Failure approach [2] which considers information on process, technology, fabrication techniques, materials used, etc. Even alone Physics of Failure does not provide the reliability of the device. So amalgamation of deterministic and probabilistic analysis is carried out.

For the most of the electronic components, the standard MilHdbk method was implemented in order to find the time to failure. But for the customized electronic components like Constant Fraction Discriminator using different technologies, this method cannot be applied as there was no proper model associating with it. Further, these new microelectronic devices often exhibit infant mortality and wear-out phenomena while in operation. Hence physics of failure approach was implemented on these components which laid emphasis on competing failure mechanisms such as electro migration, hot carrier injection, dielectric breakdown etc., that makes a device's useful life different from that predicted by empirical methods. The dominant failure mechanism that leads to device failure was found by realistic approach to reliability prediction.

Neutron Flux Monitoring System-NFMS [3]- comprises of different modules (Pulse Translator, Logarithmic Count Rate, Mean-Square Value Processor etc) that process pulse and current signals from detector. Besides, there are modules that generate trip signals. Trip signals are of 24V level and optically isolated.

It is worthwhile to study the failure mechanisms of the components involved in the signal processing chain of NFMS, as its reliability is being evaluated with conventional MIL-HDBK-217 method. The physics of failure study of these components will generate reliability data that can be eventually compared with the MTBF figures provided by MIL-HDBK-217.

A few components have been identified in this regard-They form a part of trip signal generation which has direct implication on safety. 4N-36: Optocoupler, AD-620: Instrumentation Amplifier, OP-07: A general purpose operational amplifier etc., are widely used in the trip modules of NFMS. So it is beneficial to start the P.O.F study with these components. Another candidate chosen for study is CFD-2004.This chip is used in the pulse processing circuits of NFMS. It is an indigenously developed ASIC which uses BJT process technology.

Constant fraction discriminator (CFD) is another device which is failing regularly in the field. This device is made up of BJT technology. It is a level discriminator at which it provides a pulse when the analog input reaches particular voltage level. The possible failure mechanisms for this device was electro migration and hot carrier injection. The temperature and radiation considered as stress parameters. These parameters effects the operation of BJT transistors inside to behave as it reduces the output voltage which further reduces the performance parameter which is in this case is voltage of output pulse. Constraint in the experimentation is that both the stress parameters cannot be applied simultaneously instead one after another. Effect of individual parameter is quantified on voltage output and degradation of whole device is studied. Selection of stress levels can be carried out by using Design of Experiments (DOE) [4] and accelerating testing [5] was implemented. Since there is no sufficient model for this device, modelling is to be carried out by probabilistic analysis. From the model, relation between design parameters and time to failure is observed and provided to designer.

Support Vector Machine (SVM) is a learning algorithm developed by Vapnik 1995 [6] and later improved in Vapnik 1998 [7] and Shawe-Taylor and Cristianini 2004 [8]. It is sophisticated method prevents from overfitting of the data when compared to artificial neural networks. It is extensively used in pattern recognition, prediction, classification and regression in image processing, bio-medical sciences and other fields. The SVM uses several linear and non-linear kernel functions to measure the similarities between data, and the decision function is represented by an expansion of the kernel function selected. Support Vector Regression (SVR) utilises the regression analysis from SVM with the expansion of kernel functions. This SVR was applied to the testing data for the reliability prediction of CFD.

This paper characterized the data obtained from the design of experiments and the accelerated testing to generate model and respective kernel function by sensitive analysis using the regression by classification. The degradation of the output voltage happened due to the application of stress parameters in a non-linear way, hence several non-linear kernel

functions was implemented and tested to quantify which of the kernel and its parameters suit the model with higher accuracy.

2. Reliability Prediction using Physics of Failure Approach

The following methodology demonstrated in Figure 1 was implemented on reliability prediction of constant fraction discriminator using support vector machine.

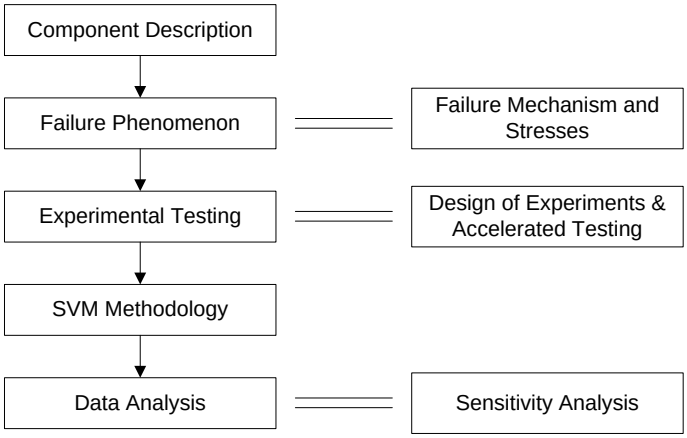

Figure 1: Prediction Methodology

2.1 Component Description

The electronic component of interest in this paper is Constant Fraction Discriminator. The construction, material characteristics, processes, operation and functioning of CFD is explained in this section.

2.2 Failure Phenomenon

From the literature survey and field inspection, the dominant failure mechanism and correspondingly the dominant stresses is analyzed. These stresses tend to degrade the performance parameter and a failure criterion is set at which it reaches the threshold level.

2.3 Experimental Testing

In order to test the component with stresses and its levels, design of experiments and accelerated testing are implemented to fail the component. A test circuit is designed and applies the input stress parameters to find the output at different runs.

2.4 SVM Methodology

The phenomenon of support vector machine is explained and a methodology is introduced.

2.5 Data Analysis

The data obtained from the DOE and accelerating testing is selected and combined for SVM modeling by finding the best kernel function and its function variables by using sensitivity analysis. A model is generated by selecting least error.

3. Reliability Prediction of CFD

The methodology proposed in figure 1 was implemented on constant fraction discriminator.

3.1. Component Description

Discriminators generate logic pulses in response to input signals exceeding a particular threshold. In general, there are two main types of discriminators, the leading edge discriminator and the constant fraction discriminator. The leading edge discriminator is the simpler one. Given an input pulse, the leading edge discriminator produces an output pulse at the time when the input pulse crosses a given threshold voltage. This, however, causes a problem in situations where the timing is important. If the amplitude is changed, but the rise time of the input pulse remains the same, a sort of "time walk" occurs (Figure 2) [9]. That is, an input pulse with smaller amplitude but with the same rise time as a larger pulse will cross the threshold at a later time. Thus, the timing of the output pulse is shifted by this change in amplitude.

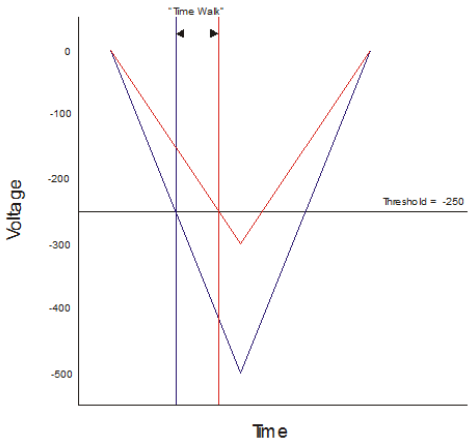

Figure 2: Leading Edge Discriminator and "Time Walk"

The constant fraction discriminator alleviates this problem by using a constant fraction, *f*, of the input pulse to precisely determine the timing of the output pulse relative to the input signal. It does this by splitting the input signal (Figure 3): attenuating one half so that it is a certain fraction, *f*, of the original amplitude (Figure 4), and delaying and inverting the other half (Figure 5).

The attenuated pulse and the delayed and inverted pulse are then added together, and the zero crossing is computed (Figure 6).

The zero crossing gives the time at which the CFD should create an output pulse, and is always independent of amplitude. For a simple linear ramp, like the one shown above, the equations for its input pulse, attenuated pulse, and delayed and inverted pulse are as follows:

$delay = t_d$, $fraction = f$, $initial\ amplitude = A$,

$input\ pulse \quad V_i = -At$,

$attenuated\ pulse \quad V_a = -fAt$,

$delayed\ and\ inverted\ pulse \quad V_d = A(t - t_d)$.

To find the zero crossing, set $0 = V_a + V_d$ and solve for t:

$$0 = -fAt + A(t - t_d) \text{ and } t_{cross} = \frac{t_d}{(1-f)}$$

Ideally, the delay is chosen such that the maximum of the attenuated pulse crosses at the desired fraction of the delayed pulse. In that case, $t_{d\_ideal} = t_{rise}(1-f)$. However, if the delay is chosen smaller than t_{d_ideal}, CFD will operate at a fraction less than that of *f*. From equation 1, we see that t_{cross} is independent of the amplitude of the input pulse. The CFD has a monitor output feature, which outputs the bipolar signal created by summing the attenuated and the delayed and inverted pulses, so that we can view how it is calculating the zero crossing [10].

As in Block diagram, Figure 6, in order to achieve a constant timing edge, it is customary to use an attenuator and a delay. The input signal is split. One part is delayed, and the other is attenuated. After these two signals are re-mixed, a comparator detects the zero cross points. The timing of the zero cross point is not influenced by the amplitude of the input signal [11].

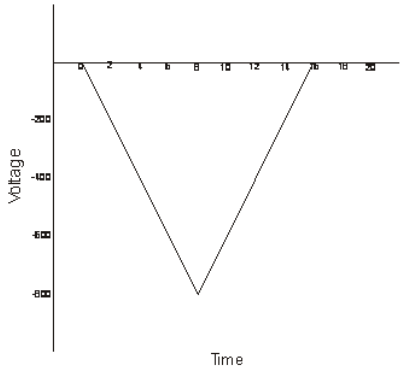

Figure 2: Input pulse to CFD

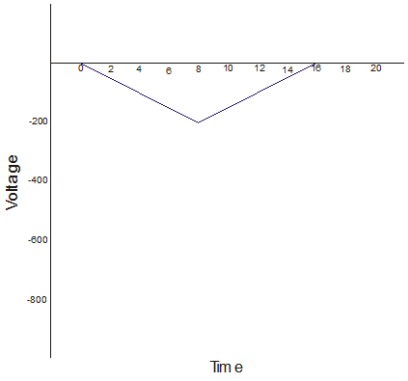

Figure 3: Attenuated Pulse

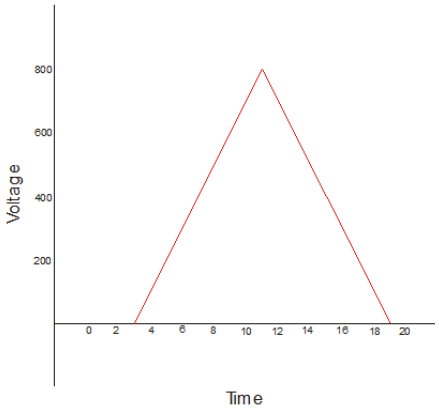

Figure 4: Delayed and Inverted Pulse

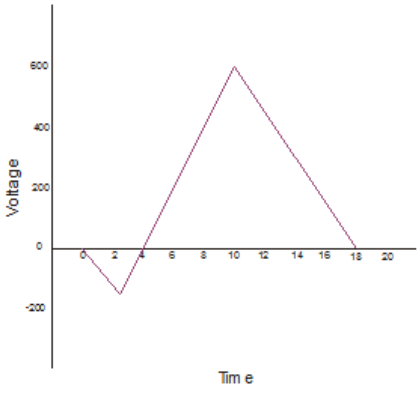

Figure 5: Sum of Attenuated and Delayed pulse

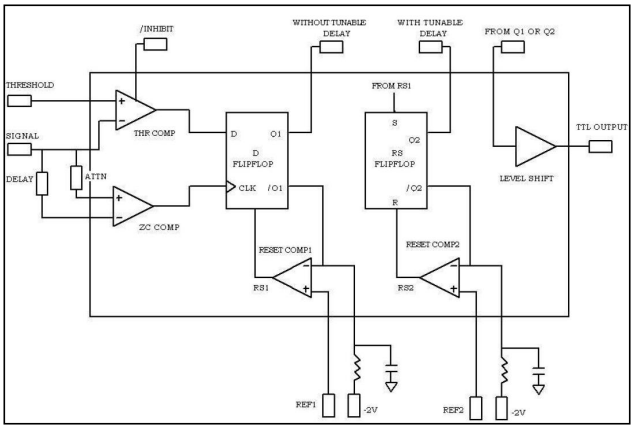

Figure 6: Block Diagram of CFD

3.2. Failure Phenomenon

Here we have taken Constant Fraction Discriminator CFD 2004 made by BEL, Bangalore, India. Comparators and flip flops as shown in Figure 6 consist of transistors made up of BJT Technology. So, the failure physics of these transistors at wafer level adversely affects the performance and failure of CFDs. As from the description, if the wave from the counter expects to cross at a threshold level, CFD must provide TTL pulse. Failure possibly happen if the threshold level at the input and the pulse width at the output varies in accordance with the prescribed level with the existing internal parameters. By the physics of failure approach, the stress parameters affect the BJT transistors to change their behavior of electrical h-parameters. Commonly, when an electrical or temperature stress applied on the transistor, they develops reverse current from emitter to base to increase in such a way to degrade the performance of output electrical characteristics such as collector current and V_{CE} voltage at the output. If these values changes inside the device, as all other devices are interconnected, this effective voltages and currents tend to vary at the larger levels of the whole device and output pulse width and time periods change. If this change is such a large that it can't detect the input pulse providing the output TTL, then it is considered as failure.

3.2.1 Effect of Temperature

The temperature dependence of bipolar transistors depends on a multitude of parameters affecting the bipolar transistor characteristics in different ways. Important effect is the temperature dependence of the current gain. Since the current gain depends on both the emitter efficiency and base transport factor [21].

The emitter efficiency depends on the ratio of the carrier density, diffusion constant and width of the emitter and base. As a result, it is not expected to be very temperature dependent. The carrier densities are linked to the doping densities. Barring incomplete ionization, which can be very temperature dependent, the carrier densities are independent of temperature as long as the intrinsic carrier density does not exceed the doping density in either region. The width is very unlikely to be temperature dependent and therefore also the ratio of the emitter and base width. The ratio of the mobility is expected to be somewhat temperature dependent due to the different temperature dependence of the mobility in n-type and p-type material.

The base transport is more likely to be temperature dependent since it depends on the product of the diffusion constant and carrier lifetime. The diffusion constant in turn equals the product of the thermal voltage and the minority carrier mobility in the base. The recombination lifetime depends on the thermal velocity. The result is therefore moderately dependent on temperature. Typically the base transport reduces with temperature, primarily because the mobility and recombination lifetime are reduced with increasing temperature. Occasionally the transport factor initially increases with temperature, but then reduces again.

Temperature affects the AC and DC characteristics of transistors. The two aspects to this problem are environmental temperature variation and self-heating. Some applications, like military and automotive, require operation over an extended temperature range. Circuits in a benign environment are subject to self-heating, in particular high power circuits.

Leakage current ICO and β increase with temperature. The DC β hFE increases exponentially. The AC β hfe increases, but not as rapidly. It doubles over the range of -55o to 85o C. As temperature increases, the increase in hfe will yield a larger common-emitter output, which could be clipped in extreme cases. The increase in hFE shifts the bias point, possibly clipping one peak. The shift in bias point is amplified in multi-stage direct-coupled amplifiers. The solution is some form of negative feedback to stabilize the bias point. This also stabilizes AC gain [22].

As from the studies from BJT technology, temperature and radiation is selected as stress parameters. The emitter and collector current of npn BJT is given Equations below

$$IE = IES\left(e^{\frac{VBE}{VT}} - 1\right)$$

$$IC = \alpha IES\left(e^{\frac{VBE}{VT}} - 1\right)$$

The output voltage VCE is given as in Equation

$$VCE = VCC - ICReff$$

Where R_{eff} is effective output resistance at the output, I_{ES} = reverse saturation current at base-emitter diode, α_T = common base forward short circuit gain, V_T = Thermal Voltage kT/q, V_{BE} = base-emitter Voltage, V_{CE} = base-collector Voltage, V_{CC} = Source Voltage typically 5V/10V. In Eber-Moll Model, IC grows at about 9% / ^{0}C if you hold VBE constant and VBE decreases by 2.1mV / ^{0}C if you hold IC constant with the temperature.

Since both the currents depend on temperature parameter V_T, the raise in the temperature leads to vary these parameters which finally lead to degrade the performance of CFD.

3.2.2 Effect of Radiation

Another stress parameter which degrades the BJT devices is Cobalt β-radiation. Degradation of many types of bipolar transistors and circuits is known to depend strongly on dose rate. For a given total dose, degradation is more severe in low dose rate exposure than high dose rate exposure. This effect has been attributed to space charge effects from trapped holes and hydrogen related species through oxygen vacancies in base oxide. There are several hardness assurance tests and most popular has been high dose rate irradiation at elevated temperatures [23].

Although radiation exposure generally leads to grain degradation in npn and pnp devices, the mechanisms by which radiation effects their gains are quite different. Ionizing radiation

degrades the current gain of npn bipolar transistors by introducing net trapped positive charge and interface traps into the oxide base. This positive oxide trapped charge spreads the emitter-base depletion region into the extrinsic base results in increase of base recombination current under forward-bias operation at the junction. Radiation-induced interface traps, especially those near mid-gap, serve as generation-recombination centers through which recombination current in the base is further increased due to enhanced surface recombination velocity. In pnp transistors [23], near-midgap interface traps in the base oxide also increase the base current by surface recombination. Compared with npn transistors, radiation-induced net positive oxide trapped charge can mitigate gain degradation by creating an imbalance in carrier concentrations at the surface of the base.

From the statistical results explained in et al. Witczak [24], Current gain degradation grows worse with decreasing dose rate regardless of dose. Excess base current, an increase in base current due to radiation exposure, increases gradually with decreasing dose rate. This effect is due to weak dependence of excess base current on radiation-induced defect densities at large total dose. Changes in collector current as compared to base current is small because it provides meaningful assessment of amount of gain degradation while relating closely to the physical mechanisms, excess base current is a convenient parameter to evaluate radiation-induced damage in these devices [24].

Although much progress has been made in understanding the effects of dose rate and temperature on radiation-induced bipolar gain degradation, still there is ambiguity in selecting the optimum values for assurance testing. From the analysis carried out by Witczak [5], the combined influence of both radiation and temperature has considerable dependence on gain degradation and excess base current enhancement. The combine effect of temperature and radiation results in degradation of performance parameters such as threshold voltage, pulse amplitude and time period of Constant Fraction Discriminator.

The induced radiation is exposed to discriminator at ISOMED, BARC at initial dose rate of 2.5Mrad. After exposure, the IC is biased with initial conditions and then admitted the IC itself to various levels of temperature by using temperature controller at IIT Bombay laboratory.

3.3. Experimental Testing

CFD 2004 of BJT technology from manufacturers of BEL is considered for this study. It is 24-pin DIP plastic package with operating conditions -5.2V to 5V and temperature 100C.

In order to monitor and test this IC for temperature and radiation considering time, a circuit is required to assess and measure it. Figure 7 shows the conditional measuring circuit for this failure testing. As we can see, along with IC, several other components also required to measure the performance parameters such as Inverter (to invert the positive pulse to negative pulse input which is not shown in figure), resistors, capacitors, etc. These components are also sensitive to temperature which effects the measurement. Hence, the circuit is divided to two parts: CFD part and measurement part. In this way, effect of temperature lies only on CFD. The board of CFD part is also holed out at the bottom of IC to expose it with sufficient temperature. A thermistor is placed across IC to continuously monitor the temperature of it.

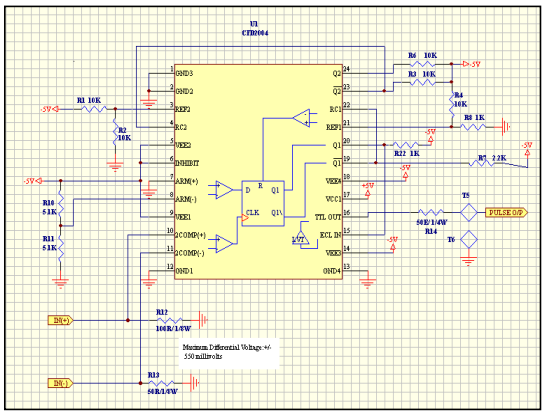

Figure 7: Circuit Diagram of CFD

From the research, temperature and radiation dose rate are considered as stress parameters for the degradation of performance of constant fraction discriminator.

The performance parameters include threshold voltage which is at the input and TTL pulse amplitude at the output. From the Taguchi method of design of experiments, selection of this temperature levels is considered such that IC provides optimum performance. Radiation and temperature are the dominant stress parameters from the failure phenomenon. Initially the device is exposed to radiation under biased conditions and further exposed to temperature. The stress parameter levels for the accelerated testing are found by using 2-stage DOE method: Basic and Extensive testing.

3.3.1 Basic testing Stage

In the basic testing stage, the behavioral effect of the stress parameters on the performance parameter is studied by limited design of experiments and accelerated testing.

3.3.1.1 Radiation Testing:

In this study, variation of pulse amplitude and time period in accordance with the radiation dose rate is calculated. Figure 8 shows the variation of output pulse amplitude with respect to the dose rate. As we can see, there is some little change in the output at higher dose rate.

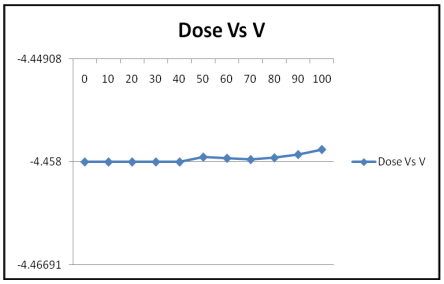

Figure 8: Variation of pulse voltage with dose rate

As from these results, dose rate at 80 rads makes considerable change in the time period. This result depicts some change in performance parameters with radiation.

3.3.1.2 Temperature Testing:

In this study, variation of pulse amplitude and time period in accordance with the temperature is calculated. Range of temperature is considered from 30^0C to 50^0C. Figure 9 shows considerable decrease in the amplitude as the temperature increased nonlinearly to 50^0C because of explanation given in above chapter. As from these results, temperature variation on CFD decreases time period linearly. This result depicts some change in performance parameters with temperature.

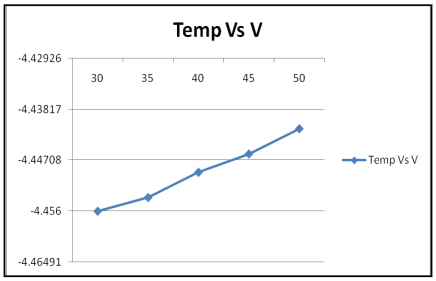

Figure 9: Variation of pulse voltage with temperature

From the screening results, we get to know that both radiation and temperature degrades the performance parameters as both the parameters increases. This experiment provides a proof of the discussion on degradation mechanisms that was explained in 3.2.

3.3.1.3 Design of Experiments:

In this stage, stress levels of both radiation and temperature is subjected to CFD circuit one after another as provided in the table 1. The response surface graphs of pulse amplitude with dose rate and temperature as the input parameters is depicted in Figure 10.

Table 1: 2X2 Matrix of radiation and temperature

Run	D	T	Avg	SD
L1	50	30	-4.452	0.013038405
L2	50	50	-4.4392	0.012316655
L3	100	30	-4.451	0.013038405
L4	100	50	-4.4382	0.012316655

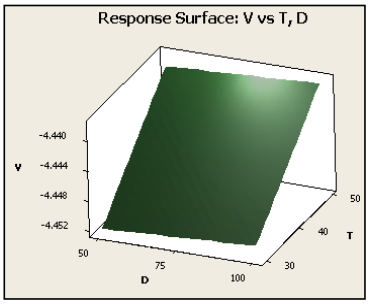

Figure 10: Response surface graph of Pulse amplitude

From DOE and these response surface graphs, the levels of input parameters is selected such that maximum degradation of performance parameter is expected and acts as input to the accelerated testing of CFD for life testing analysis.

3.3.1.4 Accelerated Testing:

From the inputs of Design of Experiments, the levels are selected such that pulse amplitude as maximum degradation. The values are provided below and experiments are carried out at regular intervals after exposure of radiation and maintaining the temperature level.

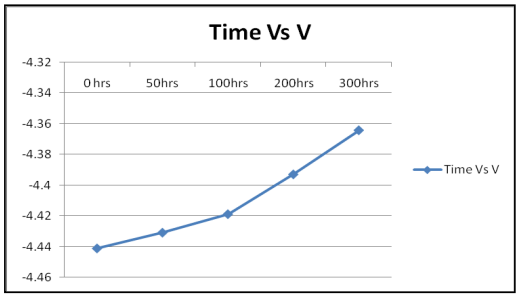

Figure 11: Accelerated testing of CFD for Voltage

As in Figure 11, the degradation of pulse amplitude happened over the time non-linearly. To quantify and model this time to failure considering dose rate and temperature need to be studied as there are no physics of failure models available in the literature.

3.3.2 Extensive testing Stage

From the input from the stage 1, as the both temperature and radiation parameters increases, the output performance factor further degrade. In this stage, the radiation parameters are selected at the higher dosages as 0 KGray, 3.14 KGray, 6.64 KGray and 10 KGray. Similarly, the testing of IC is excited to higher temperatures of 30^0C, 50^0C, 70^0C and 90^0C. From the Witczak [24], the degradation of the device by radiation increases further with the temperature. Hence the items are subjected at first to the radiation step and second to the temperature step. To get more extensive data, accelerated testing is carried out after the temperature step. This radiation-temperature-time sequence is carried out at all the stress levels of the radiation. The cumulative effect of both temperature and time factors w.r.t radiation stress level is shown below. From the table 2, temperature further degrades the effect of radiation step and shown graphically in Figure 12 where t=0.

Similarly, the degradation characteristics are observed with accelerated testing carried out 90^0C at each radiation step and results are provided in table 3. From table 3, the output parameter further degrades by the effect of accelerated time and shown graphically in Figure 13 and experiences non-linear behavior. From the above figures, it was concluded that both radiation and temperature degrades the performance parameter, the voltage of the output pulse with further accelerated time.

Table 2: Radiation Step with Temperature

Temp	**V0KG**	**V 3KG**	**V 6KG**	**V10KG**
30	-4.426	-4.368	-4.264	-4.146
50	-4.404	-4.352	-4.238	-4.124
70	-4.382	-4.334	-4.216	-4.1
90	-4.35	-4.304	-4.184	-4.068

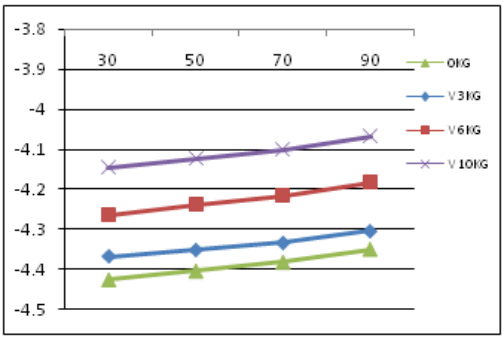

Figure 12: Degradation with radiation and temperature

Table 3: Radiation step with accelerated time

Time (in hrs)	V 3KG	V 6KG	V 10KG
0	-4.304	-4.184	-4.068
50	-4.254	-4.134	-4.016
100	-4.194	-4.074	-3.952
150	-4.122	-3.992	-3.89

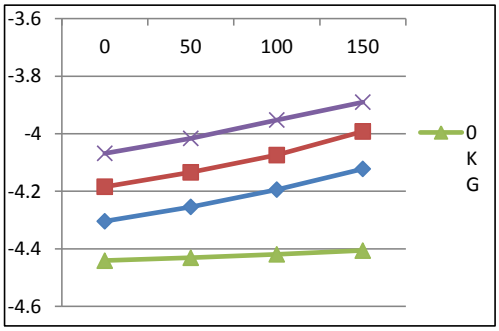

Figure 13: Degradation with radiation and accelerated time

3.4 SVM Methodology

3.4.1 What is SVM?

Support vector machine is a novel statistical learning machine based on statistical learning theory, which can repeatedly estimate dependencies among the data proposed by Vapnik [6,7], and it adheres to the principle of structural risk minimization seeking to minimize an upper bound of the generalization error rather than minimize the training error. The solutions provided SVM is theoretically elegant, computationally efficient and very effective in many large practical problems. It has a simple geometrical interpretation in a high-dimensional feature space that is nonlinearly related to input space. The classification problem assigns labels to objects, and it is a regression problem when the dependency estimates the relationship between explanatory variables and predictive variables. This induction principle is based on the bounding of the generalization error by the sum of the

training error and a confidence interval term depending on the Vapnik-Chervonenkis (VC) dimension [12]. The basic principle to solve regression prediction problem using SVM theory is to map the input data X into a high-dimensional feature space F by nonlinear mapping, to yield and solve a linear regression problem in this feature space. The SVM has been successfully applied to a number of applications ranging from particle identification, face identification, and text categorization, to engine knock detection, bioinformatics, and database marketing (Bennett and Campbell, 2000) [13].

For linear regression, assuming training set (xi,yi), for i=1,2,3…n, where xi is the actual value of input vector and yi is output, n is the number of total data pairs. It is desired to find a separator for partitioning data-set using binary classifier which separates the dark from white dots represents different sets of data. There were several possible lines L1, L2 and L3 which can separates the data into two groups as in Figure 14 [14].

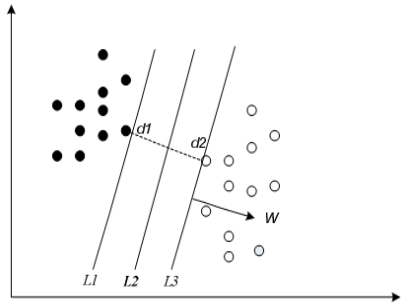

Figure 14: Linear Discriminant Function to separate data sets

In order to find the optimized solution, a linear discriminant function (or classifier) with the maximum margin was considered and this margin is defined such a way that the width of the boundary could be increased by before hitting a data point. The function is described as

$$\text{For yi} = +1, \mathrm{w^T xi} + \mathrm{b} \geq 1$$
$$\text{For yi} = -1, \mathrm{w^T xi} + \mathrm{b} \leq -1$$

and to maximize the marginal width of $\frac{2}{||w||}$ equivalent to minimize $\frac{1}{2}||w||^2$ such that $yi(w^T xi + b) \geq 1$. However in the most of the situations, it was difficult to linearly classify the data due to presence of non-separable data points. The slack variables ξi were introduced into the optimal solution to reduce the impact where formulation was deduced to

$$\text{min:} \frac{1}{2}||w||^2 + C\sum_i^m \xi\text{i such that } yi(w^T xi + b) \geq 1 - \xi\text{i}$$

where ξi ≥ 0, i = 1,2,…m and C is penalty parameter which trade-offs classification accuracy and computation complexity. C value also can be used to set how strictness the data points to be classified correctly (low C is not strict, high C is strict). To solve the convex secondary optimization and dual problem for optimal solution, Lagrangian function (dual problem) was established to calculate partial derivative for slack variables, thus

$$\min Lp(w,b,\alpha i) = \frac{1}{2}||w||^2 - \sum_{i}^{n} \alpha i(yi(w^T xi + b) - 1) \; such \; that \; 0 \leq \alpha i \leq C$$

$$\max \sum_{i}^{n} \alpha i - \frac{1}{2}\sum_{i}^{n}\sum_{ji}^{n} \alpha i \, \alpha j yiyjxi^T xj \;\; such \; that \; w = \sum_{i}^{n} \alpha iyixi \;\; and \;\; \sum_{i}^{n} \alpha iyi = 0$$

where Lp(w,b,αi) is the Lagrangain function and αi represents the Lagrangain multiplier corresponding to xi. The condition $\alpha i(yi(w^T xi + b) - 1 = 0$ should satisfy Karush–Kuhn–Tucker (KKT) conditions (also known as the Kuhn–Tucker conditions) [15] are first order necessary conditions for a solution in nonlinear programming to be optimal, provided that with some regularity conditions. The optimal solution is the Support Vector (SV), a sub set of the training data set with condition αi ≠ 0 which can influence the decision function as

$$g(x) = \sum_{i \in SV} \alpha i K(xi, x) + b$$

The function $xi^T xj$ also known as kernel function K(xi,xj) which is in this case as linear classifier. When a nonlinear kernel function is used, the optimal decision function can be obtained in the same way it is obtained in the simple inner product <xi,xj>, which is essentially a linear kernel function [16]. There are several non-linear classifiers available such as Polynomial, normalized polynomial, Gaussian etc., and selection of a function and tuning of its respective parameters plays a key role in deciding the classification accuracy. The Gaussian and polynomial functions differs in their methodologies to measure similarity in the data where former measures it by subtraction of the two vectors and later function does it by using inner product. The functions were defined as

Linear Kernel: $K(xi, xj) \; = \; xi^T xj$

Polynomial Kernel: $K(xi, xj) = (1 + xi^T xj)^p$ where p is the degree of the polynomial. It is in discrete in nature and higher the value of the polynomial, higher accurate and approximation of the model but takes higher computation time.

Gaussian or Radical Basis Function (RBF): $K(xi, xj) = e^{\left(-\frac{||xi-xj||^2}{2\sigma^2}\right)}$ where $\gamma = 1/2\sigma^2$ as kernel width parameter with bigger gamma values give the steeper functions (more flexible) while lower gamma values give the smoother functions. In order to reproduce highly irregular decision boundaries (or target functions for regression), higher gamma values are recommended.

The sequential minimal optimization algorithm (SMO) has been an effective method for training support vector machines (SVMs) on classification tasks performed on sparse data sets [17]. SMO differs from most SVM algorithms in which do not require a quadratic programming (QP) solver by segregating a sub problem into size two with each size has analytical solution. While SMO has been shown to be effective on sparse data sets and especially fast for linear SVMs, the algorithm can be extremely slow on non-sparse data sets

and on problems that have many support vectors. Regression problems are especially prone to these issues because the inputs are usually non-sparse real numbers (as opposed to binary inputs) with solutions that have many support vectors. SMO repeatedly finds two Lagrange multipliers that can be optimized with respect to each other and analytically computes the optimal step for the two Lagrange multipliers. When no two Lagrange multipliers can be optimized, the original QP problem is solved. SMO actually consists of two parts: (1) a set of heuristics for efficiently choosing pairs of Lagrange multiplier to work on, and (2) the analytical solution to a QP problem of size two [18]. Smola and Schölkopf's SMO algorithm [19] that is caused by the operation with a single threshold value was overcome by Shevade [20] suggesting two modifications the problem by efficiently maintaining and updating two threshold parameters. Their computational experiments show that these modifications speed up the SMO algorithm significantly in most situations. This paper compares and implements the sensitivity analysis of each of the tuning parameters of Gaussian and Polynomial kernels with and without of SMO.

3.4.2 Proposed methodology for comparison of SVM models

We used the following methodology as in Figure 15 to obtain the approximation kernel function with tuned parameter for the degradation of output voltage of CFD.

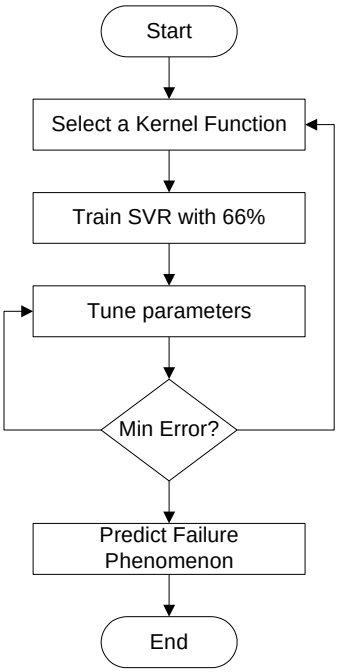

Figure 15: Proposed Methodology for comparison of different kernel functions for degradation

i. Select one of the kernel functions of RBF Kernel without hyper parameter tuning, Normalized polynomial without hyper parameter tuning and Polynomial without hyper

parameter tuning, RBF Kernel with SMO reg, Normalized polynomial and Polynomial with SMO reg.

ii. Select the parameters of SVR
iii. Train with percentage split of 66%.
iv. Tune the function parameters to get min Mean Square Error and Root Means Square Error
v. Predict the degradation phenomenon
vi. Select another function and repeat the process from (i)

3.5 Data Analysis

By combining the data from Table 1, Table 2 and 3, the table 4 as a data set was constructed with all the possible runs obtained from the design of experiments and accelerated testing of the constant fraction discriminator. In this data, temperature, time and radiation are the input parameters and Voltage as the output parameter. These 39 data points were characterized for the SVM regression analysis that was illustrated in the above section using Weka tool.

The procedure that was proposed in Figure 15 was implemented with the different kernel functions and tuning of their respective parameters. For the RBF Kernel, the complexity factor C and gamma value and for polynomial kernel, the complexity factor C and the degree of polynomial P parameters were tuned in such a way to reduce the Mean Absolute Error (MAE) and Root Means Square Error (RMSE).

Table 4: Data for SVM analysis

Temperature	Time	Radiation	Voltage	Temperature	Time	Radiation	Voltage
50	0	1	-4.441	70	0	6.5	-4.216
50	50	1	-4.431	70	0	10	-4.1
50	100	1	-4.4188	90	0	0	-4.35
50	200	1	-4.4393	90	0	3	-4.304
50	300	1	-4.3644	90	0	6.5	-4.184
30	0	0.5	-4.452	90	0	10	-4.068
50	0	0.5	-4.4392	90	50	0	-4.4308
30	0	1	-4.451	90	50	3	-4.254
50	0	1	-4.4382	90	50	6.5	-4.134
30	0	0	-4.426	90	50	10	-4.016
30	0	3	-4.368	90	100	0	-4.4188
30	0	6.5	-4.264	90	100	3	-4.194
30	0	10	-4.146	90	100	6.5	-4.074
50	0	0	-4.404	90	100	10	-3.952
50	0	3	-4.352	90	150	0	-4.4059
50	0	6.5	-4.238	90	150	3	-4.122

50	0	10	-4.124	90	150	6.5	-3.992
70	0	0	-4.382	90	150	10	-3.89
70	0	3	-4.334				

3.5.1 Sensitivity Analysis

For the Gaussian Kernel without hyper parameter tuning, the gamma value was adjusted and set to 3.5 for minimum error of 3-4% as with results shown in Table 5.

Table 5: Gamma tuning of RBF Kernel

Gamma	MAE	RMSE
20	0.0447	0.0543
10	0.035	0.0451
7.5	0.0322	0.0428
5	0.0313	0.0414
4	0.0312	0.0412
3.5	**0.0313**	**0.0411**
2.5	0.0315	0.0414
1	0.0342	0.0456
0.1	0.0727	0.0882

Similarly, the exponent of the Normalized Polykernel and Polykernel without hyper parameter tuning was adjusted to get minimum error with 8.5% and 9.1% which were higher than the RBF Kernel as shown in Table 6 and Table 7 respectively.

Table 6: Exponent Tuning of Normalized Polykernel

Exponent	MAE	RMSE
2	0.0941	0.1122
3	0.0858	0.1017
4	0.0818	0.096
5	0.0789	0.093
10	0.073	0.0871
20	0.0718	0.0856
25	0.0718	0.0855
30	**0.0718**	**0.0854**
35	0.0719	0.0855
50	0.0727	0.0859

Sequential Minimal Optimization with regression had 3 tuning parameters: C, exponent and Epsilon parameter (the insensitive loss function). By varying these parameters, the MAE was reduced to 3% and RMSE reduced to 6.3% for normalized Polykernel with C = 15, Exponent

= 45 and Epsilon = 0.0001 in Table 8 which was not recommended. Similarly, by setting the parameters to get minimum errors, the MAE was reduced to 2.6% and RMSE was reduced to 5.6% for Polykernel with C = 30 and Exponent = 27 in Table 9 which was also not recommended.

Table 7: Exponent Tuning of Polykernel

Exponent	MAE	RMSE
1	0.1104	0.1248
5	0.0736	0.0949
10	0.0661	0.0926
15	0.063	0.0922
20	0.0618	0.0919
25	0.0606	0.0919
30	0.0605	0.0919
35	0.0603	0.0918
40	0.06	0.0918
45	0.0598	0.0917
50	0.0596	0.0917
75	0.0592	0.0916
100	**0.05914**	**0.0916**

Table 8: SMO reg with Normalized Polykernel

C	MAE	RMSE
1	0.0725	0.0988
5	0.0684	0.097
10	0.0668	0.0914
15	**0.0664**	**0.0922**
20	0.0664	0.0922
Exp	MAE	RMSE
2	0.0664	0.0922
3	0.0537	0.0773
4	0.0521	0.0728
5	0.0504	0.0778
10	0.0436	0.0837
15	0.0406	0.0774
20	0.0371	0.0702
25	0.0342	0.0686
30	0.0337	0.0679
35	0.0328	0.0665
40	0.0313	0.0648
45	0.0299	0.0639
50	**0.0298**	**0.0639**

Table 9: SMO reg with Polykernel with C = 30

Exp	MAE	RMSE
1	0.0357	0.0481
2	0.036	0.0478
3	0.0347	0.0449
5	0.0295	0.0499
10	0.0277	0.0555
15	0.0271	0.0562
20	0.0268	0.0562
25	0.0262	0.0562
27	**0.0263**	**0.0562**
30	0.0289	0.0549

But for the RBF Kernel, the error was 0.06% which was so low when compared to the other kernel functions. In the paper Shuzen Li [25], they were considered the RBF kernel for accelerated degradation testing results using the data from monte-carlo simulation. The optimized tuned parameters for SMO reg with RBF kernel were C =100 and gamma is 15 from the results tabulated in Table 10 and 11. With epsilon = 0.0001, the errors were further reduced to 0.0003 and 0.0005. Hence RBF kernel best suited for degradation.

Table 10: SMO Reg with RBF Kernel with C tuning

C	MAE	RMSE
1	0.0903	0.1195
5	0.0403	0.0575
10	0.0369	0.0564
15	0.0358	0.0532
20	0.0352	0.0508
25	0.0349	0.0591
30	0.0346	0.0486
35	0.0341	0.0466
40	0.0338	0.0463
45	0.0336	0.0461
50	0.0334	0.0459
75	0.0325	0.0451
100	**0.0317**	**0.0441**

Table 10: SMO Reg with RBF Kernel with Gamma Tuning

Gamma	MAE	RMSE
0.01	0.0317	0.0441
0.1	0.0171	0.0273
1	0.0051	0.0104

5	0.001	0.0014
10	0.0007	0.0008
15	**0.0006**	**0.0008**

The optimized support vectors were -93.28437484337455 * k[0]+0.040257228770170024 * k[1]-0.22793205333831948 * k[2]-0.2817526828692522 * k[3]-0.16891291918032977 * k[4]-6.792562217468341 * k[5]-12.159262158450781 * k[6]+3.738817498294129 * k[7]+100.0 * k[8]+3.136432650141998 * k[9]-0.40548305118697636 * k[10]-0.017686862789814694 * k[11]+0.14142421495665403 * k[12]+5.8972372165834095 * k[13]-0.590734211920628 * k[14]+0.05207817633637825 * k[15]+0.13923829757449374 * k[16]-0.16307291228062248*k[17]-0.08479230240257521 * k[18]+0.010018497184633142 * k[19]+0.1664237846610784*k[20]+0.15714402054772972 * k[21]-0.22342312817692356 * k[22]-0.036205478232958915* k[23]+0.1225132753217027 * k[24]-0.5132086855567924 *k[25]+0.30454974450294453*k[26]+0.1872978002657113 * k[27]+0.20949944853703384 * k[28]+0.23888524680828016 * k[29]-0.2590720408770739 * k[30]-0.180202691026668 * k[31]-0.061199087083700046 * k[32]-0.4254874566893895 * k[33]+0.37184630434488447 * k[34]+0.3928517912643163 * k[35]+0.5688495868096197 * k[36] + 0.3783

The failure data from the physics of failure methodology was supplied to the support vector machine to find the model with optimum kernel function to find the reliability of the constant fraction discriminator.

Conclusion

In this paper, failure phenomenon of constant fraction discriminator was studied and found that the radiation and temperature with accelerated testing over time led to degradation of the output voltage from the data obtained by design of experiments and accelerated degradation test. Support vector machine was discussed to model the reliability prediction of this electronic component and proposed a model to obtain the optimum kernel function with the respective tuning parameters. It was concluded from the sensitivity analysis of all functions, SMO regression with RBF kernel was best suited for the degradation of the output parameters with least amount of error.

References

[1]. "Military Handbook, Reliability prediction of electronic component, MIL-HDBK-217F"

[2]. Mark White, "Microelectronics reliability : Physics-of-failure based modeling and lifetime evaluation", *JPL Publication* 08-05, NASA, Feb 2008

[3]. Susumu Harasawa, Atsushi Nakamoto, Yoshinori Hayakawa, Jun Egawa, Otohiko Aizawa, Tetsuya Nozaki, Takashi Minobe, Hiroshi Hatanaka, "Improved Monitoring System of Neutron Flux during Boron-Neutron Capture Therapy", *Radiation Research*, 88, 187-193 (1981)

[4]. Lloyd W. Condra, "Reliability improvement with design of experiments", 2nd edn, *Marcel Dekker*, 2001.

[5]. Wayne Nelson, "Accelerated Testing: Statistical Models, Test Plans, and Data Analysis", *John Wiley & Sons*, 2004

[6]. Vapnik, V.N., “The Nature of Statistical Learning Theory”, *Springer*: New York; 1995.
[7]. Vapnik, V.N., “Statistical Learning Theory”, *John Wiley and Sons*, Inc: New York; 1998.
[8]. Shawe Taylor, J. & Cristianini, N., “Kernel methods for pattern analysis”, *Cambridge, Cambridge University Press*, 2004
[9]. Kristin Luery, "Failure of the Constant Fraction Discriminator", July 9, 2003.
[10]. Vladimir Vassiliev, Jeremy Smith, David Kieda, "VERITAS L1 trigger Constant Fraction Discriminator",
[11]. B. Van Zeghbroeck, "Principles of Electronic Devices", University of Colarado, 2011.
[12]. Nello Cristianini, John Shawe-Taylor, “An Introduction to Support Vector Machines and Other Kernel-based Learning Methods”, *Cambridge University Press*, 2000.
[13]. Bennett, K. P. & Campbell, C., “Support Vector Machines: Hype or Hallelujah?”, *SIGKDD Explorations*, Vol 2 Issue 2, Page 1-13, 2000.
[14]. Yuan Fuqing, Uday Kumar, K B Mishra, "Complex System Reliability Evaluation using Support Vector Machine for Incomplete Data-set*", International Journal of Performability Engineering*, Vol. 7, No. 1, January 2010, pp.32-42.
[15]. Kuhn, H. W., Tucker, A. W., "Nonlinear programming", *Proceedings of 2nd Berkeley Symposium*, Berkeley: University of California Press. pp. 481–492. 1951
[16]. Yuan Fuqing, "Failure Diagnostics Using Support Vector Machine", Doctoral Thesis, Printed by *Universitetstryckeriet*, Luleå 2011
[17]. John, C Platt, "Sequential Minimal Optimization: A Fast Algorithm for Training Support Vector Machines", *Microsoft Research*, April 21, 1998
[18]. Gary William Flake, Steve Lawrence, "Efficient SVM Regression Training with SMO", *Machine Learning*, 2001
[19]. A. Smola and B. Sch¨olkopfm, “A tutorial on support vector regression”, *Technical Report* NC2- TR-1998-030, NeuroCOLT2, 1998
[20]. S. K. Shevade, S. S. Keerthi, C. Bhattacharyya, and K. R. K. Murthy, "Improvements to the SMO Algorithm for SVM Regression", *IEEE Transactions on Neural Networks*, vol. 11, no. 5, September 2000
[21]. "The temperature characteristics of bipolar transistors fabricated in CMOS technology", Guijie Wang, Gerard C.M. Meijer, Elsevier, Sensors and Actuators 87 2000 81–89.
[22]. Theodore F Bogart, Jeffrey Beasley, Guillerno Rico, "Electronic Devices and Circuits", *Pearson Prentice Hall*, 2009
[23]. Ronald L. Pease, M. C. Maher, M. R. Shaneyfelt, M. W. Savage, P. Baker, J. Krieg, T. L. Turflinger, "Total-Dose Hardening of a Bipolar-Voltage Comparator", *IEEE Transactions on Nuclear Science*, vol. 49, no. 6, December 2002
[24]. "Hardness assurance testing of bipolar junction transistors at elevated irradiation temperatures", S.C. Witczak, R.D. Schrimpf, D.M. Fleetwood, K. F. Galloway, R.C.Lacoe, D.C. Mayer, J.M. Puhl, R.L.Pease, J.S. Suehle, IEEE transaction on Nuclear Science, Vol 44, No. 6, Dec 1997
[25]. Shuzhen Li, Xiaoyang Li, Tongmin Jiang, "Life and Reliability Forecasting of the CSADT using Support Vector Machines", *Proceedings - Annual Reliability and Maintainability Symposium (RAMS)*, Page(s): 1 - 6, 25-28 Jan. 2010

CONF. IV

C6

Comparison ff Reliability Prediction Methods using Life Cycle Cost Analysis

Thaduri, A., Verma, A.K., Kumar, U. (2013). Comparison Of Reliability Prediction Methods Using Life Cycle Cost Analysis. *IEEE Proceedings on the 59th Annual Reliability and Maintainability Symposium (RAMS 2013)*, January 28-31, Orlando, Florida, USA, pp. 1-7.

Comparison Of Reliability Prediction Methods Using Life Cycle Cost Analysis

Adithya Thaduri, Lulea University of Technology
A K Verma, PhD, Stord/Haugesund University College
Uday Kumar, PhD, Lulea University of Technology

Keywords: 217+, BJT Transistor, Instrumentation Amplifier, Life cycle cost, Physics of Failure, Reliability prediction

SUMMARY AND CONCLUSION

In this paper, it was discussed on the several reliability prediction models for electronic components and comparison of these methods was also illustrated. A combined methodology for comparing the cost incurring for prediction was designed and implemented with an instrumentation amplifier and a BJT transistor. By using the physics of failure approach, the dominant stress parameters were selected on basis of research study and were subjected to both instrumentation amplifier and BJT transistor. The procedure was implemented using the methodology specified in this paper and modeled the performance parameters accordingly. From the prescribed failure criteria, mean time to failure was calculated for both the components. Similarly, using 217 plus reliability prediction book, MTTF was also calculated and compared with the prediction using physics of failure. Then, the costing implications of both the components were discussed and compared them. From the results, it was concluded that for critical components like instrumentation amplifier though the initial cost of physics of failure prediction is too high, the total cost incurred including the penalty costs were lower than that of traditional reliability prediction method. But for non-critical components like BJT transistor, the total cost of physics of failure approach was too higher than traditional approach and hence traditional approach was much efficient. Several other factors were also compared for both reliability prediction methods.

1 INTRODUCTION

The important considerations for the customer to select an item depend on the reliability, cost, availability and maintainability. To deal with the perfect repair/replacement costs, selection of the time to repair or time to replace was properly calculated or else inaccuracy in reliability prediction of this values leads to increase in the excessive costs even the actual component has higher reliability. Hence, reliability prediction of these components along with life cycle costs was needed to be considered for effective working of the system. Accordingly, there would not be same replacement times for all the components with variable reliability and costs due to the variability in criticality of the each component. This paper concentrates on this issue on which reliability prediction method was to be selected for calculation of replacement human factors, time and reputation costs.

The efficient reliability prediction is needed before the installation of the components and appropriate changes can be made at the design stages. Conventional reliability prediction methods such as Mil-Hdbk 217F, Telcordia, Bell Core, PRISM etc implements constant failure methods and believed to be true in the era of 1980s and 1990s [3]. But due to the advancements in the technology, these methods are no longer adequate to define the characteristics as there are so much variability in the design and fabrication of devices. Especially, electronics spreads out rapid developments in all the aspects and for control aspects, miniature and cost effectiveness. Some of the devices are used in safety, security and military areas where the availability is the major concern and incorrect operation leads to the unsafe shutdown. Moreover reliability aspects and prediction is critical for these components and this paper provides advanced physics of failure methodology for finding failure characteristics and reliability indices. The following Table 1 demonstrates various traditional prediction methods the differences between the values of time to failures of DC-DC converter constraints the ambiguity and risk in selecting appropriate figure [1].

Table 1: Comparisons of different reliability prediction models [1]

Reliability Prediction Model[1]	Company	1 Watt DC-DC Converter[2]				100W AC-DC PSU[3]	
		25°C		85°C		40°C	
		Hours	Years[4]	Hours	Years[4]	Hours	Years[4]
MIL-HDBK-217F (EXAR 7.0)	A	31,596,574	3606.9			686,771	78.4
MIL-HDBK-217F Notice 2	B	832,000	95.0	86,000	9.8		
MIL-HDBK-217F Notice 1	C	156,000	17.8	124,000	14.2		
Telcordia SR332 Parts count	D	89,380,000	10203.2	29,260,000	3340.2		
Telcordia SR332 Parts stress	D	104,200,000	11895.0	57,160,000	6525.1		
Siemens SN29500 (IEC61709)	A	80,978,217	9244.1			1,554,055	177.4
HRD5 Parts stress	B	2,465,000	281.4	849,000	96.9		
HRD4 Parts count	B	1,132,000	129.2	1,132,000	129.2		
MIL-HDBK-217F (EXAR 7.0)	A	31,596,574	3606.9			686,771	78.4
Telcordia SR332 Parts count	E					1,418,000	162.0

Physics of failure prediction methodology lay emphasis on the root cause of failure following fundamentals of physics of materials also considered as white box testing. Electronic devices were fabricated of different materials like Silicon,

978-1-4673-4711-2/13/$31.00 ©2013 IEEE

Germanium, Copper, Aluminum etc., with predefined technology and processes like deposition, etching and masking under controlled environment [5]. Most of failures happened due to changes in thermal activation, changes in defects of molecules, activation energy in the materials and correspondingly there was degradation in the technology and performance factors. Depends on the failure characteristics, several failure mechanisms were modeled and categorized according to the cause, material, and failure point location etc., produced in the literature. This method requires sophisticated tools for failure analysis and advanced tools for analyzing the simulated data. Still, this methodology also has challenges like insufficient data from the manufacturer, needs expert judgment and also time taking process.

Figure 1: Short idea of Modified approach

On the other hand, statistical methods were widely available in order to find out the reliability indices from the test data. This method was also considered as black box testing which concentrate on available data and proper model was selected depends on the application. There were possibilities to analyze the data and generated model to extract enormous amount of information to characterize the performance parameters. Some of them include design of experiments, accelerated testing, regression analysis, etc. Even, there were several tools available for model selection, mathematical formulation and model analysis. This methodology has some advantages like time consuming, no need for manufacturer data and parameter analysis.

Inclusion of multidisciplinary science and engineering approaches was very effective in solving of real life problems and our modified approach was combination of both physics of failure (deterministic) and statistical (probabilistic) approaches in Figure 1. This advancement methodology first starts with the proper understanding of basic failure physics of the component and process the physics of failure methodology. This knowledge was fed to the statistical approach to further refining of data for accurate models. Finally, we get three faces of models; history and literature, white box and black box models and these were sent to decision support system. Simultaneously, the cost of each prediction method was also compared for the decision on which method needed to be implemented on the criticality of the component. Other hidden costs include the amount of time that was spent on the entire processing of the prediction as it also takes care of the entire decision strategy. These details were also incorporated in this paper. The next section provides the entire block diagram for the reliability prediction with life cycle costs of each stage.

2 METHODOLOGY

The block diagram shown in Figure 2 describes the flow of prediction mechanism adopted in this paper.

2.1 Component Description

The first step in this methodology was to describe the component with all the necessary and essential information for analyzing the failure and calculating the reliability indices. The sources required for the information on the component were: materials, processes, layout diagrams, technology, architecture, design, criticality, cost, datasheet, manuals, field data and any similar item analysis that was analyzed earlier.

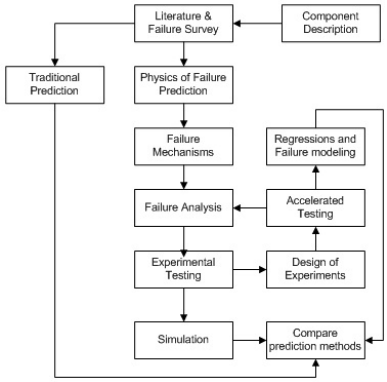

Figure 2: Reliability prediction methodology for comparisons

2.2 Literature Survey and Failure Survey

To study the failure behavior of the component, the literature survey was required to understand the behavior of several factors that affecting the performance. The information essential for this study were: expert reviews, stress factors, failure criteria, failure mechanisms, failure modes, failure analysis, degradation analysis and other factors.

2.2.1 Traditional Reliability Methodology

Based on the operational stresses and field environment, reliability indices were calculated using MilHdbk 217F and other traditional methods.

2.2.2 Physics of Failure Methodology

The advanced methodology, physics of failure lay emphasis on the root cause of failure inherently depends on the operational stress factors, environment and physical characteristics of the device [5]. From the information on component description and literature survey, appropriate failure phenomenon and failure criteria were selected.

2.3 Failure Mechanisms

There was several failure mechanisms reported in the literature characterized on operational environment, stress parameters, level of approach, technology etc. Some of list of the failure mechanisms that was not limited to electromigration, hot carrier defects, time dependent dielectric breakdown, negative bias temperature instability, corrosion, fatigue, solder reliability, stress migration, soft errors (radiation effects) etc [5,6]. There were several failure time to failure models associated with each mechanism and appropriate model was picked for the application. According to the selected component, the appropriate failure mechanism or degradation mechanisms were studied.

2.4 Failure Analysis

From the literature, an appropriate failure analysis was selected to examine and illustrate the failure of the component and root cause of failure by electrical characterization or by using non-destructive testing by making use of sophisticated instruments like scanning electron microscope, infrared spectroscopy, thermal analysis etc [9]. For some of the components where there was no information on the failure mechanism, this step was need to be implemented beforehand to acquire information on failure characteristics.

2.5.1 Experimental Planning

From the acquired data, the next process of experimentation was planned for testing and reliability prediction. The desired circuitry was designed and fabricated using printed circuit board. This step also includes the number of samples, stress parameters and experimental setup for further testing of the component.

2.5.2 Simulations

There are several tools were available to carry out simulations depends on finite element analysis, circuit simulations and parametric analysis. This step was performed simultaneous to the experiment testing to reduce the time effort for the procedure.

2.6 Design of Experiments

Design of Experiments was very advanced and efficient methodology to find the prominent factors, component selection and variability analysis of the component. The prominent approach, Taguchi method was implemented here. In order to get best out of design of experiments, a modified methodology was designed as two-step DOE. In general, there was uncertainty in selecting the stress factors for design of experiments and accelerated testing. Hence, at first screening step, the test was designed to know variability of stress on the effect of performance parameters. In the second testing step, the levels of the stress were aggressive which defines the degradation of the performance parameters.

2.7 Accelerated Testing

The input pattern obtained for degradation from modified design of experiments was applied in the accelerated testing step [13]. As from the analysis, this particular pattern leads to further degradation over the accelerated time.

2.8 Regressions and Failure Modeling

The data collected from both design of experiments and accelerated testing was used for statistical data and modeling analysis using various methods such as response surface regressions, regression methods, support vector regression and other tools to quantify the stress parameters and its behavior on the performance of the device. This data was also useful for failure models obtained from failure mechanisms.

2.9 Compare prediction models

The reliability indices calculated from traditional approaches, physics of failure models, models generated from statistical analysis and simulations were compared in this step. In accordingly, the reliability growth techniques were implemented and appropriately the repair/replacement mechanism was discussed. The actual decision was selected on basis of available inventory, importance of the component, resources available, selection of vendor and several other factors such as risk, uncertainty and human factors.

2.10 Factor Calculations

In parallel, the factors like time taken, human factors and risk was calculated at each step. With regarding the cost, this cost only provides the prediction cost of the entire block diagram in Fig 2. The total cost thus calculated including the penalty cost that was incurred by the repair/replacement costs. In the most of electronic components, the probability of replacement was more than the repair. In this case study, we are considering the replacement cost of the component.

3 FAILURE STUDIES OF COMPONENTS

3.1 Instrumentation Amplifier

An instrumentation amplifier is a gain differential device that provides the output with high common mode rejection ratio and high accuracy. This differential amplifier is widely used in several electronic applications even precise environments and also considered as most versatile amplifier. This device (INA118) require very high input impedance, low bias and offset currents, low noise and balanced inputs in order to minimize common mode gain. The basic building blocks of the instrumentation amplifier are op-amps. Technically, it is equivalent to standard op-amp, the each of the inputs of it is driven by two another op-amps to buffer the inputs and to produce desired output for impedance matching.

The gain of the amplifier is defined as the output voltage divided by input voltage [10]

$$G = Vout/(V1 - V2) = (1 + 2R1/Rgain)\ R3/R2 \quad (1)$$

Since, the voltage across Rgain equals Vin (V1-V2), the current through Rgain will equal (VIn/Rgain). Amplifiers A1 and A2 on left side will operate with gain and amplify the input signal. Rgain can be useful to tune for desired gain without effecting common mode gain and error. The

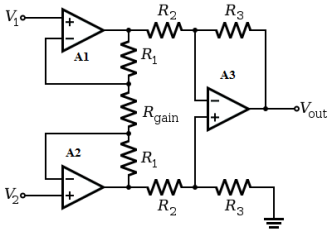

Fig 3: Test circuit for Instrumentation Amplifier, INA118

differential signal will be increased by gain, but the common-mode error will not increases, so the ratio (Gain (VDIFF)/(VError CM)) will increase. Thus, CMRR will theoretically increase in direct proportion to gain—a very useful property. CMMR is the tendency of the devices to reject the input signals common to both input leads. Ideally, a differential amplifier takes the voltages V1 and V2 on its two inputs and produces an output voltage

$$Vout = Ad(V1 - V2) \quad (2)$$

where Ad is the differential gain. But the output of a real differential amplifier is described as

$$Vout = Ad(V1 - V2) + \frac{1}{2}Acm(V1 + V2) \quad (3)$$

where Acm is the common-mode gain, which is typically much smaller than the differential gain. Thus CMRR is defined as the ratio of the powers of the differential gain over the common-mode gain, measured in decibels

$$CMMR = 10log_{10}\left(\frac{Ad}{Acm}\right)^2 = 20log_{10}\left(\frac{Ad}{|Acm|}\right) \quad (4)$$

3.1.1 Effect of Input Voltage Difference

The both gain and CMMR equations were considered as performance parameters and sensitive to the input voltage difference that further degrades the amplifier. Hence, the input voltage was selected as stress parameter.

3.1.2 Effect of Temperature

The temperature dependence of bipolar transistors depends on a multitude of parameters affecting the bipolar transistor characteristics in different ways. Important effect is the temperature dependence of the current gain. Since the current gain depends on both the emitter efficiency and base transport factor [15].

The emitter efficiency depends on the ratio of the carrier density, diffusion constant and width of the emitter and base. As a result, it is not expected to be very temperature dependent. The carrier densities are linked to the doping densities. Barring incomplete ionization, which can be very temperature dependent, the carrier densities are independent of temperature as long as the intrinsic carrier density does not exceed the doping density in either region. The width is very unlikely to be temperature dependent and therefore also the ratio of the emitter and base width. The ratio of the mobility is expected to be somewhat temperature dependent due to the different temperature dependence of the mobility in n-type and p-type material.

Leakage current *ICO and* β increase with temperature. The DC β hFE increases exponentially. The AC β *hfe* increases, but not as rapidly. It doubles over the range of -55^o to 85^{o}C. As temperature increases, the increase in *hfe* will yield a larger common-emitter output, which could be clipped in extreme cases. The increase in *hFE* shifts the bias point, possibly clipping one peak. The shift in bias point is amplified in multi-stage direct-coupled amplifiers. The solution is some form of negative feedback to stabilize the bias point. This also stabilizes AC gain [11].

As from the studies from BJT technology, temperature and radiation is selected as stress parameters. The emitter and collector current of npn BJT is given as Equation (5) and (6).

$$I_E = I_{ES}\left(e^{\frac{VBE}{VT}} - 1\right) \quad (5)$$

$$I_C = \alpha_T I_{ES}\left(e^{\frac{VBE}{VT}} - 1\right) \quad (6)$$

The output voltage VCE is given as in Equation

$$V_{CE} = V_{CE} - I_C R_{eff} \quad (7)$$

Where R_{eff} is effective output resistance at the output, I_{ES} = reverse saturation current at base-emitter diode, α_T = common base forward short circuit gain, V_T = Thermal Voltage kT/q, V_{BE} = base-emitter Voltage, V_{CE} = base-collector Voltage, V_{CC} = Source Voltage typically 5V/10V.

In Eber-Moll Model, I_C grows at about 9%/^{0}C if you hold *VBE* constant and *VB*E decreases by 2.1mV/ ^{0}C if you hold IC constant with the temperature.

Since both the currents depend on temperature parameter V_T, the raise in the temperature leads to vary these parameters which finally lead to degrade the performance of op-amps in turn the instrumentation amplifier. Hence, temperature was considered as another stress parameter which leads to reduce the gain and CMMR of instrumentation amplifier. In this paper, we selected IN128 for failure investigation. Since there was no possible failure mechanism associated with it in the literature, the failure model was not considered. But from this root cause analysis, the appropriate information was drawn out to make further testing.

The failure mechanism involved in the instrumentation was the degradation of the device parameters like gains, thermal voltage and intrinsic voltage and currents. This failure could be assessed using the standard failure analysis method which is electrical characterization.

3.2 BJT Transistor

In this study we selected 2N2222, a normal BJT transistor for failure study. At the field, this component was exposed to nuclear radiation and hence we interested to test the IC for radiation. As BJT technology was sensitive to the temperature as described in case of instrumentation amplifier, we are considering it as another stress parameter. Even in this case also, there were no failure models for failure mechanisms observed from the literature, the methodology was continued on the information gathered from the root cause analysis and field environment failed data. For further hypothesis testing, experimentation was conducted to achieve the results of

failure data. The test circuit of 2N2222 is given below in Fig 4. The stress parameters of BJT transistor was selected as temperature and radiation.

3.2.1 Effect of Radiation

Another stress parameter which degrades the BJT devices is β-radiation. Degradation of many types of bipolar transistors and circuits is known to depend strongly on dose rate. For a given total dose, degradation is more severe in low dose rate exposure than high dose rate exposure [12]. This effect has been attributed to space charge effects from trapped holes and hydrogen related species through oxygen vacancies in base oxide. There are several hardness assurance tests and most popular has been high dose rate irradiation at elevated temperatures.

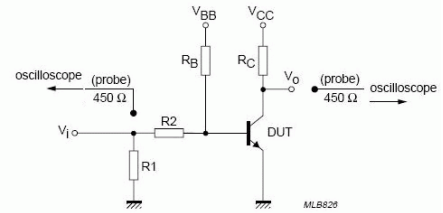

Figure 4: Test circuit for 2N2222 BJT transistor

4 RELIABILITY PREDICTIONS

By applying the above modified methodology for reliability prediction, reliability indices of both the devices were calculated using MILHDBK 217+ and by using experimental analysis considering the accelerated testing since there were no standard physics of failure models available for developing failure model. The work also carried out the simulation results to verify the behavior of both the stress parameters on the subject of interested component.

4.1 Instrumentation Amplifier

Using RIAC 217 + [7], the failure rate equation for plastic encapsulated integrated circuit was:

$$\lambda_P = \pi_G(\lambda_{OB}\pi_{DCO}\pi_{TO} + \lambda_{EB}\pi_{DCN}\pi_{RHT} + \lambda_{TCB}\pi_{CR}\pi_{DT}) + \lambda_{SIB}\pi_{SIDT} + \lambda_{EOS} \quad (8)$$

Where λ_P = Predicted failure rate, π_G = Reliability growth rate multiplier, λ_{OB} = base failure rate, π_{DCO} = failure rate multiplier of duty cycle, π_{TO} = failure rate multiplier for temperature, λ_{EB} = environmental base failure rate, π_{DCN} = failure rate multiplier of duty cycle for non operating, π_{RHT} = failure rate multiplier for temperature-humidity, λ_{TCB} = base failure rate for temperature cycling, π_{DCO} = failure rate multiplier for cycling rate, π_{DT} = failure rate multiplier for delta temperature, λ_{SIB} = base failure rate for solder joint, , π_{DT} = failure rate multiplier for solder joint delta temperature and λ_{EOS} = failure rate overstress.

There is no specific assigned model for the instrumentation amplifier. Based on its internal diagram, there are 2 portions for analysis to be needed: precision amplify and overload-protection. Comparatively, overload protection was smaller than the precision amplifier and hence precision amplifier was only analyzed. Selecting the required parameters for the INA118 instrumentation amplifier, the MTTF was calculated as $67x10^6$ hrs.

The test circuit for instrumentation amplifier in Fig 3 was subjected to both temperature and voltage simultaneously using set of runs depicted by design of experiments. From the experimentation, the stress levels of temperature 55^0C and voltage 11V produces higher degradation than other set of stress levels. These values were considered as input to the accelerated testing for extended period of time. The output voltage in terms of temperature, input stressed voltage and accelerated time was generated by response surface regression and calculated by using equation (9)

$$Vout = -4.4588 + 0.00029T - 4.035t + 0.033 + 5.546x10^{-6}T^2 + 3.797x10^{-6}t^2 - 6.624x10^{-4}V^2 + 4.459x10^{-5}TV + 0.00012tT \quad (9)$$

By considering the 5% degradation as failure in the gain and normal operating temperatures of temperature, the MTTF was calculated as $52x10^7$ hrs. There was reduction in MTTF figure when compared to traditional prediction because this experimentation considers another stress parameter as input voltage which reduces the degradation of the output variable. The CMMR of the instrumentation was also degraded when applied to the stress parameters within 5-10% with respective stress levels. The simulation studies verified the behavior of both stress parameters on degradation of output variables.

4.2 BJT Transistor

Using RIAC 217+ [7], the failure rate equation for transistors was:

$$\lambda_P = \pi_G(\lambda_{OB}\pi_{DCO}\pi_{TO}\pi_S + \lambda_{EB}\pi_{DCN}\pi_{TE} + \lambda_{TCB}\pi_{CR}\pi_{DT}) + \lambda_{SIB}\pi_{SIDT} + \lambda_{IND} \quad (10)$$

Where, π_S = stress failure rate multiplier, π_{TE} = failure rate multiplier, temperature environment and λ_{IND} = induced failure rate. The remaining factor representation was same as in Eqn .By selecting and calculating the above equation, the MTTF was calculated as $1.5x10^6$ hrs.

The test circuit for BJT transistor was subjected to temperature and then radiation as these parameters cannot be applied simultaneously. The run for stress levels for maximum degradation were temperature as 90^0C and radiation exposure of 1M rad. The voltage was generated by using response surface regression and shown below in equation

$$Vout = -2.321 + 0.00027T - 3.035t + 0.0452R + 5.235x10^{-6}T^2 + 2.535x10^{-6}t^2 - 5.644x10^{-4}R^2 + 4.487x10^{-5}TR + 0.00026tR \quad (11)$$

Under the normal conditions with 5% degradation as failure, MTTF was calculated as $1.2x10^7$ hrs. The gain over the traditional methodology was that the physics of failure considers the actual stress parameter in this case, the radiation.

4.3 Life Costing Calculations

For the instrumentation amplifier, the initial costs of both prediction methodologies were produced (in Indian equivalent of dollars). The initial cost of traditional methodology was

$$C_{it} = C_{hdbk|eqv} \quad (12)$$

Where C_{it} = initial cost for traditional methodology and $C_{hdbk|eqv}$ = cost of handbook for equivalent component. The actual cost of RIAC 217 plus handbook was 200$. The assumption was that the figure of each calculation was 200. Hence, C_{it} was assumed as 1$. The cost of physics of failure methodology was calculated as

$$C_{ip} = C_{er} + C_{rs} + C_{fa} + C_{exp} + C_{model} \quad (13)$$

Where C_{ip} = initial cost for physics of failure methodology, C_{er} = expert reviews as consultation fee, C_{rs} = cost of research papers, C_{fa} = cost of failure analysis, C_{exp} = cost of experimentation includes design, fabrication of PCB boards, sources and measurement instruments and other miscellaneous and C_{model} = cost of tools required for modeling. By considering the figure of each calculation as 200, the total cost consumed by physics of failure methodology was C_{ip} = 50+120+50+250+30 = 500$ (approximately).

Similarly, the initial or prediction costs of BJT transistor was calculated as C_{it} = 1$ and C_{ip} = 500$.

For calculating the penalty costs, it was needed to consider costs of the instrumentation amplifier as C_{IA} = 15$ and cost of BJT transistor as C_{BT} = 1$, time period and also the number of replacements over time. Hence, penalty costs were computed for both the components. For instrumentation amplifier, the cost of penalty cost by using traditional method,

$$C_{pt} = Cc\left(1 + \frac{(1+i)^t - 1}{i(1+i)^t} * 2 * \frac{t0}{MTTF_t}\right) \quad (14)$$

Where C_c = cost of the component, MTTFt = time to failure using traditional methodology, Cf = 2*Cc = failure cost as it was assumed as doubled for traditional methods, i = interest rate, t0 = age of replacement =1(assumed) and t is the design life. Similarly the cost of penalty using physics of failure methodology was shown in equation.

$$C_{pp} = Cc\left(1 + \frac{(1+i)^t - 1}{i(1+i)^t} * \frac{t0}{MTTF_p}\right) \quad (15)$$

Where MTTFp = time to failure by physics of failure.

The total cost of the reliability prediction was summation of initial and penalty costs. For traditional prediction methodology,

$$C_{tt} = C_{it} + C_{pt} \quad (16)$$

Similarly for physics of failure prediction, the total cost was

$$C_{pp} = C_{ip} + C_{pp} \quad (17)$$

To compare the total cost incurred by both the prediction methods for both the components, it was assumed that the design life was 10 years and ratio of number of replacements for a component was equal to the ratio of individual time to failures.

$$\frac{n_p}{n_t} = \frac{MTTF_p}{MTTF_t}$$

By considering these assumptions, for an instrumentation amplifier, the total cost expended on traditional methodology (1052) was more than the proposed methodology (650) for n replacements. But for the BJT transistor, the total cost expended on traditional methodology (88) was less than the proposed methodology (508) for n replacements.

4.4 Other Factors

In the traditional reliability prediction, there was a certain amount of risk associated with it and uncertainty over the selection of several standard books available. There was no possible inclusion of human factors, needed less amount of time, space and man power. But in the case of physics of failure reliability prediction methodology, it requires large amount of time, space, man power and human factors regarding the implementation of experimentation and modeling. Also, it provides the approximate figure of the failure time and had higher accuracy than previous prediction models. The difference between both the prediction methods was tabulated as in table [2].

Table 2: Comparison of Reliability Prediction methods

Factor	Traditional	PoF
Initial Cost	Low	High
Penalty Cost	High	Low
Total Cost for Critical	High	Low
Total Cost for non-critical	Low	High
Time	Less	Large
Space	Less	Large
Expertise	Low	High
Human factors	Less	More
Risk	High	Low
Uncertainty	High	Low
Man Power	Few	Large

REFERENCES

1. "European power supply manufacturers association, MTBF Report", June 2005
2. "Military Handbook, Reliability prediction of electronic component, MIL-HDBK-217F"
3. Jeff Jones, Joseph Hayes, "A Comparison of Electronic-Reliability Prediction Models", *IEEE Transactions on Reliability*, vol. 48, no. 2,1999 june
4. B. Foucher, J. Boullie, B. Meslet, D. Das, "A review of reliability prediction methods for electronic devices", *Microelectronics Reliability* 42 (2002) 1155–1162
5. "Failure Mechanisms and Models for Semiconductor Devices", *JEDEC Publication*, JEP122E, Originally published as JEP122D.01 March 2009
6. "Semiconductor Device Reliability Failure Models", *International SEMATECH*, May 31, 2000
7. "Handbook Of 217Plus Reliability Prediction Models, *Reliability Information Analysis Center (RIAC)*", 26 May 2006
8. Lloyd W. Condra, "Reliability improvement with design of experiments", 2nd edn, *Marcel Dekker*, 2001.

9. Perry L Martin, “Electronic Failure Analysis Handbook, Techniques and Applications for Electronic and Electrical Packages, Components, and Assemblies”, *McGraw Hill*, 1999
10. Charles Kitchin, Lew Counts, “A Designer's guide to Instrumentation Amplifiers”, *Analog Devices*, 2006
11. Guijie Wang, Gerard C.M. Meijer, "The temperature characteristics of bipolar transistors fabricated in CMOS technology", *Elsevier, Sensors and Actuators* 87 2000 81–89.
12. S.C. Witczak, R.D. Schrimpf, D.M. Fleetwood, K. F. Galloway, R.C.Lacoe, D.C. Mayer, J.M. Puhl, R.L.Pease, J.S. Suehle, "Hardness assurance testing of bipolar junction transistors at elevated irradiation temperatures", *IEEE transaction on Nuclear Science*, Vol 44, No. 6, Dec 1997

BIOGRAPHIES

Adithya Thaduri: He studied electronics and instrumentation engineering in bachelors and reliability engineering in masters. Presently, he is doing PhD at IIT Bombay India and Lulea University of Technology, Sweden in association with Bhabha Atomic Research center India. His core area of research on predicting the life of critical electronic components using physics of failure approach.

A.K. Verma received the B.Tech (Hons) and Ph.D. (Engg.) degrees from Department of Electrical Engineering, IIT Kharagpur. He has been with IIT Bombay as a faculty since 1988. He is a professor in the Department of Electrical Engineering at IIT Bombay. He has over 180 research papers to his credit and has supervised twenty eight Ph.D. thesis and eight four Masters Thesis at IIT Bombay. He is the Editor in Chief of the International Journal of Systems Assurance and Engineering Management. He has been a guest editor of special issues of various international journals He is a senior member of IEEE and life fellow of IETE. His research interests on reliability engineering include interdisciplinary applications in software engineering, computing, maintenance, and power systems.

Uday Kumar obtained his B. Tech from India during the year 1979. After working for 6 years in Indian mining industries, he joined the postgraduate program of Lulea University of Technology, Lulea, Sweden and obtained a PhD degree in field of Reliability and Maintenance during 1990. He worked as a Senior Lecturer and Associate Professor at Lulea University 1990-1996. In 1997, he was appointed as a Professor of Mechanical Engineering (Maintenance) at University of Stavanger, Stavanger, Norway. Since July 2001, he has taken up the position as a Professor of Operation and Maintenance Engineering at Lulea University of Technology, Lulea, Sweden. Currently he is the Director of Lulea Railway Research Center. His research interests are equipment maintenance, reliability and maintainability analysis, etc. He is also member of the editorial boards and reviewer for many international journals. He has published more than 150 papers in International Journals and Conference Proceedings.